

การเปลี่ยนชื่อมวลิกโนเซลลูโลสโดยการจัดลำดับการปรับสภาพด้วยกรดและเบสอินทรีย์



นางสาว อังคนา วงศ์ศิริวรรณ

ศูนย์วิทยทรัพยากร

จุฬาลงกรณ์มหาวิทยาลัย

วิทยานิพนธ์นี้เป็นส่วนหนึ่งของการศึกษาตามหลักสูตรปริญญาวิทยาศาสตรดุษฎีบัณฑิต

สาขาวิชาเคมีเทคนิค ภาควิชาเคมีเทคนิค

คณะวิทยาศาสตร์ จุฬาลงกรณ์มหาวิทยาลัย

ปีการศึกษา 2553

ลิขสิทธิ์ของจุฬาลงกรณ์มหาวิทยาลัย

LIGNOCELLULOSIC BIOMASS CONVERSION BY SEQUENTIAL COMBINATION OF
ORGANIC ACID AND BASE TREATMENTS



Miss Ungkana Wongsiriwan

A Dissertation Submitted in Partial Fulfillment of the Requirements
for the Degree of Doctor of Philosophy Program in Chemical Technology
Department of Chemical Technology

Faculty of Science

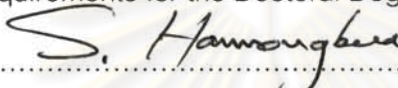
Chulalongkorn University

Academic year 2010

Copyright of Chulalongkorn University

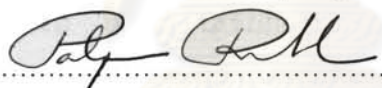
Thesis Title LIGNOCELLULOSIC BIOMASS CONVERSION BY SEQUENTIAL
COMBINATION OF ORGANIC ACID AND BASE TREATMENTS
By Miss Ungkana Wongsiriwan
Field of Study Chemical Technology
Thesis Advisor Professor Pattarapan Prasassarakich, Ph.D.
Thesis Co-Advisor Professor Chunshan Song, Ph.D.

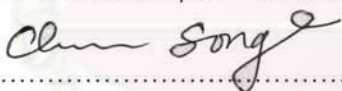
Accepted by the Faculty of Science, Chulalongkorn University in Partial
Fulfillment of the Requirements for the Doctoral Degree



..... Dean of the Faculty of Science
(Professor Supot Hannongbua, Dr. rer. nat.)

THESIS COMMITTEE


..... Chairman
(Associate Professor Tharapong Vitidsant, Doctorat de l'INPT)



..... Thesis Advisor
(Professor Pattarapan Prasassarakich, Ph.D.)


..... Thesis Co-Advisor
(Professor Chunshan Song, Ph.D.)


..... Examiner
(Associate Professor Pornpote Piumsomboon, Ph.D.)


..... Examiner
(Associate Professor Somkiat Ngamprasertsith, Doctorat de l'INPT)


..... Examiner
(Assistant Professor Chawalit Ngamcharussrivichai, Ph.D.)


..... External Examiner
(Boonyawan Yoosuk, Ph.D.)

อังคณา วงศ์ศิริวรรณ : การเปลี่ยนชีวมวลลิกโนเซลลูโลสโดยการจัดลำดับการปรับสภาพด้วยกรดและเบสอินทรีย์. (LIGNOCELLULOSIC BIOMASS CONVERSION BY SEQUENTIAL COMBINATION OF ORGANIC ACID AND BASE TREATMENTS) อ. ที่ปรึกษาวิทยานิพนธ์หลัก: ศ.ดร. ภัทรพรพรรณ ประศาสน์สารกิจ, อ. ที่ปรึกษาวิทยานิพนธ์ร่วม: Prof. Chunshan Song, 195 หน้า.

จุดประสงค์ของงานวิจัยนี้ เพื่อศึกษาหาวิธีการไฮโดรไลซิสแบบใหม่โดยใช้การจัดลำดับการปรับสภาพแบบสองขั้นตอนด้วยกรดอินทรีย์ (กรดออกซาลิก) และเบสอินทรีย์ (เตตระเมทิลแอมโมเนียมไฮดรอกไซด์) เพื่อเปลี่ยนไม้สนซึ่งเป็นชีวมวลลิกโนเซลลูโลสที่ภาวะปานกลางในเครื่องปฏิกรณ์แบบแบตช์ การจัดลำดับการปรับสภาพด้วยกรดออกซาลิกตามด้วยเบสเตตระเมทิลแอมโมเนียมไฮดรอกไซด์ แสดงผลเสริมอย่างมีนัยสำคัญในการเปลี่ยนเทียบกับปฏิกิริยาหนึ่งขั้นตอนหรือสองขั้นตอนด้วยกรดหรือเบสอย่างเดียว การตรวจสอบลักษณะสมบัติเชิงวิเคราะห์ของผลิตภัณฑ์ด้วยเทคนิคต่างๆแสดงว่า การเปลี่ยนพอลิแซ็กคาไรด์เพิ่มเนื่องจากการเสริม การตรวจสอบกากไม้สนด้วยกล้องจุลทรรศน์อิเล็กตรอนแบบส่องกราดแสดงว่า ไฮโดรไลซิสด้วยกรดทำลายโครงสร้างเซลลูโลสบางส่วนจึงช่วยให้เซลลูโลสเกิดปฏิกิริยาด้วยเบสในขั้นตอนที่สองได้ดีขึ้น การบวมไม้สนก่อนการทำปฏิกิริยาด้วยน้ำ กรด และเบสไม่แสดงผลต่อการเปลี่ยนในภาวะที่ใช้ การเปลี่ยนของเซลลูโลสแสดงผลเสริมในทิศทางเดียวกับไม้สน การคลายโครงสร้างผลึกเซลลูโลสในไม้สนทำให้เกิดการเปลี่ยนที่มากขึ้น แต่ไม่มีส่วนช่วยเหลือผลเสริมในการเปลี่ยนของไม้สน ปัจจัยทางเคมีอื่นเช่น การเพิ่มปริมาณปลายของเซลลูโลสที่มีสมบัติรีดิวซ์จากการทำปฏิกิริยาด้วยกรด อาจมีส่วนในการเกิดผลเสริม

ภาควิชา.....เคมีเทคนิค.....ลายมือชื่อนิสิต.....Ungkana Wongsiriwan.....

สาขาวิชา.....เคมีเทคนิค.....ลายมือชื่อ อ.ที่ปรึกษาวิทยานิพนธ์หลัก.....

ปีการศึกษา.....2553.....ลายมือชื่อ อ.ที่ปรึกษาวิทยานิพนธ์ร่วม.....

4973867823 : MAJOR CHEMICAL TECHNOLOGY

KEYWORDS : LIGNOCELLULOSE / HYDROLYSIS / ALKALINE PEELING /
OXALIC ACID / TETRAMETHYLAMMONIUM HYDROXIDE

UNGKANA WONGSIRIWAN : LIGNOCELLULOSIC BIOMASS
CONVERSION BY SEQUENTIAL COMBINATION OF ORGANIC
ACID AND BASE TREATMENTS. THESIS ADVISOR : PROF.
PATTARAPAN PRASASSARAKICH, THESIS CO-ADVISOR : PROF.
CHUNSHAN SONG, 195 pp.

The purpose of this research is to explore a new hydrolysis approach using sequential two-step combinations of organic acid (oxalic acid) and base (tetramethylammonium hydroxide, TMAH) to convert lignocellulosic biomass at mild conditions using a spruce wood sample in a batch reactor. A sequential combination of oxalic acid followed by TMAH shows a strong synergistic conversion compared with single- or two-step reactions with either acid or base alone. Analytical characterization of products with several techniques suggests conversion of polysaccharides was enhanced. Examination of spruce residues by SEM suggests acid hydrolysis caused partial structural breakdown of cellulose that facilitates base reaction in the second step. Pre-swelling of spruce with water, oxalic acid, and TMAH showed no significant impact on conversion under the condition employed. Cellulose conversion exhibited synergy in the same trend as that in spruce. Loosening crystalline structure of cellulose lead to higher conversion of spruce, but did not contribute to the synergistic effect. Other chemical factor such as increase in cellulose reducing end could also contribute in part to the cause of the synergy.

Department : Chemical Technology

Field of Study : Chemical Technology

Academic Year : 2010

Student's Signature Ungkana Wongsiriwan

Advisor's Signature

Co-Advisor's Signature

[Handwritten signatures of Prof. Pattarapan Prasassarakich and Prof. Chunshan Song]

ACKNOWLEDGEMENTS

I would like to express thanks to my research advisors Prof. Pattarapan Prasassarakich and Prof. Chunshan Song for their guidance. It has been an honor to work with them and learn their inspiring vision. I would like to thank all of my thesis committee members including the chairman, Assoc. Prof. Tharapong Vitidsant, Assoc. Prof. Pornpote Piumsomboon, Assoc. Prof. Somkiat Ngamprasertsith, Asst. Prof. Chawalit Ngamcharussrivichai, and Dr. Boonyawan Yoosuk for their constructive advice and suggestions.

This work would not have been accomplished without the following excellent people at the Pennsylvania State University. I would like to acknowledge Yu Noda for all the great time and work. He is a very fantastic co-worker, colleague, co-author, and friend. I have learned a lot from him. I would like to extend thanks to the people who helped me during my research years including Dr. Dania Alvarez-Fonseca, Dr. Alan Benesi, Mark Angelone, Lee Stover, Glenn Decker, and Ronnie Wasco for their assistance to instrumental analysis. I also would like to thank Dr. Jae Hyung Kim and Dr. Xiaoliang Ma for their guidance during my early days at Penn State. I also appreciate the help from technicians and secretaries at Chulalongkorn University, and the assistances of staff members at the EMS Energy Institute.

I feel very fortunate to have an opportunity to study at Chulalongkorn University and Pennsylvania State University. Chulalongkorn University gives me fundamental knowledge from the faculty at the Department of Chemical Technology. The Pennsylvania State University provides exceptional working environment and facilities. I am really grateful for being a part of these prestigious institutions. I am also indebted to the Royal Golden Jubilee program that provides financial support through the Thailand Research Fund. The Pennsylvania State University is also gratefully acknowledged for sponsorship and facilities.

I would like to thank all the CFCP members at the EMS Energy Institute, and all friends who always stay with me in good and bad times. Last but not least, I would like to express my deepest thanks to my family, especially my mother, who are always supportive, confident in me, and patient with me.

CONTENTS

	PAGE
ABSTRACT (in Thai)	iv
ABSTRACT (in English).....	v
ACKNOWLEDGMENTS	vi
CONTENTS.....	vii
LIST OF TABLES	xi
LIST OF FIGURES	xiii
NOMENCLATURES	xxi
CHAPTER 1: INTRODUCTION	1
1.1 Motivation	1
1.2 Composition and Structure of Lignocellulosic Biomass	3
1.2.1 Cellulose	6
1.2.2 Hemicellulose.....	9
1.2.3 Lignin.....	13
1.3 Traditional Conversion of Second Generation Biomass	17
1.3.1 Gasification	20
1.3.2 Pyrolysis and Liquefaction	21
1.3.3 Enzymatic Hydrolysis.....	24
1.3.4 Acid Hydrolysis	26
1.3.5 Kraft Pulping.....	29
1.3.6 Organosolv Pulping	31
1.4 Proposing a New Process for Biomass Conversion	32
1.5 Reactions of Biomass by Acids and Bases	33
1.5.1 Hydrolysis by Acid	33
1.5.2 Cleavage of Lignin Bonds by Acid	36
1.5.3 Lignin Cleavage by Base	37
1.5.4 Peeling Reaction by Base	38
1.6 Objectives and Scope	39

CONTENTS (continued)

	PAGE
CHAPTER 2: EXPERIMENTAL AND CHARACTERIZATION	41
2.1 Materials and Reagents	41
2.2 Sample Preparation for Batch Reaction	42
2.2.1 Typical Sample Preparation.....	42
2.2.2 Second-step Sample Preparation.....	43
2.2.3 Pre-swelling of Wood Samples.....	43
2.2.4 Dissolution of Wood Samples.....	44
2.3 Reaction in Batch Reactor	45
2.3.1 Sequential Acid and Base Reaction for Wood Conversion	45
2.3.2 Acid and Base Reaction for Pre-swollen Wood Conversion.....	46
2.4 Gas Product Analysis	47
2.5 Liquid Product Analysis	47
2.5.1 Gas Chromatography Mass Spectroscopy of Toluene-Extracted Samples	47
2.5.2 Gas Chromatography Mass Spectroscopy of Extracted Derivatized Samples	48
2.6 Solid Product Analysis	50
2.6.1 Pyrolysis Gas Chromatography.....	50
2.6.2 Nuclear Magnetic Resonance Spectroscopy of Carbon-13	51
2.6.3 Scanning Electron Microscope	51
2.6.4 X-ray Diffraction.....	51
CHAPTER 3: PRELIMINARY STUDIES ON BIO-OIL UPGRADING	52
3.1 Experimental for Bio-oil Upgrading	52
3.1.1 Materials	52
3.1.2 Upgrading of Bio-oil in Batch Reactor.....	53
3.1.3 Gas Chromatography Mass Spectroscopy of Bio-oil.....	53
3.2 Bio-oil Characterization	53

CONTENTS (continued)

	PAGE
3.3 Upgrading of the Bio-Oil by Commercial CoMo Sulfide Catalysts.....	56
3.3.1 Effects of Temperature	56
3.3.2 Effects of Reaction Time	60
3.3.3 Effects of Bio-Oil to Catalyst Ratio	61
3.3.4 Effect of Solvents	62
3.4 Upgrading of the Bio-Oil by Unsupported CoMoS ₂ and NiMoS ₂ Catalysts	64
3.5 Solid Formation from Bio-oil Conversion	65
3.6 Conclusion on Bio-oil Upgrading	69
CHAPTER 4: SYNERGY CONVERSION OF BIOMASS BY SEQUENTIAL ACID	
AND BASE TREATMENTS	
	70
4.1 Conversion of Biomass in Single-Step Reactions	72
4.1.1 Effects of Reaction Time and Temperature	72
4.1.2 Reaction of Polysaccharides by Oxalic Acid and TMAH	75
4.1.3 Reaction of Lignin by Oxalic Acid and TMAH.....	78
4.1.4 Hydrolysis of Hemicellulose and Cellulose.....	79
4.1.5 Effect of Reaction Time on Sugar Degradation.....	82
4.1.6 Effect of Reaction Temperature on Sugar Degradation	84
4.2 Conversion of Biomass in Two-Step Reactions	86
4.2.1 Evidence of Synergy from Total Conversion	86
4.2.2 Evidence of Synergy from Analysis of Liquid Products	88
4.2.3 Evidence of Synergy from Analysis of Solid Products	92
4.3 Conversion of Biomass in Three-Step Reactions	99
4.4 Decomposition of Oxalic Acid and TMAH	101
CHAPTER 5: PHYSICAL CONTRIBUTION TO ENHANCE SPRUCE	
CONVERSION BY ACID AND BASE	
	102
5.1 Morphological Investigation of Spruce and Solid Residues by SEM.....	103
5.2 Pre-swelling of Spruce	110

CONTENTS (continued)

	PAGE
5.3 Conversion of Pre-swollen Spruce by Acid and Base Treatment	113
CHAPTER 6: ORIGIN OF SYNERGY IN CONVERSION OF SPRUCE BY ACID- BASE TREATMENTS: CELLULOSE CONVERSION AS A PROBE	115
6.1 Dissolution of Spruce and Conversion by Acid and Base Treatment	118
6.2 Characterization of the Regenerated Spruce	122
6.3 Suggestion of Cellulose Contribution to Spruce Conversion	126
6.4 Possible Chemical Effects to Synergy	128
CHAPTER 7: CONCLUSIONS AND RECOMMENDATIONS	130
7.1 Conclusions	130
7.2 Recommendations	131
REFERENCES	132
APPENDICES	158
Appendix A: Sugar Analysis by Derivatization Methods.....	159
Appendix B: Identification of Pyrolysis Products from Literature	174
Appendix C: SEM Micrographs of Spruce and Solid Residues	186
VITA	195

ศูนย์วิจัยทรัพยากร
 จุฬาลงกรณ์มหาวิทยาลัย

LIST OF TABLES

TABLE	PAGE
1.1	Chemical constituents of wood..... 4
1.2	Chemical compositions of representative softwoods..... 11
1.3	Chemical compositions of representative hardwoods..... 12
1.4	Percentages of various linkages in milled wood lignin derived from spruce and birch..... 15
1.5	Functional group of lignin in spruce and birch (per C ₉ units)..... 16
1.6	Comparison of liquefaction and pyrolysis..... 23
2.1	Proximate and ultimate analysis of spruce 41
2.2	Typical composition of white spruce 42
3.1	Effect of solvents on conversion of bio-oil to gas, liquid, and solid product over commercial CoMo sulfide catalyst 63
3.2	Effect of catalyst type on conversion of bio-oil to gas, liquid, and solid product at 200 °C 64
3.3	Composition of bio-oil models 65
3.4	Effect of catalyst type on solid product formation of model bio-oil 67
4.1	Effect of base type on conversion of cellulose at 120°C 72
4.2	Relative amount of toluene-soluble compounds analyzed by GC-MS 78
4.3	Weight percentage of sugars derived from hemicellulose and cellulose in single-step reaction 81
4.4	Conversions of spruce by single- and two-step reactions at 150 °C, 2 h 87
4.5	Weight percentages of sugars derived from hemicellulose and cellulose from acid reactions of one- and two-step reactions 89
4.6	Selected characteristic ion masses from Py-GC-MS of biomass residue 92
4.7	Polysaccharide-to-lignin ratio of solid residues from biomass reactions at various conditions based on peak area by Py-GC-MS analysis 94

LIST OF TABLES (continued)

TABLE	PAGE
5.1 Swelling ratio of spruce in water, 10% oxalic acid, and 10% TMAH.....	112
5.2 Conversions of pre-swollen spruce in comparison with non-swollen spruce by oxalic acid and TMAH at 150 °C for 2 h	113
6.1 Conversions of regenerated spruce by oxalic acid and TMAH at 150 °C for 2 h	121
6.2 Conversions of cellulose by single- and two-step reactions at 150 °C for 2 h	127
A-1 Summary of carbohydrate derivatization for octadecyl reversed-phase column equipped with a detector in the range of 200-400 nm.....	162
B-1 Identified polysaccharides-derived compounds as pyrolysis products.....	175
B-2 Identified lignin-derived compounds as pyrolysis products.....	178
B-3 Identified lignin-TMAH derived compounds as pyrolysis products	182


 ศูนย์วิทยทรัพยากร
 จุฬาลงกรณ์มหาวิทยาลัย

LIST OF FIGURES

FIGURE	PAGE
1.1 Schematic structure of plant cell walls.....	4
1.2 Schematic representation of cellulose microfibrils.....	5
1.3 Structure of cellulose I and its inter-and intra-chain hydrogen bonding pattern. Dashed lines: interchain hydrogen bonding. Dotted lines: intrachain hydrogen bonding.....	7
1.4 Simplified structural formula of softwoods hemicellulose O-acetyl- galactoglucomannan. Sugar units: Glup (Glucopyranose); Manp (Mannopyranose); Galp (Galactopyranose)	10
1.5 Simplified structural formula of softwoods hemicellulose arabino-4-O-methyl- glucuronoxylan. Sugar units: Xylp (Xylopyranose); Glup (Glucopyranose); Arap (Arabinofuranose)	10
1.6 Simplified structural formula of hardwoods hemicellulose O-acetyl-4-O- methyl-glucuronoxylan. Sugar units: Xylp (Xylopyranose); GlupA (Glucuronic acid)	12
1.7 Simplified structural formula of hardwoods hemicellulose glucomannan. Sugar units: Glup (Glucopyranose); Manp (Mannopyranose)	12
1.8 Structures of lignin precursors. (a) p-coumaryl alcohol; (b) coniferyl alcohol; (c) sinapyl alcohol.....	13
1.9 Common Linkages between phenylpropane units in lignin. Bond linkages: (a) β -O-4; (b) β -5; (c) 5-5; (d) α -O-4; (e) β -1; (f) 4-O-5; (g) β - β	14
1.10 Important structure of softwood lignin derived from spruce	16
1.11 Conventional processes for production of fuels from lignocellulosic biomass	19
1.12 Sulfidolytic cleavage of β -aryl ether bond in lignin phenolic units.....	30
1.13 Alkaline cleavage of β -aryl ether bond in lignin non-phenolic units	30
1.14 Sulfidolytic cleavage of β -aryl ether bond in lignin non-phenolic units with α - carbonyl group.....	30

LIST OF FIGURES (continued)

FIGURE	PAGE
1.15 Mechanism of acid hydrolysis of cellulose	33
1.16 Mechanism of HMF and levulinic acid formation via secondary reactions of glucose.....	35
1.17 Mechanism of furfural formation via secondary reactions of pentose.....	35
1.18 Reaction in acid delignification of α -aryl ether bonds in lignin via (a) quinone intermediate, (b) nucleophilic substitution, (c) formation of benzyl carbocation	36
1.19 Thermochemolysis cleavage of β -aryl ether bond in lignin phenolic units	37
1.20 Alkaline peeling of cellulose	38
1.21 Rearrangement of aldose and ketose in alkaline medium	38
2.1 Photograph of batch reactor.....	46
2.2 Reaction scheme of oxime formation of β -D-glucofuranose	48
2.3 Reaction scheme of silylation of glucose oxime	49
3.1 GC-MS chromatogram of bio-oil in dichloromethane	54
3.2 GC-MS chromatogram of bio-oil in tetrahydrofuran	55
3.3 GC-MS chromatogram of bio-oil in acetone	55
3.4 GC-MS chromatogram of (a) bio-oil; (b) bio-oil product from hydrotreating over commercial CoMo sulfide catalyst at 90 °C	56
3.5 Conversion of bio-oil upgrading to gas, liquid, and solid product over commercial CoMo sulfide catalyst at various reaction temperatures	57
3.6 GC-MS chromatogram of bio-oil products from hydrotreating over commercial CoMo sulfide catalyst at (a) 90 °C; (b) 200 °C; (c) 270 °C	58

LIST OF FIGURES (continued)

FIGURE	PAGE
3.7	GC-MS chromatogram of bio-oil products from hydrotreating over commercial CoMo sulfide catalyst at 200 °C; (a) liquid product; (b) acetone-soluble solid product 59
3.8	Effect of reaction time on conversion of bio-oil to gas, liquid, and solid product over commercial CoMo sulfide catalyst at 270 °C 60
3.9	Effect of bio-oil : catalyst ration on conversion of bio-oil to gas, liquid, and solid product over commercial CoMo sulfide catalyst at 270 °C, 1h 61
3.10	GC-MS chromatogram of bio-oil products from hydrotreating over commercial CoMo sulfide catalyst at 270 °C; (a) without decalin; (b) with 1:1 decalin solvent 62
3.11	GC-MS chromatogram of bio-oil products from hydrotreating over commercial CoMo sulfide catalyst at 270 °C; (a) without methanol; (b) with 1:1 methanol solvent. The sign (✕) indicates ester compounds 63
3.12	GC-MS chromatogram of bio-oil model (Model A)..... 66
3.13	GC-MS chromatogram of bio-oil model (Model A) after hydrotreating over various catalysts 68
4.1	Conversion of single-step oxalic acid reaction at various reaction time and temperature 73
4.2	Conversion of single-step TMAH reaction at various reaction time and temperature 74
4.3	GC-FID chromatogram of liquid products from biomass in single-step reaction with acid, base, or water alone at 150 °C for 2 h..... 76
4.4	Identified compounds in GC-FID of oxalic acid and TMAH reaction with spruce. 77

LIST OF FIGURES (continued)

FIGURE	PAGE
4.5	Structure of possible disaccharides derived from softwood hemicelluloses in comparison with cellobiose structure..... 81
4.6	Monomeric sugars yield from oxalic acid reactions with spruce at 150 °C, various reaction time 83
4.7	Relative yield of hexose derivatives from TMAH reactions with spruce at 150 °C, various reaction time 83
4.8	GC-FID chromatogram of (a) oxalic acid reaction at 150 °C, 2h, (b) followed by 180 °C, 5 min, (c) followed by 180 °C, 10 min, (d) followed by 200 °C, 5 min, (e) followed by 200 °C, 10 min, (f) followed by 220 °C, 5 min, (g) followed by 220 °C, 10 min. Numbers in parentheses are the % conversion . 85
4.9	Conversion by each step of reaction by oxalic acid and TMAH..... 88
4.10	Monomeric sugars yield from acid reactions of spruce at 150 °C, 2 h 90
4.11	Monomeric sugars yield from acid reactions of spruce at 215 °C, 1 h 90
4.12	GC-FID chromatogram of liquid products from base reactions of spruce at 150 °C, 2 h 91
4.13	Example of selective ion chromatogram from single-step acid reaction of biomass at 150 °C for 2 h 93
4.14	C CPMAS NMR spectra of solid residues after two-step reactions of spruce at 150 °C for 2 h compared with the original spruce 96
4.15	Conversions of spruce by single-, two-, and three-step reactions at 150 °C for 2 h 99
4.16	Monomeric sugars yield from acid reactions of spruce from single-, two-, and three-step reactions at 150 °C for 2 h. Numbers in parentheses are the % conversion 100

LIST OF FIGURES (continued)

FIGURE		PAGE
5.1	SEM micrographs of spruce and solid residues from one-step treatment (200× magnification). Designation: (a) untreated spruce; (b) water residue; (c) acid residue; (d) base residue	103
5.2	SEM micrographs of solid residues from two-step treatment (200× magnification). Designation: (a) A-A residue; (b) B B residue; (c) B-A residue; (d) A-B residue	105
5.3	SEM micrographs of solid residues from acid treatment (500× magnification). Designation: (a) A residue; (b) A-A residue	106
5.4	SEM micrographs of solid residues from base treatment (500× magnification). Designation: (a) B residue; (b) B-B residue	106
5.5	SEM micrographs of solid residues from two-step treatment at (1000× magnification). Designation: (a) A-A residue; (b) B-B residue; (c) A-B residue	107
5.6	SEM micrographs of solid residues from acid treatment (500× magnification). Designation: (a) B-A residue; (b) A-B residue.....	108
5.7	SEM micrographs of solid residues from three-step treatment A-B-A residue (200× magnification).....	108
5.8	SEM micrographs of spruce and solid residues from two- and three-step treatment (1000× magnification). Designation: (a) A-B residue; (b) A-B-A residue	109
5.9	Pre-swelling experiment of spruce before the reaction in different medium (a) water; (b) 10% oxalic acid; (c) 10% TMAH. Dashed line represents initial level of spruce before pre-swelling.....	111

LIST OF FIGURES (continued)

FIGURE	PAGE
6.1	Basic procedures for preparation of cellulose polymorphs 117
6.2	Crystal structure of cellulose I _β and cellulose II unit cell by different projection (a) along the a-b plane of cellulose I _β , (b) parallel to the (100) lattice plane of cellulose I _β , (c) along the a-b plane of cellulose II, (d) parallel to the (010) lattice plane of cellulose II 117
6.3	Chemical structures of dissolution solvents. (a) NMMO; (b) C ₄ mim ⁺ Cl ⁻ ; (c) H ₃ PO ₄ 118
6.4	Interaction between NMMO and cellulose 119
6.5	Dissolved spruce in (a) NMMO; (b) C ₄ mim ⁺ Cl ⁻ ; (c) H ₃ PO ₄ 120
6.6	Regenerated samples from dissolution in (a) NMMO; (b) C ₄ mim ⁺ Cl ⁻ ; (c) H ₃ PO ₄ 120
6.7	X-ray diffractions of (a) spruce; (b) acid-treated residue; (c) NMMO regenerated spruce; (d) C ₄ mim ⁺ Cl ⁻ regenerated spruce; (e) H ₃ PO ₄ regenerated spruce 123
6.8	Conversions of spruce and cellulose by single-, and two-step reactions at 150 °C for 2 h 127
6.9	Scheme of cellulose before and after treatments (a) before treatment; (b) after acid treatment; (c) after base treatment 129
A-1	HPLC chromatogram at 270 nm of (a) mixture of phenol, catechol, and guaiacol standard with concentration of 0.6 mg/mL each, (b) mixture of phenol, catechol, 2 pentoses, 3 hexoses, and cellobiose standard with concentration of 0.67 mg/mL each 159
A-2	Derivation of sugars with PMP 160
A-3	Reductive amination of glucose (a) with reducing agent (b) without reducing agent 161

LIST OF FIGURES (continued)

FIGURE	PAGE
A-4 Reaction scheme of BSTFA with active proton	166
A-5 Reaction scheme of glucose derivatization by BSTFA (Method A)	166
A-6 Typical chromatogram from trimethylsilylation of glucose and cellobiose standard from 6 µg/mL glucose and 70 µg/mL cellobiose standard.	167
A-7 GC-MS chromatogram of standard 200 µg/mL glucose and 40 µg/mL cellobiose with different derivatization time (a) 3h (b) 1h	167
A-8 Calibration curve of glucose standard after derivatization by method A	168
A-9 Calibration curve of cellobiose standard after derivatization by method A .	168
A-10 GC-FID chromatogram of standard 200 µg/mL glucose and 40 µg/mL cellobiose (a) with hexane extraction (b) with dichloromethane extraction (c) in aniline solvent without extraction	169
A-11 Calibration curve of glucose standard after derivatization by method B	170
A-12 Calibration curve of cellobiose standard after derivatization by method B .	170
A-13 Chromatogram of the same sample injected in (a) GC-MS (b) GC-FID	171
A-14 GC-FID chromatogram of samples from base reaction after derivatization (a) without neutralization (b) neutralized with acetic acid (b) neutralized with oxalic acid	172
C-1 SEM micrographs of spruce at various magnification. Designation: (a) 200×; (b) 500×; (c) 1000×.....	186
C-2 SEM micrographs of water residues at various magnification. Designation: (a) 200×; (b) 500×; (c) 1000×.....	187
C-3 SEM micrographs of acid residues at various magnification. Designation: (a) 200×; (b) 500×; (c) 1000×.....	188

LIST OF FIGURES (continued)

FIGURE		PAGE
C-4	SEM micrographs of base residues at various magnification. Designation: (a) 200×; (b) 500×; (c) 1000×.....	189
C-5	SEM micrographs of A-A residues at various magnification. Designation: (a) 200×; (b) 500×; (c) 1000×.....	190
C-6	SEM micrographs of B-B residues at various magnification. Designation: (a) 200×; (b) 500×; (c) 1000×.....	191
C-7	SEM micrographs of B-A residues at various magnification. Designation: (a) 200×; (b) 500×; (c) 1000×.....	192
C-8	SEM micrographs of A-B residues at various magnification. Designation: (a) 200×; (b) 500×; (c) 1000×.....	193
C-9	SEM micrographs of A-B-A residues at various magnification. Designation: (a) 200×; (b) 500×; (c) and (d) 1000×.....	194

NOMENCLATURES

A	:	Single-Step Conversion by Oxalic Acid
A-A	:	Two-Step Conversion by Acid, Followed by Acid
A-B	:	Two-Step Conversion by Acid, Followed by Base
ABEE	:	p-Aminobenzoic Ethyl Ester
AEC	:	3-Amino-9-Ethylcarbazole
AFEX	:	Ammonia Fiber Explosion
Arap	:	Arabinofuranose
ASTM	:	American Society for Testing and Materials
B	:	Single-Step Conversion by Base (TMAH)
B-A	:	Two-Step Conversion by Base, Followed by Acid
B-B	:	Two-Step Conversion by Base, Followed by Base
BSTFA	:	Bis(trimethylsilyl)trifluoroacetamide
C	:	Carbon
C ₄ mim ⁺ Cl ⁻	:	1-n-Butyl-3-Methylimidazolium Chloride
CAS	:	Chemical Abstracts Service
CHP-Process	:	Combined Heat and Power Process
CPMAS	:	Cross Polarization-Magic Angle Spinning
DAD	:	Diode Array Detector
DB	:	Dry Basis
DCM	:	Dichloromethane
DMSO	:	Dimethyl Sulfoxide
DP	:	Degree of Polymerization
ESEM	:	Environmental Scanning Electron Microscope
FE-SEM	:	Field Emission Scanning Electron Microscope
FID	:	Flame Ionization Detector
FPU	:	Filter Paper Unit
Galp	:	Galactopyranose

NOMENCLATURES (continued)

GC	:	Gas Chromatography
GC-FID	:	Gas Chromatography Flame Ionization Detector
GC-MS	:	Gas Chromatography Mass Spectroscopy
Glup	:	Glucopyranose
Glup A.	:	Glucuronic Acid
H	:	Hydrogen
HHV	:	High Heating Value
HMDS	:	Hexamethyldisilazane
HMF	:	5-Hydroxymethylfurfural
HPLC	:	High-Performance Liquid Chromatography
JCPDS	:	Joint Committee on Powder Diffraction Standard
LFD	:	Large Field Detector
m/z	:	Characteristic Ion Masses
Manp	:	Mannopyranose
MS	:	Mass Spectroscopy
MW	:	Molecular Weight
N	:	Nitrogen
NIST	:	National Institute of Standards and Technology
NMMO	:	N-Methylmorpholine N-Oxide
NMR	:	Nuclear Magnetic Resonance Spectroscopy
NREL	:	National Renewable Energy Laboratory
O	:	Oxygen
OA	:	Oxalic Acid
P/L	:	Polysaccharide-to-Lignin
p-AMBA	:	p-Aminobenzoic Acid
PMP	:	1-Phenyl-3-Methyl-5-Pyrazolone
PNA	:	p-Nitroaniline

NOMENCLATURES (continued)

Py-GC-MS	:	Pyrolysis Gas Chromatography Mass Spectroscopy
RP-C ₁₈	:	Octadecyl Reversed-Phase Column
SEM	:	Scanning Electron Microscope
SHF	:	Separate Hydrolysis and Fermentation
SIC	:	Selective Ion Chromatogram
SSF	:	Simultaneous Saccharification and Fermentation
TCD	:	Thermal Conductivity Detector
TIC	:	Total Ion Chromatogram
THF	:	Tetrahydrofuran
TMA	:	Trimethylamine
TMAH	:	Tetramethylammonium Hydroxide
TMCS	:	Trimethylchlorosilane
TMS	:	Trimethylsilyl
TOSS	:	Total Suppression of Spinning Sidebands
UHP	:	Ultra High Purity
US	:	United State
UV	:	Ultra Violet
W	:	Single-Step Conversion by Water
XRID	:	X-ray Diffraction
Xylp	:	Xylopyranose

CHAPTER 1

INTRODUCTION

1.1 Motivation

Utilization of biomass has been considered a promising option to mitigate dependency on nonrenewable fossil resources such as petroleum. Among the renewable resources, biomass has received increasing attention because of their superior advantages. Biomass is the only foreseeable sustainable resource for energy, chemicals, materials, and food [1]. Being carbon dioxide negative or neutral, lignocellulosic biomass utilization will lead to lower greenhouse gases emission in a long run [2]. Furthermore, biomass is reliable in term of availability and environmental friendliness. Last but not least, biomass processes encourage local resource exploitation and employment.

The first generation of fuels and chemicals from biomass was developed based on sugars, starches, and vegetable oils [3]. Sugars and starches are easily converted into ethanol via fermentation. Vegetable oils are an energy-intensive part of biomass, which can be converted to biodiesel via transesterification of triglycerides from oils [4]. These first-generation technologies have been proven and implemented worldwide. The limited availability of these energy-storage parts of biomass can only alleviate dependency on fossil fuel to some extent [5]. Moreover, the availability of such feedstocks is still in debate for food supply and fertile land shortage [3] and their uses for bio-fuels have been partially linked to price increase of food in the US during 2007-2008 [6]. In addition, sugar and starch crops require significant amounts of fertilizers and pesticides during cultivation, which in turn release additional greenhouse gases such as N_2O and CO_2 [7]. Some studies based on

life-cycle analysis indicate that the production of bioethanol from corn has higher net CO₂ emission than lignocellulosic biomass; the estimated net emission of corn ethanol ranged from -52% to 3% relative to gasoline, while cellulosic bioethanol has the lowest negative result of -86% [7]. Therefore, utilization of lignocellulosic biomass will play an important role in the future. Its high yield per unit area and wide availability promote exploitation while still maintain biodiversity. In order to further promote biomass utilization, lignocellulosic biomass should be used as a sustainable feedstock for production of bio-energy, fuels, chemicals, and materials.

Several initiatives are now focusing on production and utilization of bio-based fuel, chemicals and materials [8-12]. The support of the first-generation bioenergy was already implemented through government regulations and tax incentives such as those in Brazil, the European Union, and the United States. Thailand has initiated replacement of conventional gasoline and diesel with at least 10% ethanol and biodiesel blending by 2012. Specifically, ethanol from domestic feedstock has been prioritized to drive the local ethanol production [8, 9]. It is estimated that, by 2020, up to 20% of nonrenewable fuels consumption worldwide could be replaced by biofuels [9]. For the second-generation technology initiatives, the Department of Energy in the United States has an initiative for conversion of lignocellulosic material to bioproduct, referred to any product generated from biomass that would otherwise be produced from fossil fuel. The target was set to produce 35.6 billion pounds of bioproducts by 2020, and 55.3 billion pounds by 2030 [10].

Research on lignocellulosic biomass conversion has been conducted for more than two decades. However, the commercialization of lignocellulosic biomass conversion is still in an infant stage. Due to these concerns, challenges, and encouragements, it is very desirable to explore the possibility to utilize lignocellulosic biomass in new, effective and simple ways.

1.2 Composition and Structure of Lignocellulosic Biomass

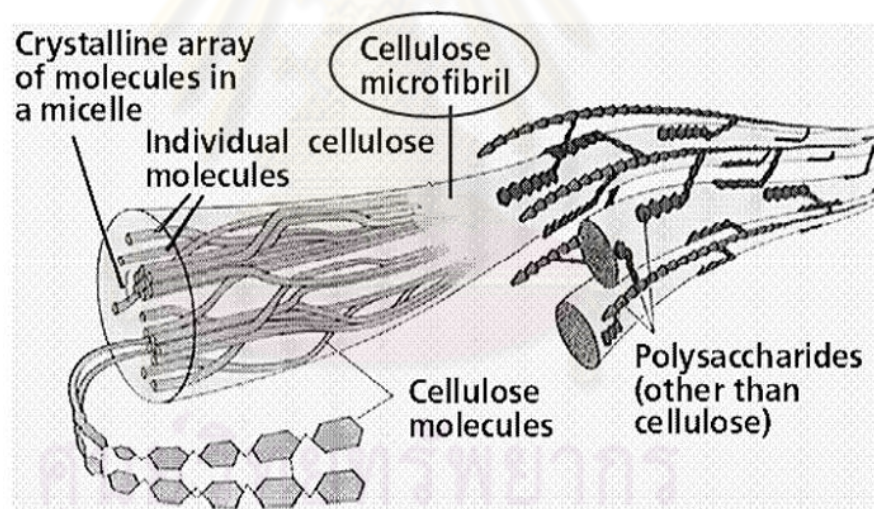
Lignocellulosic biomass is the most abundant biomass resource available. In term of energy, biomass has a capability to provide energy as much as $6-10 \times 10^{15}$ Btu (1 Btu = 1.055 kJ), 64% of which can be contributed from wood and wood wastes, followed by municipal solid waste (24%), agricultural waste (5%), and landfill gases (5%) [13]. However, only 2% of lignocellulosic biomass is currently utilized by humans, mainly for heat production, building construction, paper industry, and textile industry [14].

Lignocellulosic wood is a complex composite material consisting mainly of cellulose, hemicellulose, and lignin bonded to each other in its cell wall [15]. Other trace components such as extractives containing structural proteins, lipids and ash also exist to a minor extent. Typical constituents of wood and summary of their roles are shown in Table 1.1 [16]. The three main components in wood-cellulose, hemicellulose, and lignin are reviewed in this chapter. Cell wall is the major component in woody biomass, with mass percentage as much as 95% [16]. There are two types of cell wall: primary and secondary cell wall as shown in Figure 1.1. Each cell is separated by middle lamellae consisting primarily of lignin. The cell wall divides into primary and secondary wall, and the secondary wall further divided into S1, S2, and S3. The S2 layer is the thickest layer influencing overall cell wall thickness. Relative thickness for each layer of primary wall: S1: S2: S3 is 1: 10-22: 40-90: 2-8 [16]. From Figure 1.1, the lines in the secondary wall represent microfibrillar alignment which is parallel in each layer of the secondary wall, whereas the microfibrils in the primary wall are arranged without specific direction. Figure 1.2 shows that cellulose microfibrils are embedded in an amorphous matrix of hemicellulose and lignin. Lignin is located mainly on the outside of the microfibrils and forms covalent bonds to hemicellulose.

Table 1.1 Chemical constituents of wood [16].

	Wt.%	Polymeric nature	DP*	Molecular building blocks	Role
Cellulose	45-50	Linear, Crystalline	5,000-10,000	Glucose	Framework
Hemicellulose	20-25	Branched, Amorphous	150-200	Primarily non-glucose sugars	Matrix
Lignin	20-30	Three-dimensional	100-1,000	Phenylpropane	Matrix

* DP = degree of polymerization

**Figure 1.1** Schematic structure of plant cell walls [17].

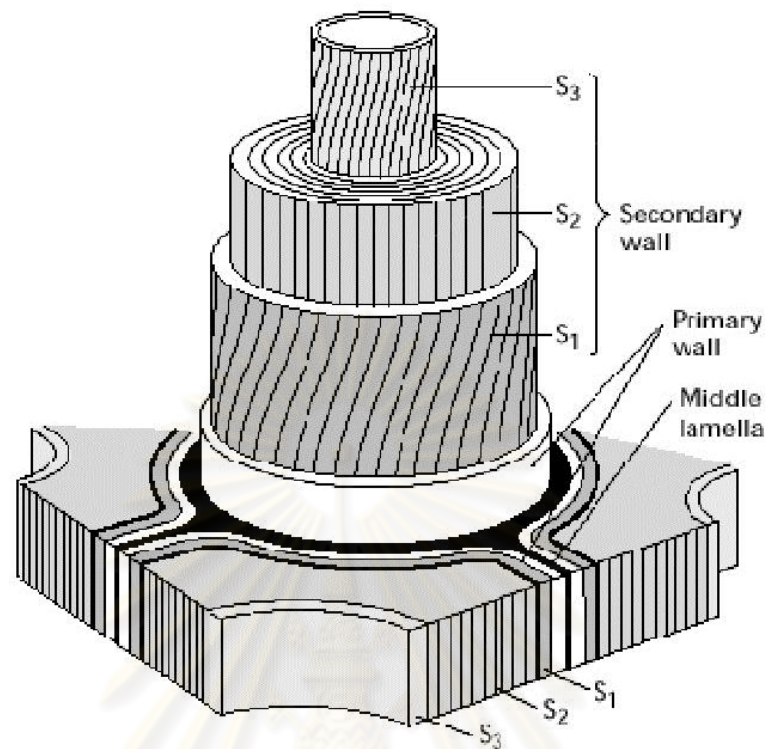


Figure 1.2 Schematic representation of cellulose microfibrils [17].

Woods from tree are categorized into softwoods and hardwoods. Both are in the same spermatophyte division. Softwoods are the common name representing gymnosperms subdivision. Softwoods are also referred as conifer or evergreen. Hardwoods are the common name for angiosperms. The hardwoods contain both vessel and fiber in order to conduct water and support structure of the tree. The softwoods contain dual functional cell called tracheid to do both water conduction and supporting roles. Leaves retention of these types of trees is also different. Softwoods hold their leave all year long, while hardwoods shred the leaves annually [16].

1.2.1 Cellulose

Cellulose is the most abundant organic polymer in the world. Its content in both softwoods and hardwoods is normally in the range of $42\pm 2\%$, making cellulose the main component in wood [16]. Cellulose is a linear homopolysaccharide of D-glucopyranose with β -(1,4) glycosidic linkages with a degree of polymerization of approximately 10000 for wood [18, 19]. In supramolecular level, cellulose structure in wood was recognized as Fringe fibrillar model for coexisting of highly and low ordered regions, known as crystalline and amorphous cellulose [20]. The crystalline form of cellulose in wood is mainly cellulose I_{β} . The monomer of cellulose is anhydroglucose or glucose. The repeating unit of cellulose is called anhydrocellobiose or cellobiose, which compose of two glucose units coupling with 180° rotated to each other, shown in Figure 1.3. This rotation leads to symmetrical hydroxyl groups of the cellulose chain. The structure of each cellulose chain is completely linear. Association of cellulose chains in parallel direction forms a microfibril. Each microfibril is composed of 36 cellulose chains and organized into 8 sheets, stabilized by hydrogen bond interactions [21, 22].

The cellulose chain end has two different structures: non-reducing end, and reducing end, as shown in Figure 1.3. The non-reducing end is terminated with C4-OH group, whereas the reducing end is terminated with C1-OH group. The non-reducing ends have closed ring structure, while the reducing ends can reversibly change its conformation between aliphatic structure with aldehyde group and cyclic hemiacetals structure [21].

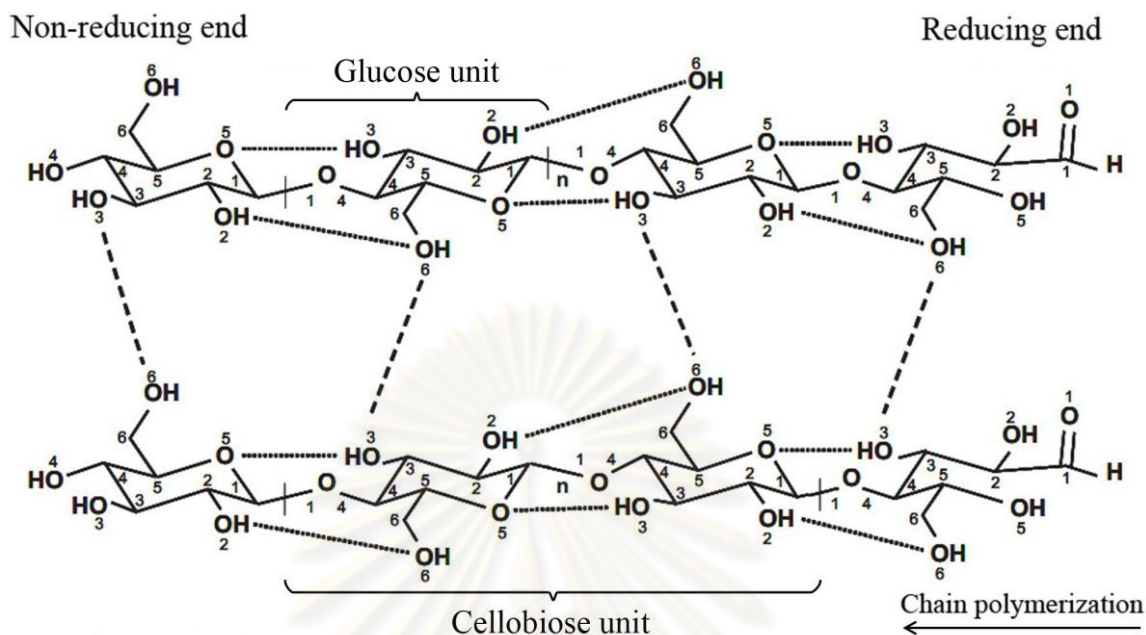


Figure 1.3 Structure of cellulose I and its inter- and intra-chain hydrogen bonding pattern. Dashed lines: interchain hydrogen bonding. Dotted lines: intrachain hydrogen bonding [21].

The hydroxyl groups in cellulose lead to hydrogen bonds which give rise to crystalline structure of cellulose. The hydrogen bonds in cellulose chains are classified as intrachain, interchain and intersheet. The intrachain and interchain hydrogen bonds are referred to the hydrogen bonds between neighboring hydrogen and oxygen of the same chain, and that between neighboring hydrogen and oxygen of different chains in the same sheet, respectively. These intermolecular hydrogen bonds are responsible for strength of cellulose and stabilize the two-fold helix conformation of crystalline cellulose [23]. Both interchain (mainly O6-H---O3 and O3-H---O6) and intrachain hydrogen bonds (O3-H---O5, O5-H---O3, O2-H---O6, and O6-H---O2) cause cellulose chains to pack in parallel to each other, and contribute to crystalline structure [17, 24, 25]. The dominant intrachain hydrogen bond is O3-H---O5. This hydrogen bond is responsible for the rigid, linear shape of the single cellulose chain by limiting the rotation of glucose units around the glycosidic linkages [26]. The

hydrogen bonding also considered as a primary factor that controls physical resistance to acid hydrolysis [27]. Interchain hydrogen bonds are also important in maintaining the structural integrity of cellulose [28]. Comparing between two interactions, intrachain bonds are more stable than interchain hydrogen bonds [22].

The intersheet interactions involve numerous C-H-O contacts and van der Waals interactions connect between neighboring sheets in a microfibril. The C-H-O interaction is reported as pseudo-hydrogen bonds due to its electrostatic energies. In cellulose I_{β} , there are 12 types of intersheet C-H-O pseudo-hydrogen bonds. Average number of hydrogen bonds for each glucose monomer inside cellulose microfibrils is descending as follows: intersheet \gg intrachain $>$ interchain. Therefore, based on both number and energy of interactions, this intersheet interaction is considered to be the main mechanism against deconstruction of the cellulose [22].

Although congested with hydroxyl groups, this unique structure favors construction of the polymer chains into tightly packed arrangements that are water insoluble [16]. Cellulose solubility decreases dramatically with increasing degree of polymerization as a consequence of hydrogen bond networks [19]. This highly order and stable structure causes cellulose to become highly resistant to hydrolysis [29]. Comparing two types of glucose polymer, cellulose is more than 100 times difficult to hydrolyze than starch [30].

Cellulose I has two crystalline structures: monoclinic unit cells for cellulose I_{β} , and triclinic unit cells cellulose I_{α} [31, 32]. Cellulose I_{β} is a more common form existed in cotton, wood and ramie fibres, whereas cellulose I_{α} is enriched in some algae and bacterial cellulose. Cellulose I_{β} has higher number of intersheet interactions than cellulose I_{α} [22]. More intersheet interaction in cellulose

I_{β} is consistent with higher stability of cellulose I_{β} that cellulose I_{β} is thermodynamically more stable as I_{α} irreversibly converts to I_{β} by heating [33].

Since the major functional group of cellulose is the hydroxyl group, cellulosic materials are hygroscopic. Hydroxyl groups have a strong affinity to polar solvents. Interaction of hydroxyl groups with polar solvents leads to swelling of the cellulose. For example, water can swell cellulose. The adsorbed moisture swells the cellulose, but does not change the crystalline structure of cellulose [16]. A similar phenomenon is observed with other polar solvents.

1.2.2 Hemicellulose

Hemicellulose is a branched amorphous heteropolymer of mainly xylose, arabinose, mannose, galactose, and glucose. Hemicellulose forms hydrogen-bond to cellulose microfibrils establishing a network that provides the structural backbone to plant cell wall [29]. Hemicellulose is found to have covalent linkages with lignin from several findings of lignin-carbohydrate complex [34-36]; however, the nature of the linkage is still uncertain. Presumably, there are more than one types of linkage associated in the lignin-carbohydrate complex. Hemicellulose also forms hydrogen-bond to lignin via hydroxyl and carbonyl groups of hemicelluloses and hydroxyl, carbonyl, and etheric oxygen of lignin.

In softwoods, the dominating hemicelluloses are partially acetylated galactoglucomannans called O-acetyl-galactoglucomannan with about 20 w/w% of the dry wood as shown in Table 1.2. Softwood O-acetyl-galactoglucomannan was reported to have an approximate degree of polymerization between 100 and 150, equivalent to a MW around 16,000–24,000. It has a backbone of β -(1→4)-D-mannopyranose and β -(1→4)-D-glucopyranose with α -(1→6)-D-galactopyranose and O-acetyl side-groups attached to the mannose as shown in Figure 1.4 [37]. The ratio

of galactose: glucose: mannose is reported to be 1:1:3, but there is also a fraction where the ratio is 0.1:1:3 [38]. The glucose: mannose ratio for white spruce (*Picea glauca*) is found to be 1:3 [39]. Presented in smaller amount, arabino-4-O-methylglucuronoxylan is also existed with 7-15 w/w% of the dry wood. The structure, shown in Figure 1.5, consists of a framework of β -(1 \rightarrow 4)-D-xylopyranose chain which is partially attached with 4-O-methyl- α -D-glucuronic acid at C-2 position. There is also α -L-arabinofuranose directly linked to C-3 of the xylose. The distribution of the acid and arabinose side chains is not known. Ratio of glucuronic acid: xylose is 1: 5-6. Ratio of arabinose: xylose is approximately 1:8 [38, 40].

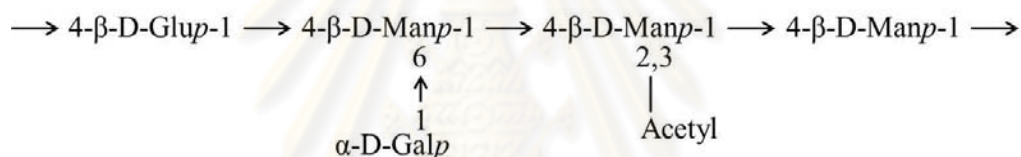


Figure 1.4 Simplified structural formula of softwoods hemicellulose O-acetyl-galactoglucomannan [38, 40]. Sugar units: Glup (Glucopyranose); Manp (Mannopyranose); Galp (Galactopyranose).

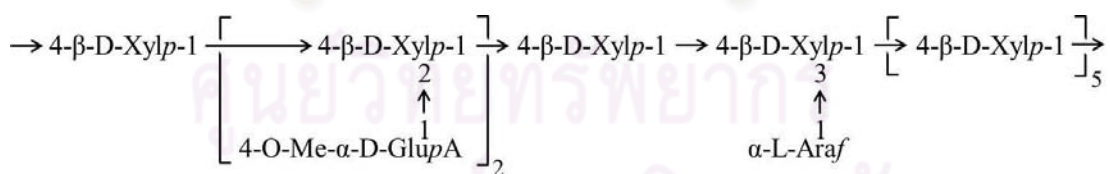


Figure 1.5 Simplified structural formula of softwoods hemicellulose arabino-4-O-methyl-glucuronoxylan [38, 40]. Sugar units: Xylp (Xylopyranose); Glup (Glucopyranose); Arap (Arabinofuranose).

Table 1.2 Chemical compositions of representative softwoods [38]*.

	White spruce	Balsam fir	Eastern White Pine	Eastern hemlock	Eastern white cedar
Cellulose	41	42	41	41	41
Hemicellulose					
O-acetyl-galacto-glucomannan	18	18	18	16	12
Arabino-4-O-methyl-glucuronoxylan	13	9	9	7	14
Lignin	27	29	29	33	31
Pectin, starch, ash, etc.	1	2	3	3	2

*All values are reported as percent of extractive-free wood.

Hemicelluloses in hardwoods are predominated by partially acetylated xylan called O-acetyl-4-O-methyl-glucuronoxylan with some extent of glucomannan. The amount of O-acetyl-4-O-methyl-glucuronoxylan varies with hardwood species in the wide range of 15-35% as shown in Table 1.3; for example, white birch contain as much as 35 % of this hemicellulose, while american elm has only 20 %. O-acetyl-4-O-methyl-glucuronoxylan structure consists of approximately 200 units of β -(1 \rightarrow 4)-D-xylopyranose, linked together by glycosidic bonds. Some of the xylose units carry a single, terminal side chain consisting of a 4-O-methyl- α -D-glucuronic acid, attached to the C-2 position of the xylose. About 70% of the xylose units attach to an O-acetyl group at C-3 position as shown in Figure 1.6. Therefore, the structure of this hemicellulose in hardwood is slightly branched. Hardwoods also contain 3-5% of a glucomannan. Ratio of glucose: mannose is ranged between 1:2 and 1:1, depending on the hardwood species. The polysaccharide consists of (1 \rightarrow 4)-linked β -D-glucopyranose and β -D-mannopyranose monomers as shown in Figure 1.7. Since

this hemicellulose is easily degraded during isolation, the complete structure of this glucomannan may be linear or slightly branched with acetyl group [38, 40].

Table 1.3 Chemical compositions of representative hardwoods [38]*.

	White birch	Red maple	American beech	Trembling aspen	American elm
Cellulose	42	45	45	48	51
Hemicellulose					
O-acetyl-4-O methyl- glucuronoxylan	35	25	26	24	19
Glucomannan	3	4	3	3	4
Lignin	19	24	22	21	24
Pectin, starch, ash, etc.	1	2	4	4	2

*All values are reported as percent of extractive-free wood.

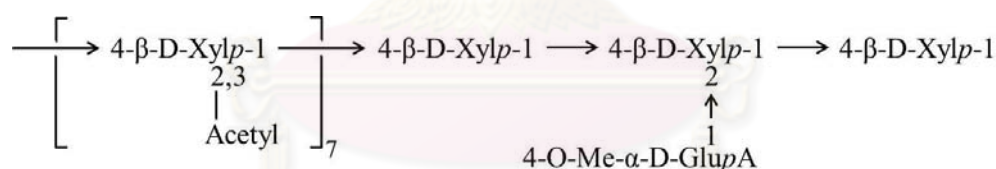


Figure 1.6 Simplified structural formula of hardwoods hemicellulose O-acetyl-4-O-methyl-glucuronoxylan [38, 40]. Sugar units: Xylp (Xylopyranose); GlupA (Glucuronic acid).



Figure 1.7 Simplified structural formula of hardwoods hemicellulose glucomannan [38, 40]. Sugar units: Glup (Glucopyranose); Manp (Mannopyranose).

1.2.3 Lignin

Lignin is a major noncarbohydrate component in the cell wall. It is a complex cross-linked three-dimensional polymer of phenylpropane units with different degree of methoxy groups. These phenolic units make lignin hydrophobic. The cross-linked three-dimensional network acts as glue and provides rigidity to cell wall. The lignin content in typical hardwood varies in the range of 18- 25 %, while the range is 25- 35 % in typical softwood [38]. The distribution of lignin in cell wall is mainly in the secondary cell wall and middle lamella, approximately 70-80%, and 15-30% of the total lignin in wood, respectively [16]. There are three lignin precursors: p-coumaryl, coniferyl, and sinapyl alcohol (also known as 4-hydroxyphenyl, guaiacyl, and syringyl monomer, respectively). The chemical structures of these precursors are shown in Figure 1.8.

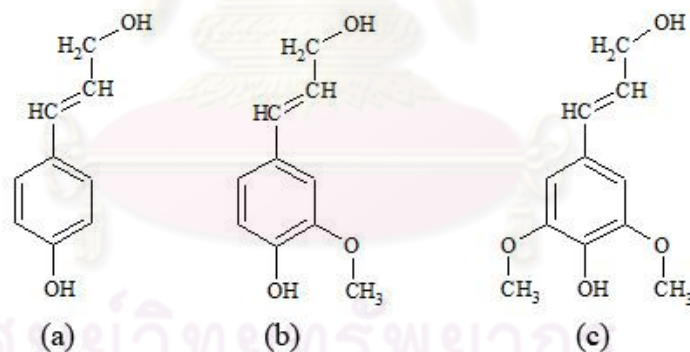


Figure 1.8 Structures of lignin precursors. (a) p-coumaryl alcohol; (b) coniferyl alcohol; (c) sinapyl alcohol.

Lignin precursors are linked by several types of bonds. The dominant bonds in lignin are shown in Figure 1.9. These links have been discovered by identification of lignin dimers and oligomers degradation products [41]. Estimated amount of these bonds in milled wood lignin of spruce (softwood) and birch (hardwood) are shown in Table 1.4.

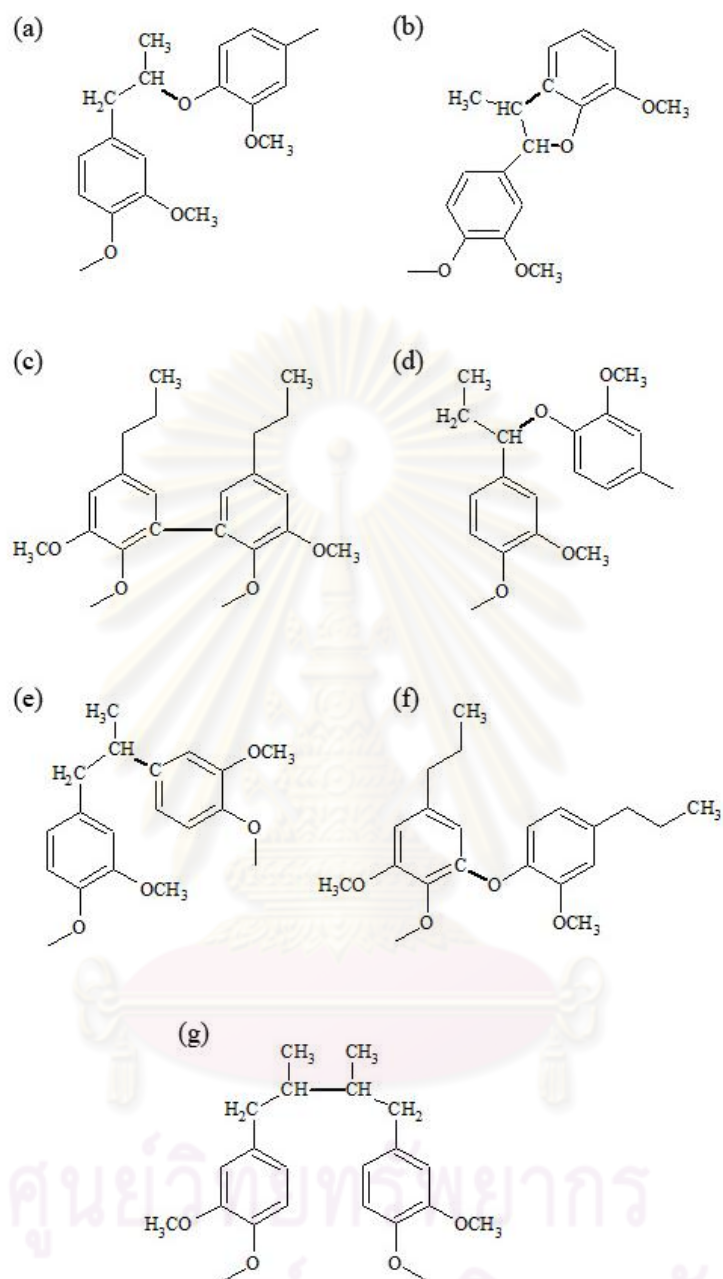


Figure 1.9 Common linkages between phenylpropane units in lignin [40]. Linkages: (a) β -O-4; (b) β -5; (c) 5-5; (d) α -O-4; (e) β -1; (f) 4-O-5; (g) β - β .

Table 1.4 Percentages of linkages in milled wood lignin from spruce and birch [40].

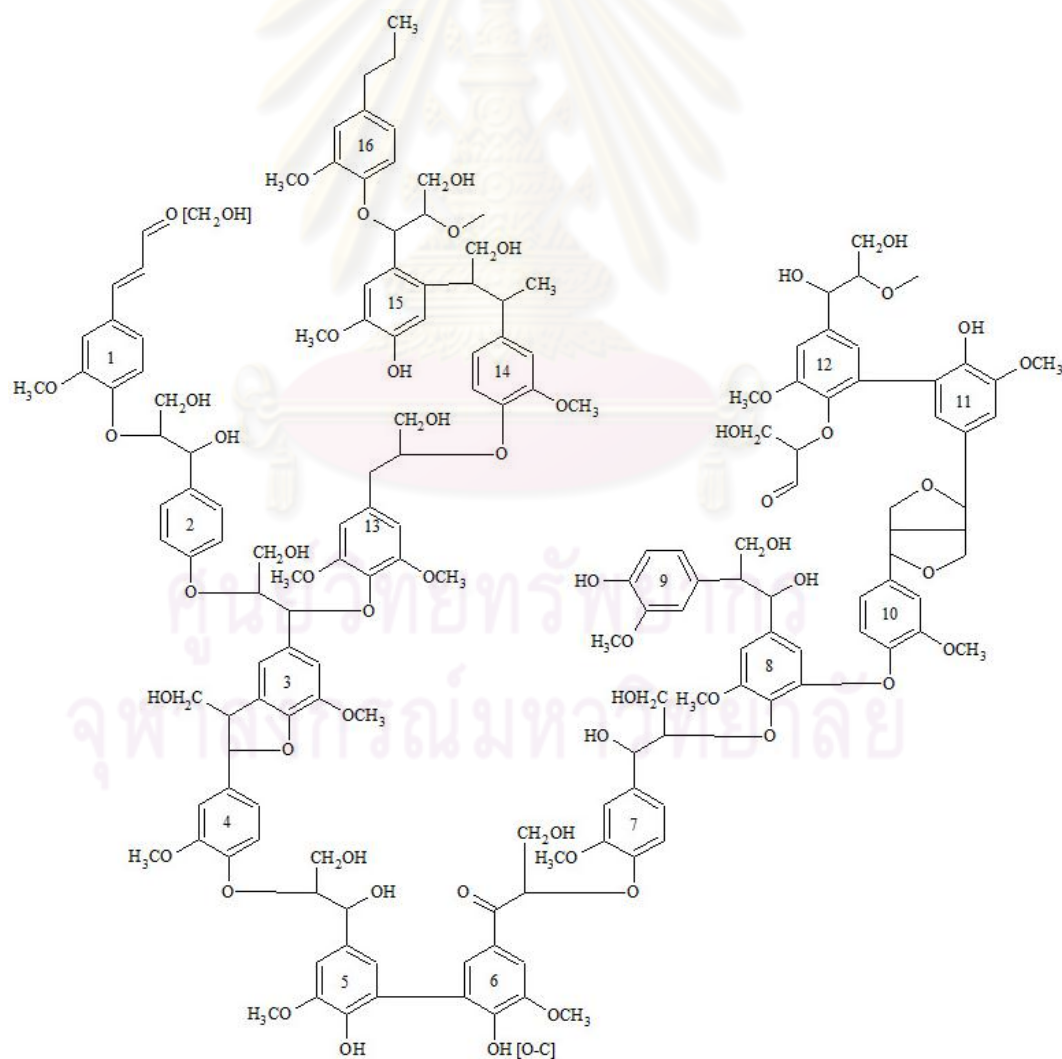
Linkage types	% of lignin in spruce	% of lignin in birch
(a) β -O-4 (Arylglycerol- β -aryl ether)	48	60
(b) β -5 (β -aryl)	9-12	6
(c) 5-5 (biphenyl)	9.5-11	4.5
(d) α -O-4 (Noncyclic benzyl aryl ether)	6-8	6-8
(e) β -1 (β -aryl)	7	7
(f) 4-O-5 (Diphenyl ether)	3.5-4	6.5
(g) β - β (β - β linked structure)	2	3

The main linkage in lignin is ether bond, dominated by β -O-4. The other bonds are carbon-carbon bonds such as β -5, 5-5, β -1, and β - β . In softwoods, the abundance of β -O-4 linkage is approximately in the range of 45-50% (corresponding to 45-50 linkages per 100 C₉ units). For hardwoods, amount of β -O-4 linkage is associated with number of syringylpropane units, whose content depends on species of hardwood. Therefore, the β -O-4 linkage of hardwoods varies with the species [16].

There are several functional groups in lignin including 4-O-alkyl, 4-O-aryl, methoxyl, aliphatic and aromatic hydroxyl groups, and carbonyl groups. Typical amount of functional groups in spruce and birch lignin are shown in Table 1.5.

Table 1.5 Functional group of lignin in spruce and birch (per C₉ units) [40].

Functional group	Spruce lignin	Birch lignin
Methoxyl	92-96	139-158
Phenolic hydroxyl	15-30	9-13
Benzyl alcohol	15-20	-
Noncyclic benzyl ether	7-9	-
Carbonyl	20	-

**Figure 1.10** Important structure of softwood lignin derived from spruce [42].

Lignin in its native state is referred to as protolignin. The exact structure of protolignin remains uncertain. For spruce, a representative scheme of lignin showing its main units and linkages is shown in Figure 1.10.

Lignin can be categorized into many groups according to the lignin structure. Guaiacyl lignin is the term used for polymerization product of coniferyl alcohol. This type of lignin is found in almost all softwoods. Guaiacyl-syringyl lignin is a copolymer of coniferyl and sinapyl alcohols with the ratio of coniferyl to sinapyl alcohol varies depending on the plant species. This latter type of lignin is normally found in hardwoods [16, 40].

1.3 Traditional Second Generation Processes for Biomass

Processing technologies for biomass can be defined into several groups, for example, the first-, second-, and third-generation processes. The first-generation processes involve conversion of energy-storage parts of biomass or employ conventional processes. Examples of the first-generation processes are transesterification of vegetable oils for the production of methyl ester or biodiesel, sugars and starch fermentation for bioethanol, anaerobic fermentation of biomass residues for biogas, combustion of organic materials for heat, and combined heat and power systems for the production of heat and electricity (CHP process). The first-generation technologies have been developed commercially.

Compared with the first-generation biofuels processes, the development of technology for second-generation processes, which involve conversion of lignocellulosic biomass, is still in an early stage. These technologies are expected to be able to handle wider range of feedstocks which are not competitive with other demands. Examples of the second-generation technologies are gasification

for syngas production, pyrolysis and liquefaction of biomass for bio-oil, enzymatic conversion of lignocellulosic biomass to ethanol, etc. These processes need further technical development and are still in an early stage of commercialization or not yet commercialized in a large scale. The third-generation technologies are defined as the processes of algae conversion. However, only an overview of major lignocellulosic biomass conversion technologies will be introduced here.

The conversion of lignocellulosic materials is related to the so called biorefinery concept, defined as a processing facility in which multiple products are coproduced from biomass feedstocks [12, 43]. Instead of focusing only on biofuels, research on the conversion of agricultural and forestry feedstocks to other valuable consumable products - such as plastics, textiles or detergents - are developed under this concept to maximize economical effectiveness. The key utilization of lignocellulosic materials is depolymerization of lignocelluloses into smaller molecules that can be used or further converted to intermediate platform chemicals [30].

The major weakness in chemical processing of lignocellulosic biomass is that it is not possible to disintegrate lignocellulose components without changing their chemical structures, neither on a technical nor on laboratory aspect. Many factors contribute to this difficulty including covalent and hydrogen bonds among and/or between each components, the macromolecular structure of cellulose and lignin. The chemical linkages between lignin and hemicelluloses hinder their separation. Three dimensional crosslinked structure of native lignin makes it insoluble in any solvent. Therefore, the lignin has to be partially degraded to lower molecular weight fragments that are soluble in the solvent and covalent bonds between lignin and hemicelluloses has to be cleaved in order to separate lignin from wood. However, the problem is that under the conditions needed for such degradation, condensation reactions in lignin also occur, which counteract the degradation. On the other hand, it

is not possible to dissolve unchanged cellulose from wood without dissolution of lignin [44]. The nature of this complex, recalcitrant composite leads to difficulties in biomass conversion. It is concerned as a fundamental bottleneck for production of fuels from renewable sources [22]. Therefore, the most challenging problem of lignocelluloses conversion is to break down the structure efficiently.

There are three conventional routes of thermochemical lignocellulose conversion as outlined in Figure 1.11. It should be noted that there are also several other processes for lignocellulosic biomass conversion which are not included in this overview such as subcritical conversion, hydrothermal conversion, and other biological processes.

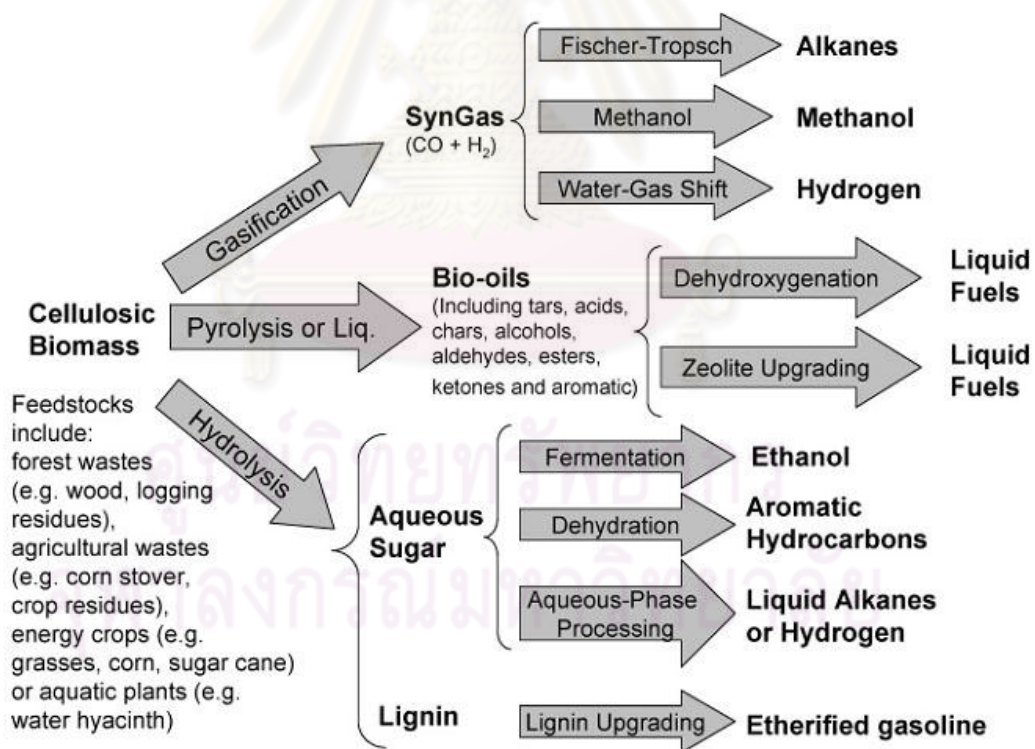


Figure 1.11 Conventional processes for production of fuels from lignocellulosic biomass [18].

1.3.1 Gasification

Gasification involves thermal partial oxidation of the biomass in order to convert it into gaseous products called synthesis gas or producer gas, which is a carbon monoxide, hydrogen, carbon dioxide, methane and nitrogen gas mixture. Small amounts of char and ash are also produced. Composition of the synthesis gas depends heavily on gasification process, gasifying agent, and the feedstock composition [45]. Gasification of wood occurs at approximately 800-1000 °C [46]. Gasification pressure ranges from normal (0.1-0.12 MPa) to high pressure (0.5-2.5 MPa). Various gasifying agents are air, oxygen, steam, CO₂ and combination of them. The heat provided in the process could be either direct (from biomass oxidation) or indirect (from external supply) [47]. The process of gasification takes place as follows. Surface and inherent moisture is evaporated first at 110-120 °C. Biomass begins to exothermically decompose at 200-300 °C to CO, CO₂, H₂ and H₂O. Then, the temperature is raised further during biomass volatilization. The volatile matter from lightweight hydrocarbons is transformed into heavy hydrocarbon, which is further gasified to gas. During this stage, tar and soot may form if insufficient gasifying agent is provided and the hydrocarbon condenses. The tar produced during gasification is one of the major problems in gasification of biomass [45]. After that, fixed carbon and ash become char, and the char is heated to provide the heat to the process. The subsequent reaction with the gasifying agent transforms the carbon into CO and CO₂ [47]. Several reactions such as decomposition, reduction, and oxidation take place during gasification [48]. Gasification is considered as an expensive process because of technological restrictions related to low conversion efficiencies, and logistic constraints. Conversion efficiencies up to 50% may be obtained for integrated gasification/combined gas–steam cycles [49].

1.3.2 Pyrolysis and Liquefaction

Biomass pyrolysis is defined as the thermal degradation of biomass in the absence of oxygen [50, 51]. Rates of pyrolysis for hemicelluloses, cellulose, and lignin are different and they also proceed via different mechanisms and pathways [51]. Hemicellulose is rapidly degraded before cellulose within a very narrow temperature range, while lignin is decomposed over a wide range due to its stability [51, 52]. The biomass pyrolysis can be categorized into three groups: conventional pyrolysis (carbonization), fast pyrolysis, and flash pyrolysis. These processes are differentiated by operating temperature, heating rate, residence time, required biomass size, and main products (char, bio-oil, and gaseous products) [51, 53, 54]. During the pyrolysis, the heat is transferred rapidly to biomass and causes volatilization releasing volatiles and forming char. The volatiles may contact the low-temperature zone in reactor and condense to tar. Quenching of volatiles leads to formation of liquid product [51]. Maximum liquid yields can be obtained from fast pyrolysis at reaction temperatures around 500 °C with high heating rates and short vapour residence times, typically 1 s, to minimize secondary reactions [52]. At these conditions, biomass decomposes to mostly vapours, aerosols and some charcoal. A dark brown liquid bio-oil is obtained from cooling and condensation of vapours and aerosols, with the maximum yields up to 80 wt% of dry feed [52]. In fast pyrolysis, very high heating and heat transfer rates is important [50]. To maximize heat transfer rate, finely ground biomass feedstock with less than 10 wt% water is required [52]. Bio-oil production requires very short vapour residence time by rapid cooling to minimize secondary reactions, but it also leads to incomplete depolymerisation of the lignin resulting in a less homogenous liquid product [52].

The bio-oil produced from fast pyrolysis is a complex homogenous hydrophilic mixture of oxygenated polar organics (about 75-80 wt%), with moisture

content ranged from 15-30 % [50, 52, 55]. Moisture in bio-oil is derived from the original moisture in the feedstock and generated by dehydration during pyrolysis and storage [55], so bio-oil always contains at least about 15% water [52]. There are more than 300 oxygenated compounds identified in bio-oil [55]. By analysis of bio-oils, it contains many types of oxygenated compounds such as cyclopentanone, methoxyphenol, acetic acid, methanol, acetone, furfural, phenol, formic acid, levoglucosan, guaiacol and their alkylated phenol derivatives [53]. Oxygenated compounds in bio-oil are not only diverse but also high in number, leading to low energy density, immiscibility with conventional fuels, and instability of bio-oil due to acidic compounds [52, 55]. Bio-oil is very thermally unstable; it starts to polymerize at 80-90 °C [56, 57]. Instability of bio-oil was observed during storage; the viscosity and molecular weight of bio-oil increases significantly as well as phase separation [57]. Acidity is responsible for bio-oil corrosive behavior, which becomes more severe at elevated temperature and adds requirements on construction materials [55]. Due to highly corrosive property and low heating value of bio-oil, it is not a good fuel for heat and power generation [58].

Biomass liquefaction is a thermochemical process with low temperature and high pressure operation for production of liquid organic products. The process parameters of liquefaction in comparison with pyrolysis are summarized in Table 1.6.

Table 1.6 Comparison of biomass liquefaction and pyrolysis [11, 59].

Process	Pyrolysis	Liquefaction
Temperature (°C)	450-550	150-420
Pressure (atm)	1-5	1-240
Resident time	1-2 sec	10-60 min
Drying	Necessary	Unnecessary
Solvent	Unnecessary	Necessary
Products properties		
Moisture (wt%)	15-30	5
pH	2.5	-
Specific gravity	1.2	1.1
Viscosity (cP)	40-100 (at 50 °C)	15000 (at 61 °C)
Elemental composition (wt%)		
C	54-58	73
H	5.5-7	8
O	35-40	16
N	0-0.2	N/A
Ash	0-0.2	N/A
HHV (MJ/kg)	16-19	34

Conventional direct liquefaction processes normally operated in hot compressed water or organic solvents such as acetone and anthracene oil alcohols (methanol, ethanol, propanol and butanol). Typical liquid products yields are usually in the range of 20–60 %, depending on process parameters such as temperature, pressure, residence time, solvents and catalysts employed. Catalysts are normally used in liquefaction, especially alkaline solution such as Na_2CO_3 , NaOH , K_2CO_3 , KOH ,

LiOH, RbOH, CsOH, and Ca(OH)₂. The function of catalysts is to minimize char formation and maximize liquid products yield [58].

1.3.3 Enzymatic Hydrolysis

Enzymatic hydrolysis is a biological process for conversion of polysaccharides into monomeric sugars. It is well developed and regarded as an effective way to hydrolyze cellulose to monosaccharides [60]. Enzymatic hydrolysis occurs in aqueous systems with pH range of 4-5, temperature range of 45–55 °C, with a concentration of cellulosic substrate between 1 and 10 %, and the amount of enzyme protein at the 1 % level of the substrate [23, 61]. Cellulase dosage of 10–30 FPU/g cellulose is often used in laboratory-scale research because high yield was obtained within reasonable time (48–72 h) and enzyme cost [60]. Enzymes for cellulose hydrolysis are called cellulases, which are produced from certain types of fungi and/or bacteria. Multienzyme system with at least three major enzymes groups, namely endo-glucanase, exo-glucanase and β-glucosidase, shows synergistic actions in catalyzing the cellulose hydrolysis [23, 60]. Endo-glucanase enzyme attacks cellulose fiber at the low crystallinity regions and creates free chain-ends. Exo-glucanase enzyme further cleaves the cellulose by removing cellobiose units from the free chain-ends. The cellobiose is then fragmented to glucose by the β-glucosidase [60].

In native biomass, the enzymatic digestibility of cellulose by enzyme is less than 20 % yield. There are several factors that hinder hydrolysis of biomass by enzyme. There is no final conclusion on which factors is the major contribution to slow hydrolysis of different lignocellulosic materials [62]. These factors have been categorized into two groups: factors related to the substrate structure and factors related to the mechanism and interactions of the enzymes [62], although there might

be some other classifications [60]. Those factors related to substrate structure are structural features of cellulose, cellulose crystallinity, degree of cellulose polymerization, accessible surface area, heterogeneous character of biomass structure, and protection of cellulose by lignin and hemicellulose [29, 63, 64]. For examples, lignin hinders hydrolysis by limiting the accessibility of the cellulose and by irreversibly binding with the enzymes [64]. Substrate concentration also affects initial rate and yield of hydrolysis at high substrate concentration [65]. The factors related to mechanism and interactions of enzymes include enzyme activity, enzyme adsorption, formation of enzyme-substrate complexes, interaction between the cellulose and the cellulases, nature of the cellulases, reaction conditions, end-product concentrations, and the inhibition effects [60, 63, 66].

Because of the above limiting factors to enzymatic hydrolysis, conversion of lignocelluloses by biological process using enzymes requires pretreatment of the substrate in order to disrupt lignin and hemicellulose barriers so that hydrolytic enzymes can penetrate to cellulose [67]. The resulting surface and porosity increase enhances enzymatic digestibility. The pretreatments involve physical, physicochemical, chemical and biological processes. Physical pretreatment are comminution (dry, wet, vibratory ball milling, or compression milling), steam explosion, and hydrothermolysis. An example of physicochemical pretreatment is ammonia fiber explosion (AFEX). Examples of chemical pretreatment are acid and alkali pretreatment, where H_2SO_4 and NaOH are the most common reagents for acid and alkali, respectively. However, pretreatment is one of the most expensive steps [18]. Furthermore, there is no single pretreatment that could meet all the requirements for enzymatic hydrolysis [60]. In addition, the enzymatic hydrolysis is a time-consuming process [60]. Enzymatic hydrolysis usually takes several days, whereas acid hydrolysis takes a few min. The enzymes for hydrolysis are still expensive [68]. Enzymatic hydrolysis is also susceptible for inhibition by several substances that

produced as by-products of pretreatment [68, 69]. Simultaneous saccharification and fermentation (SSF) was studied to solve the problem posted by a separate hydrolysis and fermentation (SHF). In SSF, the glucose is simultaneously produced and consumed to avoid inhibition by secondary products. Because the optimal temperatures of the hydrolysis and fermentation are different (45-55 °C and 30 °C), it is difficult to maximize the products [68]. Enzymatic hydrolysis of lignocellulosic materials is the most common method that has been studied for hydrolysis of lignocelluloses to produce bioethanol. However, large-scale commercialization of lignocellulosic bioethanol plant has not been implemented yet [70].

1.3.4 Acid Hydrolysis

Acid hydrolysis involves cleavage of polysaccharides in biomass into their monomer units using acid as a reagent. The main hydrolysis product from cellulose is glucose, while the hydrolysis of softwood and hardwood hemicelluloses yields mainly mannan and xylose, respectively. The typical acid widely used for acid hydrolysis is sulfuric acid (H_2SO_4) [60]. Other acids such as hydrochloric acid (HCl), phosphoric acid (H_3PO_4) were also investigated for acid hydrolysis of biomass [71]. Due to the small size of the acid, it can readily penetrate into the biomass pore structure, so the pretreatment is not required. Also, the rate of acid hydrolysis is faster than that by enzyme. However, the liberated glucose can degrade under severe acidic conditions [71]. There are two acid hydrolysis processes: concentrated acid, and diluted acid.

For concentrated acid hydrolysis, 10-30 % sulfuric acid is generally used. This method needs lower temperature and pressure, but longer time than diluted acid hydrolysis. An optimized concentrated hydrolysis could give about 80% sugars yield based on theoretical value by using 26 % H_2SO_4 for 2 h, after the 30 min mixing

time at 100 °C [72]. Lignin is reported to be mostly insoluble in mineral acid. However, concentrated acid hydrolysis consumes large amounts of acid and energy. The costs for corrosion-resistant material and acid recovery are also their disadvantages [73, 74].

In diluted acid hydrolysis, moderate conditions are used for hemicellulose liberation, while the hydrolysis of cellulose requires more severe conditions. Typically, sulfuric acid of 0.5-5 % concentration is used. Temperature is in the range of 120-180 °C or may be up to 230 °C. High pressure at about 10 atm is also used [60, 69]. The diluted acid hydrolysis was developed to overcome drawbacks on concentrated acid hydrolysis. However, when low concentration acid is used, the high temperature is required. This is a general trend for acid hydrolysis [69, 75].

A two-step acid hydrolysis was also explored. Choi and Mathews [76] studied diluted acid hydrolysis of several low-grade biomass samples including softwood from lumber processing. H₂SO₄ and HCl were used in their two-step batch process to obtain improved yields of hemicellulose in the first step, and cellulose in the second step. Optimum conditions were obtained with H₂SO₄ as the reagent at condition 2% H₂SO₄, 132 °C, 40 min in the first step, and 15% H₂SO₄, 132 °C, 70 min in the second step. The glucose and xylose yield in g/g wood was 0.026 and 0.266, respectively, in the first step, and 0.099 and 0.066, respectively, in the second step [76]. The two-step acid hydrolysis is also used in determination of carbohydrates in wood [77-80].

Xiang et al. [24] studied hydrolysis of commercial α -cellulose by H₂SO₄. The first series was conducted in the temperature range of 185-245 °C using 0.07 % H₂SO₄. Hydrolysis of cellulose is represented by the first-order rate kinetics. There is a sudden increase of the activation energy near 215 °C indicating the kinetic

behavior of cellulose is strongly dependent on physical state of the cellulose. Below 215 °C, the cellulose is in crystalline form. Above 215 °C, the physical state of cellulose changes resulting in the change in kinetic behavior of cellulose. This work also presented the two-step hydrolysis by varying acid concentration in the pretreatment step at 25 °C for 4 h before dilution to 4 % for hydrolysis in the second step at 120 °C. Acid concentration below 60 % did not affect the subsequent hydrolysis in the second step. When cellulose was pretreated with acid concentration of 65 % or higher, most of the cellulose was dissolved and some portion was reprecipitated after dilution. The reprecipitated cellulose was hydrolyzed at about the same rate as starch suggesting that the pretreatment of cellulose with concentrated acid changes physical structure of cellulose as reaffirmed by XRD and SEM of reprecipitated cellulose. This behavior required less concentration of acid at higher pretreatment temperature. The state of hydrogen bonding of cellulose was believed to correspond to the resistance in cellulose hydrolysis [24].

Hydrolysis of lignocellulosic biomass by hot-compressed, subcritical and supercritical water has also been investigated by several researchers [81-84]. Cellulose, hemicellulose, and lignin were studied separately in the initial stage; however, the results are different from the actual biomass suggesting the difference is due to interaction between biomass components. Condition at 270 °C, 2 min, with addition of mineral acid was optimized. In addition to fast hydrolysis rate in subcritical water, the degradation of glucose was also rapid.

Organic acid has been considered for hydrolysis of biomass. Dapía et al. [85] studied hydrolysis of beech wood by 80 % formic acid at 110-130 °C, 60-140 min. About 90 % of hemicellulose was hydrolyzed. The hydrolysis is very specific to hemicellulose, leaving about 98% of cellulose remaining as a pulp. In addition, 80-90% of lignin is delignified at the same time. In another work by Sun et al., 78 %

formic acid was combined with 4 % HCl to hydrolyzed cellulose at optimized condition: 75 °C, 7 h. Approximately 13% of glucose was obtained. High temperature accelerates hydrolysis of cellulose as well as degradation of hydrolysis products. Rate of degradation is faster than hydrolysis and becoming more pronounced at high temperature [75].

Hydrolysis of wood by oxalic acid was rarely studied. It was reported as a diffusible proton donor for enzymatic and non-enzymatic hydrolysis of polysaccharides in lignocelluloses [86]. Kenealy et al. studied vapor-phase pretreatment of wood chip with diethyl oxalate, which decomposed readily by combination of water and heat to oxalic acid and ethanol. Vapor-phase reaction leads to high concentration of acid for hydrolysis at 140 °C, 30 min. Oxalic acid was found to specifically hydrolyzed hemicellulose in both softwood and hardwood [87].

1.3.5 Kraft Pulping

As for the delignification by base reagents, two general alkaline pulping processes are sulfate (Kraft), and sulfite process. The Kraft pulping process is the most well-known process in papermaking industry. In this process, the lignin and hemicelluloses are cleaved from lignocellulosic substrate by mixture of alkaline solution, leaving the cellulosic fibers for paper. The aqueous solution of sodium hydroxide (NaOH) and sodium sulfide (Na_2S), or white liquor, is reacted with the wood chips at about 170 °C for several hours. Delignification takes place during the process. Lignin macromolecule is fragmented into smaller water/alkali-soluble molecules, primarily through the cleavage of β -aryl ether bonds in phenolic aryl-propane units. Only minor portion of carbon-carbon linkages are cleaved during the pulping process. In a conventional softwood kraft pulping, 95-96 wt% of lignin is removed [88]. The main reactions in delignification by Kraft pulping are shown in

Figure 1.12-1.14 [89]. Hydrosulfide ion is a stronger nucleophile than hydroxide ion and plays an important role in nucleophilic addition to the lignin structure.

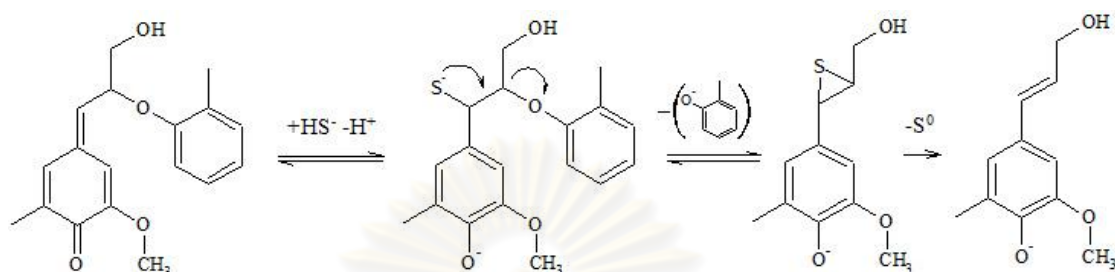


Figure 1.12 Sulfidolytic cleavage of β -aryl ether bond in lignin phenolic units [89].

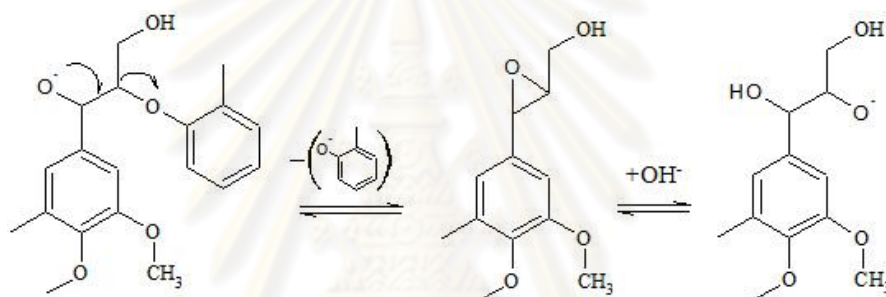


Figure 1.13 Alkaline cleavage of β -aryl ether bond in lignin non-phenolic units [89].

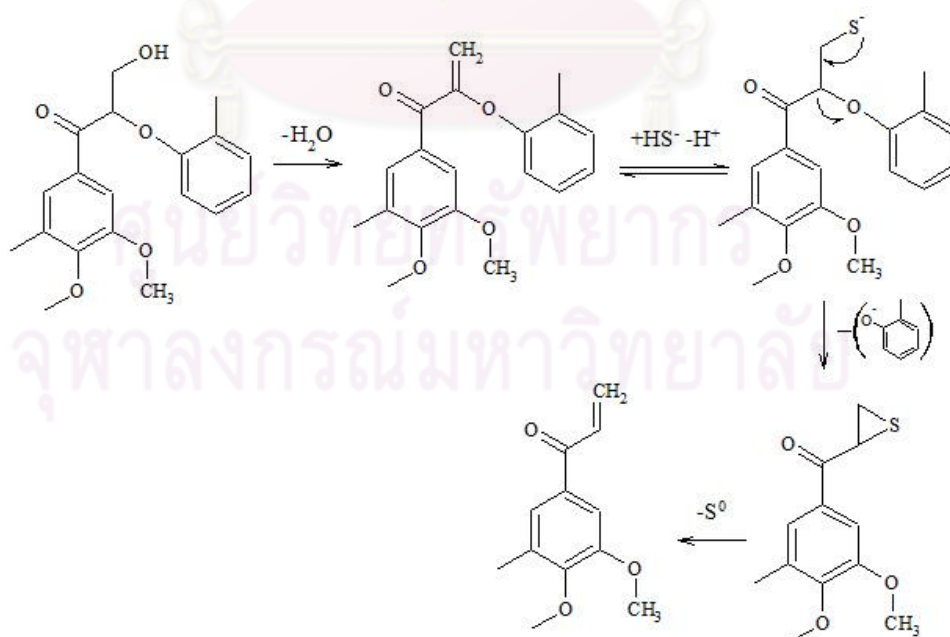


Figure 1.14 Sulfidolytic cleavage of β -aryl ether bond in lignin non-phenolic units with α -carbonyl group [89].

1.3.6 Organosolv Pulping

Organosolv pulping process involves delignification of wood which relies on chemical break down and modification of lignin until molecules in lignin become small and soluble in reaction medium. A variety of organic solvents have also been examined in order to improve the Kraft pulping process. Mixtures of alcohol-water are the most widely used solvents in organosolv pulping [90, 91]. In organosolv pulping, the cleavage of ether bonds plays a major role. For acidic conditions, α -aryl ether bonds are very easy to cleave, while β -aryl ether bonds are also subjected to cleave to some extent. In alkaline organosolv process, α -aryl ether bonds with free phenolic group are readily cleaved, while the β -aryl ether bonds is dominantly occurred similar to the Kraft process [92].

As mentioned earlier, organic acids such as formic acid and acetic acid are also investigated for organosolv delignification [90, 93-97], where both hemicellulose hydrolysis and delignification occur during the processes [90, 93]. Hydrolysis of hemicellulose and degradation of monomers in acetic acid organosolv pulping occurs in the same fashion as the conventional acid hydrolysis [93]. Comparative study suggests that formic acid is a better delignifying agent than acetic acid [96]. Formic acid was reported to effectively penetrate into the interior pore of the cellulose fiber, breaking down the cellulose crystalline structure and facilitating the hydrolysis in both amorphous and crystalline regions of cellulose [75]. No significant difference was found between eucalyptus sawdust and chip in formic acid and HCl delignification [90, 91]. High concentration (80-90 %) of formic acid is usually employed at very mild condition of 90-130 °C, 60-180 min, with or without some HCl as a catalyst [85, 90, 91]. In general, hardwoods are delignified faster and more selectively than softwoods due to differences in β -ether bonds reactivity, α -ether concentration, lignin content, and propensity to undergo condensation reactions [92].

1.4 Proposing a New Process for Biomass Conversion

Although biomass conversion has been studied for several decades, it is highly desirable to study new methods for more effective conversion of lignocellulosic biomass into more valued and utilizable forms. A new hydrolysis strategy was proposed and explored using a combination of organic acid and base treatments to convert lignocellulosic biomass under mild conditions. This process was proposed based on fundamental hypothesis of acid and base functions in conversion of lignocellulosic biomass. Since acid and base have been known to preferentially disrupt different main targets in biomass, a combination of acid and base should alternately access different wood components in the recalcitrant structure of biomass to liberate the cellulosic and lignin monomers. For example, base may be responsible for cleavage of lignin in the first step. Then, acid may hydrolyze polysaccharides more easily in the second step, and vice versa.

This work uses organic acid and base as alternative of conventional mineral ones. The organic agents are preferred since they are more environmentally friendly and require much less safety precautions than the conventional mineral acid and base such as H_2SO_4 , NaOH , etc. [98]. For example, neutralization of H_2SO_4 produce large amount of gypsum [74], while its thermal degradation could produce SO_x [99]. Oxalic acid, or ethanedioic acid, is naturally occurring as a secondary metabolite of wood rotting fungi [86, 100, 101]. Degradation of oxalic acid results in organic substances such as CO_2 , and H_2O [102, 103], which are not contaminating the products. Tetramethylammonium hydroxide (TMAH) is an organic base which has been used in methylation of lignin for analysis by pyrolysis-gas chromatography technique [104-112]. TMAH can be effectively used for pulping process [113, 114]. Decomposition of TMAH can be achieved by thermal treatment to TMA (trimethylamine), followed by selective oxidation to N_2 , CO_2 , and H_2O [115].

1.5 Reactions of Biomass by Acids and Bases

1.5.1 Hydrolysis by Acid

The mechanism of acid hydrolysis of glucose is presented in Figure 1.15. The hydrolysis is initiated by proton from acid interacting rapidly with glycosidic oxygen at ether bond between glucose monomers of cellulose. The interaction forms a conjugated acid. Then, the C-O is cleaved and the conjugated acid breaks down to carbonium ion forming half-chair conformation at this stage. Finally, rapid addition of water causes liberation of free sugar and proton [24]. The mechanism of hemicellulose hydrolysis was proposed in analogous to the cellulose hydrolysis [116].

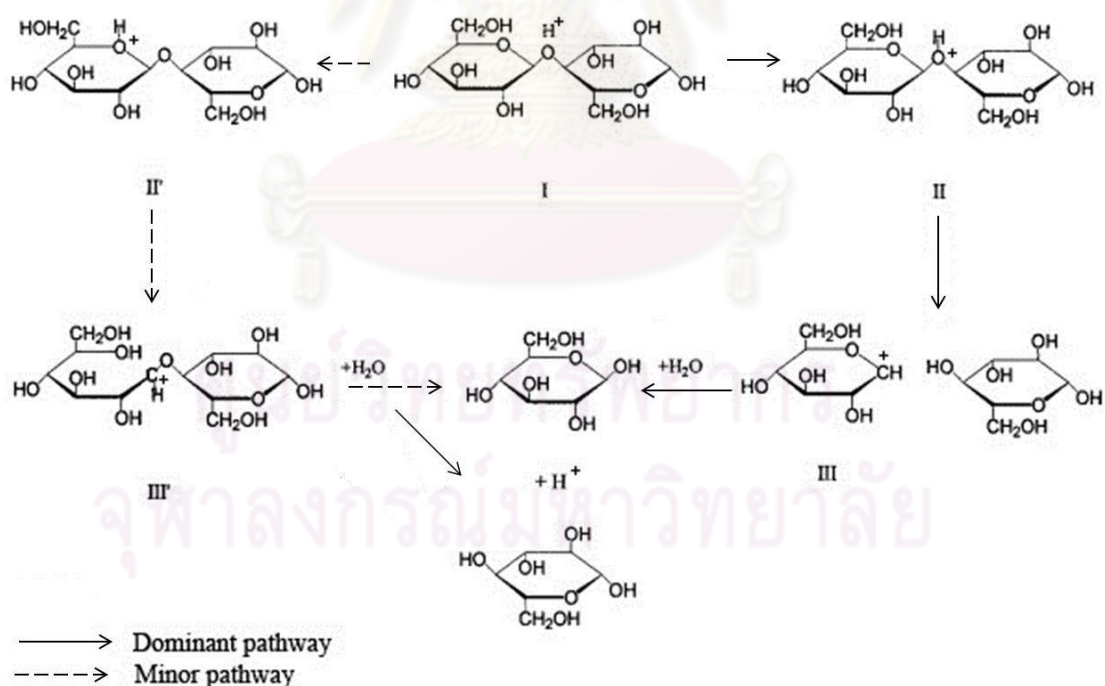


Figure 1.15 Mechanism of acid hydrolysis of cellulose [24, 117].

Acid hydrolysis of cellulose is defined as heterogeneous reaction because it is depending on physical characteristic of the cellulose [24]. Homogeneous acid hydrolysis can finally degrade cellulose into monomers, while heterogeneous hydrolysis in diluted acid levels off at a macromolecular level, approaching the level-off degree of polymerization [23]. Total heterogeneous lignocelluloses acid hydrolysis without recondensation and/or degradation of the monomers needs several treatments and condition optimization [23].

In acid hydrolysis processes, the liberated sugars can further be degraded by secondary reactions. Pentoses and uronic acid are degraded to furfural. Hexoses are degraded to 5-hydroxymethylfurfural (HMF), levulinic acid, and formic acid. Although these secondary products are not desirable for cellulosic ethanol production, where enzyme hydrolysis and fermentation are required to convert cellulose to ethanol, furfural is commercially manufactured by dilute sulfuric acid [29]. Hemicellulose is hydrolyzed to xylose and further broken down to form furfural. Although the degradation products are not desired in enzymatic hydrolysis and fermentation, they are considered as valuable chemicals. For example, HMF is produced by decomposition of fructose and has been studied by several methods [118-122]. Production of HMF from cellulose was also investigated recently [123].

Mechanism of hexose degradation to HMF and levulinic acid was proposed by Horvat et al. [124], as shown in Figure 1.16. HMF is formed through dehydration of liberated glucose and can be further degraded by rehydration to form levulinic acid and formic acid.

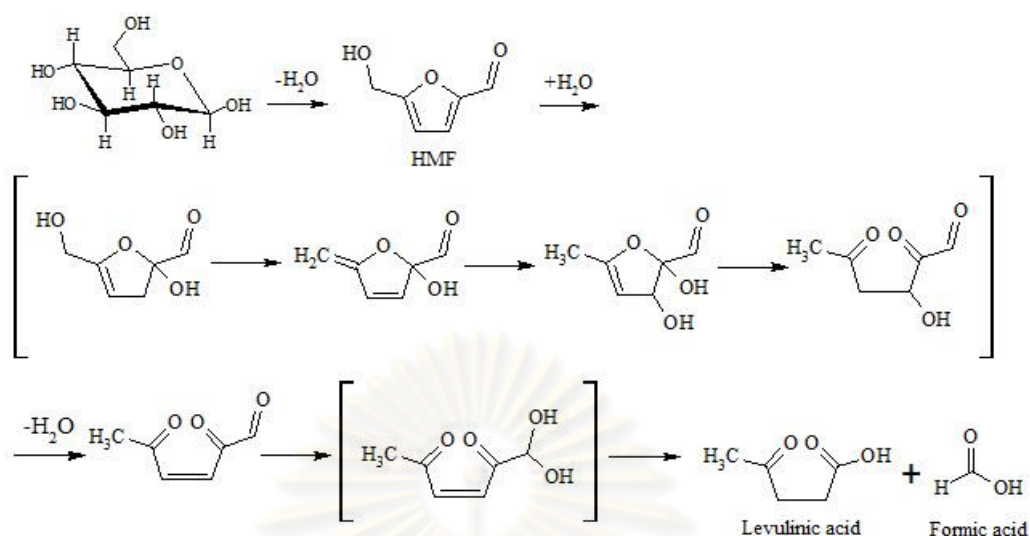


Figure 1.16 Mechanism of HMF and levulinic acid formation via secondary reactions of glucose [124].

Mechanism of furfural formation from pentose is shown in Figure 1.17 [116]. Protonation at hydroxyl group causes dehydration by dissociation of C-O bond. The C=C double bonds are formed when the positively charged carbon share two electrons from the neighboring carbon. The proton is released from the positively charged carbon then migrates within the molecule and protonates other hydroxyl group. Liberation of the second water molecule causes another C=C. Finally, the two double bonds in the molecule cause a planar structure and facilitate ring formation.

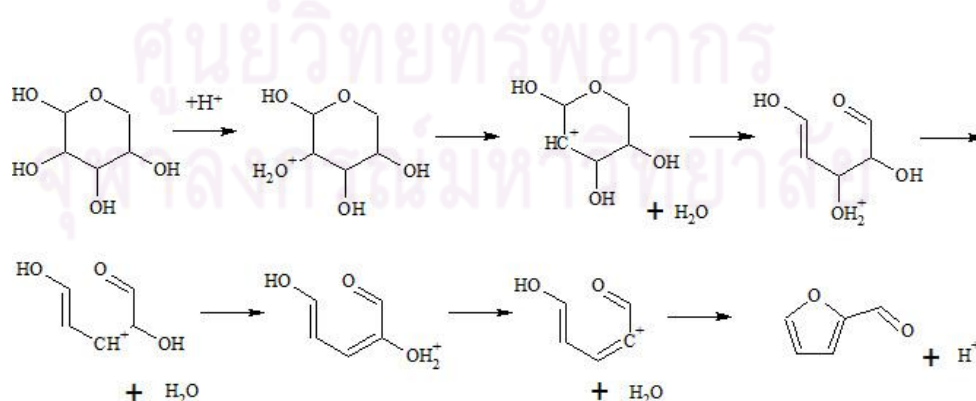


Figure 1.17 Mechanism of furfural formation via secondary reactions of pentose [116].

1.5.2 Cleavage of Lignin Bonds by Acid

Acid delignification mainly cleaves α -aryl ether bonds via three reaction paths as shown in Figure 1.18. The first path involves formation of quinone methide intermediate. The second path is a nucleophilic substitution facilitated by acid. The third path is a direct cleavage of the ether bond with formation of benzyl carbocation. The β -aryl ether bond may cleave during acid delignification with strong acid, and is more important in hardwoods than softwoods.

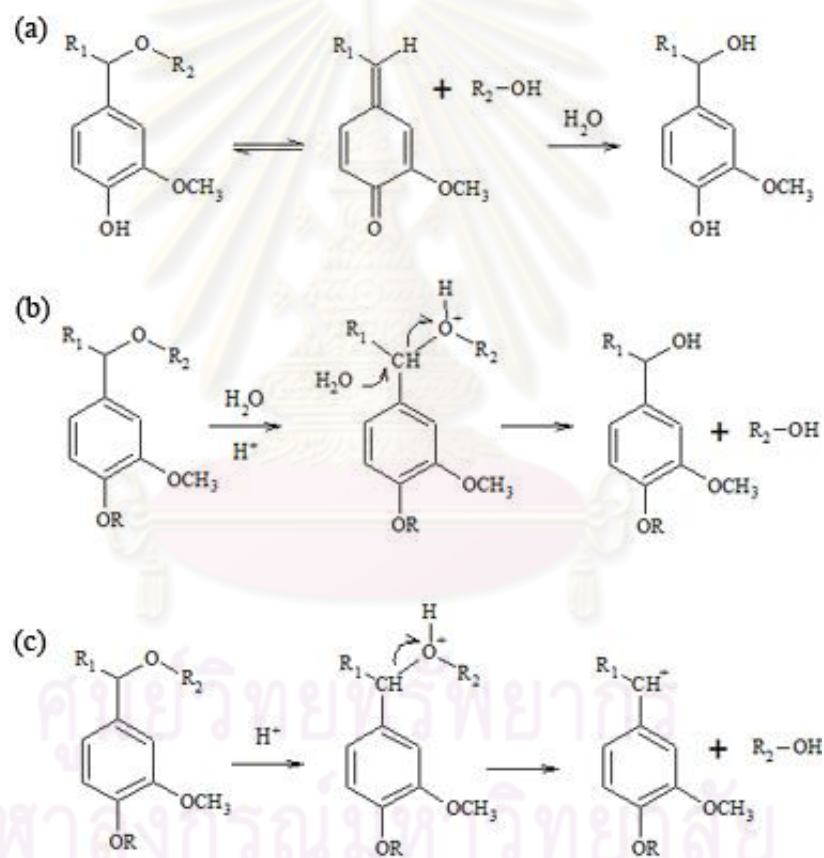


Figure 1.18 Reaction in acid delignification of α -aryl ether bonds in lignin via (a) quinone intermediate, (b) nucleophilic substitution, (c) formation of benzyl carbocation [92].

1.5.3 Lignin Cleavage by Base

The reaction of lignin bonds cleavage in TMAH can be described based on a study of TMAH thermochemolysis in lignin model [125], analogous to mechanism in alkali pulping. The main reaction path is shown in Figure 1.19. Cleavage of β -aryl ether bond by TMAH proceeds through intramolecular epoxide formation at α - and γ -carbon. The protonation at α - and γ -hydroxyl group yields 2 alkoxy salt intermediates. Then, nucleophilic displacement by α - or γ -alkoxide anion leads to formation of epoxide intermediates and cleavage of β -aryl ether bond. Other ether bond such as 4-O-etherified cinnamyl alcohol and aldehyde end groups was also reported to be cleaved by TMAH [126]. TMAH is also a methylating agent for hydroxyl groups of lignin. Methylation of phenolic hydroxyl groups partially occur by TMAH at the temperature as low as 100 °C, but complete methylation depends on chemical structure of the phenolic-containing samples [113].

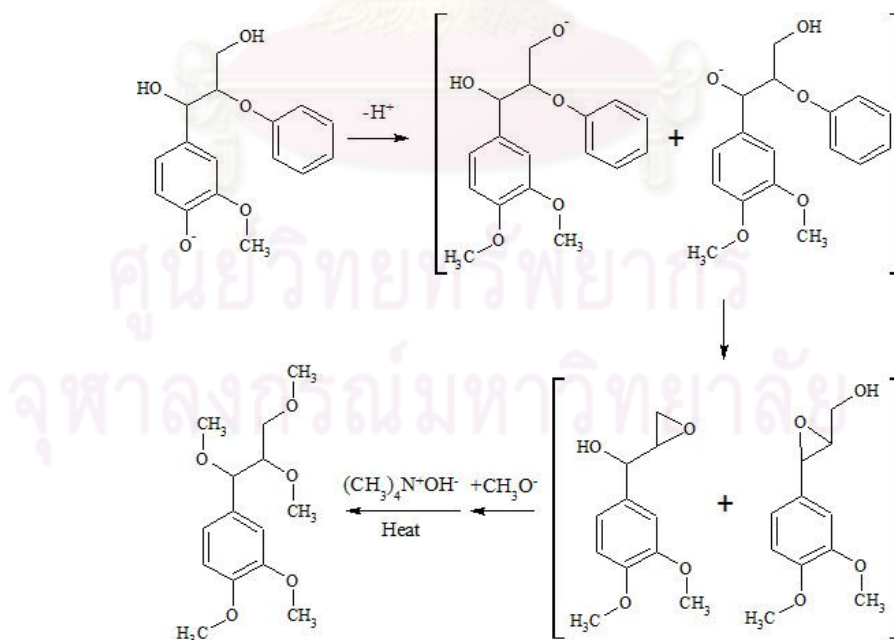
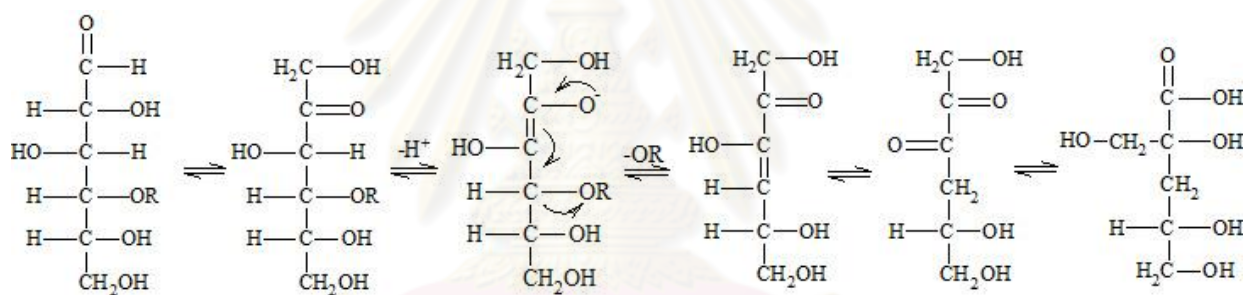


Figure 1.19 Thermochemolysis cleavage of β -aryl ether bond in lignin phenolic units [125].

1.5.4 Peeling Reaction by Base

Peeling reaction occurs at the reducing end of carbohydrates with an endwise mechanism [23, 40, 127, 128] via several reactions including isomerization, keto-enol isomerization, cleavage of glycosidic bond, keto-enol tautomerization, and rearrangement, as shown in Figure 1.20.

The stepwise peeling reaction occurs from temperature approximately 100 °C. Above 150 °C the macromolecules are mainly cleaved by alkaline hydrolysis resulting in new reducing end groups. The stepwise peeling can be stopped by a competing reaction, with formation of alkali-stable end unit [23].



R = Cellulose attached to the reducing end

Figure 1.20 Alkaline peeling of cellulose [40].

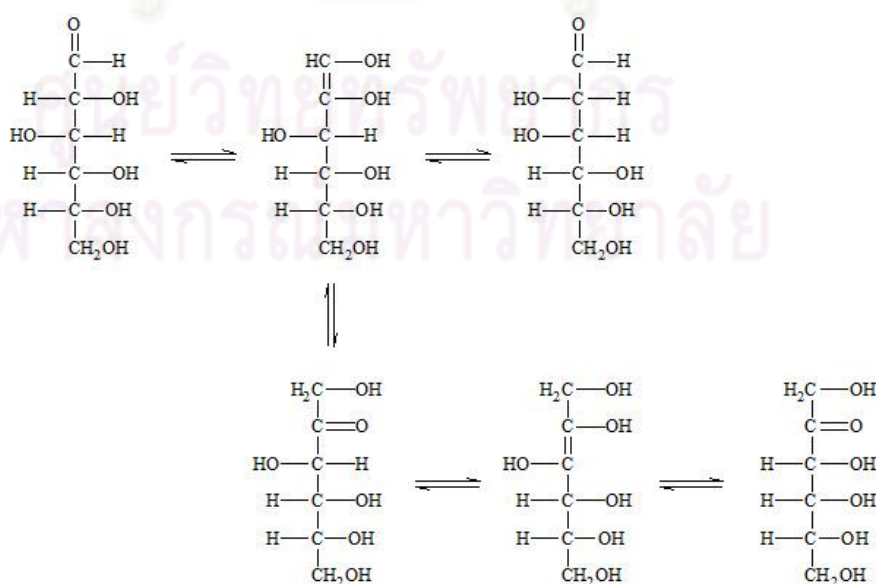


Figure 1.21 Rearrangement of aldose and ketose in alkaline medium [40].

In alkali environment, aldose and ketose sugars also subject to rearrangement, as shown in Figure 1.21.

1.6 Objectives and Scope

The specific objective of this work is to explore a new concept of sequential combination of oxalic acid and tetramethylammonium hydroxide treatments for converting lignocellulosic biomass, specifically wood, into valued-added chemical feedstocks such as fermentable sugars, furanic compounds, and phenolic compounds. The synergistic effects of the process need to be identified and the causes that lead to the synergy are needed to be clarified. This study is intended to propose a new process employing combination of acid and base for conversion of lignocellulosic biomass. The representative types of organic acid and base used in this study were chosen based on fundamental knowledge of typical acid and base reaction with biomass.

Chapter 1 introduces the background and objectives of the thesis and discusses the relevance and importance of the work by providing a general review of the lignocellulosic feedstocks and the typical processes of lignocellulosic conversion. The information on reactions occurred during conversion by both acid and base is also surveyed. Experimental procedures, conditions, and analytical techniques used in the study are described in Chapter 2.

The initial work of bio-oil upgrading is reported in Chapter 3. A bio-oil sample from biomass pyrolysis experiment at the University of Mississippi was received through a third party and was used in initial catalytic upgrading study. Several commercial catalysts were used for testing. The characterization of liquid product from the reaction was performed. However, the problem of stability of bio-oil during storage and solid formation during the reaction leads to study on bio-oil model

made of chemical mixture. The work in this chapter formulated an idea to develop a new process using mild condition to convert biomass.

Initiation of using sequential combination of acid and base to convert woody biomass is presented in Chapter 4. Spruce was used as a feedstock for two-step reaction by oxalic acid and TMAH. Characterization of the products were carried out using several analytical techniques including gas chromatography (GC) equipped with mass spectrometry (MS) and flame ionization detector (FID), pyrolysis gas chromatography mass spectroscopy (Py-GC-MS), and solid state nuclear magnetic resonance spectroscopy of carbon-13 (^{13}C -NMR). The analytical results indicate an existence of synergy by acid followed by base treatment.

Chapter 5 presents the study towards understanding of synergistic conversion in the aspect of physical properties of biomass and residue that may contribute to the enhancement of biomass conversion. First, the physical appearance of the spruce was investigated with a scanning electron microscope (SEM). Then, pre-swelling experiment of the spruce was conducted and the conversion was compared with that of the typical cases in order to identify whether the reagent accessibility in the spruce is one of the factor that limits conversion of spruce.

In Chapter 6, further investigation of main contributor of synergistic conversion is presented. Based on characterization of products in Chapter 4, it is shown that cellulose may be responsible to the synergistic conversion. The trend from cellulose experiment is also in accordance with that of lignocellulose. When cellulose in spruce was converted to different crystalline structure of cellulose II, the improvement of conversion by both acid and base was observed.

Finally, the important conclusions from this research as well as recommendations for further research are given in Chapter 7.

CHAPTER 2

EXPERIMENTAL

2.1 Materials and Reagents

White Spruce, a softwood biomass, was obtained from School of Forest Resources, The Pennsylvania State University. The proximate and ultimate analysis properties as well as a calorific value of the spruce are shown in Table 2.1. The amount of cellulose, hemicellulose, and lignin was reported in Table 2.2.

Table 2.1 Proximate and ultimate analysis of spruce.

Properties	Value
Proximate Analysis (wt.%, DB)	
Moisture (after drying)	2.56±0.10
Volatile Matter	85.40±0.17
Fixed Carbon (by diff.)	14.57
Ash	0.03±0.03
Ultimate Analysis (wt.%, DB)	
C	50.03±0.25
H	5.75±0.02
N	0.05±0.04
S	0.03±0.00
O (by diff.)	44.11
High Heating Value (MJ/kg)	20.2±0.3

Table 2.2 Typical composition of white spruce [129].

Components	Wt.% (Dry basis)
Cellulose	44.8
Hemicellulose	30.9
Lignin	27.1
Ash	0.03

The chemicals used in this experiment are oxalic acid dehydrate (99+%, Sigma-Aldrich), tetramethylammonium hydroxide solution (TMAH; 10 wt% in H₂O, Sigma-Aldrich), hydroxylamine hydrochloride (99%, Alfa Aesar), phenylbenzene (aniline; 99+%, Alfa Aesar), N,O-Bis(trimethylsilyl)trifluoroacetamide with trimethylchlorosilane (99% BSTFA with 1% TMCS, Sigma-Aldrich), hexane (98.5%+, Alfa Aesar), 2-(Hydroxymethyl)phenyl-β-D-glucopyranoside (salicin; 99+%, Sigma-Aldrich), D(+)-glucose(99%, Alfa Aesar), and D(+)-xylose (>99%, Fluka), N-methylmorpholine N-oxide (NMMO; 97%, Aldrich), n-propyl 3,4,5-trihydroxybenzoate (n-propyl gallate, 98%+, Alfa Aesar), 1-n-butyl-3-methylimidazolium chloride (C₄mim⁺Cl⁻ 99%, Alfa Aesar), and phosphoric acid (H₃PO₄, 99.999%, Sigma-Aldrich). All the chemicals were used without further purification.

2.2 Sample Preparation for Batch Reaction

2.2.1 Typical Sample Preparation

Spruce was ground in a Wiley mill with 1 mm mill mesh size and sieved to 20-40 mesh size (425-850 μm sieve opening) to get a uniform range of

particle size. Before the reaction, wood was dried overnight in a vacuum oven at 80 °C. The drying condition of 65-80 °C under vacuum at least 4 h from wet state is recommended in order to get a minimum and reproducible dry weight for wood material [130]. The dried sample was kept in a desiccator at room temperature before using in the second-step reaction. The moisture of the sample was approximately 2.5 % after drying and storage.

2.2.2 Second-step Sample Preparation

The samples for second-step reactions in a sequential combination of acid and base treatment were prepared from solid residues of the first-step reactions. When the first-step reactions complete, liquid products and solid residues were collected from the reactor and filtered. The solid residues were washed to remove excess reagent with at least 250 mL of deionized water or until the pH of filtrate is equal to that of deionized water. The solid residues were dried overnight in a vacuum oven at 80 °C. The dried sample was kept in a desiccator at room temperature.

2.2.3 Pre-swelling of Wood Samples

Preparation of pre-swollen wood for experimental in Chapter 5 was done as follows. The wood sample was weighed 0.5 g for each batch of pre-swelling experiment. The, it was immersed in water, 10 % oxalic acid, or 10 % TMAH solution for 12 h at room temperature. The pre-swollen sample was centrifuged before measuring the swelling ratio as shown in the equation (2.1).

$$\text{Swelling Ratio} = \frac{\text{Volume}_{\text{After swelling}}}{\text{Volume}_{\text{Before swelling}}} = \frac{\text{Height}_{\text{After swelling}}}{\text{Height}_{\text{Before swelling}}} \quad (2.1)$$

2.2.4 Dissolution of Wood Samples

Preparation of reprecipitated cellulose in spruce by the dissolution-regeneration process in Chapter 6 was done with three different reagents: N-methylmorpholine N-oxide (NMMO), 1-n-butyl-3-methylimidazolium chloride ($C_4mim^+Cl^-$), and phosphoric acid (H_3PO_4). In the first dissolution method, 85% NMMO was used as cellulose solvent [131-137]. N-gallate 1 wt% concentration was used as a stabilizer [136-138]. The dissolution was operated in a round-bottom flask under ultra-purity nitrogen gas and heated at 130 °C in an oil bath. The dried spruce and NMMO solution was mixed at 10 wt% wood. The mixture was stirred continuously for 3 h. The wood was dissolved in the solvent and become one phase, which was very viscous at the end of the operation. Then, 100 mL of boiling water was added to reprecipitate the cellulose in spruce. The regenerated sample was filtered and washed with boiling water. After that, it was dried in a vacuum oven at 80 °C overnight.

Dissolution of spruce by $C_4mim^+Cl^-$ ionic liquid was carried out [139-144]. Since the reagent was very hygroscopic, and water content was found to be crucial in dissolution of cellulose [142], both ionic liquid and wood were dried in a vacuum oven for 24 h prior to dissolution to remove water. The dissolution was operated at 100 °C for 8 h under ultra-purity nitrogen gas, using 10 wt% of wood in ionic liquid. The mixture was stirred continuously during the dissolution. Then, 100 mL of deionized water was added at the end of dissolution to reprecipitate the cellulose in spruce. The regenerated sample was filtered and washed with water. After that, it was dried in a vacuum oven at 80 °C overnight.

Dissolution of cellulose in wood by phosphoric acid was done according to the literature [145]. An ice-cold 83.2 % H_3PO_4 was slowly mixed with

spruce with vigorous stirring. The mixture was kept in an ice-cold bath for one hour. At the end of dissolution, 400 mL of cold water was added to reprecipitate the cellulose in spruce. The clear supernatant was removed from the top of the solution. Then, 5 mL of 2 M Na_2CO_3 and 100 mL of cold deionized water was added. The regenerated sample was filtered and washed with water. After that, it was dried in a vacuum oven at 80 °C overnight.

2.3 Reaction in Batch Reactor

2.3.1 Sequential Acid and Base Reaction for Wood Conversion

The reaction was carried out in a 25-mL horizontal stainless batch reactor, as shown in Figure 2.1. After loading with 0.5 g of biomass and 10 g of acid or base solution (10 wt% oxalic acid or TMAH in H_2O), the reactor was closed and checked for leakage with nitrogen gas for 10 min. The reactor was purged five times with nitrogen gas. The pressure of nitrogen in reactor was adjusted to 1 atm at room temperature. The reactor was placed in a preheated fluidized bed sand bath (Techne, SBL-2D), equipped with a motor to move the reactor in vertical direction. The reactor was agitated vertically during the reaction at a rate of 250 cycles per min. After the reaction, the reactor was removed from the sand bath and immediately cooled down in a water bath to room temperature. The reactor was slowly vented and opened to collect the product. The liquid and solid products were separated by filtration with 1- μm pore size filter paper. The reactor was carefully rinsed with deionized water to remove the entire solid residue remaining inside. Then, the solid residue was washed with at least 250 mL deionized water or until the pH of filtrate does not change. The solid residue was dried overnight in the vacuum oven at 80 °C.

The reaction in the second step was carried out in the same approach as the first step reaction using 0.5 g of combined solid residues from the first step

reaction and 10 g of new reagent. The conversion and overall conversion was calculated based on the solid biomass conversion. The overall conversion of two-step reactions was calculated by the following equation.

$$\text{Overall conversion} = 1 - \left(\text{wt.\% Solid}_{1^{\text{st}}\text{step}} \times \text{wt.\% Solid}_{2^{\text{nd}}\text{step}} \right) \quad (2.2)$$



Figure 2.1 Photograph of batch reactor.

2.3.2 Acid and Base Reaction for Pre-swollen Wood Conversion

The pre-weighed 0.5 g of pre-swollen wood was transferred directly to the reactor without drying to preserve the swelling structure of the wood. Before transferring, the pre-swollen wood was immersed and rinsed in the reagent to replace the swelling solvent in the pore. Based on triplicated experiments, the recovery rate of pre-swollen wood with water, oxalic acid, and TMAH was 97.15 ± 0.03 , 99.04 ± 0.55 , and 93.40 ± 0.18 %, respectively. These numbers were used to normalize the conversion by acid and base treatments in Chapter 5.

2.4 Gas Product Analysis

The gas samples were analyzed qualitatively with Shimadzu GC-17A gas chromatograph, equipped with thermal conductivity detector (TCD) and flame ionization detector (FID). The TCD was used for permanent gases (mainly CO and CO₂) analysis, and FID was used for C₁–C₅ hydrocarbon analysis. The column used for TCD was a Supelco Carboxen 1000 column, 4.6-m length and 3.17- μ m inside diameter. An Alltech Chemipack C₁₈ column, 1.8-m length and 3.17- μ m inside diameter, was used for FID detector. The gas from reactor was collected in a Tedlar™ air sampling bag. Injection volume of gas was 1 mL. The temperature profile in the oven started from initial holding temperature at 35 °C for 7.5 min, and then ramped to 200 °C at a heating rate of 20 °C/min, and held for 9.3 min. Peaks were identified based on comparison with gas standard.

2.5 Liquid Products Analysis

2.5.1 Gas Chromatography Mass Spectroscopy of Toluene-Extracted Samples

The organic solvent from binary reaction or extraction was analyzed in Shimadzu GC-17A gas chromatograph, with Shimadzu QP-5000 mass spectrometer. The capillary column was Rxi-5ms, 0.25 μ m thickness, 30-m length and 0.25-mm inside diameter. The oven temperature was set initially at 45 °C, held for 2 min, then raised 6 °C/min to 300 °C, and held 15 min at 300 °C. Injection and interface temperature were 280 °C and 230 °C, respectively. Helium gas flow rate was 1 mL/min. Injection volume was 1 μ L with 21:1 split ratio. The mass spectrometer was operated in the electron impact mode with ionization potential of 70 eV. The m/z

range was 50-500. Peaks were identified based on mass fragmentation patterns in comparison with NIST standard library.

2.5.2 Gas Chromatography and Mass Spectroscopy of Extracted Derivatized Samples

Standards and samples were derivatized to oxime trimethylsilyl (oxime-TMS) forms by the following procedure adapted from literature [146]. Prior to derivatization, liquid sample with pH higher than 7 was neutralized with 10 % oxalic acid until pH in the range of 5-7. The aqueous solution of 200 μL was measured and mixed with 50 μL of salicin internal standard solution (400 $\mu\text{g}/\text{mL}$ concentration). The mixture was evaporated under high purity nitrogen stream until completely dry. The oxime formation step was done with 50 μg of hydroxylamine hydrochloride and 1 mL aniline at 60 $^{\circ}\text{C}$ for 10 min in a water bath. In this step, reducing sugars reacted with hydroxylamine and formed oxime (Figure 2.2). After cooling to room temperature, silylation (Figure 2.3), was done by adding 250 μL BSTFA containing 1% TMCS to the mixture and sonicated at ambient temperature for 10 min. The silylated products were extracted with 1 mL hexane by sonication for 10 min. The final mixture was centrifuged before separation of the hexane phase for analysis in GC-FID.

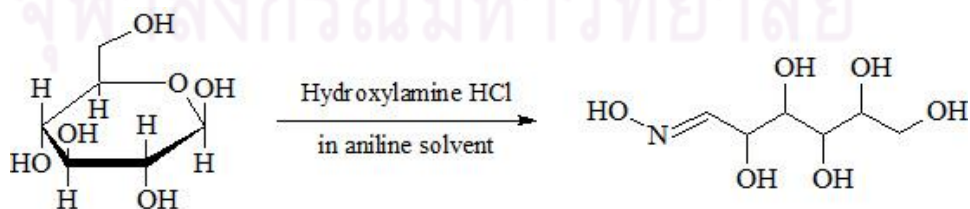


Figure 2.2 Reaction scheme of oxime formation of β -D-glucopyranose.

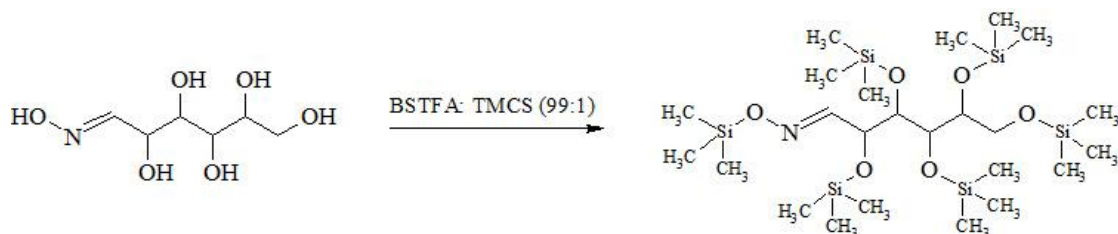


Figure 2.3 Reaction scheme of silylation of glucose oxime.

One μL of extracted derivatized sample was injected in GC-FID Varian CP-3800. The column was VF-5ms (30-m length and 0.25-mm capillary column, 0.25 μm thickness). The oven temperature was programmed to start at 160 $^{\circ}\text{C}$, hold for 1 min, and then rise at rate of 2 $^{\circ}\text{C}/\text{min}$ to 172 $^{\circ}\text{C}$, 10 $^{\circ}\text{C}/\text{min}$ to 210 $^{\circ}\text{C}$, 30 $^{\circ}\text{C}/\text{min}$ to 320 $^{\circ}\text{C}$, and held at this final temperature for 2 min. Injector and detector temperature were set to 250 $^{\circ}\text{C}$ and 320 $^{\circ}\text{C}$, respectively. Gas flow rate was 2.7 mL/min. Peaks were identified based on comparison with standard and by GC-MS identification based on mass fragmentation patterns of injected samples compared to NIST standard library.

For identification of the derivatized samples, the hexane-extracted samples were injected in GC-MS (Shimadzu GC-17A gas chromatograph, with Shimadzu QP-5000 mass spectrometer) to identify their peaks. The capillary column was Rxi-5ms, coated with 5% phenyl and 95% methyl polysiloxane 0.25 μm thickness, 30-m length and 0.25-mm inside diameter. The oven temperature was set initially at 65 $^{\circ}\text{C}$, held for 2 min, then raised 6 $^{\circ}\text{C}/\text{min}$ to 300 $^{\circ}\text{C}$, and held 15 min at 300 $^{\circ}\text{C}$. Injection and interface temperature were 280 $^{\circ}\text{C}$ and 230 $^{\circ}\text{C}$, respectively. Helium gas flow rate was 1.3 mL/min. Injection volume was 1 μL in splitless mode. The mass spectrometer was operated in the electron impact mode with ionization potential of 70 eV. The m/z range was 50-500. Peaks were identified based on mass fragmentation patterns in comparison with NIST standard library.

2.6 Solid Product Analysis

2.6.1 Pyrolysis Gas Chromatography

The solid residue from reaction was analyzed by Pyrolysis-GC-MS. The pyrolysis unit was Pyroprobe 1000. The GC-MS instrument was HP 5890 Series II, with HP 5971A mass selective detector. The GC column was Rxi-5ms capillary column, 30 m × 0.25 mm, 0.25- μ m thickness. Very small amount of solid residue with particle size less than 60 mesh was used to ensure complete pyrolysis of the samples and avoid signal overloaded. Approximately 0.1 mg of dried solid residue was measured and transferred to a thin quart tube. All of the solid residues were assumed to be entirely pyrolyzed. Since the smallest measuring unit of the balance was 0.1 mg, the sample weight may carry some error when quantitative analysis is required. The quart tube containing solid sample was inserted into horizontal filament coil in the pyrolysis unit. The pyroprobe was programmed to heat with rate of 5 °C/ms to 610 °C, and held for 10 sec. After flash pyrolysis of the solid sample, the gas was cryotrapped by liquid nitrogen at early part of the GC column in order to trap the pyrolyzates (condensable pyrolysis products). The GC oven temperature started at 35 °C, increased at a rate of 4 °C/min to reach 300 °C, and held 15 min at this final temperature. Interface temperature was 280 °C. Helium was used as a carrier gas. The mass spectrometer was operated in the electron impact mode with 70 eV of ionization potential. The setting m/z detection range of the mass spectrometer was 40-550. Peaks were identified based on comparison of mass fragmentation patterns with Wiley standard library installed in the equipment, by comparison with literatures (Appendix B) [105, 107-109, 112, 147-152], and by selective characteristic ion masses (Chapter 4, Table 4.6 and Figure 4.13).

2.6.2 Nuclear Magnetic Resonance Spectroscopy of Carbon-13

The cross polarization-magic angle spinning (CPMAS) ^{13}C spectra with total suppression of spinning sidebands (TOSS) of wood solid residues were obtained at room temperature on a Bruker AV-300 solid state NMR spectrometer operating at 75.55 MHz. 2048 scans were accumulated for each sample. A rectangular contact was used with a contact time of 2 msec. The spinning rate was 5000 Hz, and the relaxation delay was 5 sec. Spinal 128 ^1H decoupling was used during acquisition. The spectra were referenced indirectly to the aromatic ^{13}C shift of hexamethylbenzene ($\delta = 132.2$ ppm).

2.6.3 Scanning Electron Microscopy

Surface topography of wood solid residues was accessed by FEI Quanta 200 environmental scanning electron microscope (ESEM) with LFD detector. The dried wood samples were spread on a double-sided tape attached on a sample holder and placed in the chamber directly. The equipment was operated at low vacuum mode, approximately 0.6-0.9 Torr. Relative humidity of the operating room was about 2.5 % at 23 °C.

2.6.4 X-ray Diffraction

Crystalline morphology of solid residues was determined by X-ray diffraction (XRD) on an automated Scintag Powder Diffractometer with Si(Li) peltier detector and Cu-K α radiation, $\lambda = 1.54059$ Å, 30 mA, 35 kV. Diffractograms were acquired over the scanning range of 5° to 50° 2 θ with a scanning speed of 2.5 °/min. Diffractograms were analyzed using the standard JCPDS methods.

CHAPTER 3

PRELIMINARY STUDIES ON BIO-OIL UPGRADING

The most direct and conventional way to convert solid biomass to organic liquid products is by pyrolysis and liquefaction. However, the bio-oil from these processes requires upgrading, primarily by deoxygenation. This chapter presents the preliminary work on bio-oil upgrading.

3.1 Experimental for Bio-oil Upgrading

The experiments in Chapter 3 are different from Chapter 4-6 and described separately in this chapter.

3.1.1 Materials

The bio-oil liquid product from wood pyrolysis was provided by the Department of Forest Products, Mississippi State University. It was produced with Auger fast pyrolysis of softwood at 500 °C. Based on MSDS, this bio-oil contained more than 400 oxygenated organic compounds, approximately 5-10 % organic acids, 5-20 % aldehydes and hydroxyaldehydes, 20-30 % ketones and hydroxyketones, 20-30 % phenolics, and 15-30 % water based on wet liquid basis. The production date was not indicated. The catalysts used in bio-oil upgrading were commercial CoMo/Al₂O₃ catalyst, and unsupported NiMoS₂ and CoMoS₂ synthesized by hydrothermal method [153]. The commercial CoMo/Al₂O₃ catalyst was sulfided prior to reaction and kept in solvent (decalin, or water). Other chemicals used were acetone (J.T. Baker, 99.8% purity), tetrahydrofuran (VWR, 99.5% purity), dichloromethane, decahydronaphthalene (decalin, Sigma-Aldrich, 99% purity).

3.1.2 Upgrading of Bio-oil in Batch Reactor

The upgrading of bio-oil was performed in a 25-mL batch microreactor, as shown in Figure 2.1. Bio-oil and catalyst were weighed 2-4 g and 0.1 g, respectively, and loaded in the reactor. The reactor was closed and checked for leakage with nitrogen gas for 10 min. The reactor was purged five times with hydrogen to 400 psig and then placed in a preheated fluidized bed sand bath, agitated vertically during the reaction at a rate of 250 cycles per min. After the reaction, the reactor was immediately cooled down in a water bath. The reactor was slowly vented and opened to collect the product.

3.1.3 Gas Chromatography Mass Spectroscopy of Bio-oil

The organic liquid product from bio-oil upgrading was analyzed by Shimadzu GC-17A gas chromatograph, with Shimadzu QP-5000 mass spectrometer. The capillary column was Rxi-5ms, 0.25 μm thickness, 30 m long \times 0.25 mm inside diameter. The oven temperature was set initially at 45 $^{\circ}\text{C}$, held for 4 min, then raised 3 $^{\circ}\text{C}/\text{min}$ to 280 $^{\circ}\text{C}$, and held 20 min at 280 $^{\circ}\text{C}$. Injection and interface temperature were 290 $^{\circ}\text{C}$. Helium gas flow rate was 1 mL/min. Injection volume was 1 μL with 21:1 split ratio. The mass spectrometer was operated in the electron impact mode with ionization potential of 70 eV. The m/z range was 50-500. Peaks were identified based on mass fragmentation patterns in comparison with NIST standard library. Bio-oil was diluted in solvents with ratio of 20 mg bio-oil/mL solvent (approximately 2.5 wt% bio-oil in acetone) and treated with sodium sulfate to remove water. Propylbenzene was used as an internal standard (RT = 11.45 min).

3.2 Bio-Oil Characterization

Bio-oil can be dissolved in tetrahydrofuran (THF) and acetone. It is partially dissolved in dichloromethane (DCM) and water, but not soluble in hexane

and toluene. The bio-oil dissolved in THF, acetone, and DCM were injected into the GC-MS. Since the bio-oil was not completely miscible with DCM, the characterization result from DCM shows fewer peaks with less intensity than bio-oil in acetone and THF (Figure 3.1). The acetone and THF dilution gave similar results qualitatively and quantitatively (Figure 3.2 and 3.3). However, the chromatogram of bio-oil in THF shows a distinctive peak of butylated hydroxytoluene at retention time of 37 min (Figure 3.2). This result is not in agreement with MSDS and others results in literatures [59, 154]. Therefore, acetone was selected as solvent for bio-oil and its products analysis. The chromatogram from bio-oil dissolved in acetone (Figure 3.3) shows broad peak at RT = 35-36 min, which is the peak of levoglucosan decomposed from cellulose. Other peaks are mainly phenolic compounds that derived from lignin. The identification of major peaks found in bio-oil is shown in Figure 3.3. Other polar components such as acids, aldehydes, and ketones may not be compatible with the column. They are eluted very quickly and not shown in the chromatogram.

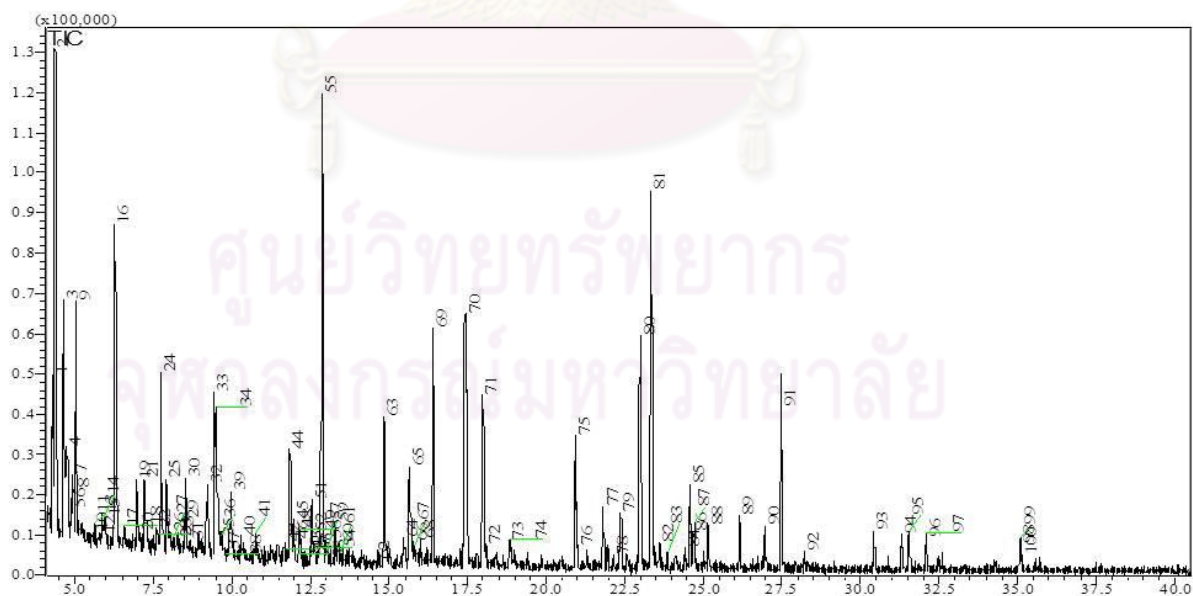


Figure 3.1 GC-MS chromatogram of bio-oil in dichloromethane.

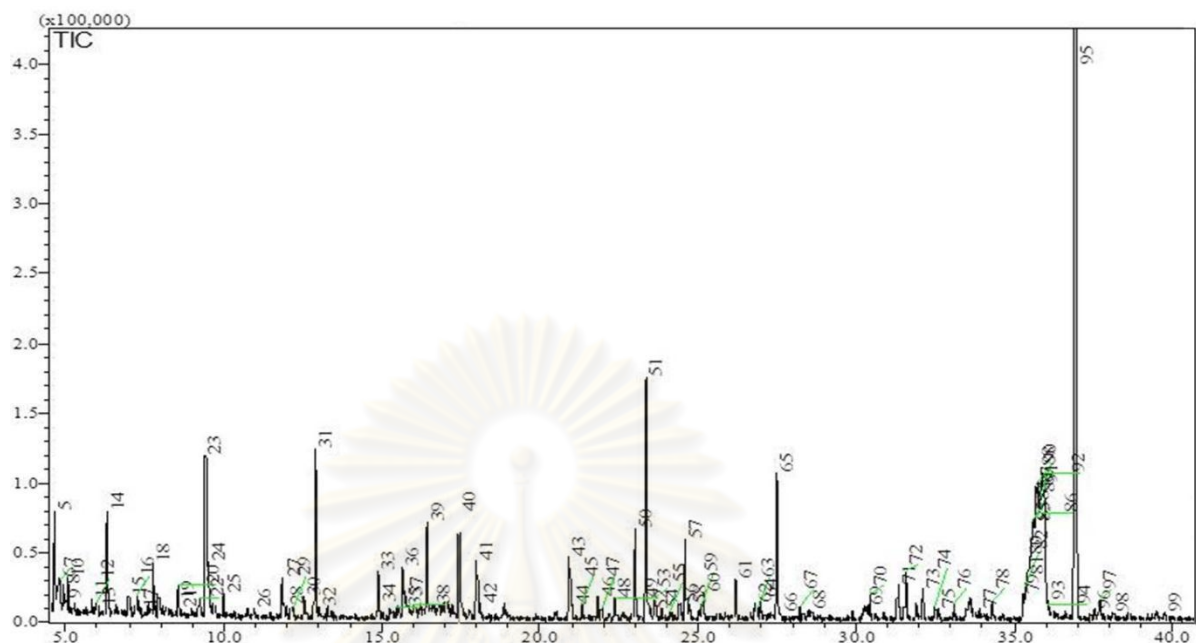


Figure 3.2 GC-MS chromatogram of bio-oil in tetrahydrofuran.

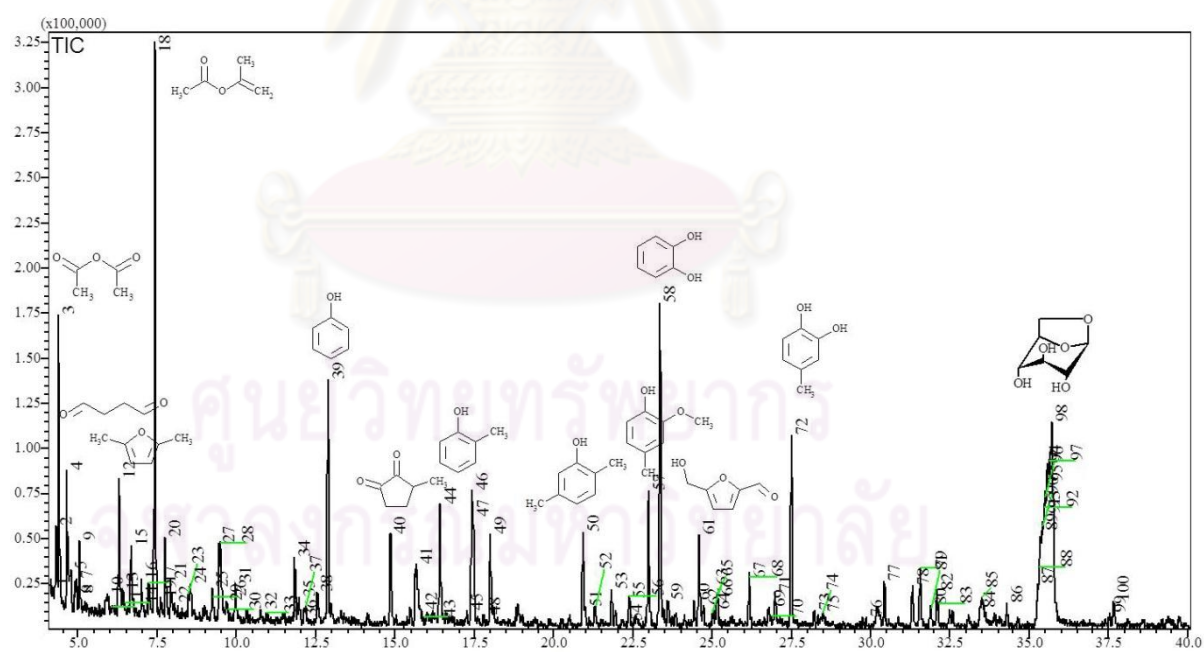


Figure 3.3 GC-MS chromatogram of bio-oil in acetone.

3.3 Upgrading of Bio-Oil by Commercial CoMo Sulfide Catalysts

The upgrading of bio-oil over CoMo sulfide catalysts has been studied widely [155, 156]. The upgrading experiments by hydrodeoxygenation were carried out using commercial CoMo sulfide as main catalyst. Several conditions were tried at temperature range of 90-270 °C, retention time range of 5-60 min, and with different solvents such as methanol, decalin, and water. The products could be separated to gas, liquid, and solid products. The main components in both uncatalyzed and catalyzed reactions are oxygenated compounds with hydroxyl, carbonyl, and carboxylic functional groups.

3.3.1 Effects of Temperature

Reaction at 90 °C do not lead to solid formation (Figure 3.5), but the bio-oil product composition based on GC-MS analysis did not significantly change from initial bio-oil (Figure 3.4). The two highest peaks in original bio-oil and in liquid product from upgrading at 90 °C were the same and identified as acetate 1-propen-2-ol and acetic acid anhydride (RT = 7.4 and 4.4 min). Thus, the temperature of 90 °C was too low for catalytic reaction over commercial CoMo sulfide catalyst.

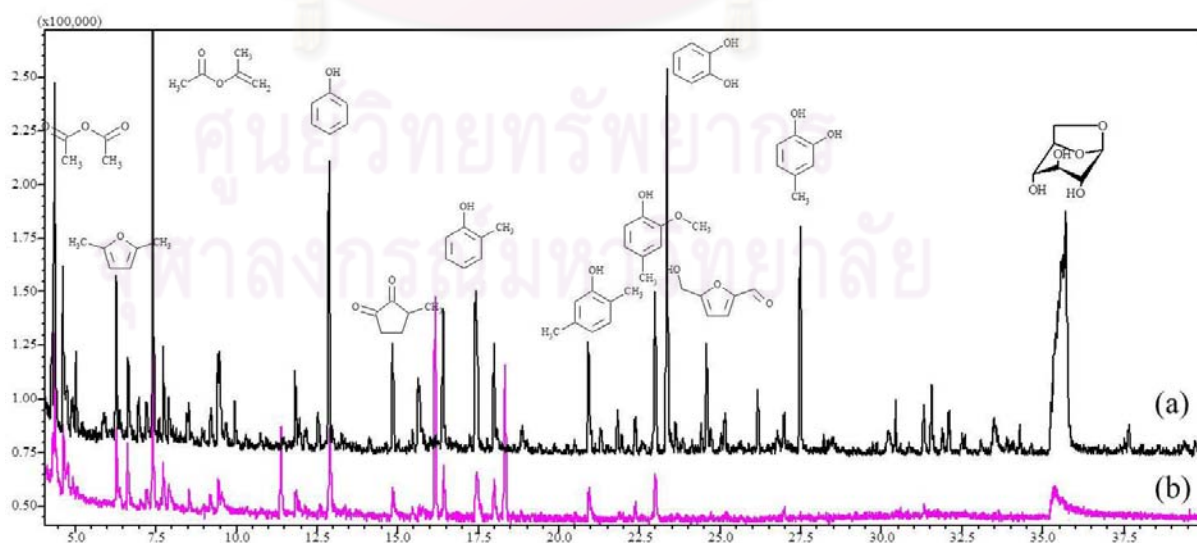


Figure 3.4 GC-MS chromatogram of (a) bio-oil; (b) bio-oil product from hydrotreating over commercial CoMo sulfide catalyst at 90 °C.

The conversion of bio-oil to gas, liquid, and solid products, as well as product analysis from hydrotreatment at 90-270 °C are shown in Figure 3.5 and 3.6, respectively. As the temperature was increased, the increase in amount of solid products was observed due to the converting of viscous liquid to very rigid solid. The main compounds in liquid products were generally decreased in amount as the temperature increased, except for the 1-hydroxy-2 propanone (RT = 6 min) increased with temperature. The formation of 1-hydroxy-2 propanone as the major product was observed in both non-catalytic hydrothermal and commercial CoMo sulfide catalyst at 270 °C. It should be noted that the high intensity of peak at RT= 11.45 min in Figure 3.6(c) was due to the high amount of the internal standard in the samples compared in the same range of sensitivity. Based on this experiment, the concentration of the internal standard should be in the range of 0.003-0.004 wt%.

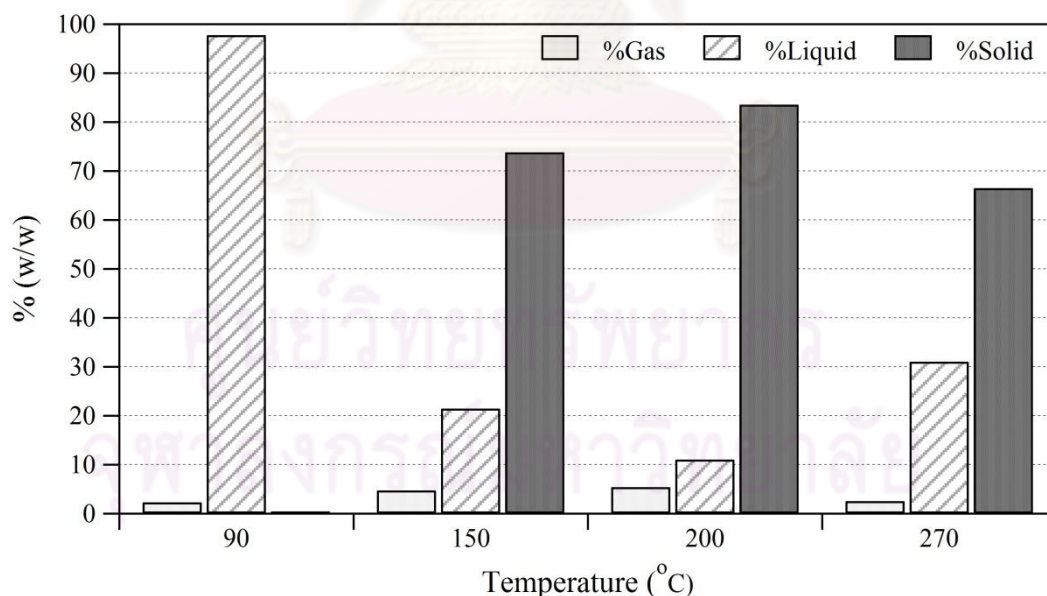


Figure 3.5 Conversion of bio-oil upgrading to gas, liquid, and solid product over commercial CoMo sulfide catalyst at various reaction temperatures.

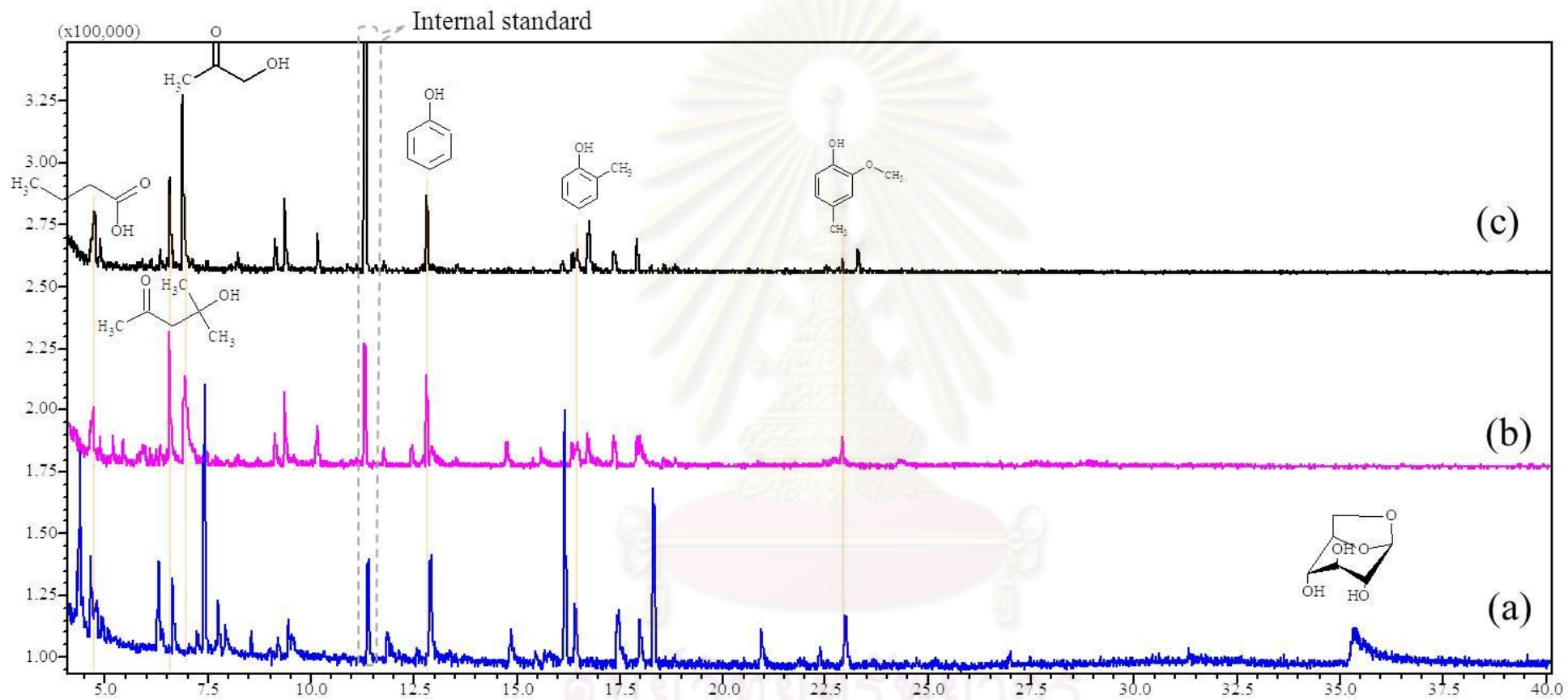


Figure 3.6 GC-MS chromatogram of bio-oil products from hydrotreating over commercial CoMo sulfide catalyst at (a) 90 °C; (b) 200 °C; (c) 270 °C.

Considering the composition and yield of the liquid products, components of the bio-oil products were still polar and hydrophilic. Also, the weight of liquid products and the water in the initial bio-oil was in the same range. This information suggests that the main components in bio-oil were converted to form solid product by condensation and polymerization after hydrotreating over commercial CoMo sulfide catalyst. The composition comparison of liquid products and acetone-soluble part of solid product from the hydrotreating at 200 °C, shown in Figure 3.7, supports the idea that most components found in liquid product were the same as those in acetone-soluble solid product.

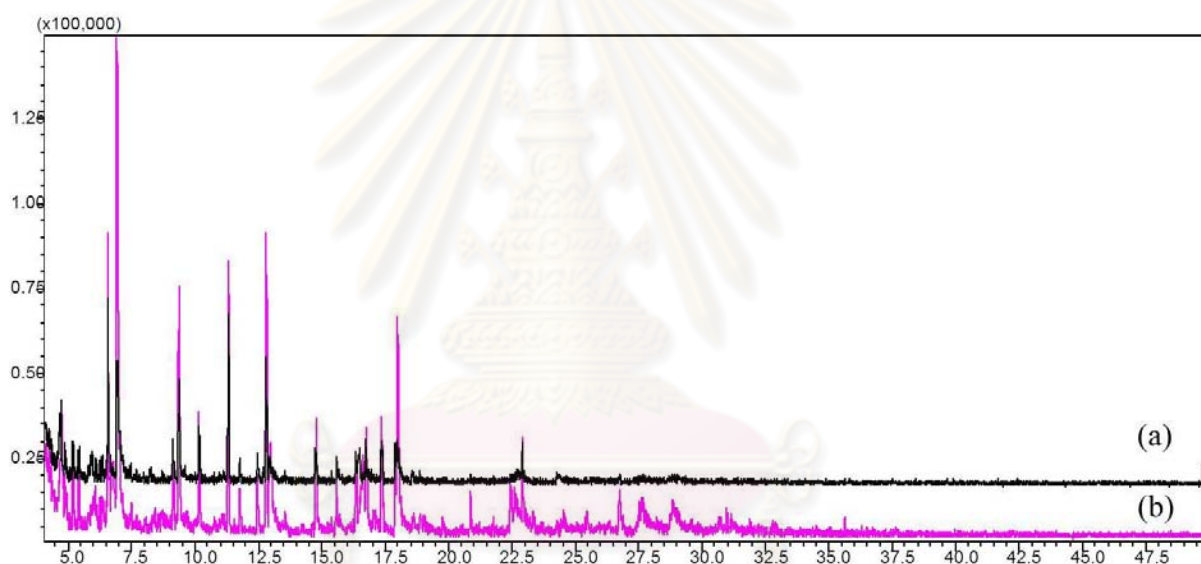


Figure 3.7 GC-MS chromatogram of bio-oil products from hydrotreating over commercial CoMo sulfide catalyst at 200 °C; (a) liquid product; (b) acetone-soluble solid product.

3.3.2 Effects of Reaction Time

In order to study the effects of retention time, particularly at the beginning of reaction, the 5 and 10 min experiment was carried out at 270 °C using commercial CoMo sulfide catalyst. The conversion of bio-oil is shown in Figure 3.8. Although the liquid products were not analyzed, the results from conversion indicated that the solid formation took place as early as 5 min. However, at 10 min, the amount of solid product was decreased suggesting that the bio-oil could undergo through cycle of melting and solidifying because of the heat and condensation of the small products during the process. The solid product from the 5 min reaction was tar-like, while that from the 10 min reaction was also tar-like but slightly less viscous than the 5 min product.

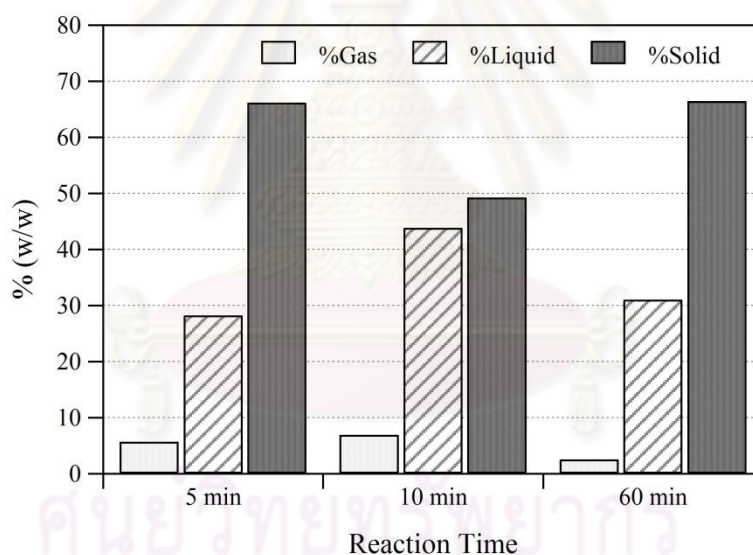


Figure 3.8 Effect of reaction time on conversion of bio-oil to gas, liquid, and solid product over commercial CoMo sulfide catalyst at 270 °C.

3.3.3 Effects of Bio-Oil to Catalyst Ratio

The typical ratio of bio-oil : commercial CoMo sulfide catalyst was 40:1. The bio-oil hydrotreating at bio-oil : catalyst ratio of 20:1 and 10:1 was studied by keeping the catalyst weight at 0.1 g and varying the bio-oil weight to 2 and 1 g. Conversion results are shown in Figure 3.9. As increasing catalyst amount, the gas product from bio-oil conversion was increased. Also, the solid product was more dry and rigid when high amount of catalyst was used. However, the low amount of bio-oil may lead to nonhomogeneous contact of bio-oil and catalyst because the viscous bio-oil adhered mostly to the reactor wall and could not mix well by shaking.

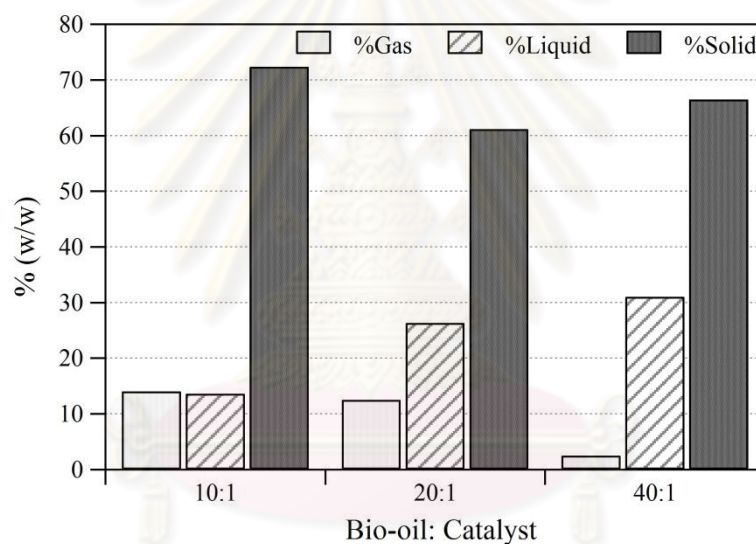


Figure 3.9 Effect of bio-oil : catalyst ratio on conversion of bio-oil to gas, liquid, and solid product over commercial CoMo sulfide catalyst at 270 °C, 1h.

3.3.4 Effect of Solvents

Several solvents have been tested to improve the hydrotreating reaction. The experiment was carried out at constant bio-oil : solvent weight ratio of 1:1. The solvents used were methanol, dichloromethane, and decalin. As for the dichloromethane, the solvent causes permanent reactor leakage possibly due to its high vapor pressure (Data not shown).

The experiment with decalin did not show any effects on the reaction for both composition (Figure 3.10) and conversion (Table 3.1). This is probably due to phase separation and thermal stability of decalin. The liquid products in decalin experiments have two phases. The decalin phase does not have any detectable compounds detected except the decalin (chromatogram not shown).

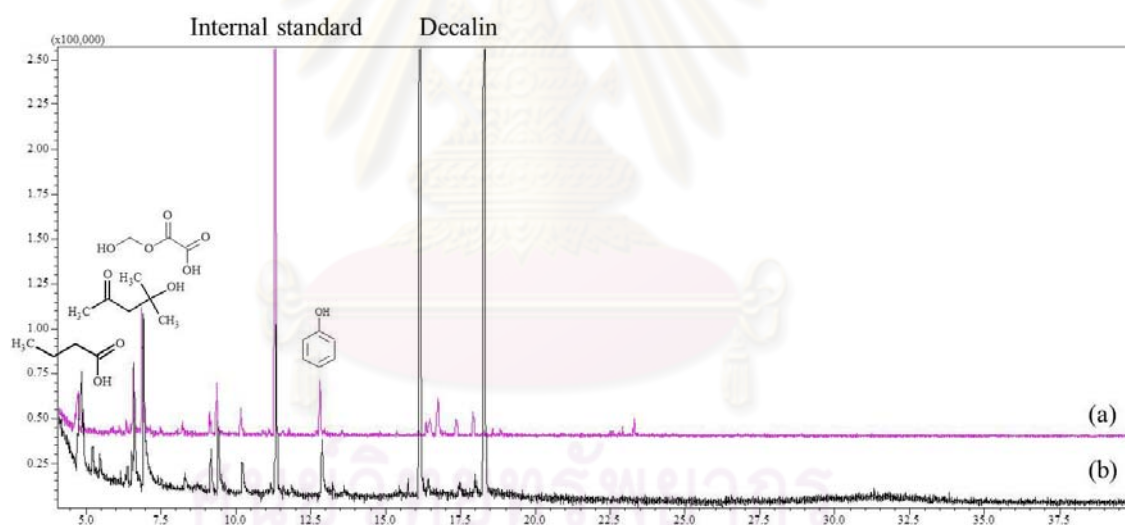


Figure 3.10 GC-MS chromatogram of bio-oil products from hydrotreating over commercial CoMo sulfide catalyst at 270 °C; (a) without decalin; (b) with 1:1 decalin solvent.

When methanol was used as reaction medium, the addition of solvent did not improve the conversion of bio-oil (Table 3.1). Bio-oil was fully miscible with the methanol. However, the solid product did not lower than the hydrotreating without methanol. The amount of liquid product was corresponding to the sum of the amount of added solvent and water (or water-soluble part) initially present in bio-oil. There

were more ester compound products found in liquid product from hydrotreating in the presence of methanol due to esterification (Figure 3.11).

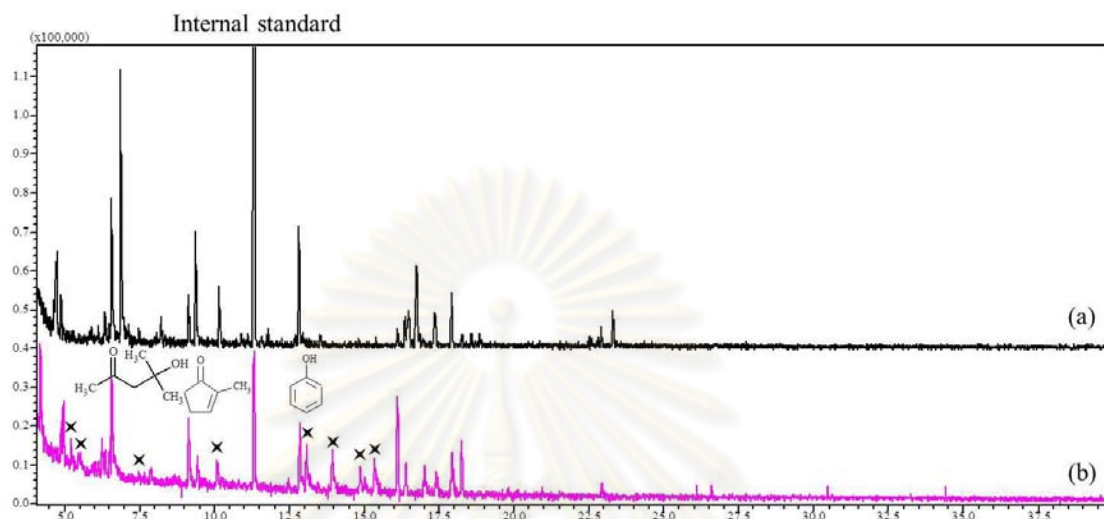


Figure 3.11 GC-MS chromatogram of bio-oil products from hydrotreating over commercial CoMo sulfide catalyst at 270 °C; (a) without methanol; (b) with 1:1 methanol solvent. The sign (X) indicates ester compounds.

Table 3.1 Effect of solvents on conversion of bio-oil to gas, liquid, and solid product over commercial CoMo sulfide catalyst.

Exp.	Feed	Solvent	Temperature (°C)	Yield		
				% Gas	% Liquid	% Solid
1	Bio-oil	-	90	2.23	97.77	0.00
2	Bio-oil	-	150	4.74	21.47	73.79
3	Bio-oil	-	270	2.50	31.03	66.47
4	Bio-oil	Decalin	90	4.15	95.85	0.00
5	Bio-oil	Decalin	150	3.83	17.42	78.76
6	Bio-oil	Decalin	270	7.41	2.99	89.60
7	Bio-oil	Methanol	270	6.36	14.55	79.09

3.4 Upgrading of Bio-Oil by Unsupported CoMoS₂ and NiMoS₂ Catalysts

The unsupported CoMoS₂ and NiMoS₂ were synthesized and their activities were investigated for conversion of the bio-oil. At the same condition with bio-oil hydrotreating over commercial CoMo sulfide catalyst, the synthesized CoMoS₂ catalysts yield high amount of solid product, probably due to high activity of the catalysts. The reaction and catalyst amount was reduced to decrease the solid product formation. From Table 3.2, the product distribution was still at least 70% solid product. From GC-MS, the major products are diacetone alcohol, pyruvic acid, and 1-hydroxy-2-propanone similar to those from hydrotreating over commercial catalyst (chromatogram not shown).

Table 3.2 Effect of catalyst type on conversion of bio-oil to gas, liquid, and solid product at 200 °C.

Exp.	Feed	Catalyst	Bio-oil: Catalyst	Time	Yield		
					% Gas	% Liquid	% Solid
8	Bio-oil	Commercial CoMo sulfide	40:1	1 h	5.41	11.03	83.56
9	Bio-oil	CoMoS ₂	20:01	1 h	6.56	3.28	90.15
10	Bio-oil	NiMoS ₂	20:01	1 h	8.82	21.37	69.81
11	Bio-oil	CoMoS ₂	40:1	30 min	6.13	23.20	70.67
12	Bio-oil	NiMoS ₂	40:1	30 min	5.69	12.15	82.16

3.5 Solid Formation from Bio-oil Conversion

Since the major problem in upgrading of bio-oil was the high amount of solid product. The solid formation of bio-oil conversion was studied using 3 bio-oil models as shown in Table 3.3. The mixture was injected in GC-MS to confirm its detectability. However, it was found that the GC can only detect phenolic compounds. It cannot detect carbohydrates and organic acids (Figure 3.12).

Table 3.3 Composition of bio-oil models.

Component	wt %		
	Model A	Model B	Model C
Water	20	17.8	22
Glucose	20	17.8	17
Acetic acid	20	17.8	17
Phenol	10	17.8	8
1,2-dihydroxybenzene	10	9.0	8
2-methylphenol	10	9.0	9
2-methoxyphenol	10	9.0	9
Acetaldehyde	-	1.8	8
Formaldehyde	-	-	2
Total	100.0	100.0	100.0

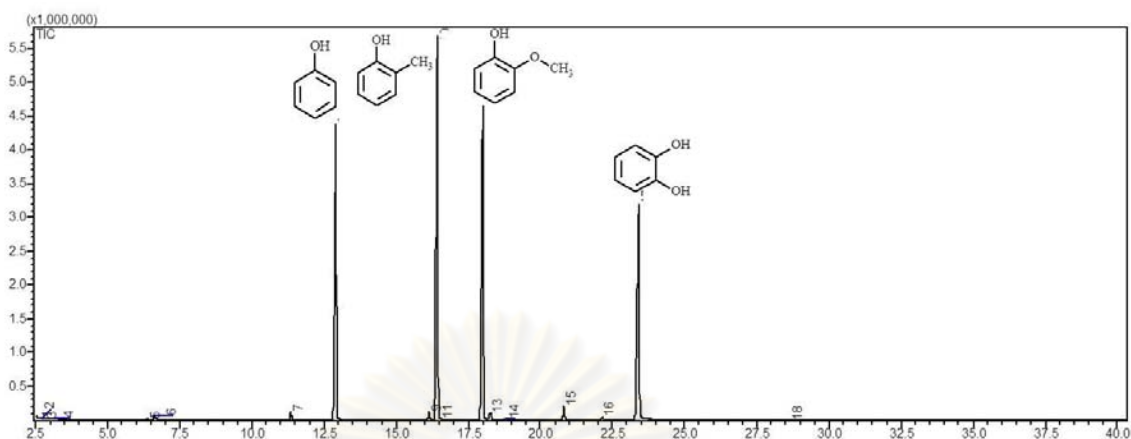


Figure 3.12 GC-MS chromatogram of bio-oil model (Model A).

As shown in Table 3.4, the individual chemicals and bio-oil model were hydrotreated at 270 °C, 400 psig H₂, 1 hour, over commercial CoMo sulfide catalyst without solid formation. This is contrast with the hydrotreating of bio-oil which forms high amount of solid product.

Reaction of the model fuel over various metal oxide catalysts such as Ni/SBA-15, CeO₂, and ZrO₂ do not significantly differ from reaction without catalyst. GC-MS analysis shows slightly decrease of the chemicals initially in bio-oil model. Only small amount of diacetone alcohol was found in Exp. 22. The product formed was very little compared to initial chemical amount and each catalyst did not show significant difference from each other and initial bio-oil model (Figure 3.13). Under the condition tested with bio-oil model, the phenolic compounds were moderately stable. Hydrotreating of bio-oil model do not lead to solid formation; the only solid found was the remaining solid catalyst.

One possible explanation for solid formation during thermal conversion could be that the phenolic compounds may recondense with formaldehyde, as occur during the production of acid-catalyzed phenol formaldehyde resin. In order to proof the origin of solid formation in bio-oil during thermal processing, bio-oil model B and C were prepared. Acetaldehyde and/or formaldehyde were included in addition to water, glucose, acid, and phenolics mixture in the Model A. After thermal reaction at 270 °C, there was no solid formed suggesting there are

other contributors in complex composition of bio-oil that leads to solid formation during heat treatment.

Table 3.4 Effect of catalyst type on solid product formation of model bio-oil.

Exp.	Feed	Catalyst	Temp (°C)	Time	Solid
15	Guaiacol	CoMo sulfide	270	1 h	No
16	Cresol	CoMo sulfide	270	1 h	No
17	Phenol	CoMo sulfide	270	1 h	No
18	Model A	-	270	1 h	No
19	90% Model A + 10% Bio-oil	-	270	1 h	No
20	Model A	CoMo sulfide	270	1 h	No
21	Model A	50% Ni/SBA-15	270	1 h	No
22	Model A	CeO ₂	270	1 h	No
23	Model A	ZrO ₂	270	1 h	No
24	Model A	SBA-15	270	1 h	No
25	Model A	Al ₂ O ₃	270	1 h	No
26	Model A	50% Ni/SBA-15	350	1 h	No
27	Model A	CeO ₂	350	1 h	No
28	Model B	-	270	1 h	No
29	Model B	50% Ni/SBA-15	270	1 h	No
30	Model C	-	270	1 h	No

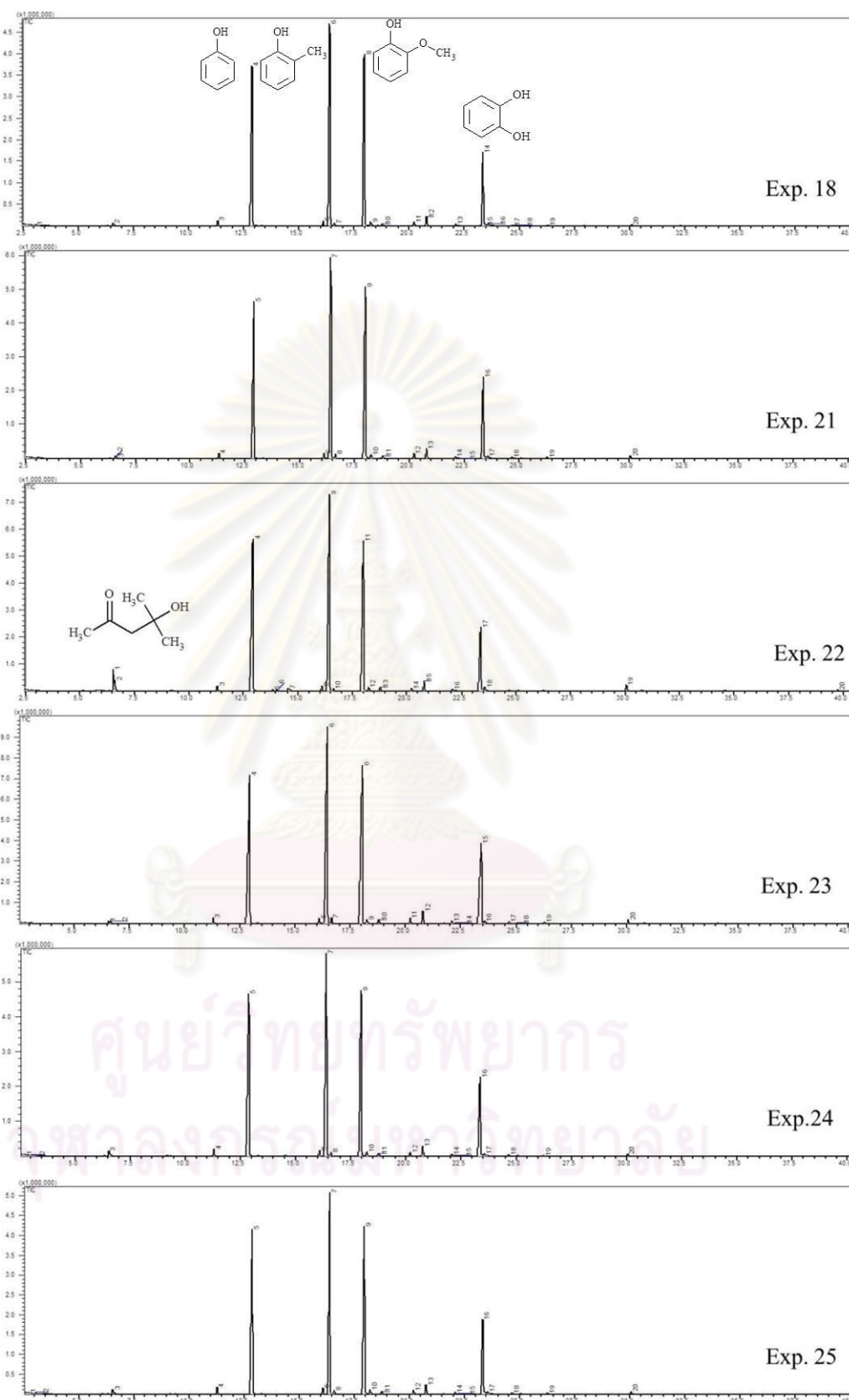


Figure 3.13 GC-MS chromatogram of bio-oil model (Model A) after hydrotreating over various catalysts.

3.6 Conclusion on Bio-oil Upgrading

The preliminary works on bio-oil upgrading demonstrate major problem in hydrotreating of bio-oil. Since the bio-oil contains huge amount of oxygenated compounds including carboxylic acids, aldehydes, ketones, and phenolics, it is very reactive, corrosive, and unstable [11]. High reactivity of bio-oil leads to undesired reactions such as repolymerization and condensation resulting in high amount of solid formation. Preliminary hydrotreating experiments of bio-oil were not successful mainly due to high amount of solid products. Investigation of solid formation using bio-oil model cannot simulate the solid formation process occurring in the bio-oil. Based on preliminary experiments, it is recommended that the reactor should be easier to clean up to prevent accumulation of product remaining in the reactor and allow better mixing of viscous substance. Stability of the bio-oil during storage was reported and it is recommended the bio-oil should be supplied on a regular basis [57]. Therefore, consistency of the experiments has to rely on aging of the bio-oil. Furthermore, the pyrolysis process for production of bio-oil involves several technical requirements such as high heating and cooling rate, low moisture content and small particle size of feedstock.

It is convinced that the utilization of lignocellulosic biomass via pyrolysis route has inherited problem on both upstream and downstream processes. A new process for conversion of lignocellulosic biomass is desired. Therefore, the following work in Chapter 4-6 involves a new thermochemical process concept on sequential combination of acid and base treatment for lignocellulosic biomass conversion.

CHAPTER 4

SYNERGY CONVERSION OF BIOMASS BY SEQUENTIAL ACID AND BASE TREATMENTS

There is a need for development of a new process for conversion of lignocellulosic biomass. Considering the conventional processes described in Chapter 1, each technology has its own benefits and disadvantages. The gasification process requires very high temperature to break down the biomass to gas compounds suitable for synthesis of large molecules. Although, the gasification technology is accepted and very useful, very high temperature used during gasification reduces energy efficiency of the process [18]. To decrease the energy consumption, development of a more efficient route to produce liquid products from biomass under mild conditions should be considered. Pyrolysis and liquefaction use high temperature to degrade biomass in a very short period of time and then quench condensable gas product into liquid; however, the bio-oil obtained from the process is highly reactive and tends to react to form polymeric solid products as illustrated in Chapter 3. This is in agreement with some recent opinions which suggest that bio-oil from conventional pyrolysis is very unstable and tends to recondense upon heating [3, 11, 157]. These thermal degradation processes consume high energy because of the high energy employed, and requirement of low moisture of less than 10 % in wood making drying process necessary. Alternatively, the low temperature process such as enzymatic hydrolysis applies biological microorganisms to convert cellulose into glucose. This method is well known and used in lignocellulosic ethanol production, but the mandatory pretreatment and long reaction time during hydrolysis are the major obstacle of the process [158]. Diluted acid hydrolysis is mainly used as a pretreatment for enzymatic hydrolysis. Inherited problem of diluted acid hydrolysis for enzymatic hydrolysis is

that the secondary products inhibit the activity of the enzymes. Alkali reagents such as NaOH are also employed for lignin depolymerization in Kraft pulping for papermaking process.

Both acid and base have been used with lignocellulosic biomass for different purposes. Since acid and base generally used for different targets in biomass, the combination of them seems promising. The first step acid or base could depolymerize polysaccharide or lignin, respectively, leaving the biomass substrate with high content of lignin or polysaccharide for second step treatment. Therefore, an effort to explore combination of acid and base is initiated in this work.

Typical acid and base reagents in lignocellulosic biomass conversion involve mineral acid and base such as H_2SO_4 , HCl, NaOH, Na_2S , etc. When these mineral reagents are disposed, they release inorganic substance into surrounding environment. This work proposes the use of organic acid and base instead of inorganic ones. However, the effects of organic acid or base types are not explored in this study. Oxalic acid and tetramethylammonium hydroxide (TMAH) were selected as a representative organic acid and base, respectively. The pK_a of organic acids are considerably weaker than a very strong acid such as H_2SO_4 . From pK_a values of various common acids: sulfuric acid (H_2SO_4 , pK_a -3, 1.9 [159]), phosphoric acid (H_3PO_4 , pK_a 2.12 [160]), oxalic acid ($(\text{COOH})_2$, pK_a 1.23, 4.19 [161]), formic acid (HCOOH , pK_a 3.77 [161]), acetic acid (CH_3COOH , pK_a 4.76 [162]), the strongest organic acid is the oxalic acid with the lowest pK_a range among organic acids [163]. For organic base, the exact pK_b values of many base compounds are unavailable. A set of simple experiment, shown in Table 4.1, was carried out with microcrystalline cellulose to test conversion in comparison with conventional NaOH. The results show that conversion by 10 % TMAH is comparable to 3 % NaOH at the testing conditions.

The specific objective of Chapter 4 is to explore a sequential combination of oxalic acid and tetramethylammonium hydroxide treatments for converting lignocellulosic biomass, specifically wood, into valued-added chemical feedstocks such as fermentable sugars, furanic compounds, and phenolic compounds.

Table 4.1 Effect of base type on conversion of cellulose at 120°C.

Base		3%	10%	10%	25%
		NaOH	TMAH	Piperidine	Tripropylamine
% Conversion	30 min	34.6	36.5	6.1	8.8
	1h	44.0	38.8	12.2	7.8

4.1 Conversion of Biomass in Single-Step Reactions

4.1.1 Effects of Reaction Time and Temperature

Effects of reaction time and temperature in acid and base conversion of single step reaction are shown in Figure 4.1 and 4.2, respectively. It can be seen that temperature shows significant effects on both oxalic acid and TMAH conversion of spruce, whereas reaction time slightly improve conversion of TMAH. This is in agreement with literature that both temperature and acid concentration affect hydrolysis rate of cellulose [23, 27] and that rate of acid hydrolysis increases remarkably with increasing temperature [71, 164]. Reaction time, in the range shown in Figure 4.1, do not significantly affect the oxalic acid reaction, probably because the reaction has level off in the operated range. At 180 and 215 °C, the conversion by oxalic acid was dropped as the reaction proceeded. This could be the result of the oxalic acid degradation at high temperature. Product degradation could also become more pronounced at high temperature. It is reported that monosaccharide degradation takes place more rapidly than hydrolysis at higher temperature [71, 75]. The

hydrolyzed cellulose may form nonhydrolyzable oligomers that cannot be converted to glucose [165]. Glucose can also recombine with acid-soluble lignin in hydrolysate, forming a lignin-carbohydrate complex [27]. These glucose reactions take place simultaneously and may explain the conversion as the effects of reaction time and temperature. Conversion by base treatment in Figure 4.2 proceeded positively with time.

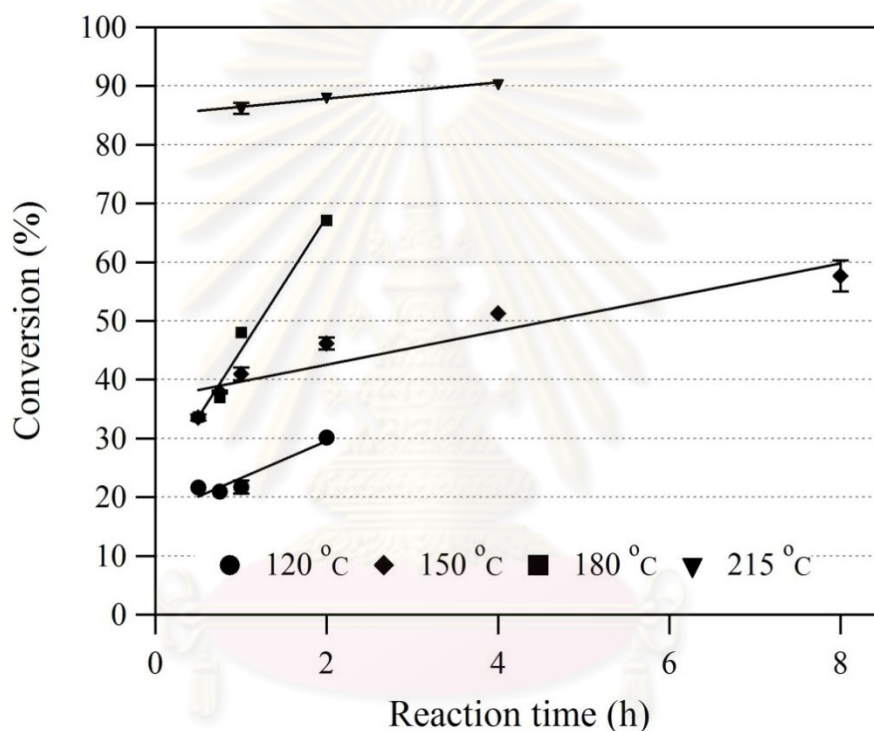


Figure 4.1 Conversion of single-step oxalic acid reaction at various reaction times and temperatures.

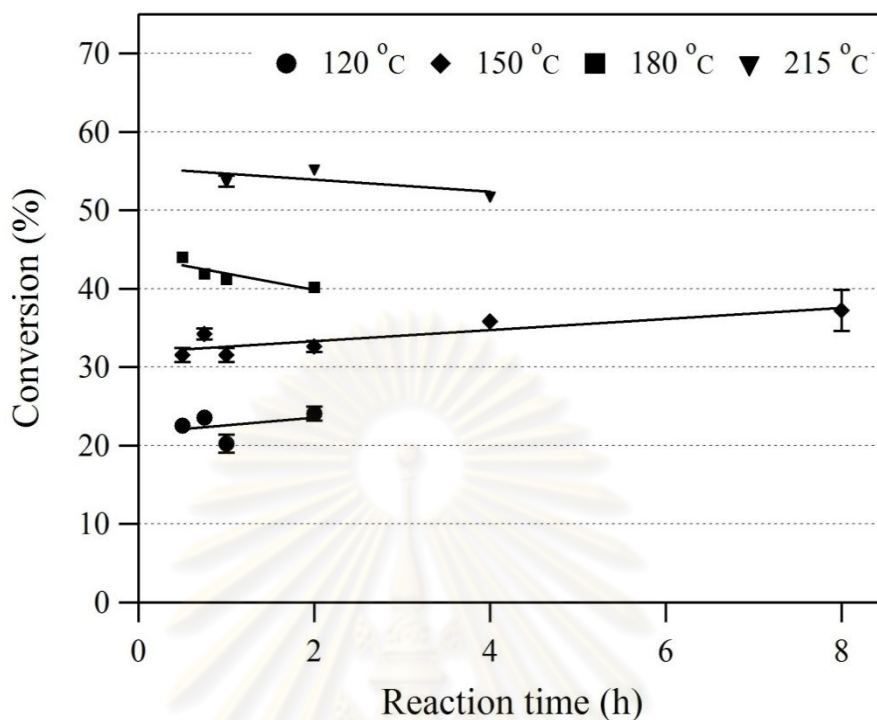


Figure 4.2 Conversion of single-step TMAH reaction at various reaction times and temperatures.

Other parameters was also studied for hydrolysis as follows. The kinetics of cellulose hydrolysis also strongly depend on the physical state of cellulose affected by temperature and acid concentration. Beyond the transitional severity, the hydrogen bonds in cellulose becomes unstable, allowing hydrolysis at higher rate [27]. Hydrogen ion concentration slightly affects the hydrolysis rate [164]. Reactor configuration affects monosaccharide yields as well. In bed-shrinking flow-through reactor, the glucose yields were 50-100% increased from that in batch reactors and percolation reactors [27]. Reactor materials such as stainless steel and iron also catalyze degradation of sugars [166]. Operation over a long reaction time leads to degradation of sugars as well [167]. These reasons explain the limited hydrolysis in lignocellulose.

The maximum glucose yields usually occur in high temperature at short reaction time such as 2-10 min [164, 168], which is difficult to operate on the instrument. Since optimization of processes parameters are not the objective of this work, it is better to use long reaction time for repeatability due to variation of elapsed time for reactor attachment to the shaker and time for heating up of the reactor between each experiments. Therefore, the sugar yields reported in this work is not the optimized and maximum values from the process.

4.1.2 Reaction of Polysaccharides by Oxalic Acid and TMAH

Monosaccharides obtained from hydrolysis in aqueous phase can be detected by GC-FID via derivatization to their oxime-TMS and TMS derivatives. The chromatograms of typical single step reaction are shown in Figure 4.3. Identification of main peaks in GC-FID chromatogram is shown in Figure 4.4. Hydrolysis reaction with water was conducted and used as a control experiment, where only small amounts of xylose and arabinose were identified. The standard error of sugar analysis ranged between 0.01 and 1.10%. From the acid reaction, the detectable products are xylose, arabinose, galactose, mannose, glucose, hexose derivatives, and cellobiose at retention time 6.6, 6.8, 10.4, 10.5, 10.6, 13, and 14.2 min, respectively. This observation is consistent with literature that reported oxalic acid as a diffusible proton donor for enzymatic and non-enzymatic hydrolysis of polysaccharides in lignocelluloses [86]. Furthermore, decomposition of oxalic acid gives carbon dioxide and formic acid, which has recently been reported as another proton donor [169].

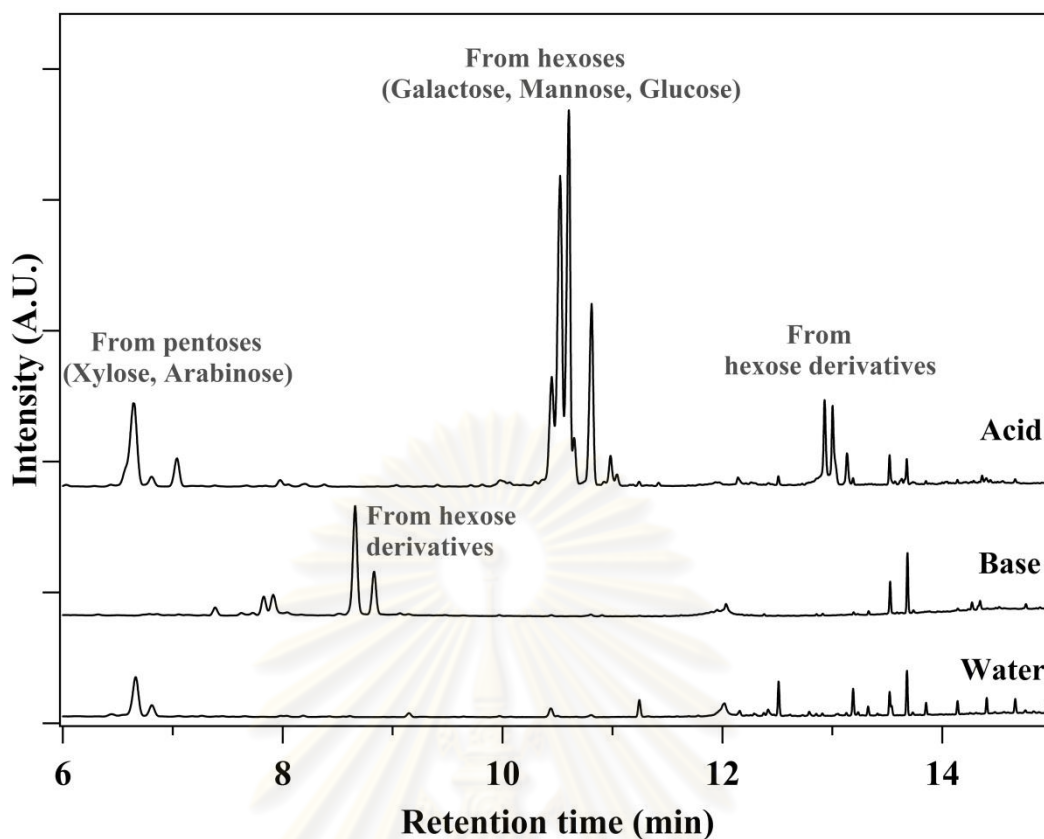


Figure 4.3 GC-FID chromatogram of liquid products from biomass in single-step reaction with acid, base, or water alone at 150 °C for 2 h.

As for base reaction, monomeric sugar derivative peaks, at retention time 8.6 and 8.8 min, is the main carbohydrate-derived product. There was no monosaccharide found from base reactions. Depolymerization of polysaccharides by TMAH may proceed via chain cleavage and peeling reaction during alkaline hydrolysis, similar to that in Kraft pulping process, resulting in oligomeric and monomeric sugar derivatives from polysaccharides. In peeling reaction, monomer of polysaccharides is cleaved one-by-one at its reducing end. The alkaline hydrolysis results in chain fragmentation and generation of new reducing end groups available for the peeling reaction. To the best of our knowledge, there is no literature related to mechanism of polysaccharides depolymerization by TMAH within the range of conditions used in this work. The identification was suggested by mass spectroscopy that both peaks are 2-keto-D-gluconic acid, shown in Figure 4.4. Based on

identification by reaction with standards and model compounds, both peaks are derived from hexoses and cellulose. The 2-keto-D-gluconic acid is likely to form by peeling reaction, and possibly rearrangement.

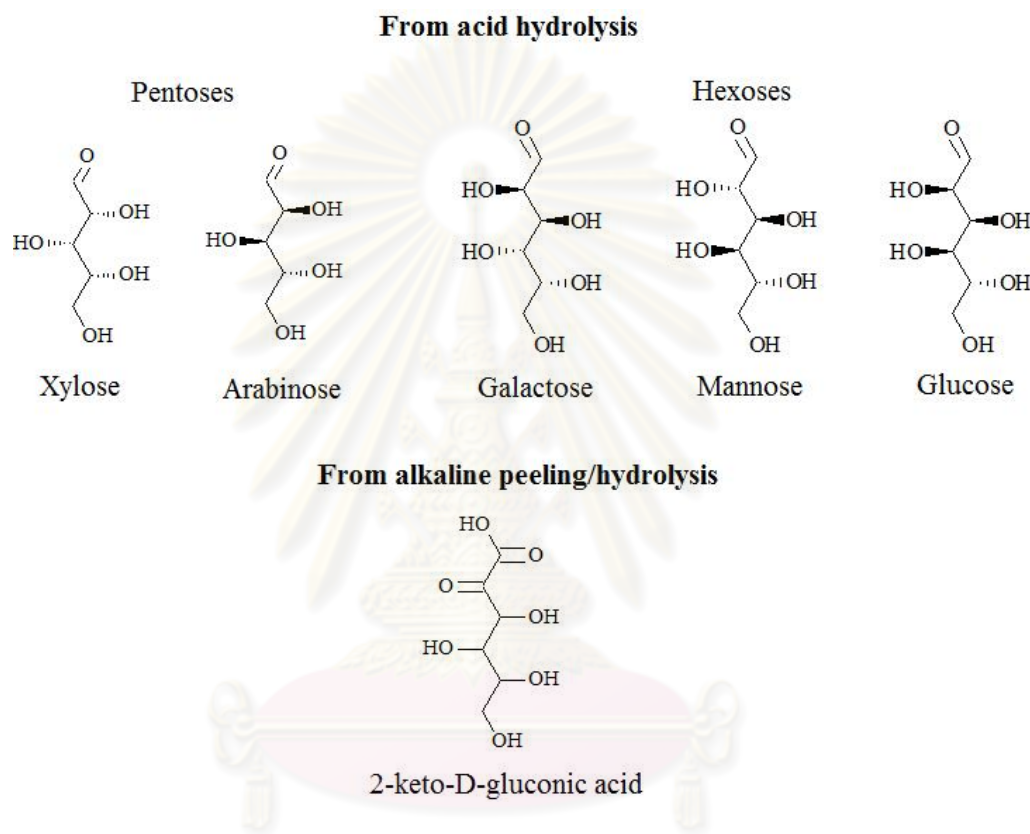


Figure 4.4 Identified compounds in GC-FID of oxalic acid and TMAH reaction with spruce.

It is important to note that the method of sugar analysis in this work is focused on analysis of monosaccharide; besides monosaccharides, only cellobiose disaccharide was identified by the current method. It is very likely that there are other dimers, trimers, and oligomers in liquid products because the glycosidic bond cleavage can occur at any ether bridge bond in polysaccharides by acid. Although the oxime-TMS derivatization technique is able to analyze di- and trisaccharide [170-

173], the method used in this study (the oven temperature, derivatization conditions, derivatization reagent, and GC system) was not optimized for oligomer analysis.

4.1.3 Reaction of Lignin by Oxalic Acid and TMAH

In addition to sugar analysis, liquid products were also analyzed for less polar compounds such as monomeric lignin precursors, which can be detected by GC after extraction with toluene to separate nonpolar phenolic compounds from aqueous liquid products. This toluene-soluble fraction was analyzed by GC-MS. Table 4.2 shows relative amounts of toluene-soluble compounds, reported as weight percentage based on the total spruce and assuming the GC-FID response factor of all compounds in this table equal to that of furfural.

Table 4.2 Relative amount of toluene-soluble compounds analyzed by GC-MS*.

Compounds	Reaction conditions			
	150 °C, 2 h		215 °C, 2 h	
	Acid	Base	Acid	Base
Furfural	2.12%	-	0.81%	-
5-Methylfurfural	0.10%	-	0.13%	-
Phenolics compounds	0.17%	-	0.22%	5.41%

*The response factor of each compounds are assumed to equal to that of furfural.

From oxalic acid reaction, furfural and 5-methylfurfural were detected from single step oxalic acid reaction. This result reveals that monosaccharides liberated from acid reaction undergo secondary reactions. For example, 5-hydroxymethylfurfural is derived from dehydration and acetal formation of glucose, as also reported in the literature [174, 175]. Phenolic compounds are also detected

indicating that the oxalic acid can cleave bonds between lignin monomers, possibly the α -aryl ether bond that is most susceptible to cleavage by acid via mechanisms shown in Figure 1.18 [92].

The TMAH reaction resulted in several phenolic compounds such as 1,2-dimethoxybenzene and 2-methoxyphenol at high temperature (215 °C), as shown in Table 4.2. Phenolic compounds detected from liquid product by base reaction could be derived from ether bond cleavage of lignin, since TMAH has been reported to break β -O-4 aliphatic aryl ether bonds in lignin [112]. TMAH reaction at 150 °C do not give phenolic compounds. This is probably because the liberated lignin is in oligomer form, which is not detected well in GC instrument.

4.1.4 Hydrolysis of Hemicellulose and Cellulose

The amount and types of liberated monosaccharides from acid reaction at 150 °C implies that hydrolysis of both hemicellulose and cellulose may contribute to the observed sugars. Since glucose can be found in both hemicellulose and cellulose, the amount of glucose originating from hemicellulose has been estimated based on the following information. In white spruce, the major types of hemicelluloses are O-acetyl-galactoglucomannan and arabino-4-O-methyl-glucuronoxylan, approximately 18 and 13% of extractive-free wood, respectively [38]. Therefore, arabino-4-O-methyl-glucuronoxylan should be the main contributor for xylose and arabinose. Its structure consists of β -D-xylopyranose polymer, with some 4-O-methyl- α -D-glucuronic acid and small amount of α -L-arabinofuranose terminal. The ratio of β -D-xylopyranose : 4-O-methyl- α -D-glucuronic acid : α -L-arabinofuranose is 10 : 2 : 1.3. The mannose and galactose should primarily depolymerized from O-acetyl-galactoglucomannan. In water-soluble galactoglucomannan, the ratio of α -D-galactopyranose : β -D-glucopyranose : β -D-

mannopyranose is 1 : 1 : 3, while this ratio is 0.1 : 1 : 3 in alkali-soluble galactoglucomannan. The difference in these two types of galactoglucomannan is the amount of terminal galactose attached to the glucomannan backbone. However, the ratio of glucose : mannose is constant at 1 : 3. Based on this information, the amount of glucopyranose liberated from hemicellulose can be estimated to be equal to 1/3 of the mannose, assuming the rate of depolymerization of them is the same.

Table 4.3 shows the weight percentages of sugars derived from hemicellulose and cellulose in the liquid products based on this simple calculation, noted that the percentages are on the basis of total mass of the starting wood. In the first step of acid reaction, the reaction time and temperature significantly affect the yield of sugars, possibly by the secondary reactions that degrade the liberated monosaccharides. Without degradation, hydrolysis by oxalic acid in one-step reaction at 150 °C is specific to hemicellulose, which is in agreement with literature [87]. When reaction time at 150 °C was extended from 30 min to 8 h, yields of sugars from hemicellulose were reduced. Increasing reaction temperature to 180 °C also decreased sugars yields. At 215 °C, there is only small amount of sugars derived from cellulose implying that the sugars from hemicellulose may be completely degraded. Noted that cellobiose was detected from 215 °C reactions. The presence of cellobiose indicates the cleavage of glycosidic bonds in cellulose structure at this temperature (215 °C) since the possible disaccharides derived from two main hemicelluloses are xylobiose, xyloarabinose, mannobiose, mannoglucose, and mannogalactose, as shown in Figure 4.5.

Table 4.3 Weight percentage of sugars derived from hemicellulose and cellulose in single-step reaction.

Experiments	% Conversion	Wt% sugars (hemicellulose)	Wt% sugars (cellulose)
A, 150 °C, 30 min	31.6	24.2	0.7
A, 150 °C, 45 min	34.3	19.5	0.1
A, 150 °C, 1h	31.5	15.4	1.9
A, 150 °C, 2h	32.7	13.1	3.4
A, 150 °C, 4h	35.8	3.0	2.4
A, 150 °C, 8h	37.2	2.0	1.2
A, 180 °C, 2h	40.2	3.3	2.5
A, 215 °C, 1h	53.8	-	0.1

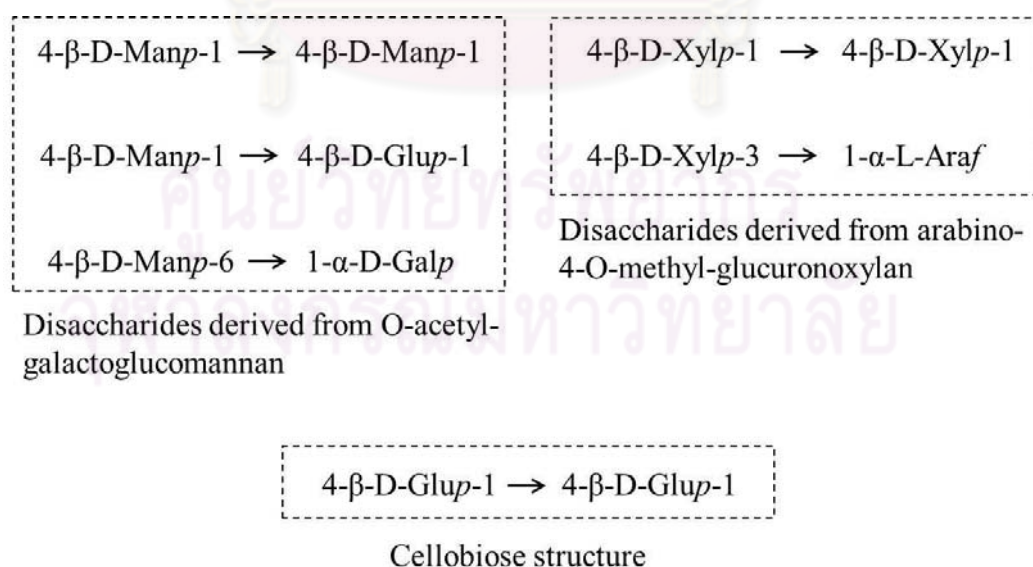


Figure 4.5 Structure of possible disaccharides derived from softwood hemicelluloses in comparison with cellobiose structure.

4.1.5 Effect of Reaction Time on Sugar Degradation

Sugar yields from oxalic acid and TMAH reactions at 150 °C and various times are shown in Figure 4.6 and 4.7, respectively. For reaction by oxalic acid, monomeric sugars from hemicelluloses are liberated and degraded with reaction time. Glucose was cleaved from hemicellulose then increased due to cellulose cleavage and degraded as well. The degradation products from pentoses and hexoses such as furfural and 5-methylfurfural, respectively, was detected by GC-MS as shown in Table 4.2. The relative amount of two hexose derivatives derived from TMAH reaction was in the same range regardless of increasing conversion as shown in Figure 4.2, suggesting that there is degradation of the products in TMAH solution in a similar rate with the peeling rate.

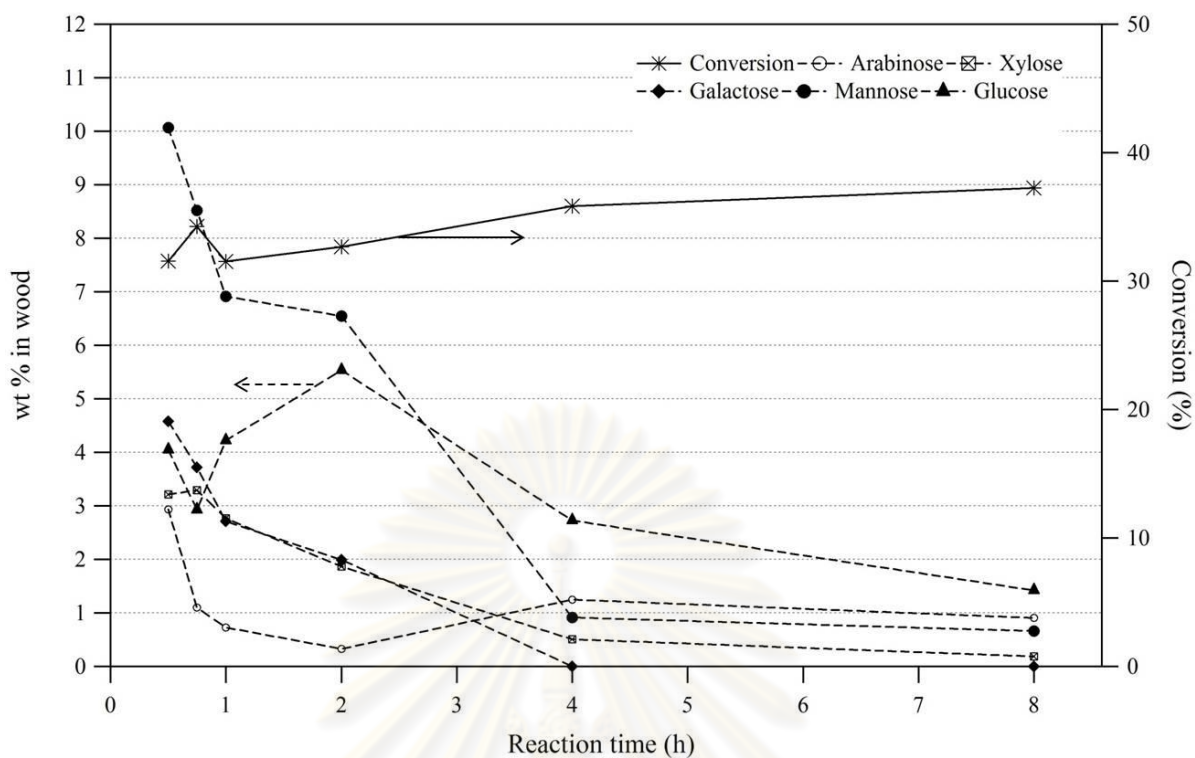


Figure 4.6 Monomeric sugars yield from oxalic acid reactions with spruce at 150 °C, various reaction time.

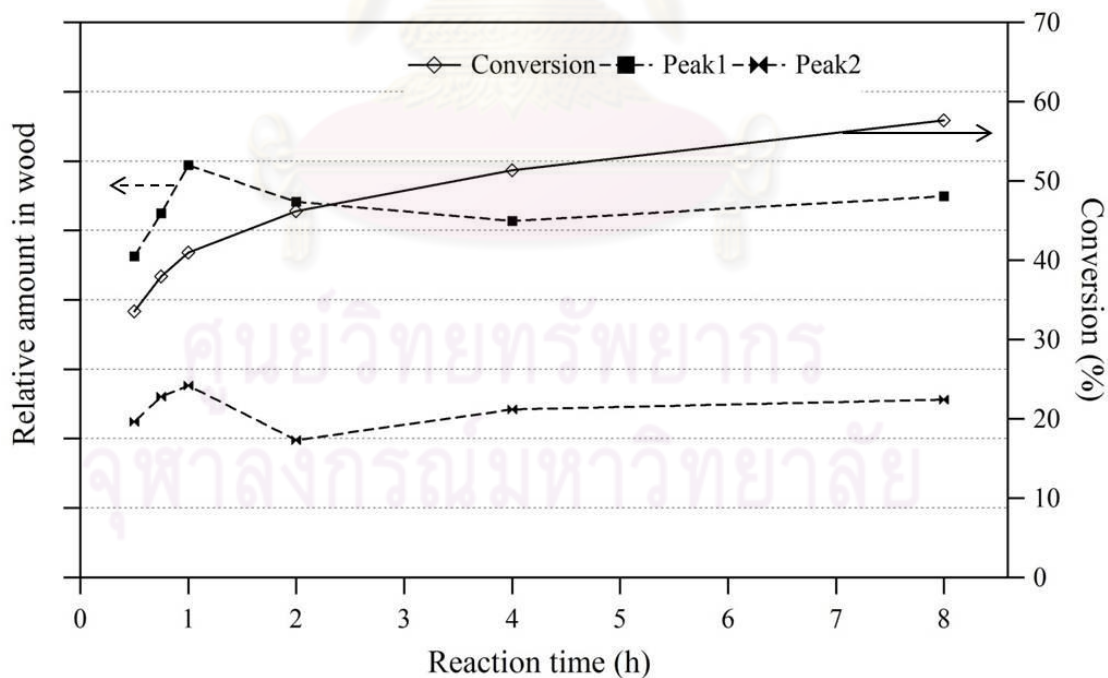


Figure 4.7 Relative yield of hexose derivatives from TMAH reactions with spruce at 150 °C, various reaction time.

4.1.6 Effect of Reaction Temperature on Sugar Degradation

Degradation of monomeric sugars was observed in oxalic acid reaction with a short further heating at the end of the experiment. A set of experiment with oxalic acid and spruce at 150 °C, 2 h was carried out. At the end of the experiment, the reactor was further heated up to 180-220 °C and kept at these temperature for 5 and 10 min. The results on sugar yields are presented in Figure 4.8. It can be seen that by adding secondary hydrolysis at 180 °C, 5 min, the amount of arabinose and glucose peaks were higher, but that of xylose and mannose were slightly lower than the original acid case at 150 °C, 2h. When the time at 180 °C was extended to 10 min, the increase of the glucose peaks were more prominent, while yields of other sugars decrease. The secondary reaction at 200 °C, 5 min shows the same effects to the amount of sugars as previous one. However, when the time at 200 °C was extended to 10 min, the amount of all the sugars apparently diminished. Degradation of sugars leads to lower sugar yields. The higher sugars yields may result from hydrolysis of the solid remaining spruce or oligomer in the hydrolyzate. The results are correspond with literature that the degradation rate may become higher than the hydrolysis rate as the temperature increases [71, 75].

The two-step acid hydrolysis was normally used mainly for the determination of total carbohydrate in biomass [77-80]. There are also experiments on two-step acid hydrolysis of biomass in order to hydrolyze hemicelluloses in the first step, and then hydrolyze cellulose in the second step [27, 176-178]. Without removal of liquid product in the first step, the generated sugars could quickly degrade as shown in Figure 4.8. In this work, the two-step acid-acid reactions are used and analyzed in each step in order to compare with acid-base combination.

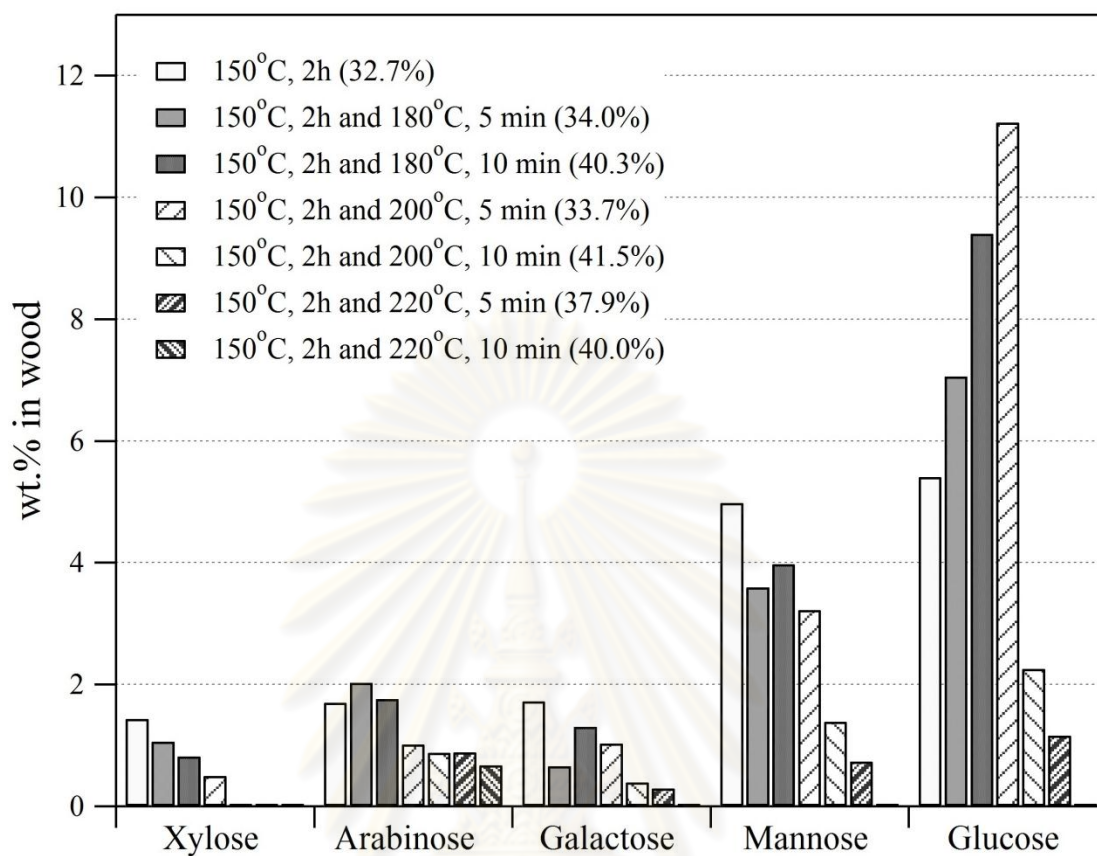


Figure 4.8 GC-FID chromatogram of (a) oxalic acid reaction at 150 °C, 2h, (b) followed by 180 °C, 5 min, (c) followed by 180 °C, 10 min, (d) followed by 200 °C, 5 min, (e) followed by 200 °C, 10 min, (f) followed by 220 °C, 5 min, (g) followed by 220 °C, 10 min. Numbers in parentheses are the % conversion.

4.2 Conversion of Biomass in Two-Step Reactions

As the initial phase of exploring the new process, the synergistic of the process was studied first to determine whether the process is promising. With an intention of using the solid residue from the first step treatment as a starting material for the second-step treatment, mild temperature was preferred in order to combine solid residue to the same amount as those in the first step to keep the same solid-to-liquid ratio in both steps. Therefore, the condition was fixed at 150 °C, 2 h for each step, and 1 atm of N₂ at room temperature unless indicated otherwise. Noted that some data in this chapter has been published in *Energy & Fuels*, Volume 24, 2010 [179].

4.2.1 Evidence of Synergy from Total Conversion

Conversions of the spruce were determined from solid residue weight after reactions and neutralization of the liquid products. Table 4.4 shows conversions in single- and two-step reactions at 150 °C. For the single-step reactions, the conversion by hydrolysis with the following reagents increased in the order of: water < 10% oxalic acid < 10% TMAH. This is consistent with the general trends reported for acid and base hydrolysis in the literature [82].

On the other hand, a different trend was observed in the two-step hydrolysis reactions, where certain combinations of acid and base treatments can give much higher conversion of the biomass that cannot be achieved by prolonged treatments with either the acid or the base alone. As shown in Table 4.4, the overall biomass conversion by the two-step hydrolysis reactions increased in the order of A-A < B-B ≈ B-A < A-B. There was no direct comparison of conversion with the present work on the two-step tests found the literature.

Table 4.4 Conversions of spruce by single- and two-step reactions at 150 °C, 2 h.

	Conversion (%)						
	Water	Acid	A-A	B-A	Base	B-B	A-B
1st-step	18.5	32.7	-	-	46.2	-	-
2nd-step	-	-	9.9	25.0	-	26.5	51.1
Overall	-	-	39.3	59.6	-	60.5	67.1
Standard Error (%)	0.2	0.7	2.5	2.1	1.1	2.7	1.6

Sequential combinations of acid and base treatments clearly exhibited a positive promoting effect compared to the two-step reactions with either acid or base alone. For the conversion for each step shown in Figure 4.9, the conversion with acid in the second step after base (B-A, 25.0%) was more than twice of that by A-A, and that by base reaction of A-B (51.1%) was almost twice of that by B-B. The A-B conversion in the second step was also higher than that in the first step of B. When the same reagent was applied in the two-step reactions, conversion from acid reaction dropped from 33% in the first step to 10% in the second step, while conversion from base reaction in the first step (46%) decreased to 27% in the second step. This could be due to limited accessible sites (hemicellulose/cellulose/lignin) for acid and base. Using acid after base can increase accessibility for acid in the second step. In the same manner, base may be able to access more sites in the second step after acid reaction in the first step. Simple comparisons of conversions implied the different chemistry of hydrolysis between acid and base. This is further clarified by the following analysis of liquid and solid products.

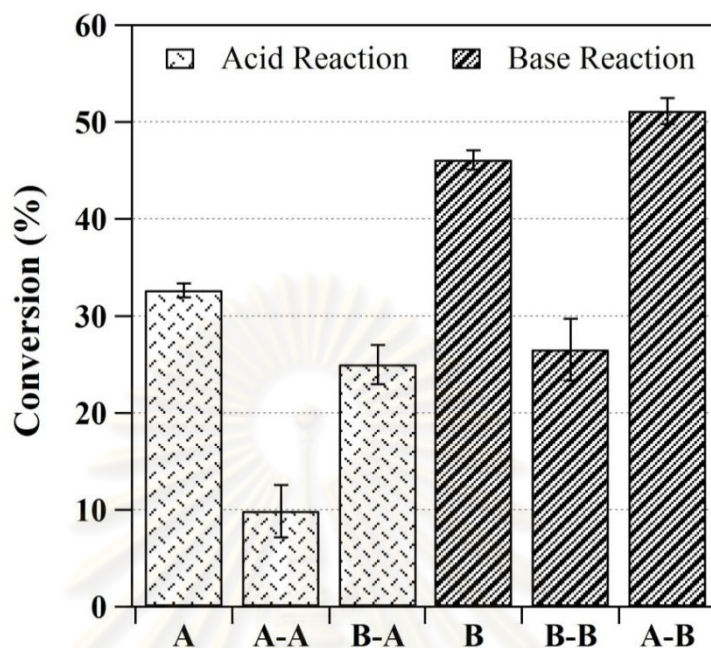


Figure 4.9 Conversion by one and second step of spruce by oxalic acid and TMAH.

4.2.2 Evidence of Synergy from Analysis of Liquid Products

From GC-MS of extracted liquid products, furfural was observed from B-A reaction, with the concentration of 0.79% (w/w), but not from A-A reaction. This could be due to low hydrolysis capability in the second step acid hydrolysis, since these furfural compounds are produced from degradation of monosaccharides generated from hydrolysis.

From GC-FID of derivatized sugars, weight percentages of sugars derived from hemicellulose and cellulose from acid reactions from one- and two-step reactions are shown in Table 4.5. Considering the two acid reactions at 150 °C for 2h (A and A-A), a clear contrast is spotted. A-A yields less sugars from hemicellulose (2.9%), while slightly more from cellulose (5.6%) than A. This result confirms the fact that hemicellulose can readily be hydrolyzed while cellulose is more resistant to hydrolysis, in agreement with several literature [71, 74, 76, 167, 176, 180].

Hemicellulose is susceptible to acid hydrolysis because of amorphous structure [180] and weaker bond in hemicellulose [167]. B-A reaction produces slightly lower yield of hemicellulose than A, suggesting that some hemicellulose may be removed from the wood during the first step by base reaction and lack of synergy in B-A reaction based on polysaccharide conversion.

Table 4.5 Weight percentages of sugars derived from hemicellulose and cellulose from acid reactions of one- and two-step reactions.

Experiments	Wt% sugars (hemicellulose)	Wt% sugars (cellulose)
A, 150 °C, 2h	13.1	3.4
A-A, 150 °C, 2h	2.9	5.6
B-A, 150 °C, 2h	10.0	3.3

Sugar yields from acid reactions at 150 °C based on the total weight of wood are shown in Figures 4.10. The sugars from B-A was comparable to the single-step acid, but higher than that from A-A. At higher temperature of 215 °C, although the sugars are degrading at this temperature, higher glucose yields from B-A compared to A-A suggests that the sugars liberated from hydrolysis of B-A is higher than from A-A (Figure 4.11).

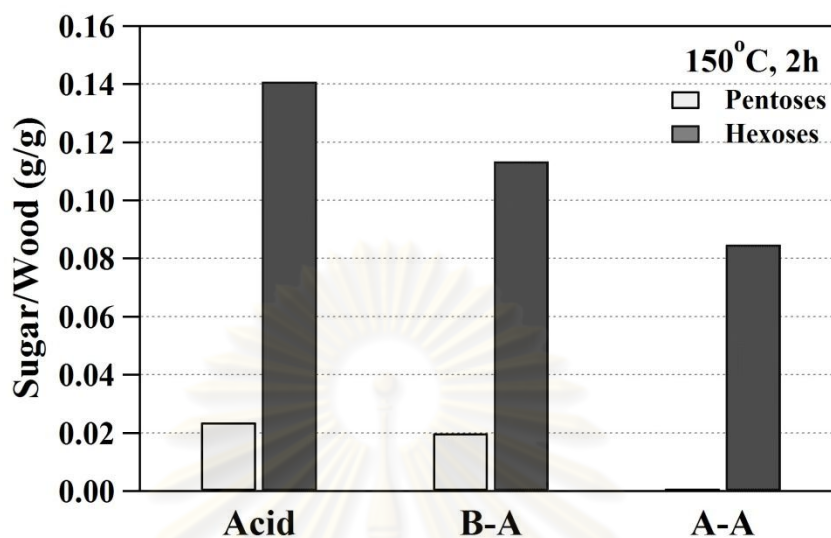


Figure 4.10 Monomeric sugars yield from acid reactions of spruce at 150 °C, 2 h.

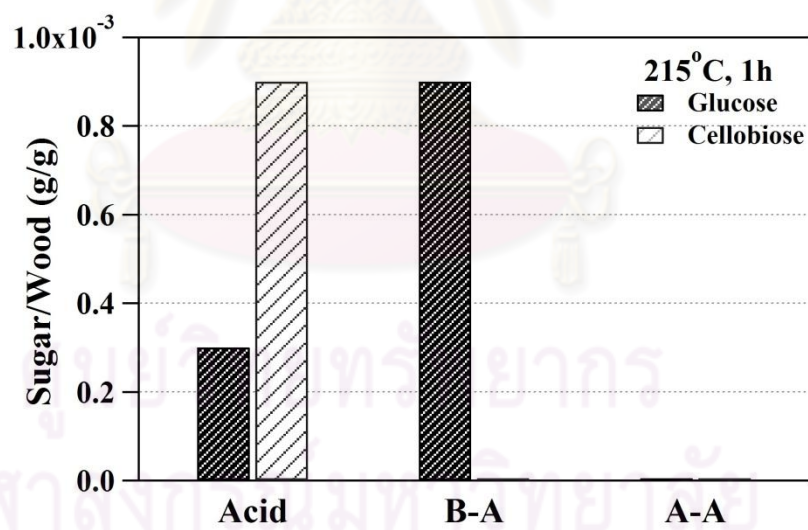


Figure 4.11 Monomeric sugars yield from acid reactions of spruce at 215 °C, 1 h.

For base reactions, the chromatogram of liquid samples after derivatization is shown in Figure 4.12. Accurate quantification was not possible without standard of the 2-keto-D-gluconic acid, but based on relative peak area comparison, it is observed that A-B reaction yields the 2-keto-D-gluconic acid most. A positive effect of the sequential combination was confirmed for A-B reaction. High conversion of A-B was achieved in agreement with the results of products analysis.

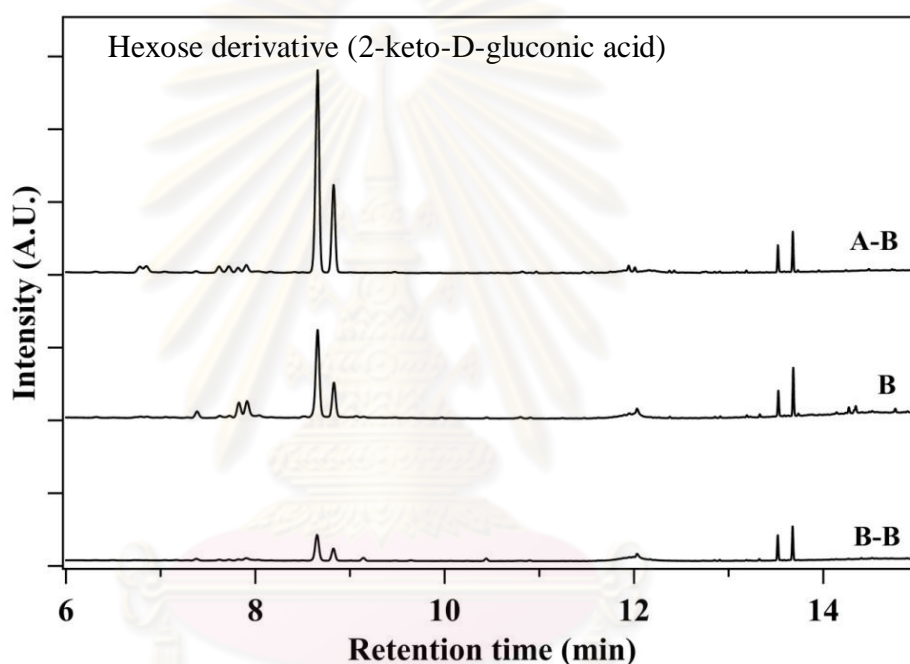


Figure 4.12 GC-FID chromatogram of liquid products from base reactions of spruce at 150 °C, 2 h.

From conversion and liquid products analysis, specific combination of acid followed by base was the most effective combination for spruce conversion. Acid and base treatments produce different monomers. The monomeric product from base treatment was not previously identified in literature. Therefore, existing knowledge does not account for the synergy and product from the acid-base sequential combination.

4.2.3 Evidence of Synergy from Analysis of Solid Products

Solid products were analyzed by Py-GC-MS and ^{13}C -NMR. For Py-GC-MS, several characteristic ion masses (m/z) were selected to identify certain compounds from the total ion chromatogram. Details of the selected characteristic ion masses are shown in Table 4.6.

Table 4.6 Selected characteristic ion masses from Py-GC-MS of biomass residue.

m/z	Origin	Type	Compounds
43	Polysaccharides	Aliphatic compound	Acetaldehyde and acetic acid
55	Polysaccharides	Anhydrosugar pentofuranose	5-Methyl-2(5H)-furanone
60	Polysaccharides	Anhydrosugar hexopyranose	1,6-Anhydro- β -D-glucopyranose
96	Polysaccharides	Anhydrosugar pentofuranose	2-Furancarboxaldehyde
98	Polysaccharides	Anhydrosugar pentofuranose	2-Furanmethanol
112	Polysaccharides	Cyclopentene-type compound	2-Hydroxy-3-methyl-2-cyclopenten-1-one
94	Lignin	Phenol	Phenol
107	Lignin	Alkylated phenol	4-Methylphenol
109	Lignin	Guaiacol	2-Methoxyphenol
110	Lignin	Catechol	1,2-Benzenediol
137	Lignin	Alkylated guaiacol	2-Methoxy-4-methylphenol
151	Lignin	Aldehyde/ketone side-chain guaiacol	4-Hydroxy-3-methoxy-benzaldehyde
164	Lignin	Propenyl guaiacol	2-Methoxy-4-(1-propenyl)-phenol

A typical total ion chromatogram of pyrolysis-GC-MS from solid residues (Figure 4.13) exhibits a broad peak for carbohydrates derived from polysaccharides at around 28-31 min, which is significantly larger than other small peaks from carbohydrates. In contrast, several peaks from lignin-derived phenolic compounds appear with similar intensities. From all other ion chromatograms of other samples, chemical composition of all the samples contains similar types of structural units derived from lignin and polysaccharides.

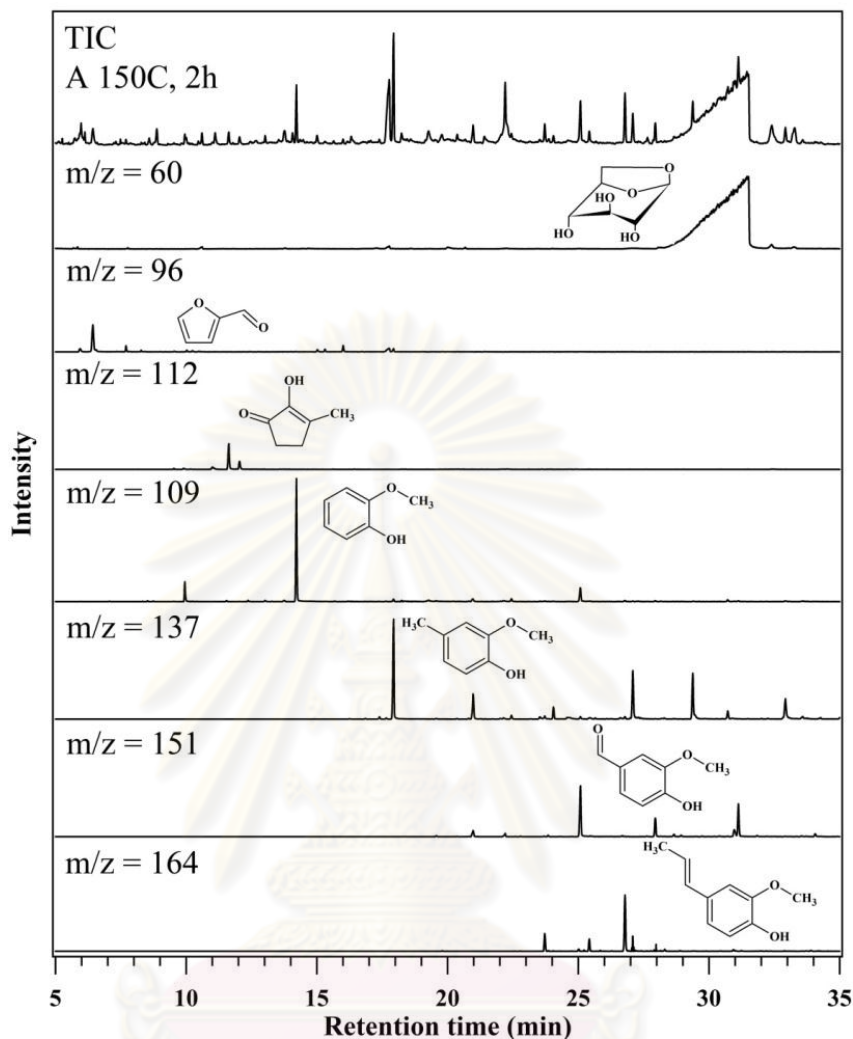


Figure 4.13 Example of selective ion chromatogram from single-step acid reaction of biomass at 150 °C for 2 h.

Since the peaks intensities depend on amount of material used in pyrolysis, which had been weighed 0.1-0.3 mg for analysis by Py-GC-MS. The accuracy of sample weight measurement was critical and carried uncertainty for very small samples. Also, there are some unidentified peaks where their origins cannot be determined.

In order to compare the intensities across different samples, the ratio of peak area of carbohydrates to lignin in solid residues (denoted as P/L ratio), shown in Table 4.7, was used instead of area% or absolute area. This type of comparison should be regarded as semi-quantitative, because it did not consider the difference in response factor of each compound.

Table 4.7 Polysaccharide-to-lignin ratio of solid residues from biomass reactions at various conditions based on peak area by Py-GC-MS analysis.

Sample	P/L
Spruce	1.6
W, 150 °C, 2h	2.9
A, 150 °C, 2h	3.2
B, 150 °C, 2h	9.9
A-A, 150 °C, 2h	2.9
A-B, 150 °C, 2h	1.3
B-A, 150 °C, 2h	30.9
B-B, 150 °C, 2h	42.0
W, 215 °C, 1h	3.8
A, 215 °C, 1h	0.9
B, 215 °C, 1h	24.2

P/L ratio for solid residues from single-step reactions increases from 1.6 (Spruce) to 9.9 and 24.2 for base reactions at 150 °C and 215 °C, respectively. This increasing trend of P/L ratio is more likely due to reduction of lignin by base reaction. Although there was no lignin monomer observed from toluene extraction by base reaction at 150 °C, an increase in P/L ratio shows that lignin potentially be fragmented from the biomass, but not in the forms of lignin monomer. Unexpectedly, P/L ratios of reactions with water and acid at 150 °C and water at 215 °C are slightly higher than that of original spruce. This increase, although relatively small, is not consistent with the results from liquid product analysis by GC-FID, where we concluded that acid primarily reacts with carbohydrates under these conditions. This could be due to swelling effect from water and acid that allows more cellulose in solid residues to be pyrolyzed. As for acid reaction at 215 °C, on the other hand, P/L ratio decreased from the initial spruce, suggesting considerable conversion of polysaccharides during the hydrolysis reaction. Again, the information from Py-GC-MS analysis of solid residue from single-step reactions confirms selectivity of oxalic acid to polysaccharides. TMAH is more preferentially reacting with lignin, even though it can react with both lignin and polysaccharides. These trends in P/L ratios sufficiently confirmed the different features between acid and base treatment in the single step. It is better demonstrated at 215 °C with greater changes in the P/L ratios.

P/L ratios for two-step reactions can be better interpreted based on ^{13}C Solid-NMR results. Figure 4.14 shows solid-state ^{13}C CPMAS NMR spectra of solid residues after two-step reactions at 150 °C for 2 h with the original spruce as reference. The NMR signals are assigned to the different wood components according to the literature [181-185] as follows: methyl carbon of acetyl group in hemicellulose at 22 ppm; aryl methoxy carbon in lignin at 56 ppm; cellulose C-6 at 63 ppm;

cellulose C-2, 3, 5 at 74 ppm; cellulose C-4 at 89 ppm; cellulose C-1 at 105 ppm; aromatic carbon of lignin in the region between 110-160 ppm; carboxyl carbon of acetyl group in hemicellulose at 172 ppm. The general NMR assignment is also useful to delineate chemical structural changes in solid biomass: aliphatic band in the range of 0-80 ppm; methyl group at 0-25 ppm; methylene carbon at 25-50 ppm; methoxyl group at 50-65 ppm; ether group at 65-80 ppm; aromatic band in the range of 90-170 ppm; catechol type carbon at 142 ppm; phenolic carbon at 152 ppm; carboxyl group at 170-190 ppm; carbonyl group at 190-230 ppm [186].

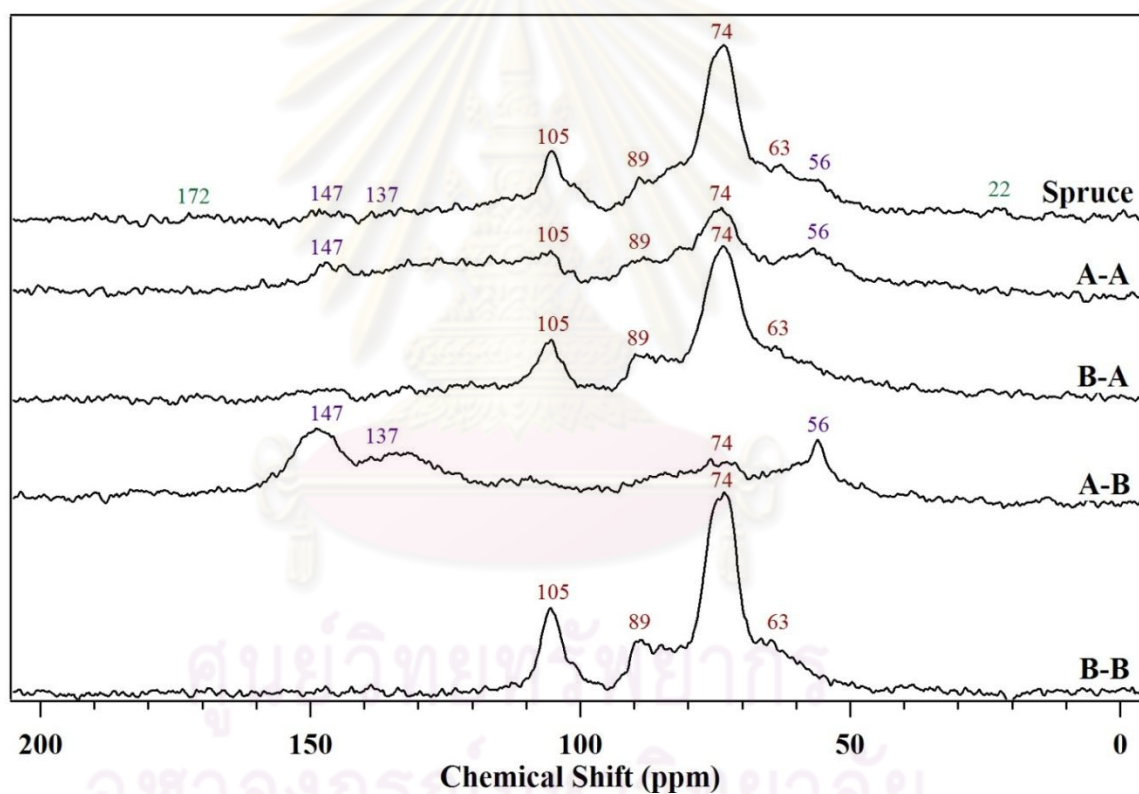


Figure 4.14 ^{13}C CPMAS NMR spectra of solid residues after two-step reactions of spruce at 150 °C for 2 h compared with the original spruce.

In general, the spectra from wood samples shows mainly ether group, methoxyl group, and aromatics. There was very low signal from methyl group, methylene carbon, carboxyl group, and carbonyl group. The decrease of signal from ether group in A-A indicates ether bond cleavage by acid reaction. The signal from ether group almost disappears in residue from A-B, suggesting that TMAH in the second step also plays a role in cleavage of ether bond so that only the signal from lignin was observed in A-B residues. B-A and B-B residues were dominated by ether group suggesting the lignin was cleaved by TMAH in the first step.

The signals from hemicellulose are very weak in all samples because the dominant signals from hemicellulose are from acetyl groups; their content is generally very low in softwood [38, 181]. The hemicellulose signal at 22 ppm disappeared after the treatment by acid or base. The signals from lignin are also weak in the original spruce. However, they slightly increase in A-A residue probably because the decrease in polysaccharides by acid led to increase in lignin concentration in the solid residue, making lignin signals more noticeable. This is in agreement with the lower P/L ratio of A-A residue from that of the first-step acid residue (from 3.2 to 2.9). The lignin signals in B-A remains almost the same in 110-160 ppm range and slightly decreases at 56 ppm, while the cellulose signals slightly increase at 89 ppm, resulting in significantly higher P/L ratio. In A-B residue, the lignin signals at 56, 147, and 137 ppm become strongly intense. In addition to this, surprisingly, the cellulose signals are almost unnoticeable. The P/L ratio of A-B correspondingly decreased to 1.3. The B-B residue shows no significant lignin signal and more intense cellulose signals at 105, 89, and 74 ppm. P/L ratio of B-B is very high due to lignin removal.

The results from GC-FID, Py-GC-MS and NMR are in agreement. For example, the A-B reaction exhibited high conversion of polysaccharides in wood, as is also reflected by the GC-FID results. For solid residue analysis, the results

demonstrate a considerable difference of A-B and B-B results indicating that base reaction in the second step of A-B can remarkably converts cellulose in the biomass. This interpretation is in contrast to the conclusion from the single step reaction that base specifically removes lignin more preferentially to polysaccharide portion in wood. This suggests that the acid reaction in the first step facilitates conversion by base reaction in the second step, probably due to removal of hemicellulose by acid in the first step providing more accessibility to base in the second step. This synergistic effect of sequential acid-base combination leads to enhanced conversion of wood.

From liquid and solid product analysis, formation of glucose indicates cellulose breakdown, while that of galactose, mannose, xylose, and arabionose suggests hemicellulose decomposition by oxalic acid treatment. Reaction with acid in the first step causes more breakdown of hemicellulose and cellulose, as revealed by GC-FID and ^{13}C -NMR. Reaction with base in the first step promotes lignin decomposition without major impact on cellulose as shown by Py-GC-MS and ^{13}C -NMR.

ศูนย์วิทยทรัพยากร
จุฬาลงกรณ์มหาวิทยาลัย

4.3 Conversion of Biomass in Three-Step Reactions

A three-step reaction of A-B-A was also explored in the same manner as the two-step experiments. The result of conversion and sugars yield in comparison with one-, and two-step reaction is shown in Figure 4.15 and 4.16. Actual conversion during the third step of A-B-A was 6.6%, while it was 9.9% in A-A, and 25% in B-A.

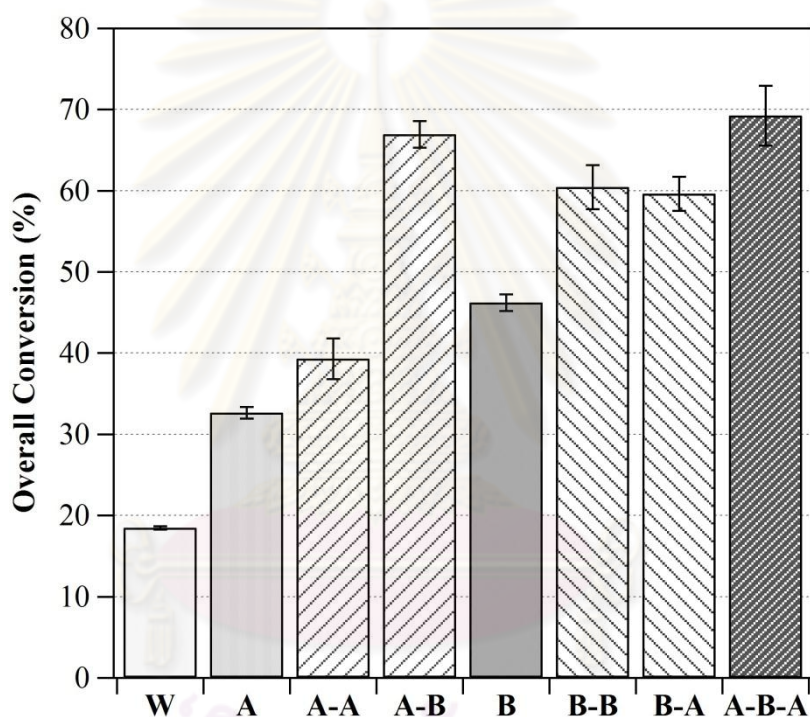


Figure 4.15 Conversions of spruce by single-, two-, and three-step reactions at 150 °C for 2 h.

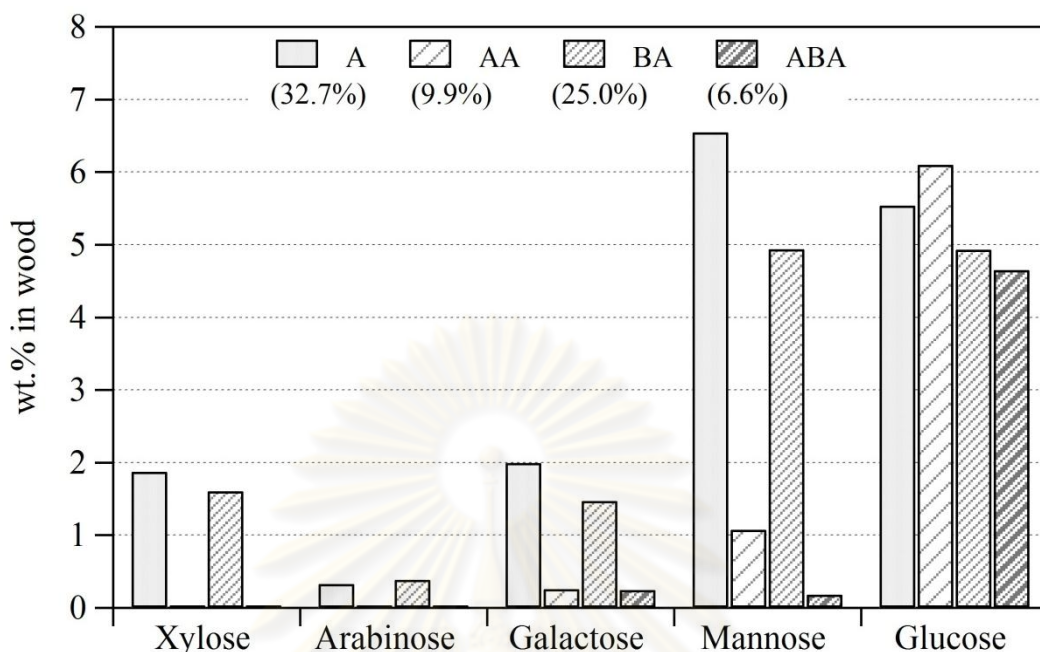


Figure 4.16 Monomeric sugars yield from acid reactions of spruce from single-, two-, and three-step reactions at 150 °C for 2 h. Numbers in parentheses are the % conversion.

Sugar yield of A-B-A (Figure 4.16) shows no significant improvement, except for high ratio of sugar derived from cellulose indicating that the hemicellulose in A-B substrate may have been hydrolyzed during the prior treatments. This is supported by disappearance of hemicellulose signal in ^{13}C NMR result (Figure 4.14), and because the hemicellulose is more susceptible to hydrolysis than cellulose, as concluded in the two-step A-A reaction and in literature [71, 74, 76, 167, 176, 180].

Since there is no evidence supporting the synergy of the treatment of acid after base (B-A, and A-B-A), it is concluded that the synergistic conversion was found on in the case of A-B.

4.4 Decomposition of Oxalic Acid and TMAH

The biomass decomposition into gas products has been investigated qualitatively. The reaction of biomass with TMAH at 150 °C, 2h did not produce observable amount of gas products. In the reaction of biomass by oxalic acid, there was CO and CO₂ formed from the reaction. It is not yet clear whether the gases were formed from biomass or oxalic acid. In order to clarify whether the reagents were decomposed during hydrolysis, the blank experiment with TMAH and oxalic acid reagent were carried out at 150 °C for 2 h. Heating of TMAH reagent alone did not produce any gas at this condition. The pH of the solution did not change and remained higher than 14 before and after reaction. Therefore, degradation of TMAH solution, if any, is expected to be limited within the conditions in this study. Tanczos et al. indicates that TMAH decomposition temperature in the presence of cellulose is about 230 °C [113]. However, oxalic acid is partially decomposed to gas and water-soluble compounds. In the blank experiment using oxalic acid solution heated at 150 °C for 2h, degradation of oxalic acid produced some gas containing mostly CO and CO₂. The amount of gas formed in the reaction of biomass with oxalic acid was in the same order of magnitude with that from oxalic acid in the blank test. The previous work by Kakumoto et al. suggests two main decomposition pathway of oxalic acid producing CO₂ + HCOOH and CO₂ + CO + H₂O [187]. Further quantitative analysis of gas products from biomass decomposition should be conducted in the future study.

Since the process parameters in this study have not yet been optimized, it is possible to further minimize degradation of oxalic acid by using lower temperature and/or shorter retention time. For practical application, recovery and reuse of reagents may become a crucial issue. The issue of reagent recovery should be studied in the future to decrease operation cost. Moreover, the product selectivity is likely to be further improved by tailoring the reaction conditions.

CHAPTER 5

PHYSICAL CONTRIBUTION TO ENHANCE SPRUCE CONVERSION BY ACID AND BASE

Due to the finding of synergistic effect in sequential combination of acid and base treatment of spruce highlighted in Chapter 4, it is interesting to find out the reason contributing to the synergy. Possible contributions to synergistic conversion of the proposed process may involve physical contribution, chemical contribution, or the combination of both. This chapter investigates the physical characteristics of spruce that may be responsible to the aforementioned synergistic phenomena. The physical property that may be responsible for conversion of acid and base is the morphology of the spruce that could be collapse or widen because of the treatment. Also, widening of the spruce pore structure may facilitate the acid and base diffusion and enhance conversion by acid and base. Pre-swelling of the wood structure was carried out to examine effect of enlarged pore structure of spruce. In case of coal, swelling is beneficial pretreatment for coal catalytic liquefaction by expansion of the coal structure [188, 189], facilitating dispersion of catalyst on the coal surface, and improving hydrogen transfer, resulting in higher conversion and better oil quality [190]. For lignocellulosic materials such as wood, the part that can be swollen is the cellulose by interaction between hydroxyl group of cellulose and functional groups or polar part of the swelling solvents [23].

The objective of Chapter 5 is to investigate the physical contribution to the spruce conversion by oxalic acid and TMAH, and to the synergy of A-B conversion found in Chapter 4. The physical contribution was studied by morphology observation of the spruce and the residues, and by pre-swelling of spruce, followed by conversion of the pre-swollen spruce by acid and base.

5.1 Morphological Investigation of Spruce and Solid Residues by SEM

The spruce and solid residues after each treatment were examined by scanning electron microscope (SEM). The SEM micrographs for spruce and the single-step treatment at 200 \times magnification are shown in Figure 5.1. The features of tracheid in raw spruce are observed in Figure 5.1(a). Bordered pits and cross-field pits were found in some region at higher magnification, which are in agreement with literature [191].

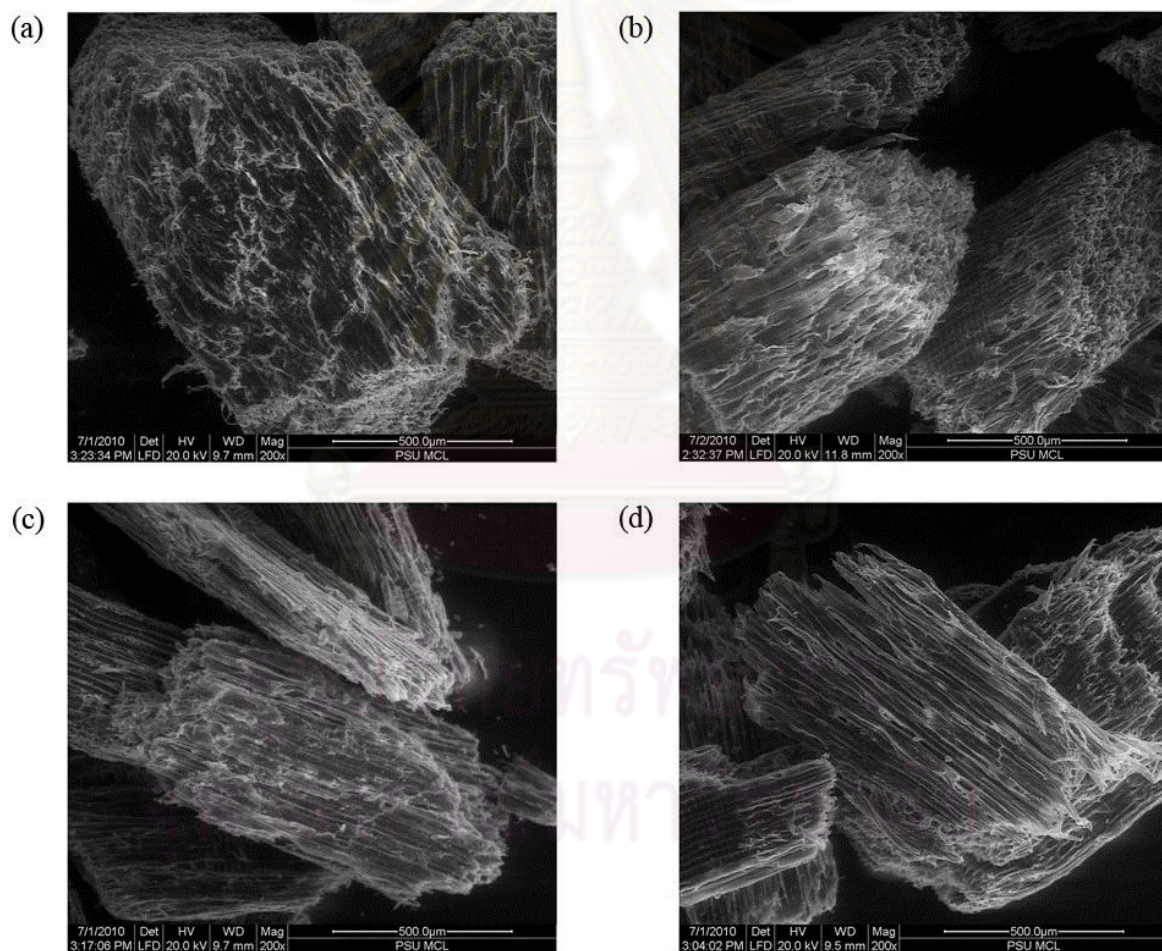


Figure 5.1 SEM micrographs of spruce and solid residues from one-step treatment (200 \times magnification). Designation: (a) untreated spruce; (b) water residue; (c) acid residue; (d) base residue.

The fiber shape of solid residue was maintained after acid or base treatments (Figure 5.1 (c),(d)). Although treatment by TMAH causes lignin liberation indicated by Py-GC-MS and ^{13}C -NMR in Chapter 4, there was adequate amount of lignin to hold the fiber as shown in Figure 5.1 (d). Since most of the samples were in horizontal direction, it was difficult to see ones in perpendicular direction; however, the structure of spruce did not seem to significantly collapse after drying. The surface of spruce initially has a lot of fringes at the edges and around the surface (Figure 5.1(a)). However, these fringes decreased when the spruce was treated in water (Figure 5.1(b)) indicating that the edges of spruce surface were more sensitive to treatment. Since the main macromolecular structural of the residual spruce is preserved, it is suggested that the treatments do not disrupt lignocellulose structurally but possibly by penetration of ion into the structure of spruce.

Figure 5.2 shows the 200 \times magnification SEM micrographs of two-step reaction. The residues after the two-step treatment do not significantly different from those from one-step treatment and the initial spruce. Another feature observed in A-B residues (Figure 5.2 (d)) was the formation of small particles, which could form as a result of recondensation of glucose or lignin monomers liberated from the reaction.

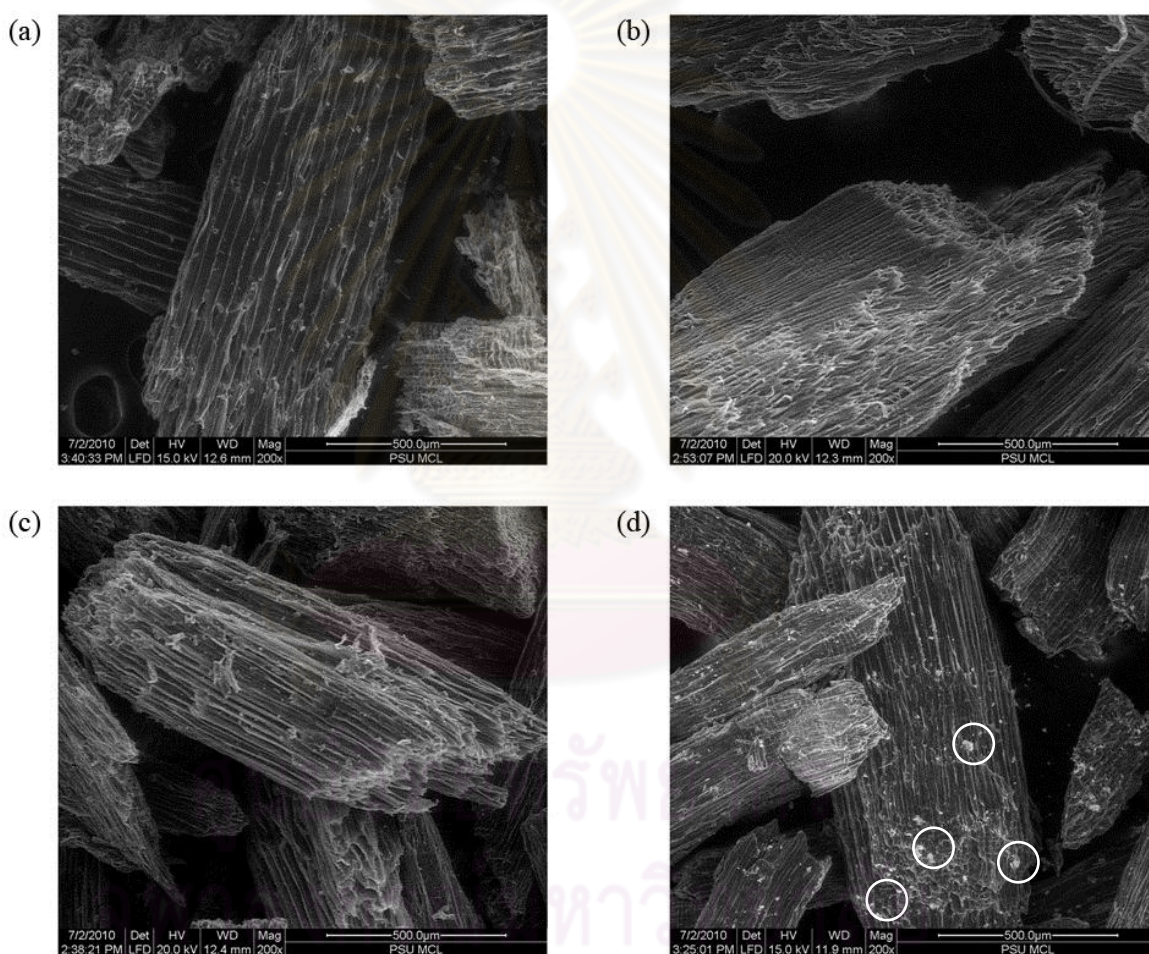


Figure 5.2 SEM micrographs of solid residues from two-step treatment (200 \times magnification). Designation: (a) A-A residue; (b) B-B residue; (c) B-A residue; (d) A-B residue.

Figure 5.3 shows surface of the spruce after acid treatment (A and A-A) at higher magnification of 500 \times . Disrupted surface in Figure 5.3 indicates cellulose breakdown as a result of acid treatment.

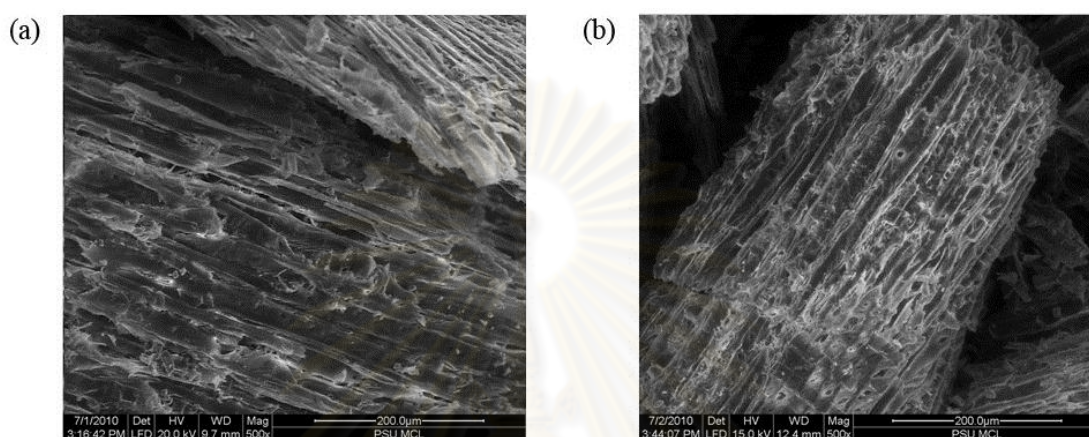


Figure 5.3 SEM micrographs of solid residues from acid treatment (500 \times magnification). Designation: (a) A residue; (b) A-A residue.

On the other hand, surface of the spruce after base treatment (Figure 5.4) shows different feature from the acid-treated ones. Lignin was partially removed from spruce, leaving clearer cellulose shape on the surface.

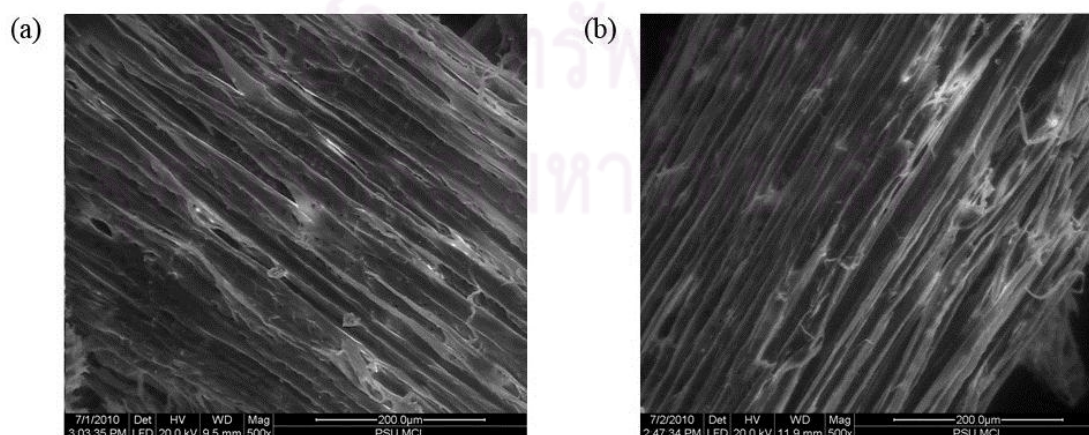


Figure 5.4 SEM micrographs of solid residues from base treatment (500 \times magnification). Designation: (a) B residue; (b) B-B residue.

Investigation of the spruce at the particle ends is also in agreement with surface observation. Cellulose was disrupted by acid treatment (Figure 5.5 (a)). Clear cellulose fiber shape was spotted due to lignin dissolution after base treatment (Figure 5.5 (b)). However, the wide gap observed in sequential treatment of acid followed by base (Figure 5.5 (c)) shows that both cellulose and lignin were significantly liberated by the treatment. This feature was not observed in the B-A treatment (Figure 5.6 (a)).

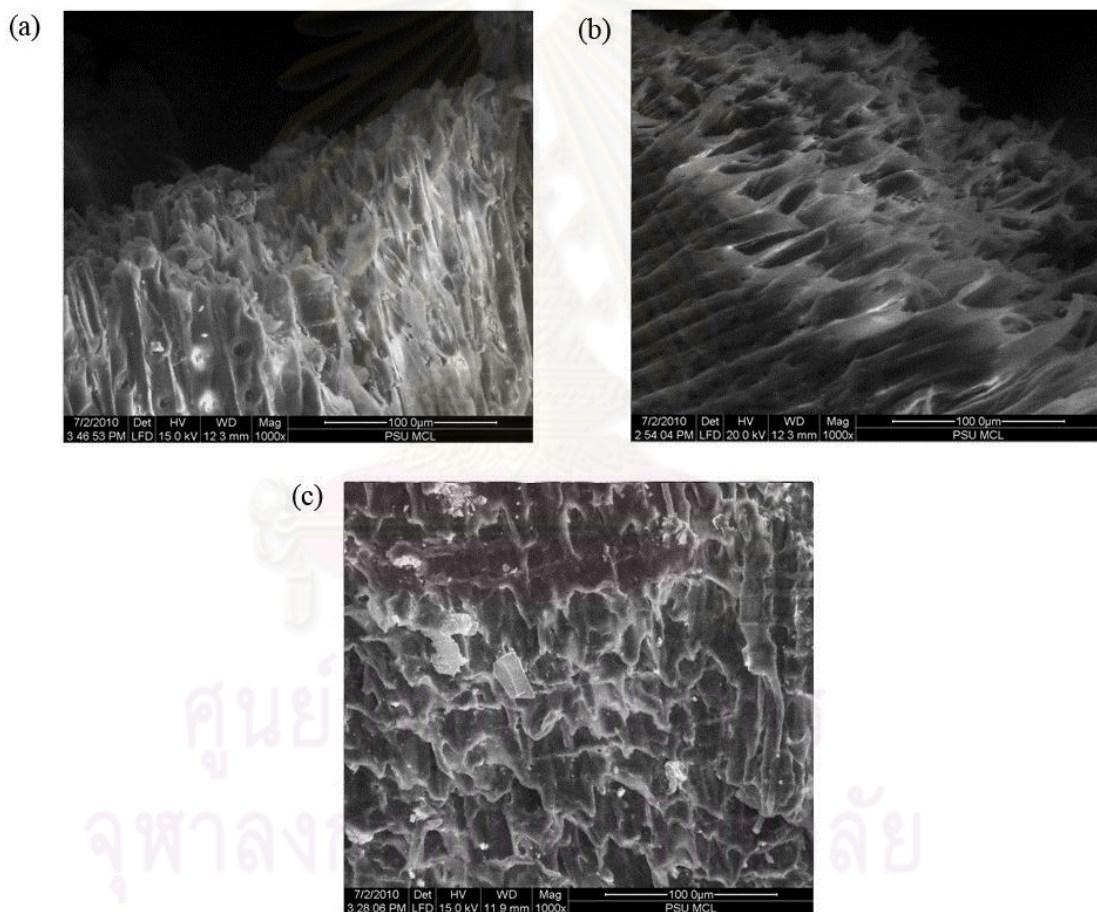


Figure 5.5 SEM micrographs of solid residues from two-step treatment at (1000× magnification). Designation: (a) A-A residue; (b) B-B residue; (c) A-B residue.

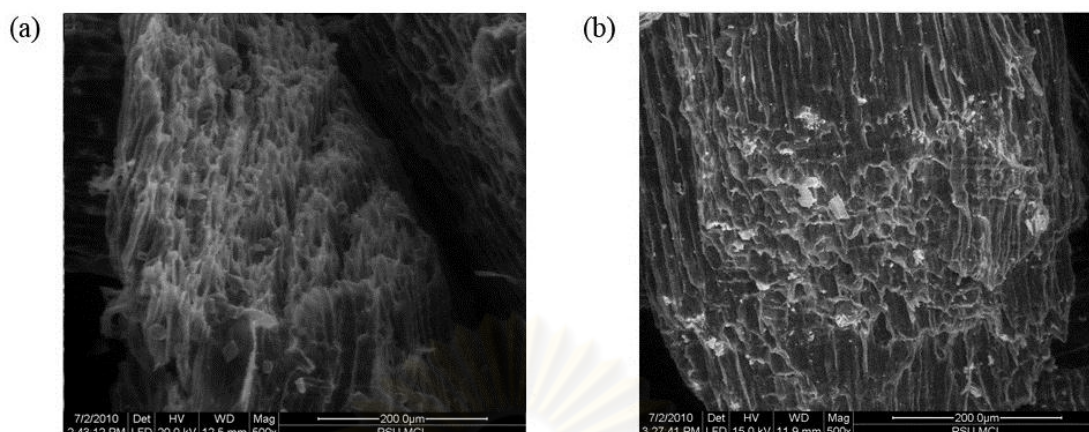


Figure 5.6 SEM micrographs of solid residues from acid treatment (500× magnification). Designation: (a) B-A residue; (b) A-B residue.

The 200× magnification SEM micrograph of three- step reaction (A-B-A) is shown in Figure 5.7. There are more particles formed in the A-B-A residue. The existence of these particles in A-B and A-B-A residues is more distinct at higher magnification, as shown in Figure 5.8. However, the main structure of the residues remained the same as in the spruce.

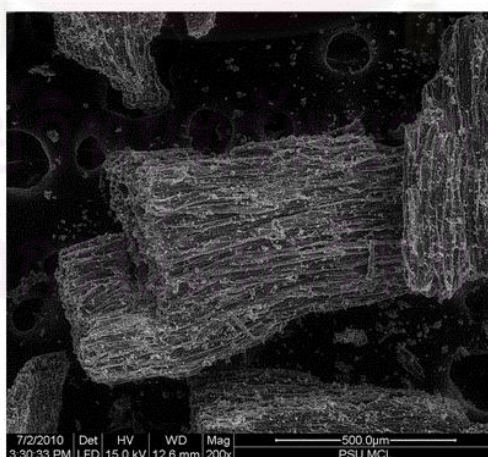


Figure 5.7 SEM micrographs of solid residues from three-step treatment A-B-A residue (200× magnification).

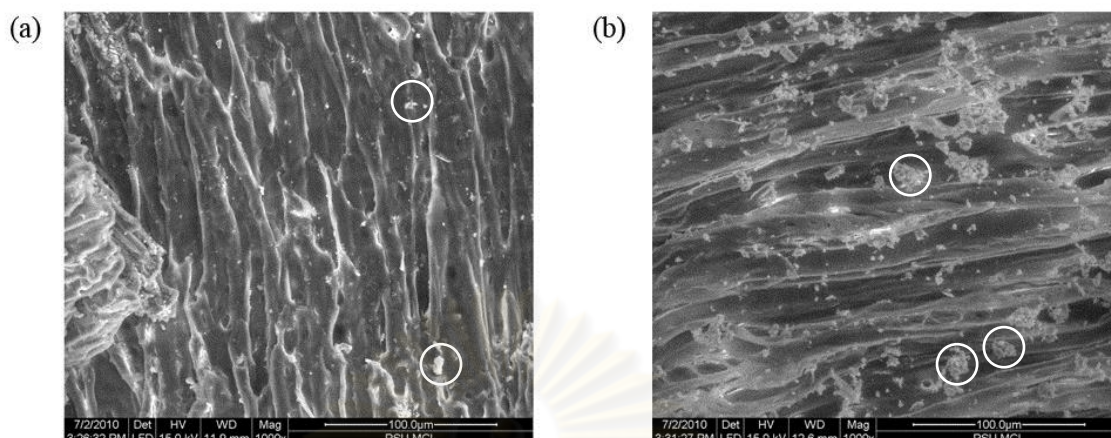


Figure 5.8 SEM micrographs of spruce and solid residues from two- and three-step treatment (1000 \times magnification). Designation: (a) A-B residue; (b) A-B-A residue.

From SEM investigation, it can be concluded that cellulose was disrupted by the acid treatment. This cellulose breakdown by oxalic acid could facilitate further cellulose conversion by TMAH in the second step of A-B.

ศูนย์วิทยทรัพยากร
จุฬาลงกรณ์มหาวิทยาลัย

5.2 Pre-swelling of Spruce

In general, swelling of cellulose in protic and aprotic organic solvents of high swelling power can swell native cellulose quickly within 5 min [192]. Examples of strong swelling solvents for cellulose are water, DMSO, ethanolamine [192]. Swelling power can be described as an ability of the solvent to overcome hydrogen bond between cellulose units and form a new hydrogen bond with them [23, 193]. This process preserves the entire structure of cellulose as a moiety; however, physical properties of cellulose are significantly changed and sample volume is increased due to uptake of the swelling solvent [145]. Swelling takes place as a result of transportation of the swelling solvent through pores system of cellulose. Initial swelling mainly depends on the void system. The swelling proceeds by interaction of solvents with hydroxyl groups in the accessible cellulose, which leads to breaking of hydrogen bonds [23, 131], and by the change in distribution and structure of voids. Further swelling is then influenced by the molar volume, and polar part of the swelling agents, and also affected by the initial state and the change of cellulose structure during the swelling process [192]. Fidale et al. concluded that three parameters correlated to cellulose swelling are molar volume, basicity, and dipolarity of the solvent [193].

The pre-swelling experiment was done according to the procedure in Chapter 2. Water, oxalic acid and TMAH solution was selected as the swelling solvent to avoid inherent effects from other solvents. Very high swelling power solvent such as DMSO was not used because strong solvent-cellulose interaction hinders complete removal of the solvent. Interactions between DMSO-water, and DMSO-hydroxyl groups of cellulose were reported to be very strong [193]. It could be difficult to remove DMSO by rinsing with water for the subsequent reactions. Figure 5.9 shows the pre-swollen spruce by water, oxalic acid aqueous solution, and

TMAH aqueous solution. The dashed line is the level of spruce before the pre-swelling.

The swelling ratio was measured based on the height of bulk spruce before and after the pre-swelling process. The swelling ratio is shown in Table 5.1. Standard errors of the swelling ratio are within 3%. The % recovery of pre-swollen wood was used to normalize the conversion from swelling experiments. The results of the swelling ratio are in agreement with the swelling capability of the solvents reported in literature. Water is known for ability to swell the cellulose [23, 192]. In the presence of oxalic acid, the swelling ratio is reduced, in agreement with literature that reported decrease in swelling of cellulose by oxalic acid [194]. TMAH is among the strongest swelling solvent in this experiment, as reported for its capability to swell cellulose [195].

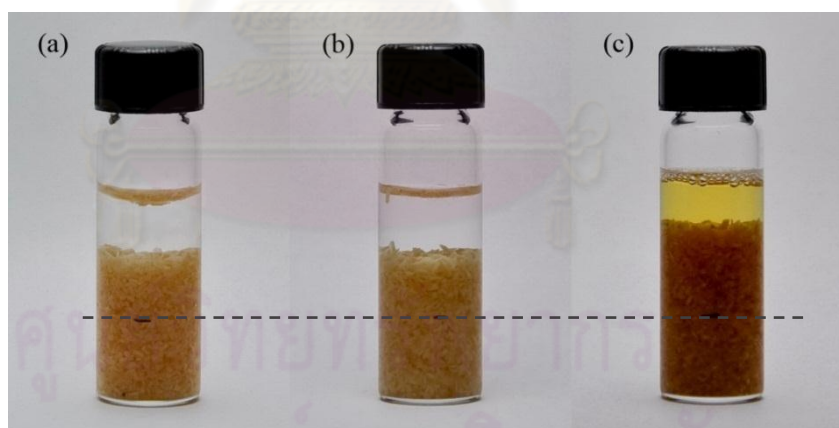


Figure 5.9 Pre-swelling experiment of spruce before the reaction in different medium (a) water; (b) 10% oxalic acid; (c) 10% TMAH. Dashed line represents initial level of spruce before pre-swelling.

Table 5.1 Swelling ratio of spruce in water, 10% oxalic acid, and 10% TMAH.

Solvent	Swelling ratio	% Recovery
Water	1.92	97.15±0.03
10% Oxalic Acid	1.78	99.04±0.55
10% TMAH	2.14	93.40±0.18

Swelling of cellulose in water takes place rapidly due to hygroscopicity of the hydroxyl groups in cellulose, but the highly ordered supramolecular structure of cellulose prevents it from dissolution. In some solvent systems, the swelling phenomenon depends on the concentration of the solvent that may cause limited swelling or unlimited swelling (dissolution) [23]. Tetraalkylammonium hydroxides such as TMAH can act as cellulose solvent similar to NaOH which is normally used in mercerization of cellulose [195]. It should be noted that mercerization involves dissolution of cellulose, but at concentration of NaOH less than 10%, it acts as the swelling solvent [23, 196]. In a similar way, tetraalkylammonium hydroxide can swell and dissolve cellulose depending on structure and concentration of the solvent. Interaction of TMAH during swelling involves hydroxyl group of cellulose and water molecule and polar end of the $R_4N^+OH^-$ ion dipole forming a hydrate complex. The nonpolar end of tetraalkylammonium hydroxide is responsible for widening the gap between the cellulose chains. The size of nonpolar end determines the swelling power of the solvent. Minimum molecular weight of 150 is suggested for dissolution effect [23, 195]. TMAH, molecular weight of 91.18, is the smallest tetraalkylammonium hydroxide. Based on the molecular weight requirement, TMAH can only swell, but cannot dissolve cellulose. However, there was almost 7% lost during the pre-swelling process suggesting some part of spruce was dissolved in TMAH.

5.3 Conversion of Pre-swollen Spruce by Acid and Base Treatment

The swollen spruce was subjected to single-step treatment with oxalic acid or TMAH. The conversion results are shown in Table 5.2. It is found that there is no significant enhancement from the pre-swelling process. The conversion of pre-swollen spruce ranged closely within 1% different from the spruce subjected to acid treatment without the pre-swelling, and with 3.6% for base treatment.

Table 5.2 Conversions of pre-swollen spruce in comparison with non-swollen spruce by oxalic acid and TMAH at 150 °C for 2 h.

Exp.	Pretreatment	Reaction	% Conversion	Standard Error
1	None	10% Oxalic acid	32.7	0.7
2	Pre-swelling by water	10% Oxalic acid	32.3	1.9
3	Pre-swelling by 10% OA	10% Oxalic acid	33.3	1.3
4	Pre-swelling by 10% TMAH	10% Oxalic acid	31.7	1.9
5	None	10% TMAH	46.2	1.0
6	Pre-swelling by water	10% TMAH	47.5	1.5
7	Pre-swelling by 10% OA	10% TMAH	46.9	3.1
8	Pre-swelling by 10% TMAH	10% TMAH	49.8	2.9

From the conversion of pre-swollen spruce in Table 5.2, the pre-swelling of spruce did not improve conversion by oxalic acid and TMAH probably due to two reasons. First, the swelling process may already occur rapidly during the typical reaction, as supported by literature that most swelling takes place very quickly [23]. Although it was not indicated specifically in the literature for swelling by 10% oxalic acid and 10% TMAH, the long reaction time employed in this treatment could allow the swelling process to complete.

Second, the hydrogen and hydroxide ions from acid and base may readily penetrate into the spruce due to small particle size of the spruce and small size of the ions. The diffusivity of the oxalic acid and TMAH is expected to occur rapidly due to small molecules of both reagents. In a study on diffusivity of sulfuric acid in wood, critical chip size for hydrolysis at 140 and 160 °C is 2000 and 1000 μm , respectively [197]. At chip size more than the critical size, gradient concentration will reduce the sugar yield, especially in the first 10 min of reaction [197]. Since the particle size of spruce in the experiment was in the range of 425-850 μm , it is expected that there was no variation of reagent concentration within the particles. Also, it was reported that the conversion of smaller particles size (less than 250 μm) of spruce with oxalic acid and TMAH at the same condition exhibited very small improvement on spruce conversion (3.4% by oxalic acid, and 0.6% by TMAH) [198], suggesting the diffusivity in two size of the spruce are the same and both particle sizes are smaller than the critical size.

It is concluded that the pre-swelling process of spruce did not have apparent impact on conversion of spruce by acid or base under the condition employed in this work and therefore does not contribute to the synergy conversion in A-B.

CHAPTER 6

ORIGIN OF SYNERGY IN CONVERSION OF SPRUCE BY ACID-BASE TREATMENTS: CELLULOSE CONVERSION AS A PROBE

In this chapter, the possible contributors to the synergy conversion in parallel with the previous chapter were further investigated. The cellulose contribution to spruce was proposed based on analytical results from Chapter 4 and experiments with commercial cellulose. Then, the investigation was further divided to physical contribution of cellulose and chemical contribution of cellulose. In order to study the physical contribution of cellulose in spruce, various cellulose solvent systems were used to dissolve cellulose in spruce to modify crystalline structure of the cellulose in spruce.

Both swelling and dissolution processes are known to disrupt the hydrogen bonds in cellulose and form new H-bonds between the swelling or dissolving solvents and the hydroxyl groups of cellulose [132]. The process of swelling and dissolution is closely related; high severity of swelling leads to dissolution [23, 131]. Dissolution of cellulose is distinguished by transition from a two-phase to a one-phase mixture due to a breakdown of the cellulose supramolecular structure [145]. Some solvents can act as either swelling or dissolution solvents for cellulose depending the operating conditions and the properties of cellulose [145]. There are several types of cellulose solvent systems, which can be classified as nonderivatizing and derivatizing solvents [23]. The nonderivatizing solvents involve only intermolecular interactions, while the derivatizing solvents also involve covalent derivatization in addition to the solvation effects [23, 131]. After dissolution, the dissolved cellulose can be regenerated by changing the conditions such as % water by

adding water to the system, which is the most general method used. For examples, the regenerated cellulose from cellulosic materials/N-methylmorphine-N-oxide (NMMO) is identified as cellulose II and amorphous cellulose [132]. The cellulose II structure of regenerated cellulose is more accessible than cellulose I due to lower degree of crystallinity [132].

There are six types of cellulose crystalline polymorphs: cellulose I, II, III_I, III_{II}, IV_I, and IV_{II}. Cellulose I is a native cellulose found in nature, whereas others are regenerated forms of cellulose I as shown in Figure 6.1. Specifically, cellulose I can undergo an irreversible transition to cellulose II by two conventional processes: regeneration and mercerization. Regeneration involves either dissolution of cellulose with an appropriate solvent followed by coagulation/precipitation and recrystallization/regeneration. Mercerization involves intracrystalline swelling of cellulose in concentrated aqueous NaOH followed by washing and recrystallization. The alkalization by NaOH is the method generally used for cellulose activation in commercial processes. Cellulose III is produced from cellulose I or II with ammonia treatment, followed by ammonia evaporation. Cellulose III_I is obtained from treatment of cellulose I. When cellulose II is used as a starting material, cellulose III_{II} is formed. It is assumed that cellulose III_I may have a parallel structure and cellulose III_{II} possesses an antiparallel structure. Similarly, cellulose IV has two polymorphs and two structures depending on the precursor (cellulose III_I or III_{II}) [199].

Cellulose II is thermodynamically the most stable crystalline form. The distinction between cellulose I and cellulose II is that cellulose II has an antiparallel packing whereas the chains in cellulose I run in parallel direction. The difference found in the inter-chain bonding: the prevalent hydrogen bond for cellulose I is the O6-H---O3 whereas cellulose II has O6-H---O2 as shown in Figure 6.2 [17, 21, 200].

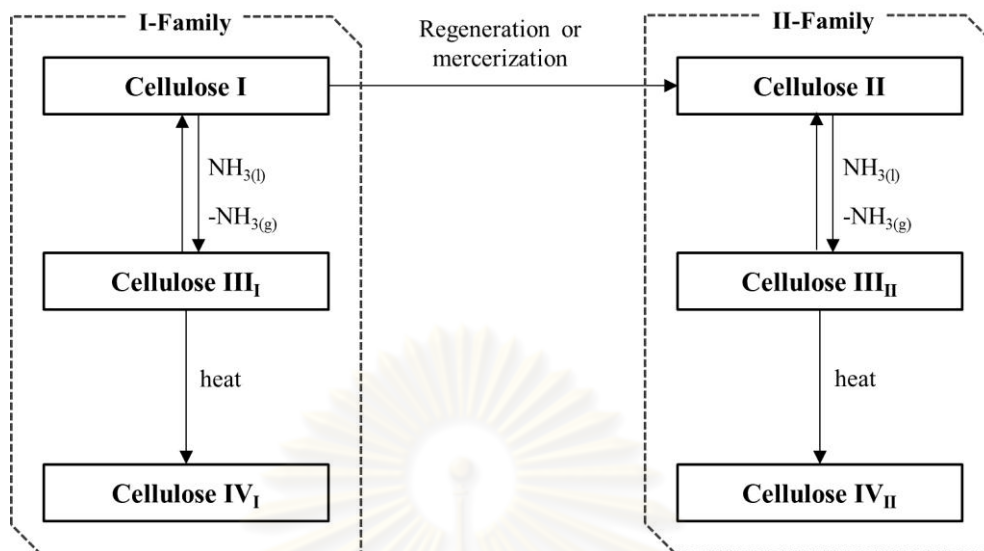


Figure 6.1 Basic procedures for preparation of cellulose polymorphs [199].

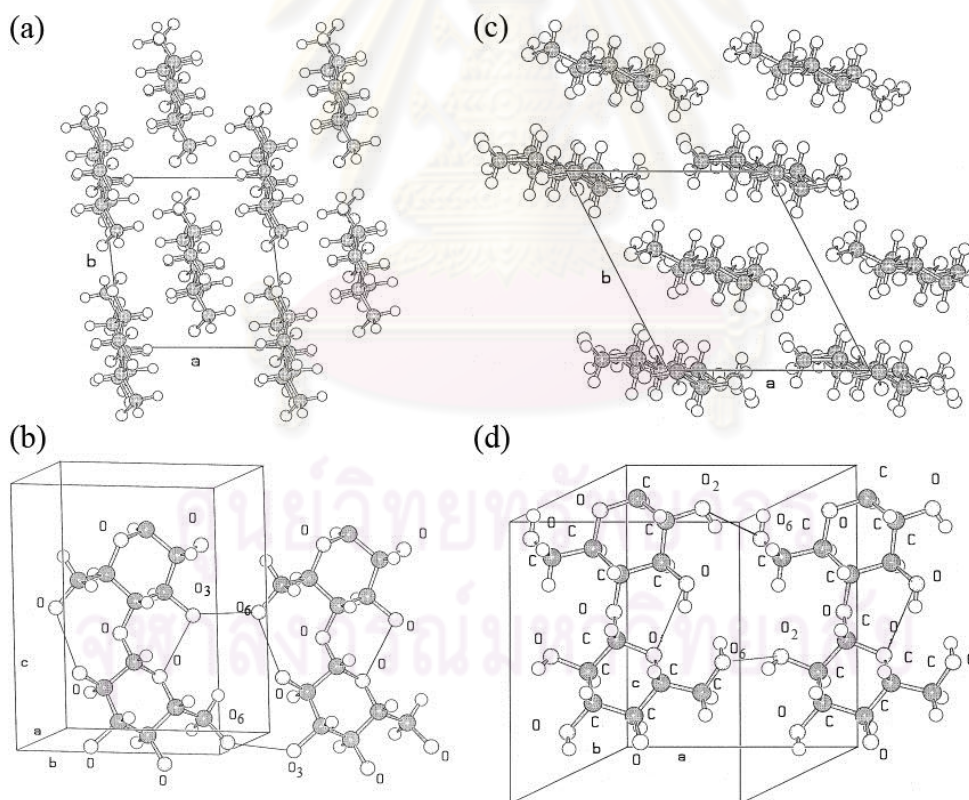


Figure 6.2 Crystal structure of cellulose I_β and cellulose II unit cell by different projection (a) along the a-b plane of cellulose I_β, (b) parallel to the (100) lattice plane of cellulose I_β, (c) along the a-b plane of cellulose II, (d) parallel to the (010) lattice plane of cellulose II [200].

The objective of Chapter 6 is to investigate cellulose contribution and physical contribution of cellulose to the synergy in Chapter 4. The possible chemical contribution of cellulose on synergistic conversion of spruce was also proposed at the end of this chapter.

6.1 Dissolution of Spruce and Conversion by Acid and Base Treatment

The experiments of spruce cellulose dissolution was carried out by three cellulose dissolution systems: 4-methylmorpholine N-oxide (NMMO), 1-n-butyl-3-methylimidazolium chloride ($C_4mim^+Cl^-$), and phosphoric acid (H_3PO_4). NMMO and $C_4mim^+Cl^-$ are nonderivatizing solvents [23, 132, 139, 140], whereas H_3PO_4 is a derivatizing solvent, with ether bond interaction with cellulose forming cellulose phosphate (Cellulose-O- PO_3H_2) [23, 145]. The chemical structure of the dissolution solvents used in the experiments is shown in Figure 6.3.

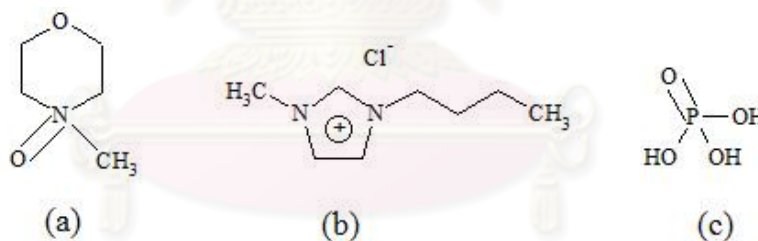


Figure 6.3 Chemical structures of dissolution solvents. (a) NMMO; (b) $C_4mim^+Cl^-$; (c) H_3PO_4 .

NMMO has been commercially used for cellulose dissolution [140]. It forms ionic and electron donor-acceptor interaction with hydroxyl groups of cellulose, as shown in Figure 6.4 [23]. The NMMO monohydrate (13% H_2O) is effective cellulose solvent. Its dissolution function can change to swelling by increasing the water amount [131, 136]. Since sugar composition of untreated and treated wood by NMMO remained unchanged, NMMO treatment was reported to maintain sugar composition of carbohydrates. Acid-soluble lignin was not affected by the NMMO

dissolution process [135]. Solid recovery after regeneration of cellulose from various cellulosic and lignocellulosic samples were reported to be in the range of 81-97%, with the lost due to handling and loss of water-extractives [134-136].

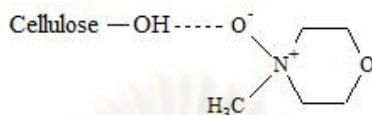


Figure 6.4 Interaction between NMMO and cellulose [23].

1-n-butyl-3-methylimidazolium chloride ($C_4mim^+Cl^-$) is ionic liquid, with chloride anions and 1-butyl-3-methylimidazolium cations. Chloride ion was proved as a superior proton acceptor for cellulose dissolution of ionic liquid because it is small and can form strong hydrogen bond with cellulose [139]. Performance of cellulose dissolution decreases with an increase in size of the alkyl chain in imidazolium cation [139]. $C_4mim^+Cl^-$ is effective for wood dissolution [141, 142]. Its optimum dissolution power was higher than NMMO [131, 133, 143]. The dissolution mechanism in NMMO and $C_4mim^+Cl^-$ progresses in the same way [143, 144] and is believed to depend on the nature of cellulose [143]. Degree of polymerization of cellulose is slightly affected by dissolution-regeneration [140, 144]. Lignin may slightly dissolve in $C_4mim^+Cl^-$ solvent [141, 142]. Water content in the solution considerably affects solubility [139, 142, 201].

Phosphoric acid (H_3PO_4) was claimed as an effective cellulose solvent due to small proton that can diffuse into cellulose easier than other cellulose solvents [145]. H_3PO_4 with concentration higher than 81% was reported to cause dissolution for microcrystalline cellulose. The regenerated cellulose was identified as amorphous cellulose [145]. The interactions between H_3PO_4 and cellulose occurring simultaneously are competition of hydrogen bond and esterification. Acid hydrolysis

may be minimized at low temperature. No change of DP was observed by this dissolution method [145].

During dissolution, the color of cellulose/solvents mixtures changed. As the dissolution proceeded, the slurry became more viscous and transit to one phase, as shown in Figure 6.5. After regeneration, the recoverable solid from dissolution and regeneration for spruce/NMMO, spruce/ $C_4mim^+Cl^-$, and spruce/ H_3PO_4 was 93.04 %, 94.88 %, and 99.61 %, respectively. The regenerated solids are shown in Figure 6.6.

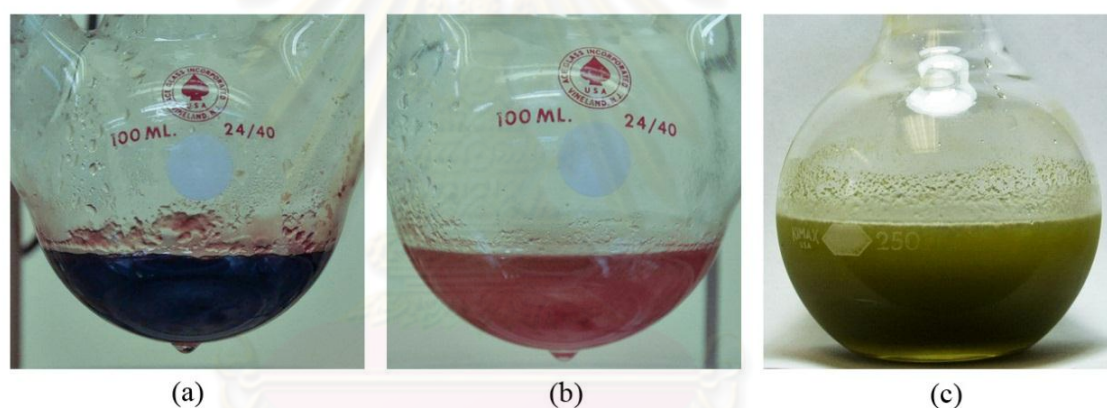


Figure 6.5 Dissolved spruce in (a) NMMO; (b) $C_4mim^+Cl^-$; (c) H_3PO_4 .

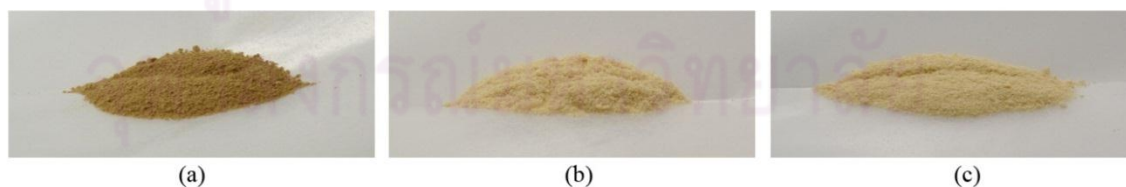


Figure 6.6 Regenerated samples from dissolution in (a) NMMO; (b) $C_4mim^+Cl^-$; (c) H_3PO_4 .

After regeneration, the solids were subjected to oxalic acid/TMAH single-step reaction. The conversion results are shown in Table 6.1. About 17-40 % conversion improvement was observed in oxalic acid treatment, while TMAH treatment increased the conversion about 24 %. This enhancement could be due to lossening of crytralline structure of cellulose in spruce by the dissolution-regeneration process.

Table 6.1 Conversions of regenerated spruce by oxalic acid and TMAH at 150 °C for 2 h.

Exp.	Cellulose modification	Reaction	Conversion (wt.%)	Standard Error
1	None	10% Oxalic acid	32.7	0.7
2	By NMMO	10% Oxalic acid	46.0	0.6
3	By C ₄ mim ⁺ Cl ⁻	10% Oxalic acid	38.3	0.6
4	By H ₃ PO ₄	10% Oxalic acid	41.6	1.7
5	None	10% TMAH	46.2	1.0
6	By NMMO	10% TMAH	57.0	1.2
7	By C ₄ mim ⁺ Cl ⁻	10% TMAH	57.4	1.0
8	By H ₃ PO ₄	10% TMAH	57.6	1.8

The conversion of spruce after cellulose structure modification was enhanced. The cellulose structure was further investigated in the next section.

6.2 Characterization of the Regenerated Spruce

The X-ray diffractions of spruce, acid-treated spruce, and regenerated spruces by NMMO, $C_4mim^+Cl^-$, and H_3PO_4 are shown in Figure 6.7. For cellulose I, the XRD pattern shows the peaks at $2\theta = 14.8, 16.25,$ and 22.6° . For cellulose II, the diffraction peaks are observed at $2\theta = 12.0, 20.2,$ and 21.8° [196]. It is observed that the dissolution-regeneration process causes loosening of crystalline structure of cellulose. Although it is reported that the dissolution-regeneration method generally yields cellulose II, the peak for cellulose II in regenerated spruces by NMMO, $C_4mim^+Cl^-$, and H_3PO_4 in this work is barely observed. On the other hand, the diffraction peaks of regenerated spruces, in Figure 6.7 (c), (d), and (e), was close to the combination of the original cellulose I and amorphous cellulose, represented by broad peak around 21.5° [202]. The generation of amorphous cellulose instead of cellulose II was in agreement with regenerated spruce in ionic liquid [142]. The appearance of amorphous cellulose could be due to the presence of lignin and other wood components, and the regeneration method which could affect the crystallinity of the regenerated cellulose [142, 203].

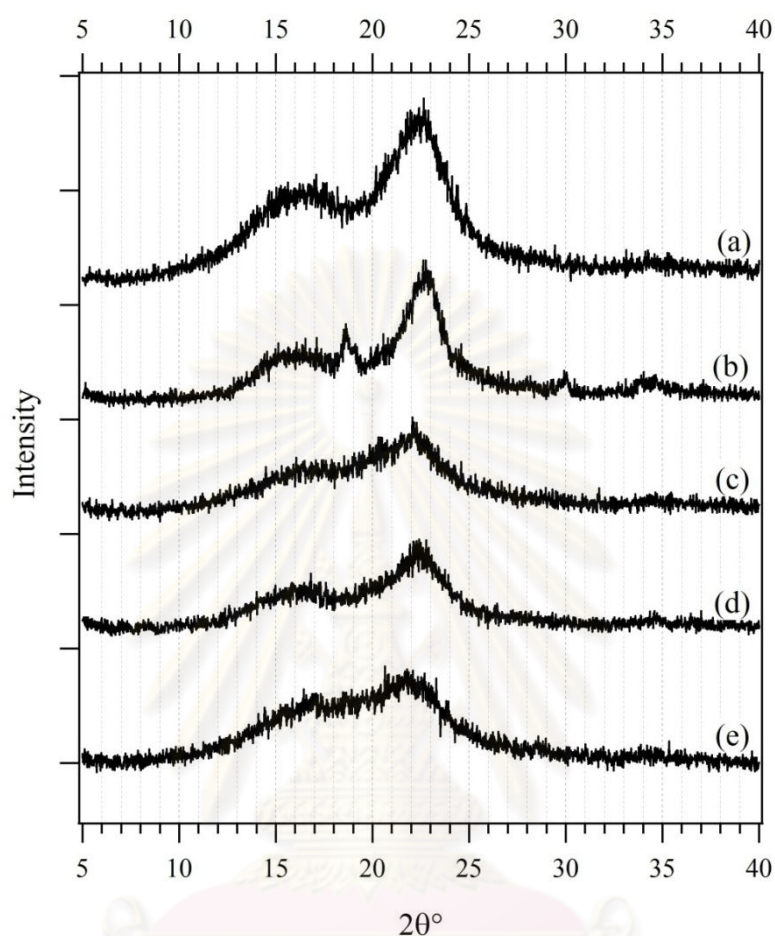


Figure 6.7 X-ray diffractions of (a) spruce; (b) oxalic acid-treated residue; (c) NMMO regenerated spruce; (d) $C_4mim^+Cl^-$ regenerated spruce; (e) H_3PO_4 regenerated spruce.

Comparing the conversion of regenerated spruce with the XRD results suggesting the generation of amorphous cellulose was the main contribution to the enhanced conversion by the dissolution-regeneration method (Table 6.1). The XRD intensity of NMMO-pretreated spruce was the lowest indicating less crystalline structure of the regenerated spruce, hence it yielded high conversion by oxalic acid. The XRD intensity of $C_4mim^+Cl^-$ pretreated spruce was comparable to that of H_3PO_4 pretreated spruce, but the peak of H_3PO_4 pretreated spruce has shifted more indicating

higher amorphous cellulose than that in $C_4mim^+Cl^-$ pretreated spruce; accordingly the H_3PO_4 pretreated spruce was converted more than the $C_4mim^+Cl^-$ pretreated spruce. In other word, the amorphous structure of regenerated spruce increased in the order of $C_4mim^+Cl^- < H_3PO_4 < NMMO$, corresponding to the conversion trend by acid treatment shown in Table 6.1.

For the conversion by TMAH, there is very limited information for conversion. However, the polysaccharides conversion by alkaline NaOH reagent was discussed since both NaOH and TMAH proceed via action of hydroxide ion. Crystalline structure and reducing ends of cellulose was proved to affect the alkaline conversion of cellulose [204]. In the samples with high number of reducing ends, the crystalline structure showed less effect to the conversion [204]. Alkaline conversion in cellulose was also reported to take place preferentially in the amorphous zone of cellulose [205]. So, the change in cellulose crystalline structure from cellulose I to other structure was likely to promote the conversion by TMAH, which explained the enhanced conversion in Table 6.1. Also, the change in degree of polymerization (DP) of cellulose was reported to indirectly affect the peeling reaction of cellulose [206, 207]. Since the regenerated spruce could lower cellulose DP, it could be another factor resulting in the increased conversion by TMAH. Therefore, the conversion by TMAH could be enhanced due to combined effects of lower crystallinity of cellulose and change in DP.

Considering the XRD of the acid-treated spruce, the characteristic peaks remained the same as those in original spruce indicating that the acid treatment did not significantly affect the crystallinity of spruce. There was an unidentified diffraction peak at $2\theta = 18.6^\circ$, which cannot be removed even the residue was rinsed by hot water prior to the analysis. The existence of the unidentified peak hindered crystallinity determination based on Segal's empirical equation (equation 6.1) [208].

$$\text{Crystallinity Index} = \frac{(I_{002} - I_{AM})}{I_{002}} \times 100 \quad (6.1)$$

where I_{002} is the maximum intensity of the 002 lattice diffraction, and I_{AM} is the intensity at $2\theta = 18^\circ$ [208].

Although the crystallinity of cellulose in acid-treated residue could not be calculated, it is observed in Figure 6.7 (b) that the peak at 22.6° was sharper compared to the spruce, possibly by less broad peak around 21.5° suggesting the amorphous cellulose was converted during acid treatment. This is in agreement with literature indicating that the amorphous cellulose was easier to be hydrolyzed than crystalline cellulose, leaving the residue with higher crystallinity than the initial spruce [209]. It is concluded that the enhanced conversion of the regenerated spruce was due to the loosening of crystalline structure of cellulose, while the actual acid treatment cause lower content of amorphous cellulose. Therefore, it is unlikely that the change in crystalline form of cellulose caused by acid treatment could enhance conversion and lead to synergy in the two-step A-B reaction of spruce presented in Chapter 4.

6.3 Suggestion of Cellulose Contribution to Spruce Conversion

Although crystallinity of cellulose in spruce may not contribute to the synergistic A-B conversion, there is a possibility that cellulose may influence the synergy. First, cellulose is the main component in wood. Second, the analysis in Chapter 4 indicated that polysaccharide conversion was enhanced and lead to synergy, but hemicellulose was mostly converted in the one-step treatment. Third, experiment on microcrystalline cellulose also exhibits synergistic conversion in similar way as in the conversion of spruce, as shown in Figure 6.8 and Table 6.2 [210]. For the single-step reactions, the conversion by hydrolysis with the following reagents increased in the order of: water < 10% oxalic acid < 10% TMAH. In the pure cellulose conversion, the oxalic acid conversion is slightly lower than that of spruce in the same condition. This is probably because the conversion during the one-step acid reaction in spruce converts mainly hemicellulose in contrast to the cellulose conversion.

In the two-step treatments, the overall cellulose conversion increased in the order of A-A < B-B < B-A < A-B. For the conversion for each step shown in Table 6.2, the conversion of B-A (24.4%) was more than twice of that by A-A (10.4%), and conversion by base reaction of A-B (61.9%) was more than six times of that by B-B (9.2%). The A-B conversion in the second step was also higher than that in the first step of B (58.1%). When the same reagent was applied in the two-step reactions, conversion from acid reaction dropped from 29.1% in the first step to 10.4% in the second step, while conversion from base reaction in the first step (58.1%) decreased to 9.2% in the second step.

Based on the conversion results, sequential combinations of acid and base treatments for pure cellulose also exhibited the synergy. The enhanced conversion of A-B combination in cellulose was more prominent than that in spruce suggesting that the synergistic conversion was contributed largely by conversion of

cellulose. Further investigation on pure cellulose conversion is currently being carried out at the Pennsylvania State University.

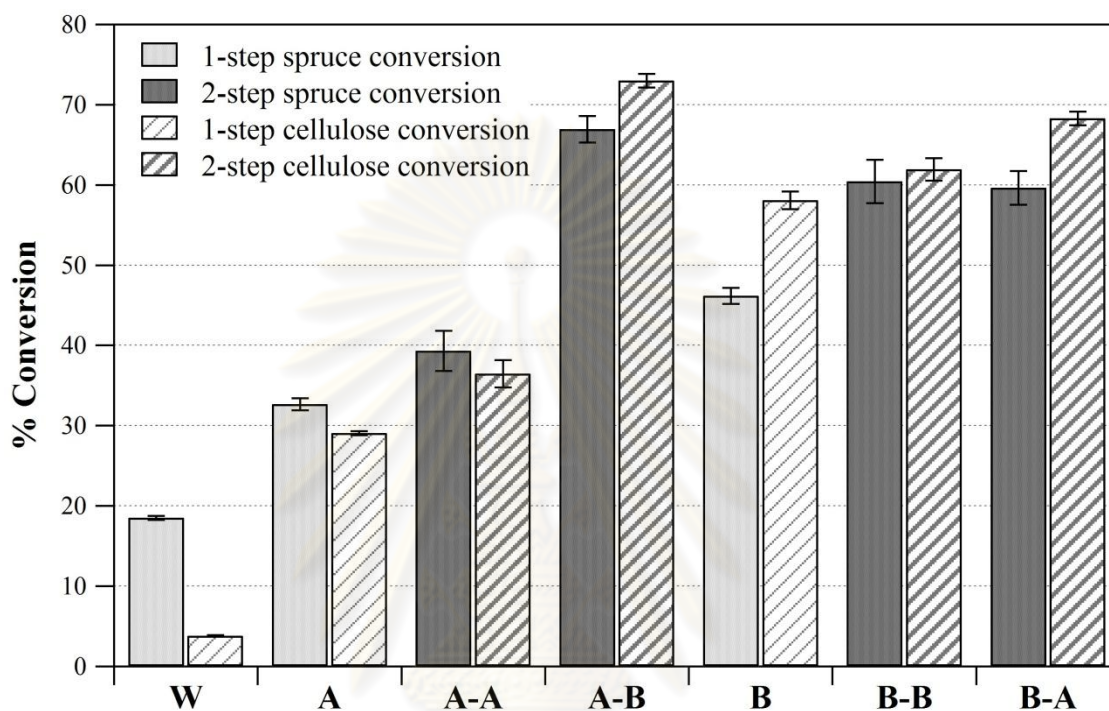


Figure 6.8 Conversions of spruce and cellulose by single-, and two-step reactions at 150 °C for 2 h [210].

Table 6.2 Conversions of cellulose by single- and two-step reactions at 150 °C for 2 h [210].

	Conversion (%)						
	Water	Acid	A-A	B-A	Base	B-B	A-B
1st-step	3.8	29.1	-	-	58.1	-	-
2nd-step	-	-	10.4	24.4	-	9.2	61.9
Overall	-	-	36.5	68.3	-	61.9	73.0
Standard Error (%)	0.1	0.2	2.1	2.2	1.1	0.7	0.9

6.4 Possible Chemical Effects to Synergy

During alkaline reaction in cellulose, there are four concurrent processes that dictate the progress of cellulose conversion: peeling-off reaction, chemical stopping reaction, physical stopping by crystalline cellulose, and alkaline hydrolysis [211]. Based on kinetic study of cellulose conversion in alkaline medium, the dominant reaction was the endwise peeling-off reaction [205-207], while the alkaline hydrolysis was relatively very slow. The parameters that affect peeling reaction are the amount of reducing ends, DP, and amount of amorphous cellulose [211]. The reducing end contributes most to the peeling reaction. Also, formation of reducing ends was reported as the rate-limiting step in the peeling reaction of cellulose [211]. This assumption based on NaOH reagent also in agreement with study of TMAH thermochemolysis of carbohydrates and it indicates that the TMAH cleaves bonds in carbohydrates by endwise depolymerization at reducing end group [127, 128]. The new reducing ends could be formed by glycosidic bond cleavage by acid hydrolysis or alkaline hydrolysis [205, 206]. As shown in Figure 6.9, the original cellulose is consisting of crystalline and amorphous cellulose. Amorphous cellulose is more susceptible to acid hydrolysis and cleaved first (Figure 6.9 (b)) [212]. For base reaction, the cellulose peeling must be originated at the reducing end of cellulose initiated by alkaline hydrolysis. The peeling reaction is ended when the stopping reaction takes place (Figure 6.9 (c)).

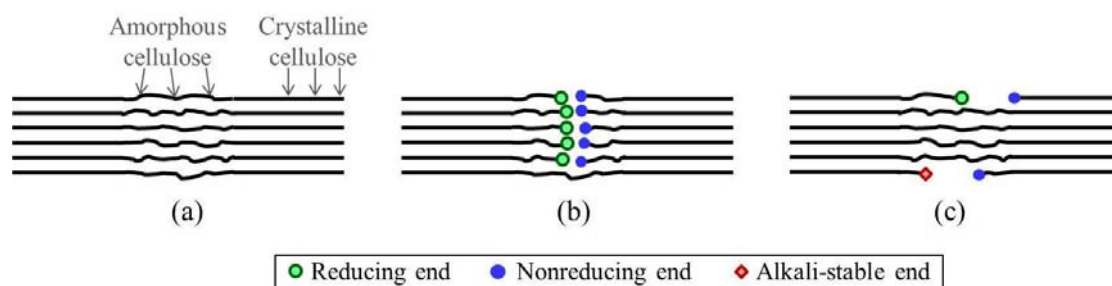


Figure 6.9 Scheme of cellulose before and after treatments (a) before treatment; (b) after acid treatment; (c) after base treatment.

The synergistic conversion of A-B could be due to the enhanced conversion in TMAH reaction by change in number of reducing ends in cellulose. The oxalic acid reaction in the first-step reaction could enhance the second-step TMAH conversion by increasing the number of reducing ends in spruce, which leads to higher conversion by peeling reaction. Since the contribution by physical properties (morphology and swelling effect of spruce) and crystalline structure is less likely to enhance the A-B conversion, this aspect of chemical contribution should be more feasible.

ศูนย์วิทยทรัพยากร
 จุฬาลงกรณ์มหาวิทยาลัย

CHAPTER 7

CONCLUSIONS AND RECOMMENDATIONS

7.1 Conclusions

Utilization of lignocellulosic biomass is encouraged due to many reasons. Several thermochemical processes have been applied for conversion of lignocellulose. Development for a new, effective and simple process using mild condition that allows the energy-efficient utilization of the abundant lignocellulosic biomass is still highly desirable.

A new process of acid-base combination at mild condition has been established for conversion of lignocellulosic biomass into liquid phase for woody biomass, specifically spruce. The organic acid (oxalic acid) and base (TMAH) has also been used in place of mineral ones. There is a strongly synergistic conversion in the sequential two-step reaction, namely the acid followed by base (A-B) treatment. The existence of synergy has also been verified by analytical investigation of the products. The total conversion results are in agreement with independent analytical results. The acid treatment produces sugar monomers, while the base treatment produces non-sugar hexose derivative from polysaccharides in biomass. The first-step acid treatment causes more cellulosic structural breakdown, which facilitates base treatment in the second step. The base treatment after acid one enhances polysaccharide conversion, while the base treatment alone does not. The enhanced conversion of cellulose is one cause of synergy, as suggested by product characterizations. Further investigation of the swelling effects leads to a conclusion that the physical structure enhancements by pre-swelling are not the factor leading to the synergy in the condition employed. Loosening of cellulose crystalline structure by

dissolution-regeneration process can improve the conversion for both acid and base but does not involve in the synergy of A-B. There is a possibility that the synergistic conversion has been chemically promoted by formation of new reducing end groups in cellulose that leads to enhancement in peeling reaction by TMAH.

7.2 Recommendations

Based on the current work on acid-base combination process to convert lignocelluloses, the following are recommendations for further research.

1. Validation of the proposed chemical promoting factor

The chemical aspect of promoting factor for synergistic conversion by acid-base combination is remaining to be done. Although the information base on sulfuric acid hydrolysis and sodium hydroxide alkaline conversion of cellulose support the chemical contribution, it is interesting to prove its validity.

2. Application to other lignocellulosic materials

In this study, only the softwood spruce has been utilized in the process. Application to other lignocellulosic feedstock will help to validate the synergistic conversion. Also, the effects of composition in lignocelluloses should be further studied.

3. Optimization of the process

Since this study is the initial development of the new conversion process, there are many possibilities to modify or redesign the process based on this concept. For example, the yield of sugars and 2-keto-D-gluconic acid in the first- and second-step acid treatment could be maximized.

REFERENCES

- [1] Lynd, L. R., et al. The role of biomass in America's energy future: Framing the analysis. Biofuels, Bioproducts and Biorefining. 2009. 3(2): 113-123.
- [2] Antizar-Ladislao, B. and Turrion-Gomez, J. L. Second-generation biofuels and local bioenergy systems. Biofuels, Bioproducts and Biorefining. 2008. 2(5): 455-469.
- [3] Lange, J.-P. Lignocellulose conversion: An introduction to chemistry, process and economics. Biofuels, Bioproducts and Biorefining. 2007. 1(1): 39-48.
- [4] Naik, S. N., Goud, V. V., Rout, P. K., and Dalai, A. K. Production of first and second generation biofuels: A comprehensive review. Renewable and Sustainable Energy Reviews. 2010. 14(2): 578-597.
- [5] Srinivasan, S. The food v. Fuel debate: A nuanced view of incentive structures. Renewable Energy. 2009. 34(4): 950-954.
- [6] Timilsina, G. R. and Shrestha, A. How much hope should we have for biofuels? Energy. 2010. In Press, Corrected Proof.
- [7] Wang, M., Wu, M., and Huo, H. Life-cycle energy and greenhouse gas emission impacts of different corn ethanol plant types. Environmental Research Letters. 2007. 2(2): 024001.
- [8] Jull, C., Redondo, P. C., Mosoti, V., and Vapnek, J. Recent trends in the law and policy of bioenergy production, promotion and use. 2007 [Accessed 10/16/2010]. FAO Legal Papers Online #68. Available from: www.fao.org/legal/prs-ol/lpo68.pdf.
- [9] Zarrilli, S. The emerging biofuels market: Regulatory, trade and development implication. 2006 [Accessed 09/20/2010]. Available from: http://r0.unctad.org/ghg/events/biofuels/UNCTAD_DITC_TED_2006_4.Final.pdf.

- [10] DOE and USDA. Vision for bioenergy and biobased products in the United States. Report by US DOE and USDA 2006 [Accessed 06/11/2009]. Available from: http://www1.eere.energy.gov/biomass/pdfs/final_2006_vision.pdf
- [11] NSF. Breaking the chemical and engineering barriers to lignocellulosic biofuels: Next generation hydrocarbon biorefineries. Final Report based on NSF-DOE-ACS Workshop 2008 [Accessed 06/11/2009]. Available from: <http://www.ecs.umass.edu/biofuels/Images/Roadmap2-08.pdf>.
- [12] Fernando, S., Adhikari, S., Chandrapal, C., and Murali, N. Biorefineries: Current status, challenges, and future direction. Energy & Fuels. 2006. 20(4): 1727-1737.
- [13] Demirbas, M. F., Balat, M., and Balat, H. Potential contribution of biomass to the sustainable energy development. Energy Conversion and Management. 2009. 50(7): 1746-1760.
- [14] Pauly, M. and Keegstra, K. Cell-wall carbohydrates and their modification as a resource for biofuels. The Plant Journal. 2008. 54(4): 559-568.
- [15] DOE. Breaking the biological barriers to cellulosic ethanol: A joint research agenda. DOE/SC-0095 2006 [Accessed 09/30/2010]. Available from: <http://genomicscience.energy.gov/biofuels/b2bworkshop.shtml>.
- [16] Lewin, M. and Goldstein, I. S. Wood structure and composition. International fiber science and technology series. New York: Wiley-VCH Verlag GmbH, 1991.
- [17] Kontturi, E. Surface chemistry of cellulose : From natural fibres to model surfaces: Eindhoven University of Technology, 2005.

- [18] Huber, G. W., Iborra, S., and Corma, A. Synthesis of transportation fuels from biomass: Chemistry, catalysts, and engineering. Chemical Reviews. 2006. 106(9): 4044-4098.
- [19] Yi-Heng Percival, Z. and Lee, R. L. Toward an aggregated understanding of enzymatic hydrolysis of cellulose: Noncomplexed cellulase systems. Biotechnology and Bioengineering. 2004. 88(7): 797-824.
- [20] Hearle, J. W. S. A fringed fibril theory of structure in crystalline polymers. Journal of Polymer Science. 1958. 28(117): 432-435.
- [21] Festucci-Buselli, R. A., Otoni, W. C., and Joshi, C. P. Structure, organization, and functions of cellulose synthase complexes in higher plants. Brazilian Journal of Plant Physiology. 2007. 19: 1-13.
- [22] Gross, A. S. and Chu, J.-W. On the molecular origins of biomass recalcitrance: The interaction network and solvation structures of cellulose microfibrils. The Journal of Physical Chemistry B. 2010. 114 (42): 13333–13341.
- [23] Klemm, D., Philipp, B., Heinze, T., Heinze, U., and Wagenknecht, W. Comprehensive cellulose chemistry. Vol. 1: Fundamentals and Analytical Methods. Weinheim: Wiley-VCH, 1998.
- [24] Xiang, Q., Lee, Y., Pettersson, P., and Torget, R. Heterogeneous aspects of acid hydrolysis of α -cellulose. Applied Biochemistry and Biotechnology. 2003. 107(1): 505-514.
- [25] Gardner, K. H. and Blackwell, J. The hydrogen bonding in native cellulose. Biochimica et Biophysica Acta (BBA) - General Subjects. 1974. 343(1): 232-237.
- [26] Tashiro, K. and Kobayashi, M. Theoretical evaluation of three-dimensional elastic constants of native and regenerated celluloses: Role of hydrogen bonds. Polymer. 1991. 32(8): 1516-1526.

- [27] Xiang, Q., Kim, J. S., and Lee, Y. Y. A comprehensive kinetic model for dilute-acid hydrolysis of cellulose. Applied Biochemistry and Biotechnology. 2003. 105-108: 337-352.
- [28] Kondo, T. The relationship between intramolecular hydrogen bonds and certain physical properties of regioselectively substituted cellulose derivatives. Journal of Polymer Science Part B: Polymer Physics. 1997. 35(4): 717-723.
- [29] Mosier, N., et al. Features of promising technologies for pretreatment of lignocellulosic biomass. Bioresource Technology. 2005. 96(6): 673-686.
- [30] Hayes, D. J. An examination of biorefining processes, catalysts and challenges. Catalysis Today. 2009. 145(1-2): 138-151.
- [31] Nishiyama, Y., Sugiyama, J., Chanzy, H., and Langan, P. Crystal structure and hydrogen bonding system in cellulose I_α from synchrotron X-ray and neutron fiber diffraction. Journal of the American Chemical Society. 2003. 125(47): 14300-14306.
- [32] Nishiyama, Y., Langan, P., and Chanzy, H. Crystal structure and hydrogen-bonding system in cellulose I_β from synchrotron X-ray and neutron fiber diffraction. Journal of the American Chemical Society. 2002. 124(31): 9074-9082.
- [33] Horii, F., Yamamoto, H., Kitamaru, R., Tanahashi, M., and Higuchi, T. Transformation of native cellulose crystals induced by saturated steam at high temperatures. Macromolecules. 1987. 20(11): 2946-2949.
- [34] Morrison, I. M. Lignin-carbohydrate complexes from *lolium perenne*. Phytochemistry. 1974. 13(7): 1161-1165.
- [35] Azuma, J.-I. and Tetsuo, K. Lignin-carbohydrate complexes from various sources. Methods in Enzymology. 1988. Volume 161: 12-18.

- [36] Singh, R., et al. Lignin-carbohydrate complexes from sugarcane bagasse: Preparation, purification, and characterization. Carbohydrate Polymers. 2005. 62(1): 57-66.
- [37] Lundqvist, J., et al. Characterization of galactoglucomannan extracted from spruce (*picea abies*) by heat-fractionation at different conditions. Carbohydrate Polymers. 2003. 51(2): 203-211.
- [38] Timell, T. E. Recent progress in the chemistry of wood hemicelluloses. Wood Science and Technology. 1967. 1(1): 45-70.
- [39] Tyminski, A. and Timell, T. E. The constitution of a glucomannan from white spruce (*picea glauca*). Journal of the American Chemical Society. 1960. 82(11): 2823-2827.
- [40] Sjöström, E. Wood chemistry: Fundamentals and applications. 2 ed: Gulf Professional Publishing, 1993.
- [41] Nimz, H. Beech lignin - proposal of a constitutional scheme. Angewandte Chemie International Edition in English. 1974. 13(5): 313-321.
- [42] Adler, E. Lignin chemistry—past, present and future. Wood Science and Technology. 1977. 11(3): 169-218.
- [43] Lynd, L. R., Jin, H., Michels, J. G., Wyman, C. E., and Dale, B. E. Bioenergy: Background, potential, and policy: Center for Strategic and International Studies. Washington, DC, 2003.
- [44] Nimz, H. and Casten, R. Chemical processing of lignocellulosics. European Journal of Wood and Wood Products. 1986. 44(6): 207-212.
- [45] Balat, M., Balat, M., Kirtay, E., and Balat, H. Main routes for the thermo-conversion of biomass into fuels and chemicals. Part 2: Gasification systems. Energy Conversion and Management. 2009. 50(12): 3158-3168.

- [46] Agbontalor, E. a. Overview of various biomass energy conversion routes. American-Eurasian Journal of Agricultural & Environmental Sciences. 2007. 2(6): 662-671.
- [47] Yokoyama, S. and Mutsumura, Y. The Asian biomass handbook: A guide for biomass production and utilization. Tokyo, Japan: Japan Institute of Energy, 2008.
- [48] Puig-Arnavat, M., Bruno, J. C., and Coronas, A. Review and analysis of biomass gasification models. Renewable and Sustainable Energy Reviews. 2010. 14(9): 2841-2851.
- [49] Caputo, A. C., Palumbo, M., Pelagagge, P. M., and Scacchia, F. Economics of biomass energy utilization in combustion and gasification plants: Effects of logistic variables. Biomass and Bioenergy. 2005. 28(1): 35-51.
- [50] Meier, D. and Faix, O. State of the art of applied fast pyrolysis of lignocellulosic materials -- a review. Bioresource Technology. 1999. 68(1): 71-77.
- [51] Babu, B. V. Biomass pyrolysis: A state-of-the-art review. Biofuels, Bioproducts and Biorefining. 2008. 2(5): 393-414.
- [52] Bridgwater, A. V., Meier, D., and Radlein, D. An overview of fast pyrolysis of biomass. Organic Geochemistry. 1999. 30(12): 1479-1493.
- [53] Demirbas, A. The influence of temperature on the yields of compounds existing in bio-oils obtained from biomass samples via pyrolysis. Fuel Processing Technology. 2007. 88(6): 591-597.
- [54] Demirbas, A. Combustion characteristics of different biomass fuels. Progress in Energy and Combustion Science. 2004. 30(2): 219-230.
- [55] Zhang, Q., Chang, J., Wang, T., and Xu, Y. Review of biomass pyrolysis oil properties and upgrading research. Energy Conversion and Management. 2007. 48(1): 87-92.

- [56] Iojoiu, E. E., Domine, M. E., Davidian, T., Guilhaume, N., and Mirodatos, C. Hydrogen production by sequential cracking of biomass-derived pyrolysis oil over noble metal catalysts supported on ceria-zirconia. Applied Catalysis A: General. 2007. 323: 147-161.
- [57] Diebold, J. P., A review of the chemical and storage stability of fast pyrolysis bio-oils, National Renewable Energy Laboratory, Golden, Colorado, 2000.
- [58] Xu, C. and Etcheverry, T. Hydro-liquefaction of woody biomass in sub- and super-critical ethanol with iron-based catalysts. Fuel. 2008. 87(3): 335-345.
- [59] Demirbas, A. Mechanisms of liquefaction and pyrolysis reactions of biomass. Energy Conversion and Management. 2000. 41(6): 633-646.
- [60] Talebnia, F., Karakashev, D., and Angelidaki, I. Production of bioethanol from wheat straw: An overview on pretreatment, hydrolysis and fermentation. Bioresource Technology. 2010. 101(13): 4744-4753.
- [61] Galbe, M. and Zacchi, G. A review of the production of ethanol from softwood. Applied Microbiology and Biotechnology. 2002. 59(6): 618-628.
- [62] Palonen, H., Role of lignin in the enzymatic hydrolysis of lignocellulose, in *VTT Biotechnology*. 2004, Helsinki University of Technology: Espoo, Finland.
- [63] Walker, L. P. and Wilson, D. B. Enzymatic hydrolysis of cellulose: An overview. Bioresource Technology. 1991. 36(1): 3-14.
- [64] McMillan James, D., Pretreatment of lignocellulosic biomass, in *Enzymatic conversion of biomass for fuels production*. 1994, American Chemical Society. p. 292-324.
- [65] Enzymatic conversion of biomass for fuels production. ACS symposium series, ed. Himmel, M. E., Baker, J. O., and Overend, R. P.: American Chemical Society, 1994 518.

- [66] Cheung, S. W. and Anderson, B. C. Laboratory investigation of ethanol production from municipal primary wastewater solids. Bioresource Technology. 1997. 59(1): 81-96.
- [67] Kumar, P., Barrett, D. M., Delwiche, M. J., and Stroeve, P. Methods for pretreatment of lignocellulosic biomass for efficient hydrolysis and biofuel production. Industrial & Engineering Chemistry Research. 2009. 48(8): 3713-3729.
- [68] Taherzadeh, M. J. and Niklasson, C. Ethanol from lignocellulosic materials: Pretreatment, acid and enzymatic hydrolyses, and fermentation Lignocellulose biodegradation, ed. Saha, B. C. and Hayashi, K.: American Chemical Society, 2004.
- [69] Larsson, S., et al. The generation of fermentation inhibitors during dilute acid hydrolysis of softwood. Enzyme and Microbial Technology. 1999. 24(3-4): 151-159.
- [70] Balat, M. Production of bioethanol from lignocellulosic materials via the biochemical pathway: A review. Energy Conversion and Management. 2010. 52(2): 858-875.
- [71] Lenihan, P., et al. Dilute acid hydrolysis of lignocellulosic biomass. Chemical Engineering Journal. 2010. 156(2): 395-403.
- [72] Iranmahboob, J., Nadim, F., and Monemi, S. Optimizing acid-hydrolysis: A critical step for production of ethanol from mixed wood chips. Biomass and Bioenergy. 2002. 22(5): 401-404.
- [73] Sun, Y. and Cheng, J. Hydrolysis of lignocellulosic materials for ethanol production: A review. Bioresource Technology. 2002. 83(1): 1-11.
- [74] Taherzadeh, M. J. and Karimi, K. Acid-based hydrolysis processes for ethanol from lignocellulosic materials: A review. Bioresources. 2007. 2(3): 472-499.

- [75] Sun, Y., Zhuang, J., Lin, L., and Ouyang, P. Clean conversion of cellulose into fermentable glucose. Biotechnology Advances. 2009. 27(5): 625-632.
- [76] Choi, C. H. and Mathews, A. P. Two-step acid hydrolysis process kinetics in the saccharification of low-grade biomass: 1. Experimental studies on the formation and degradation of sugars. Bioresource Technology. 1996. 58(2): 101-106.
- [77] Bose, S. K., et al. An improved method for the hydrolysis of hardwood carbohydrates to monomers. Carbohydrate Polymers. 2009. 78(3): 396-401.
- [78] Saeman, J. F., Moore, W. E., Mitchell, R. L., and Millett, M. A. Techniques for the determination of pulp constituents by quantitative paper chromatography. TAPPI Journal. 1954. 37(8): 336-343.
- [79] Sluiter, A., et al., Determination of structural carbohydrates and lignin in biomass, laboratory analytical procedure, National Renewable Energy Laboratory, Golden, Colorado, 2008.
- [80] ASTM Standard E 1721, Standard test method for determination of acid-insoluble residues in biomass, ASTM International, West Conshohocken, PA, 2009, DOI: 10.1520/E1721-01R09, www.astm.org.
- [81] Song, C., Hu, H., Zhu, S., Wang, G., and Chen, G. Nonisothermal catalytic liquefaction of corn stalk in subcritical and supercritical water. Energy & Fuels. 2004. 18(1): 90-96.
- [82] Yu, Y., Lou, X., and Wu, H. Some recent advances in hydrolysis of biomass in hot-compressed water and its comparisons with other hydrolysis methods Energy & Fuels. 2008. 22(1): 46-60.
- [83] Kumar, S. and Gupta, R. B. Biocrude production from switchgrass using subcritical water. Energy & Fuels. 2009. 23(10): 5151-5159.

- [84] Asghari, F. S. and Yoshida, H. Conversion of Japanese red pine wood (*Pinus densiflora*) into valuable chemicals under subcritical water conditions. Carbohydrate Research. 2010. 345(1): 124-131.
- [85] Dapía, S., Santos, V., and Parajó, J. C. Study of formic acid as an agent for biomass fractionation. Biomass and Bioenergy. 2002. 22(3): 213-221.
- [86] Shimada, M., Akamitsu, Y., Tokimatsu, T., Mii, K., and Hattori, T. Possible biochemical roles of oxalic acid as a low molecular weight compound involved in brown-rot and white-rot wood decays. Journal of Biotechnology. 1997. 53(2-3): 103-113.
- [87] Kenealy, W., Horn, E., Davis, M., Swaney, R., and Houtman, C. Vapor-phase diethyl oxalate pretreatment of wood chips: Part 2. Release of hemicellulosic carbohydrates. Holzforschung. 2007. 61(3): 230-235.
- [88] Chakar, F. S. and Ragauskas, A. J. Review of current and future softwood kraft lignin process chemistry. Industrial Crops and Products. 2004. 20(2): 131-141.
- [89] Gierer, J. Chemistry of delignification. Wood Science and Technology. 1985. 19(4): 289-312.
- [90] Baeza, J., et al. Organosolv pulping -- V: Formic acid delignification of eucalyptus globulus and eucalyptus grandis. Bioresource Technology. 1991. 37(1): 1-6.
- [91] Erismann, N. d. M., Freer, J., Baeza, J., and Duran, N. Organosolv pulping-VII: Delignification selectivity of formic acid pulping of eucalyptus grandis. Bioresource Technology. 1994. 47(3): 247-256.
- [92] McDonough, T. J. The chemistry of organosolv delignification. IPST technical paper series. 1992. 455.
- [93] Parajó, J. C., Alonso, J. L., and Vázquez, D. On the behaviour of lignin and hemicelluloses during the acetosolv processing of wood. Bioresource Technology. 1993. 46(3): 233-240.

- [94] Lachenal, D., Mortha, G., Sevillano, R.-M., and Zaroubine, M. Isolation of residual lignin from softwood kraft pulp. Advantages of the acetic acid acidolysis method. Comptes Rendus Biologies. 2004. 327(9-10): 911-916.
- [95] Kham, L., Le Bigot, Y., Delmas, M., and Avignon, G. Delignification of wheat straw using a mixture of carboxylic acids and peroxyacids. Industrial Crops and Products. 2005. 21(1): 9-15.
- [96] Ligeró, P., Villaverde, J. J., de Vega, A., and Bao, M. Delignification of eucalyptus globulus saplings in two organosolv systems (formic and acetic acid): Preliminary analysis of dissolved lignins. Industrial Crops and Products. 2008. 27(1): 110-117.
- [97] Ligeró, P., Villaverde, J. J., Vega, A., and Bao, M. Acetosolv delignification of depithed cardoon (*cynara cardunculus*) stalks. Industrial Crops and Products. 2007. 25(3): 294-300.
- [98] Marafi, M. and Stanislaus, A. Spent hydroprocessing catalyst management: A review: Part II. Advances in metal recovery and safe disposal methods. Resources, Conservation and Recycling. 2008. 53(1-2): 1-26.
- [99] EHS Guidelines, Large volume inorganic compounds manufacturing and coal tar distillation, International Finance Corporation, Washington, DC, 2007, <http://www.ifc.org/ifcext/sustainability.nsf/Content/EHSGuidelines>.
- [100] Shimada, M., Ma, D.-B., Akamatsu, Y., and Hattori, T. A proposed role of oxalic acid in wood decay systems of wood-rotting basidiomycetes. FEMS Microbiology Reviews. 1994. 13(2-3): 285-295.
- [101] Tsao, G. T.-N. Production of oxalic acid by a wood-rotting fungus. Appl. Environ. Microbiol. 1963. 11(3): 249-254.
- [102] Higgins, J., Zhou, X., Liu, R., and Huang, T. T. S. Theoretical study of thermal decomposition mechanism of oxalic acid. The Journal of Physical Chemistry A. 1997. 101(14): 2702-2708.

- [103] Lapidus, G., Barton, D., and Yankwich, P. E. Kinetics and stoichiometry of the gas-phase decomposition of oxalic acid. The Journal of Physical Chemistry. 1964. 68(7): 1863-1865.
- [104] Poerschmann, J., Rauschen, S., Langer, U., Augustin, J., and Górecki, T. Molecular level lignin patterns of genetically modified bt-maize mon88017 and three conventional varieties using tetramethylammonium hydroxide (TMAH)-induced thermochemolysis. Journal of Agricultural and Food Chemistry. 2008. 56(24): 11906-11913.
- [105] Vane, C. H. The molecular composition of lignin in spruce decayed by white-rot fungi (*phanerochaete chrysosporium* and *trametes versicolor*) using pyrolysis-GC-MS and thermochemolysis with tetramethylammonium hydroxide. International Biodeterioration & Biodegradation. 2003. 51(1): 67-75.
- [106] Kuroda, K.-I., Nishimura, N., Izumi, A., and Dimmel, D. R. Pyrolysis of lignin in the presence of tetramethylammonium hydroxide: A convenient method for S/G ratio determination. Journal of Agricultural and Food Chemistry. 2002. 50(5): 1022-1027.
- [107] Filley, T. R., et al. Lignin demethylation and polysaccharide decomposition in spruce sapwood degraded by brown rot fungi. Organic Geochemistry. 2002. 33(2): 111-124.
- [108] Vane, C. H., Martin, S. C., Snape, C. E., and Abbott, G. D. Degradation of lignin in wheat straw during growth of the oyster mushroom (*pleurotus ostreatus*) using off-line thermochemolysis with tetramethylammonium hydroxide and solid-state ¹³C NMR. Journal of Agricultural and Food Chemistry. 2001. 49(6): 2709-2716.
- [109] Vane, C. H., Abbott, G. D., and Head, I. M. The effect of fungal decay (*agaricus bisporus*) on wheat straw lignin using pyrolysis-GC-MS in the

- presence of tetramethylammonium hydroxide (TMAH). Journal of Analytical and Applied Pyrolysis. 2001. 60(1): 69-78.
- [110] Kuroda, K.-I., Ozawa, T., and Ueno, T. Characterization of sago palm (*metroxylon sagu*) lignin by analytical pyrolysis. Journal of Agricultural and Food Chemistry. 2001. 49(4): 1840-1847.
- [111] Challinor, J. M. Review: The development and applications of thermally assisted hydrolysis and methylation reactions. Journal of Analytical and Applied Pyrolysis. 2001. 61(1-2): 3-34.
- [112] Clifford, D. J., Carson, D. M., McKinney, D. E., Bortiatynski, J. M., and Hatcher, P. G. A new rapid technique for the characterization of lignin in vascular plants: Thermochemolysis with tetramethylammonium hydroxide (TMAH). Organic Geochemistry. 1995. 23(2): 169-175.
- [113] Tanczos, I., Pokol, G., Borsa, J., Tóth, T., and Schmidt, H. The effect of tetramethylammonium hydroxide in comparison with the effect of sodium hydroxide on the slow pyrolysis of cellulose. Journal of Analytical and Applied Pyrolysis. 2003. 68-69: 173-185.
- [114] Tanczos, I. and Schmidt, H. Quatam process: New sulfur-free delignification. Journal of Wood Chemistry and Technology. 2002. 22(4): 219 - 233.
- [115] Hirano, K., et al. An efficient treatment technique for TMAH wastewater by catalytic oxidation. IEEE transactions on semiconductor manufacturing. 2001. 14(3): 202-206.
- [116] Mamman, A. S., et al. Furfural: Hemicellulose/xylose-derived biochemical. Biofuels, Bioproducts and Biorefining. 2008. 2(5): 438-454.
- [117] Philipp, B., Dan, D. C., Fink, H.-P., Kasulke, U., and Loth, F. Comparative studies in acid and enzymic hydrolysis of cellulose of different structure. Plaste und Kautschuk. 1981. 28: 481-485.

- [118] Musau, R. M. and Munavu, R. M. The preparation of 5-hydroxymethyl-2-furaldehyde (HMF) from D-fructose in the presence of DMSO. Biomass. 1987. 13(1): 67-74.
- [119] Bicker, M., Kaiser, D., Ott, L., and Vogel, H. Dehydration of d-fructose to hydroxymethylfurfural in sub- and supercritical fluids. The Journal of Supercritical Fluids. 2005. 36(2): 118-126.
- [120] Asghari, F. S. and Yoshida, H. Dehydration of fructose to 5-hydroxymethylfurfural in sub-critical water over heterogeneous zirconium phosphate catalysts. Carbohydrate Research. 2006. 341(14): 2379-2387.
- [121] Amarasekara, A. S., Williams, L. D., and Ebede, C. C. Mechanism of the dehydration of d-fructose to 5-hydroxymethylfurfural in dimethyl sulfoxide at 150 °C: An NMR study. Carbohydrate Research. 2008. 343(18): 3021-3024.
- [122] Hansen, T. S., Woodley, J. M., and Riisager, A. Efficient microwave-assisted synthesis of 5-hydroxymethylfurfural from concentrated aqueous fructose. Carbohydrate Research. 2009. 344(18): 2568-2572.
- [123] Su, Y., et al. Single-step conversion of cellulose to 5-hydroxymethylfurfural (HMF), a versatile platform chemical. Applied Catalysis A: General. 2009. 361(1-2): 117-122.
- [124] Horvat, J., Klaic, B., Metelko, B., and Sunjic, V. Mechanism of levulinic acid formation. Tetrahedron Letters. 1985. 26(17): 2111-2114.
- [125] Filley, T. R., Minard, R. D., and Hatcher, P. G. Tetramethylammonium hydroxide (TMAH) thermochemolysis: Proposed mechanisms based upon the application of ¹³C-labeled TMAH to a synthetic model lignin dimer. Organic Geochemistry. 1999. 30(7): 607-621.
- [126] Kuroda, K.-I. and Nakagawa-Izumi, A. Tetramethylammonium hydroxide (TMAH) thermochemolysis of lignin: Behavior of 4-o-etherified cinnamyl

- alcohols and aldehydes. Journal of Agricultural and Food Chemistry. 2005. 53(23): 8859-8865.
- [127] Fabbri, D. and Helleur, R. Characterization of the tetramethylammonium hydroxide thermochemolysis products of carbohydrates. Journal of Analytical and Applied Pyrolysis. 1999. 49(1-2): 277-293.
- [128] Schwarzingler, C. On the mechanism of thermally assisted hydrolysis and methylation of carbohydrates: The contribution of aldol and retroaldol reactions. Journal of Analytical and Applied Pyrolysis. 2003. 68-69: 137-149.
- [129] Fengel, D. and Wegener, G. Wood: Chemistry, ultrastructure, reactions: Walter De Gruyter, 1989.
- [130] Hergt, H. F. A. and Christensen, G. N. Variable retention of water by dry wood. Journal of Applied Polymer Science. 1965. 9(7): 2345-2361.
- [131] Cuissinat, C. and Navard, P. Swelling and dissolution of cellulose part 1: Free floating cotton and wood fibres in n-methylmorpholine-n-oxide-water mixtures. Macromolecular Symposia. 2006. 244(1): 1-18.
- [132] Zhao, H., et al. Interactions between cellulose and N-methylmorpholine-N-oxide. Carbohydrate Polymers. 2007. 67(1): 97-103.
- [133] Cuissinat, C. and Navard, P. Swelling and dissolution of cellulose, part III: Plant fibres in aqueous systems. Cellulose. 2008. 15(1): 67-74.
- [134] Kuo, C.-H. and Lee, C.-K. Enhanced enzymatic hydrolysis of sugarcane bagasse by N-methylmorpholine-N-oxide pretreatment. Bioresource Technology. 2009. 100(2): 866-871.
- [135] Shafiei, M., Karimi, K., and Taherzadeh, M. J. Pretreatment of spruce and oak by N-methylmorpholine-N-oxide (NMMO) for efficient conversion of their cellulose to ethanol. Bioresource Technology. 2010. 101(13): 4914-4918.
- [136] Jeihanipour, A., Karimi, K., and Taherzadeh, M. J. Enhancement of ethanol and biogas production from high-crystalline cellulose by different modes of

- NMO pretreatment. Biotechnology and Bioengineering. 2010. 105(3): 469-476.
- [137] Ramakrishnan, S., Collier, J., Oyetunji, R., Stutts, B., and Burnett, R. Enzymatic hydrolysis of cellulose dissolved in n-methyl morpholine oxide/water solutions. Bioresource Technology. 2010. 101(13): 4965-4970.
- [138] Konkin, A., et al. Degradation processes in the cellulose/ n - methylmorpholine- n -oxide system studied by HPLC and ESR. Radical formation/recombination kinetics under UV photolysis at 77 K. Cellulose. 2007. 14(5): 457-468.
- [139] Swatloski, R. P., Spear, S. K., Holbrey, J. D., and Rogers, R. D. Dissolution of cellose with ionic liquids. Journal of the American Chemical Society. 2002. 124(18): 4974-4975.
- [140] Heinze, T., Schwikal, K., and Barthel, S. Ionic liquids as reaction medium in cellulose functionalization. Macromolecular Bioscience. 2005. 5(6): 520-525.
- [141] Fort, D. A., et al. Can ionic liquids dissolve wood? Processing and analysis of lignocellulosic materials with 1-n-butyl-3-methylimidazolium chloride. Green Chemistry. 2007. 9(1): 63-69.
- [142] Kilpeläinen, I., et al. Dissolution of wood in ionic liquids. Journal of Agricultural and Food Chemistry. 2007. 55(22): 9142-9148.
- [143] Cuissinat, C., Navard, P., and Heinze, T. Swelling and dissolution of cellulose. Part IV: Free floating cotton and wood fibres in ionic liquids. Carbohydrate Polymers. 2008. 72(4): 590-596.
- [144] Kosan, B., Michels, C., and Meister, F. Dissolution and forming of cellulose with ionic liquids. Cellulose. 2008. 15(1): 59-66.
- [145] Zhang, Y. H. P., Cui, J., Lynd, L. R., and Kuang, L. R. A transition from cellulose swelling to cellulose dissolution by o-phosphoric acid: evidence

- from enzymatic hydrolysis and supramolecular structure. Biomacromolecules. 2006. 7(2): 644-648.
- [146] Rojas-Escudero, E., Alarcón-Jiménez, A. L., Elizalde-Galván, P., and Rojo-Callejas, F. Optimization of carbohydrate silylation for gas chromatography. Journal of Chromatography A. 2004. 1027(1-2): 117-120.
- [147] Stout, S. A., Boon, J. J., and Spackman, W. Molecular aspects of the peatification and early coalification of angiosperm and gymnosperm woods. Geochimica et Cosmochimica Acta. 1988. 52(2): 405-414.
- [148] Faix, O., Meier, D., and Fortmann, I. Thermal degradation products of wood. Holz als Roh- und Werkstoff. 1990. 48(7): 281-285.
- [149] Faix, O., Fortmann, I., Bremer, J., and Meier, D. Thermal degradation products of wood. Holz als Roh- und Werkstoff. 1991. 49(5): 213-219.
- [150] del Rio, J. C., et al. Determining the influence of eucalypt lignin composition in paper pulp yield using Py-GC/MS. Journal of Analytical and Applied Pyrolysis. 2005. 74(1-2): 110-115.
- [151] Alves, A., Schwanninger, M., Pereira, H., and Rodrigues, J. Analytical pyrolysis as a direct method to determine the lignin content in wood: Part 1: Comparison of pyrolysis lignin with Klason lignin. Journal of Analytical and Applied Pyrolysis. 2006. 76(1-2): 209-213.
- [152] Fahmi, R., et al. Prediction of klason lignin and lignin thermal degradation products by Py-GC/MS in a collection of lolium and festuca grasses. Journal of Analytical and Applied Pyrolysis. 2007. 80(1): 16-23.
- [153] Yoosuk, B., Kim, J. H., Song, C., Ngamcharussrivichai, C., and Prasassarakich, P. Highly active MoS₂, CoMoS₂ and NiMoS₂ unsupported catalysts prepared by hydrothermal synthesis for hydrodesulfurization of 4,6-dimethyldibenzothiophene. Catalysis Today. 2008. 130(1): 14-23.

- [154] Oasmaa, A. and Meier, D. Norms and standards for fast pyrolysis liquids: 1. Round robin test. Journal of Analytical and Applied Pyrolysis. 2005. 73(2): 323-334.
- [155] Elliott, D. C., et al. Developments in direct thermochemical liquefaction of biomass: 1983-1990. Energy & Fuels. 1991. 5(3): 399-410.
- [156] Elliott, D. C. Historical developments in hydroprocessing bio-oils. Energy & Fuels. 2007. 21(3): 1792-1815.
- [157] Faaij, A. P. C. Bio-energy in europe: Changing technology choices. Energy Policy. 2006. 34(3): 322-342.
- [158] Talebnia, F., Karakashev, D., and Angelidaki, I. Production of bioethanol from wheat straw: An overview on pretreatment, hydrolysis and fermentation. Bioresource Technology. 2009. 101(13): 4744-4753.
- [159] Kolthoff, I. M. and Elving, P. J. Treatise on analytical chemistry. New York: The Interscience Encyclopedia Inc., 1959.
- [160] Bjerrum, J., Schwarzenbach, G., and Sillen, L. G. Stability constants. London: The Chemical Society, 1958.
- [161] Brown, H. C., McDaniel, D. H., and Häflinger, O. Determination of organic structures by physical methods, ed. Braude, E. A. and Nachod, F. C. Vol. 1. New York: Academic Press, 1955.
- [162] Dippy, J. F. J., Hughes, S. R. C., and Rozanski, A. 498. The dissociation constants of some symmetrically disubstituted succinic acids. Journal of the Chemical Society (Resumed). 1959: 2492-2498.
- [163] Lee, J.-W., Rodrigues, R. C. L. B., and Jeffries, T. W. Simultaneous saccharification and ethanol fermentation of oxalic acid pretreated corncob assessed with response surface methodology. Bioresource Technology. 2009. 100(24): 6307-6311.

- [164] López-Arenas, T., Rathi, P., Ramírez-Jiménez, E., and Sales-Cruz, M., Factors affecting the acid pretreatment of lignocellulosic biomass: Batch and continuous process, in *Computer aided chemical engineering*, Pierucci, S. and Ferraris, G. B., Editors. 2010, Elsevier. p. 979-984.
- [165] Mok, W. S., Antal, M. J., and Varhegyi, G. Productive and parasitic pathways in dilute acid-catalyzed hydrolysis of cellulose. Industrial & Engineering Chemistry Research. 1992. 31(1): 94-100.
- [166] Xiang, Q., Lee, Y., and Torget, R. Kinetics of glucose decomposition during dilute-acid hydrolysis of lignocellulosic biomass. Applied Biochemistry and Biotechnology. 2004. 115(1): 1127-1138.
- [167] Aguilar, R., Ramírez, J. A., Garrote, G., and Vázquez, M. Kinetic study of the acid hydrolysis of sugar cane bagasse. Journal of Food Engineering. 2002. 55(4): 309-318.
- [168] Abasaheed, A. E. and Mansour, M. E. Thermal effects on acid hydrolysis of cellulose. Bioresource Technology. 1992. 40(3): 221-224.
- [169] Kleinert, M. and Barth, T. Phenols from lignin. Chemical Engineering & Technology. 2008. 31(5): 736-745.
- [170] Ruiz-Matute, A. I., Brokl, M., Soria, A. C., Sanz, M. L., and Martínez-Castro, I. Gas chromatographic-mass spectrometric characterisation of tri- and tetrasaccharides in honey. Food Chemistry. 2010. 120(2): 637-642.
- [171] Sanz, M. L., et al. GC behavior of disaccharide trimethylsilyl oximes. Journal of Chromatographic Science. 2003. 41: 205-208.
- [172] Sanz, M., Sanz, J., and Martínez-Castro, I. Characterization of o-trimethylsilyl oximes of disaccharides by gas chromatography-mass spectrometry. Chromatographia. 2002. 56(9): 617-622.
- [173] Brokl, M., Soria, A. C., Martínez-Castro, I., Sanz, M. L., and Ruiz-Matute, A. I. Characterization of o-trimethylsilyl oximes of trisaccharides by gas

- chromatography-mass spectrometry. Journal of Chromatography A. 2009. 1216(22): 4689-4692.
- [174] Shen, D. K. and Gu, S. The mechanism for thermal decomposition of cellulose and its main products. Bioresource Technology. 2009. 100(24): 6496-6504.
- [175] Scalarone, D., Chiantore, O., and Riedo, C. Gas chromatographic/mass spectrometric analysis of on-line pyrolysis-silylation products of monosaccharides. Journal of Analytical and Applied Pyrolysis. 2008. 83(2): 157-164.
- [176] Nguyen, Q., et al. Dilute acid hydrolysis of softwoods. Applied Biochemistry and Biotechnology. 1999. 77(1): 133-142.
- [177] Nguyen, Q., Tucker, M., Keller, F., and Eddy, F. Two-stage dilute-acid pretreatment of softwoods. Applied Biochemistry and Biotechnology. 2000. 84-86(1-9): 561-576.
- [178] Karimi, K., Kheradmandinia, S., and Taherzadeh, M. J. Conversion of rice straw to sugars by dilute-acid hydrolysis. Biomass and Bioenergy. 2006. 30(3): 247-253.
- [179] Wongsiriwan, U., Noda, Y., Song, C., Prasassarakich, P., and Yeboah, Y. Lignocellulosic biomass conversion by sequential combination of organic acid and base treatments. Energy & Fuels. 2010. 24(5): 3232-3238.
- [180] Marzioletti, T., et al. Dilute acid hydrolysis of loblolly pine: A comprehensive approach. Industrial & Engineering Chemistry Research. 2008. 47(19): 7131-7140.
- [181] Wikberg, H. and Liisa Maunu, S. Characterisation of thermally modified hard- and softwoods by ¹³C CPMAS NMR. Carbohydrate Polymers. 2004. 58(4): 461-466.
- [182] Bardet, M., Foray, M. F., Maron, S., Goncalves, P., and Tr an, Q. K. Characterization of wood components of portuguese medieval dugout canoes

- with high-resolution solid-state NMR. Carbohydrate Polymers. 2004. 57(4): 419-424.
- [183] Freitas, J. C. C., Bonagamba, T. J., and Emmerich, F. G. Investigation of biomass- and polymer-based carbon materials using ^{13}C high-resolution solid-state NMR. Carbon. 2001. 39(4): 535-545.
- [184] Bardet, M., et al. Investigation with ^{13}C NMR, EPR and magnetic susceptibility measurements of char residues obtained by pyrolysis of biomass. Fuel. 2007. 86(12-13): 1966-1976.
- [185] Sievers, C., et al. Quantitative solid state NMR analysis of residues from acid hydrolysis of loblolly pine wood. Bioresource Technology. 2009. 100(20): 4758-4765.
- [186] Song, C., Hou, L., Saini, A. K., Hatcher, P. G., and Schobert, H. H. CPMAS ^{13}C NMR and pyrolysis-GC-MS studies of structure and liquefaction reactions of montana subbituminous coal. Fuel Processing Technology. 1993. 34(3): 249-276.
- [187] Kakumoto, T., Saito, K., and Imamura, A. Unimolecular decomposition of oxalic acid. The Journal of Physical Chemistry. 1987. 91(9): 2366-2371.
- [188] Artok, L., Davis, A., Mitchell, G. D., and Schobert, H. H. Swelling pretreatment of coals for improved catalytic liquefaction. Fuel. 1992. 71(9): 981-991.
- [189] Pinto, F., Gulyurtlu, I., Lobo, L. S., and Cabrita, I. Effect of coal pre-treatment with swelling solvents on coal liquefaction. Fuel. 1999. 78(6): 629-634.
- [190] Joseph, J. T. Beneficial effects of preswelling on conversion and catalytic activity during coal liquefaction. Fuel. 1991. 70(3): 459-464.
- [191] Trtik, P., et al. 3D imaging of microstructure of spruce wood. Journal of Structural Biology. 2007. 159(1): 46-55.

- [192] Philipp, B., Schleicher, H., and Wagenknecht, W. The influence of cellulose structure on the swelling of cellulose in organic liquids. Journal of Polymer Science: Polymer Symposia. 1973. 42(3): 1531-1543.
- [193] Fidale, L. C., Ruiz, N., Heinze, T., and Seoud, O. A. E. Cellulose swelling by aprotic and protic solvents: What are the similarities and differences? Macromolecular Chemistry and Physics. 2008. 209(12): 1240-1254.
- [194] Blanca Roncero, M., Colom, J. F., and Vidal, T. Why oxalic acid protects cellulose during ozone treatments? Carbohydrate Polymers. 2003. 52(4): 411-422.
- [195] Tanczos, I., et al. Effect of tetramethylammonium hydroxide on cotton cellulose compared to sodium hydroxide. Macromolecular Chemistry and Physics. 2000. 201(17): 2550-2556.
- [196] Moharram, M. A. and Mahmoud, O. M. X-ray diffraction methods in the study of the effect of microwave heating on the transformation of cellulose I into cellulose II during mercerization. Journal of Applied Polymer Science. 2007. 105(5): 2978-2983.
- [197] Tillman, L., Lee, Y., and Torget, R. Effect of transient acid diffusion on pretreatment/hydrolysis of hardwood hemicellulose. Applied Biochemistry and Biotechnology. 1990. 24-25(1): 103-113.
- [198] Noda, Y. Unpublished work. 2009.
- [199] Takahashi, M. and Ookubo, M. CP/MAS ¹³C NMR and waxes studies on the effects of starting cellulose materials on transition between cellulose polymorphs. Kobunshi Ronbunshu. 1994. 51(2): 107-113.
- [200] Zugenmaier, P. Conformation and packing of various crystalline cellulose fibers. Progress in Polymer Science. 2001. 26(9): 1341-1417.

- [201] Zakrzewska, M. G. E., Bogel-L•Ukasik, E., and Bogel-L•Ukasik, R. Solubility of carbohydrates in ionic liquids. Energy & Fuels. 2010. 24(2): 737-745.
- [202] Park, S., Baker, J., Himmel, M., Parilla, P., and Johnson, D. Cellulose crystallinity index: Measurement techniques and their impact on interpreting cellulase performance. Biotechnology for Biofuels. 2010. 3(1): 10.
- [203] Zhu, S., et al. Dissolution of cellulose with ionic liquids and its application: A mini-review. Green Chemistry. 2006. 8(4): 325-327.
- [204] Meller, A. The effect of crystalline structure on the alkaline degradation of cellulose fibers. Journal of Polymer Science. 1961. 51(155): 99-109.
- [205] Haas, D. W., Hrutfiord, B. F., and Sarkanen, K. V. Kinetic study on the alkaline degradation of cotton hydrocellulose. Journal of Applied Polymer Science. 1967. 11(4): 587-600.
- [206] Van Loon, L. and Glaus, M. Review of the kinetics of alkaline degradation of cellulose in view of its relevance for safety assessment of radioactive waste repositories. Journal of Polymers and the Environment. 1997. 5(2): 97-109.
- [207] Van Loon, L. R., Glaus, M. A., Laube, A., and Stallone, S. Degradation of cellulosic materials under the alkaline conditions of a cementitious repository for low- and intermediate-level radioactive waste. II. Degradation kinetics. Journal of Polymers and the Environment. 1999. 7(1): 41-51.
- [208] Segal, L., Creely, J. J., Martin, A. E., and Conrad, C. M. An empirical method for estimating the degree of crystallinity of native cellulose using the x-ray diffractometer. Textile Research Journal. 1959. 29(10): 786-794.
- [209] Zhao, H., et al. Effects of crystallinity on dilute acid hydrolysis of cellulose by cellulose ball-milling study. Energy & Fuels. 2005. 20(2): 807-811.
- [210] Noda, Y., Wongsiriwan, U., Prasassarakich, P., Yeboah, Y., and Song, C. Sequential combination of organic acid and base treatments for converting

- lignocellulosic biomass and cellulose. Preprint Paper-American Chemical Society, Division of Fuel Chemistry. 2010. 55(2): 941-943.
- [211] Pavasars, I., Hagberg, J., Borén, H., and Allard, B. Alkaline degradation of cellulose: Mechanisms and kinetics. Journal of Polymers and the Environment. 2003. 11(2): 39-47.
- [212] Berggren, R., Molin, U., Berthold, F., Lennholm, H., and Lindström, M. Alkaline degradation of birch and spruce: Influence of degradation conditions on molecular mass distributions and fibre strength. Carbohydrate Polymers. 2003. 51(3): 255-264.
- [213] Sanz, M. L. and Martínez-Castro, I. Recent developments in sample preparation for chromatographic analysis of carbohydrates. Journal of Chromatography A. 2007. 1153(1-2): 74-89.
- [214] Scherz, H. and Bonn, G. Analytical chemistry of carbohydrates. Stuttgart: Thieme Medical Publishers, 1998.
- [215] Ball, G. F. M. The application of HPLC to the determination of low molecular weight sugars and polyhydric alcohols in foods: A review. Food Chemistry. 1990. 35(2): 117-152.
- [216] Binder, H. Separation of monosaccharides by high-performance liquid chromatography: Comparison of ultraviolet and refractive index detection. Journal of Chromatography A. 1980. 189(3): 414-420.
- [217] Shen, X. and Perreault, H. Characterization of carbohydrates using a combination of derivatization, high-performance liquid chromatography and mass spectrometry. Journal of Chromatography A. 1998. 811(1-2): 47-59.
- [218] Lamari, F. N., Kuhn, R., and Karamanos, N. K. Derivatization of carbohydrates for chromatographic, electrophoretic and mass spectrometric structure analysis. Journal of Chromatography B. 2003. 793(1): 15-36.

- [219] Zhang, L., Xu, J., Zhang, L., Zhang, W., and Zhang, Y. Determination of 1-phenyl-3-methyl-5-pyrazolone-labeled carbohydrates by liquid chromatography and micellar electrokinetic chromatography. Journal of Chromatography B. 2003. 793(1): 159-165.
- [220] Lv, Y., et al. Separation and quantification of component monosaccharides of the tea polysaccharides from *Gynostemma pentaphyllum* by HPLC with indirect UV detection. Food Chemistry. 2009. 112(3): 742-746.
- [221] Fischer, K., Wacht, M., and Meyer, A. Simultaneous and sensitive HPLC determination of mono- and disaccharides, uronic acids, and amino sugars after derivatization by reductive amination. Acta hydrochimica et hydrobiologica. 2003. 31(2): 134-144.
- [222] Momenbeik, F. and Khorasani, J. Separation and determination of sugars by reversed-phase high-performance liquid chromatography after pre-column microwave-assisted derivatization. Analytical and Bioanalytical Chemistry. 2006. 384(3): 844-850.
- [223] Zhang, Y., Huang, L. J., and Wang, Z. F. A sensitive derivatization method for the determination of the sugar composition after pre-column reductive amination with 3-amino-9-ethylcarbazole (AEC) by high-performance liquid chromatography. Chinese Journal of Chemistry. 2007. 25(10): 1522-1528.
- [224] Abreu, P., Pereira, A., and Relva, A. Characterisation of a sugar fraction from *Sarcocephalus latifolius* stem bark extract. Carbohydrate Polymers. 2001. 45(2): 155-160.
- [225] Medeiros, P. M. and Simoneit, B. R. T. Analysis of sugars in environmental samples by gas chromatography-mass spectrometry. Journal of Chromatography A. 2007. 1141(2): 271-278.
- [226] Little, J. L. Artifacts in trimethylsilyl derivatization reactions and ways to avoid them. Journal of Chromatography A. 1999. 844(1-2): 1-22.

- [227] Kootstra, A. M., Beefink, H., Scott, E., and Sanders, J. Optimization of the dilute maleic acid pretreatment of wheat straw. Biotechnology for Biofuels. 2009. 2(1): 31.
- [228] Springer, E. L. Prehydrolysis of hardwoods with dilute sulfuric acid. Industrial & Engineering Chemistry Product Research and Development. 1985. 24(4): 614-623.



ศูนย์วิทยทรัพยากร
จุฬาลงกรณ์มหาวิทยาลัย



APPENDICES

ศูนย์วิทยทรัพยากร
จุฬาลงกรณ์มหาวิทยาลัย

Appendix A

Sugar Analysis by Derivatization Methods

A.1 HPLC Analysis of Sugars

In general, underivatized sugars can be analyzed by HPLC with refractive index, mass spectroscopy, or evaporative light-scattering detectors [213, 214] with an aminopropylsilane-bonded silica stationary phase column [215]. A test with HPLC shows that sugars cannot be detected with HPLC equipped with octadecyl reversed-phase column (Pinnacle II PAH 5 μm \times 250 mm) and photodiode array detector (Waters 996), operated to monitor UV-vis spectra in the range of 200-400 nm. As shown in Figure A-1, only phenolic compounds are detected.

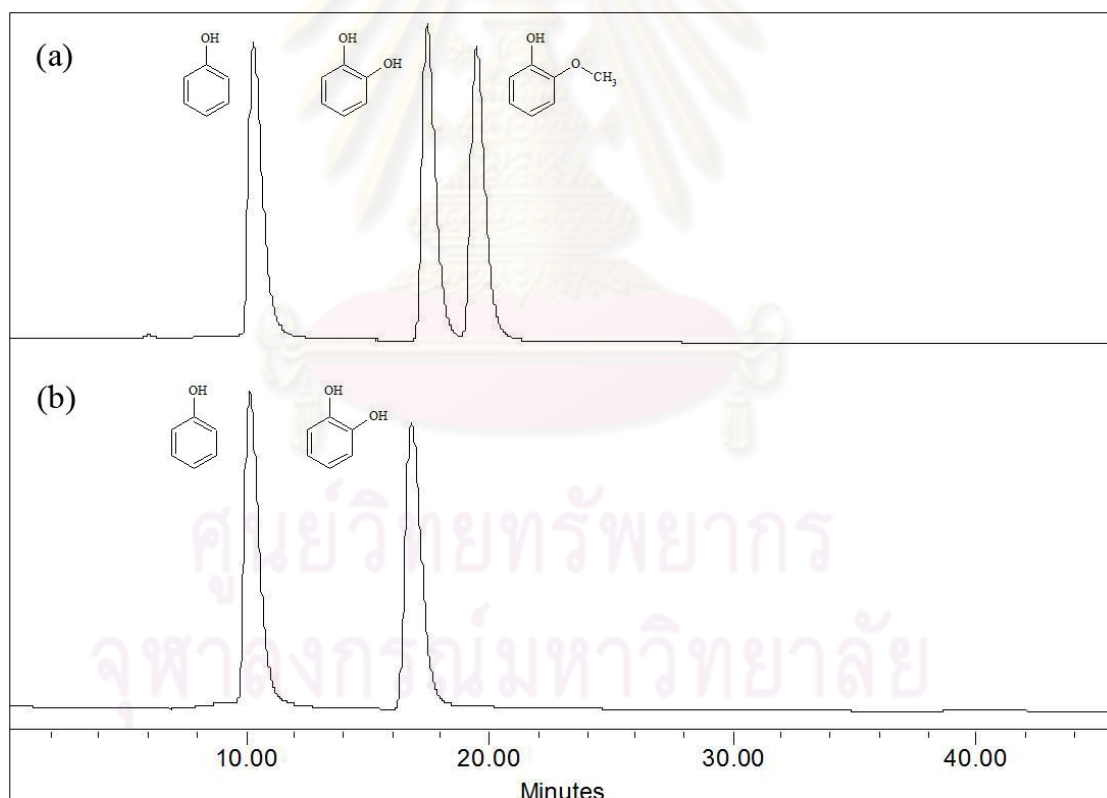


Figure A-1 HPLC chromatogram at 270 nm of (a) mixture of phenol, catechol, and guaiacol standard with concentration of 0.6 mg/mL each, (b) mixture of phenol, catechol, 2 pentoses, 3 hexoses, and cellobiose standard with concentration of 0.67 mg/mL each.

In alkylated-bonded silica gels column such as C₁₈ reversed-phase one, monosaccharides are eluted very quickly as a single unresolved peak and only less polar sugars can be separated in this type of column [214]. Also, the photodiode array detector is not a suitable detector for sugars, because the maximum absorption for sugars occurs around 188 nm from carbonyl group, but it usually overlap with peaks from contaminant and solute [216]. Therefore, pre-column derivation should be done for analysis in the existing HPLC. There are several methods for derivatization that applied to the similar type of the existing HPLC as shown in Table A-1.

The more common derivatization approach is called reductive amination, where carbonyl group in sugar in reducing state is labeled with an amino group, as shown in Figure A-3. Another common procedure, shown in Figure A-2, using 1-phenyl-3-methyl-5-pyrazolone (PMP) as a labeling agent to the carbonyl group of sugars is suggested as a preferred technique due to better resolution than reductive amination by 2-aminopyridine agent [217]. Other derivatization methods are also existing, but less common.

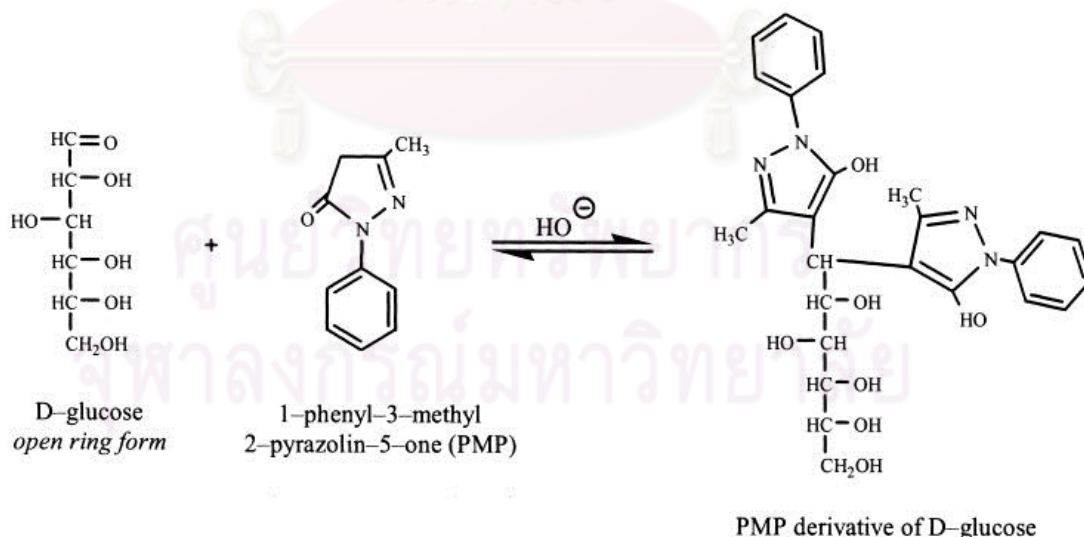


Figure A-2 Derivation of sugars with PMP [218].

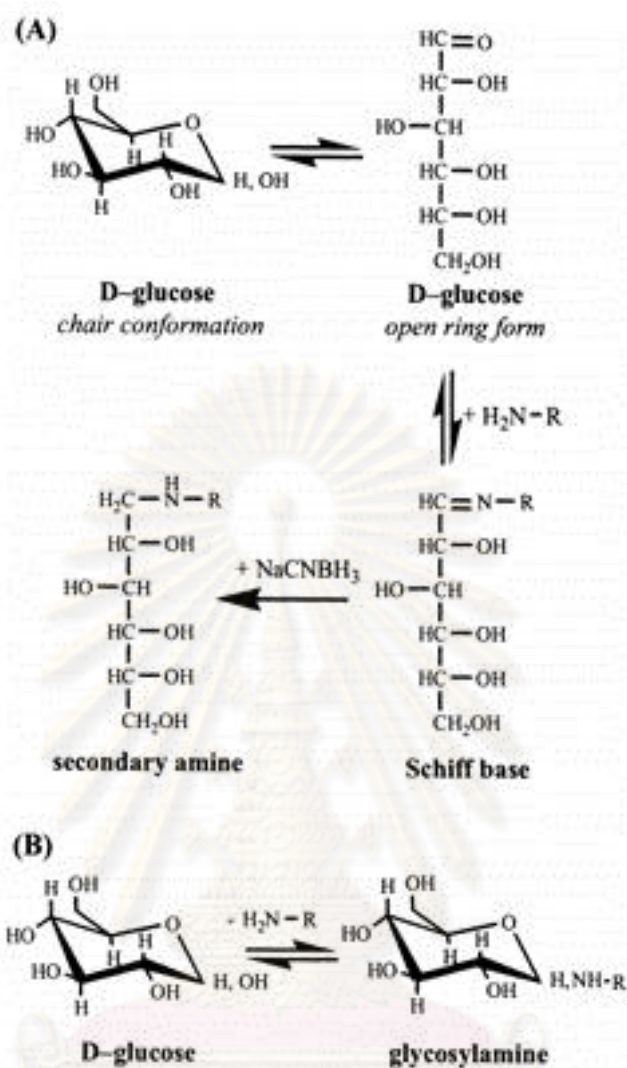


Figure A-3 Reductive amination of glucose (a) with reducing agent (b) without reducing agent [218].

A test for derivatization of sugars for HPLC was carried out with PMP reagent with a procedure from literature [219]. However, only one broad peak of PMP was shown after derivatization. The data was not shown due to the loss during instrument collapse.

Table A-1 Summary of carbohydrate derivatization for octadecyl reversed-phase column equipped with a detector in the range of 200-400 nm.

Sample	Reagents	Derivatives	WL (nm)	Conditions	Column	Detector	Ref.
Small sugar standards	PMP	bis-PMP-sugars	245	70 °C, 2 h	Inertsil ODS-3 (15x0.46 cm, 5 mm)	8450 UV-vis SpectraPhysics	[217]
Oligosaccharide standards	PMP	bis-PMP-sugars	245	70 °C, 2 h	Hypersil ODS (25x0.46 cm, 5 mm)	Varian 9050 UV-vis	[217]
Sugar standards	PMP	PMP-sugars	245	30 min	Hypersil ODS2 (15x0.45 cm, 5 mm)	UV200II	[219]
Conc. Aloe powder	PMP	PMP-sugars	245	30 min	Hypersil ODS2 (15x0.45 cm, 5 mm)	UV200II	[219]
Candy	PMP	PMP-sugars	245	30 min	Hypersil ODS2 (15x0.45 cm, 5 mm)	UV200II	[219]
Beer	PMP	PMP-sugars	245	30 min	Hypersil ODS2 (15x0.45 cm, 5 mm)	UV200II	[219]
Green tea	PMP	PMP-sugars	250	70 °C, 60 min	RP-C ₁₈ 35 °C	UV-vis	[220]

Table A-1 Summary of carbohydrate derivatization for octadecyl reversed-phase column equipped with a detector in the range of 200-400 nm. (continued)

Sample	Reagents	Reducing reagent	Derivatives	WL (nm)	Conditions	Column	Detector	Ref.
Small sugar standards	2-aminopyridine	borane-dimethylamine complex in mixture of acetic acid solution	Pyridylamino (PA)	318	80-90 °C, 60 min	Vydac 218TP54 Protein and Peptide C18 (25x0.46 cm, 5 mm)	Waters 486 Tunable Absorbance UV	[217]
Sugar standards	p-AMBA	NaBH ₃ CN	-	303	60 °C, 15 min	RP-C ₁₈ (AQUA 5 C ₁₈)	Dual beam UV detector SPD-10 AVP & DAD detector SPD-M 10 AVP	[221]
Sugar standards	p-AMBA propyl ester	NaBH ₃ CN	-	287	90 °C, 75 min	RP-C ₁₈ (AQUA 3 C ₁₈)	Dual beam UV detector SPD-10 AVP & DAD detector SPD-M 10 AVP	[221]
Sugar standards	4-aminoazobenzene	NaBH ₃ CN	-	377	90 °C, 60 min	RP-C ₁₈ (Nucleosil 100 C ₁₈)	Dual beam UV detector SPD-10 AVP & DAD detector SPD-M 10 AVP	[221]
Sugar standards	1-aminopyrene	NaBH ₃ CN	-	241	90 °C, 90 min	RP-C ₁₈ (Nucleosil 100 C ₁₈)	Dual beam UV detector SPD-10 AVP & DAD detector SPD-M 10 AVP	[221]
Sugar standards	2-(2-aminophenyl)-indole	NaBH ₃ CN	-	223	60 °C, 90 min	RP-C ₁₈ (AQUA 3 C ₁₈)	Dual beam UV detector SPD-10 AVP & DAD detector SPD-M 10 AVP	[221]

Table A-1 Summary of carbohydrate derivatization for octadecyl reversed-phase column equipped with a detector in the range of 200-400 nm. (continued)

Sample	Reagents	Reducing reagent	Derivatives	WL (nm)	Conditions	Column	Detector	Ref.
Sugar standards	PNA	NaBH ₃ CN	PNA-sugars	380	microwave, 600 W, 5 min	Nucleosil ODS & LiRP-18-5-10C at 40 °C	PU4255 UV	[222]
Milk powder	PNA	NaBH ₃ CN	PNA-sugars	380	microwave, 600 W, 5 min	Nucleosil ODS & LiRP-18-5-10C at 40 °C	PU4255 UV	[222]
Sugar standards	AEC	NaBH ₃ CN	AEC-sugars	254	70 °C, 60 min	RP-C ₁₈ (25x0.46 cm, 5 mm) 30 °C	Water 2996 UV	[223]
Stem bark of <i>S. latifolius</i>	Benzoyl chloride	-	Benzoylated-sugars	200-450	0 °C	Lichrospher Si60 & Lichrospher 100 RP18 (250x8 mm ² , 10 mm) (normal phase)	Diode array detector L7450A	[224]

Reagent abbreviation: 1-phenyl-3-methyl-5-pyrazolone (PMP), p-aminobenzoic acid (p-AMBA), p-aminobenzoic ethyl ester (ABEE), p-nitroaniline (PNA), 3-amino-9-ethylcarbazole (AEC).

A.2 GC Analysis of Sugars

HPLC operation seems more complicate than GC, while GC offer automated injection, better quantitative sugar determination [214], and identification of the substance by mass spectroscopy. When gas chromatography was used for analysis, derivatization is required to convert nonvolatile sugars to volatile ones [218]. Besides increasing sugar volatility, derivatization also improves stability of organic compounds containing active hydrogens, chromatographic characteristics, and mass spectroscopic behavior of the analyte by decreasing polarity and increase the detector sensitivity of analyte. The separation of derivatized compounds is also better for relatively non-polar capillary columns, such as DB-5, VF-5, and Rtx-5. A test on nonderivatized mixture of glucose, acetic acid, phenolic compounds was shown in Figure 3.12; only phenolic compounds are detected in GC-MS.

Derivatization of carbohydrate for gas chromatography is different from that for HPLC. Most GC derivatization involves replacing the active hydrogen atoms with non-polar substituents such as methyl, trifluoroacetyl, trimethylsilyl groups.

Trimethylsilylation is by far one of the major derivatization method for increasing the volatility and GC characteristics of a substance. It also has the added advantage in that trimethylsilyl groups increase the total ion current and the sensitivity of it mass spectrum. Derivatization of monosaccharides and disaccharides in this work was carried out by two trimethylsilylation methods.

A.2.1 Derivatization Method A

Method A is a trimethylsilylation of sugars with BSTFA [N,O-bis(trimethylsilyl)trifluoroacetamide] in non-protic solvent pyridine. BSTFA is a common trimethylsilylation agent that react with active proton as the following Figure A-4. Therefore, hydroxyl groups in sugars are silylated as shown in Figure A-5. In the method A adapted from Medeiros and Simoneit [225], 200 μL of standards or samples were dried in a stream of nitrogen gas (UHP nitrogen) until a complete dryness was achieved. Then, 200 μL of BSTFA and 1 mL of pyridine were added. The sealed vial was heated in a water bath at 70 $^{\circ}\text{C}$ for 3 h before injection in the GC.

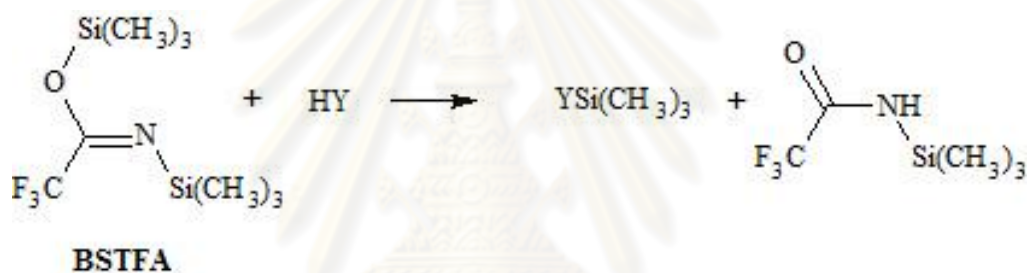


Figure A-4 Reaction scheme of BSTFA with active proton [226].

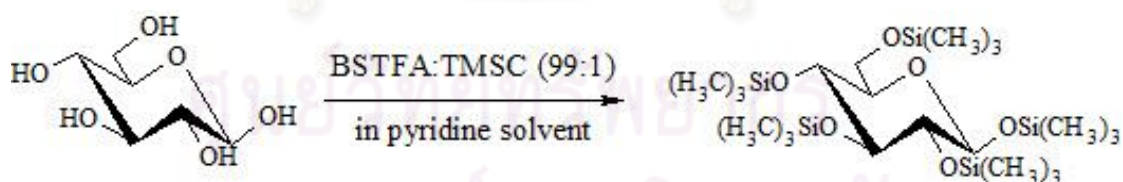


Figure A-5 Reaction scheme of glucose derivatization by BSTFA (Method A) [226].

As an initial trial, a standard containing glucose and cellobiose was injected into the GC. A typical chromatogram from GC-MS is shown in Figure A-6. Peak 1 and 2 at 24.75 and 26.25 min are trimethylsilyl derivatives of glucose. Peak 3 and 4 at 36.1 and 37.3 min are trimethylsilyl derivatives of cellobiose.

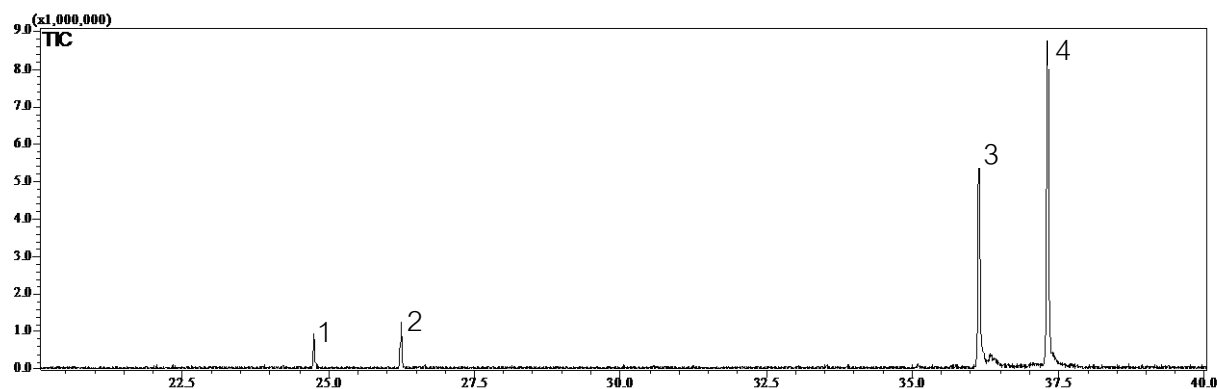


Figure A-6 Typical chromatogram from trimethylsilylation of glucose and cellobiose standard from 6 $\mu\text{g}/\text{mL}$ glucose and 70 $\mu\text{g}/\text{mL}$ cellobiose standard.

One of the drawbacks of this procedure is that the long derivatization time is required as shown in Figure A-7; when the reaction time was reduced, the amounts of silylation products were significantly affected. The long reaction time is an obstacle to do routine derivatization because the temperature and water level of the water bath has to be controlled manually during this step.

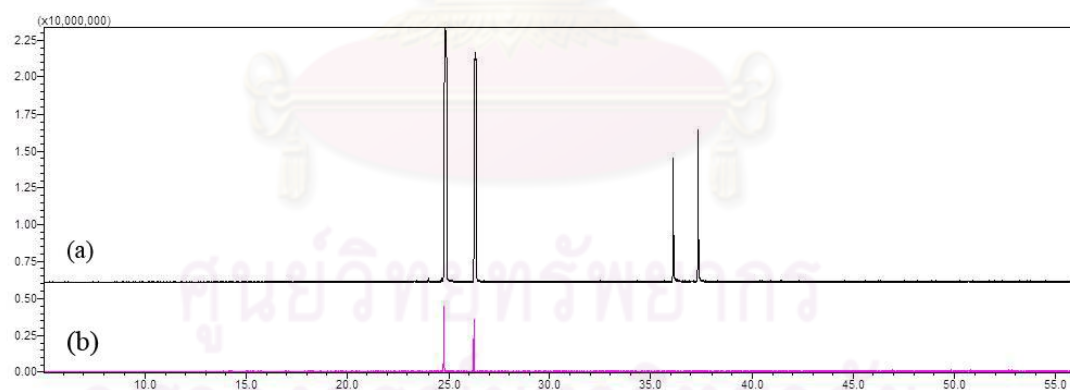


Figure A-7 GC-MS chromatogram of standard 200 $\mu\text{g}/\text{mL}$ glucose and 40 $\mu\text{g}/\text{mL}$ cellobiose with different derivatization time (a) 3h (b) 1h.

In order to quantify the amount of sugars in other samples, a calibration curve from peak area of sugar standard was created. However, there was a problem in reproducibility of the procedure, as demonstrated in Figure A-8 and Figure

A-9, which could partly due to the long reaction time render it difficult to reproduce the result with minimal error. Therefore, another method to derivatize sugars was explored in order to decrease reaction time and increase reproducibility of the derivatization method.

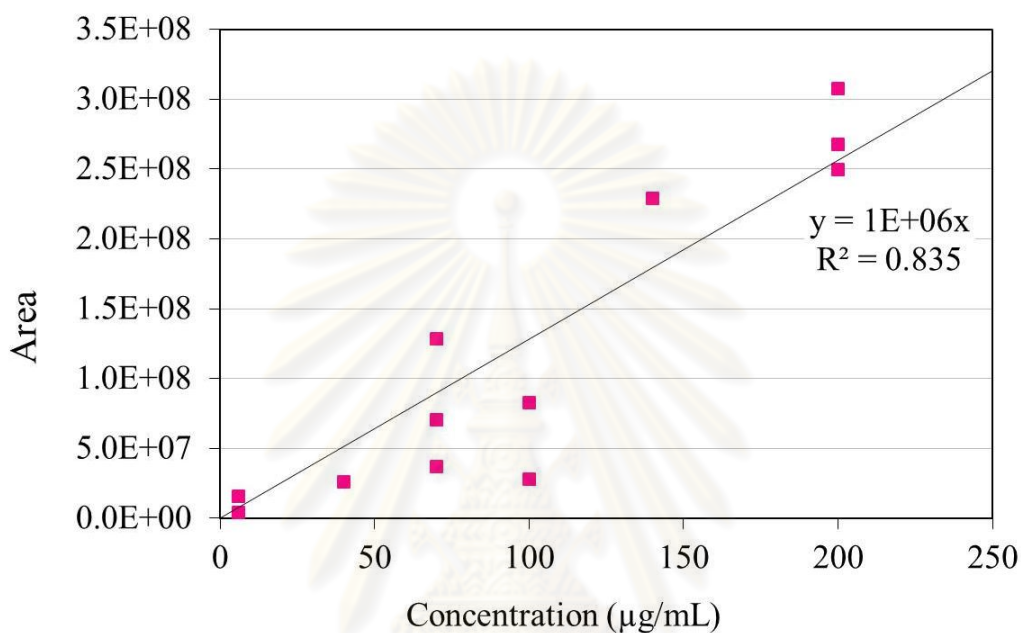


Figure A-8 Calibration curve of glucose standard after derivatization by method A.

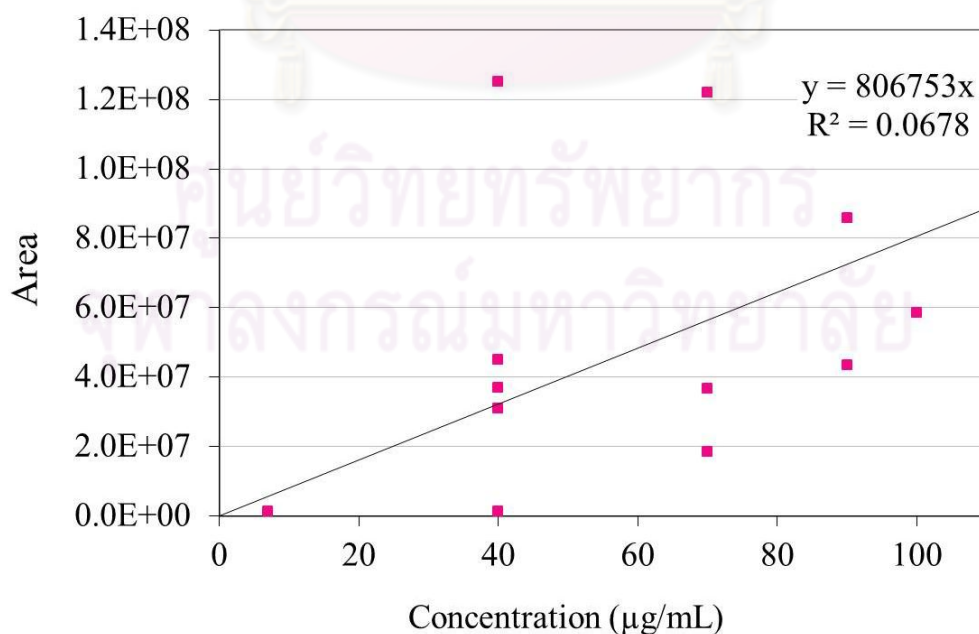


Figure A-9 Calibration curve of cellobiose standard after derivatization by method A.

A.2.2 Derivatization Method B

In method B, oxime-trimethylsilylation of sugars was performed in two steps, oxime formation and silylation step, as described in Chapter 2. This derivatization method yields fairly stable derivatives [213]. The optimized reaction conditions for both step from Rojas-Escudero et al. [146] was used without modification. Additional post-derivatization extraction step was added to the method. As shown in Figure A-10, the extraction with hexane gives the most distinct peaks of the derivatized standards. Also, it was found in the samples with high sugar concentration that the reaction medium may become very viscous and cannot be transferred to an injection vial for GC. Therefore, the extraction step was added at the end of the derivatization. Also, the GC oven temperature program was modified with slower heating rate to improve separation of the hexose sugars.

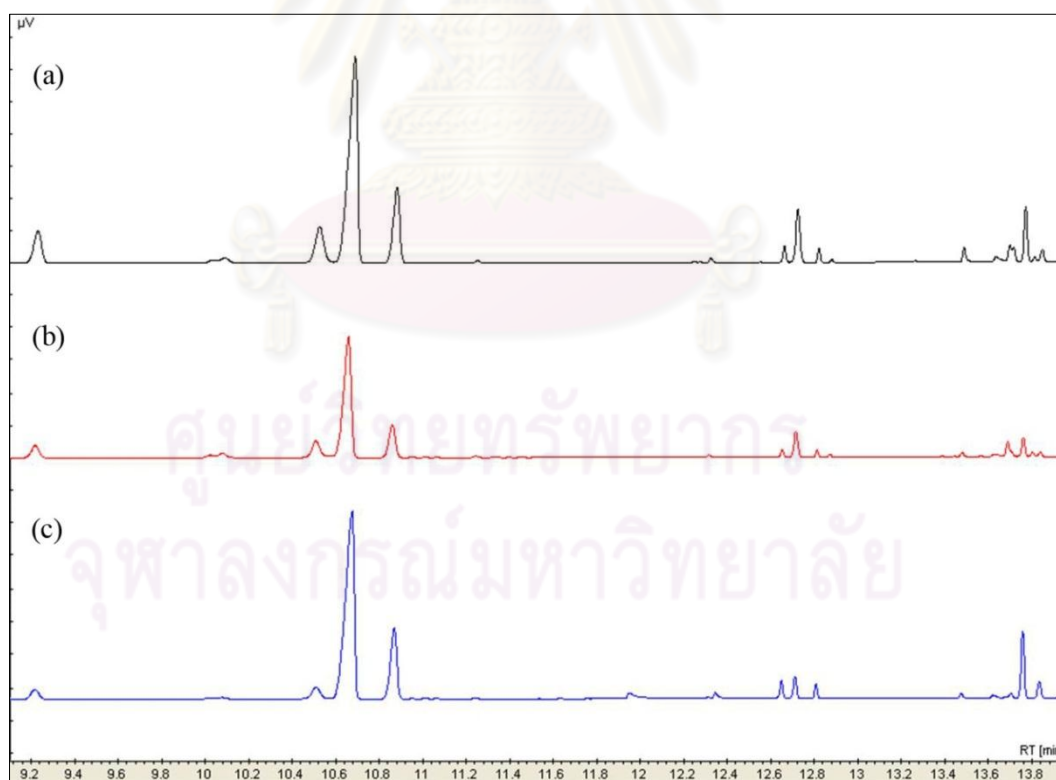


Figure A-10 GC-FID chromatogram of standard 200 µg/mL glucose and 40 µg/mL cellobiose (a) with hexane extraction (b) with dichloromethane extraction (c) in aniline solvent without extraction.

Calibration with standard for the derivatization method B of glucose and cellulose are shown in Figure A-11 and A-12. Repeatability of the derivatization method B was also tested and gives satisfactory results.

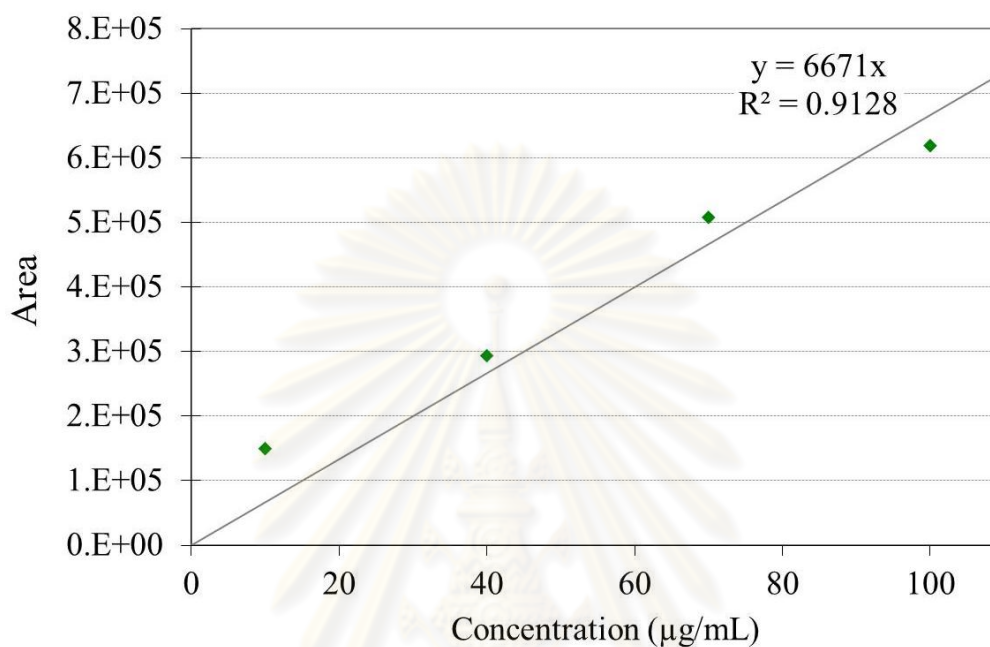


Figure A-11 Calibration curve of glucose standard after derivatization by method B.

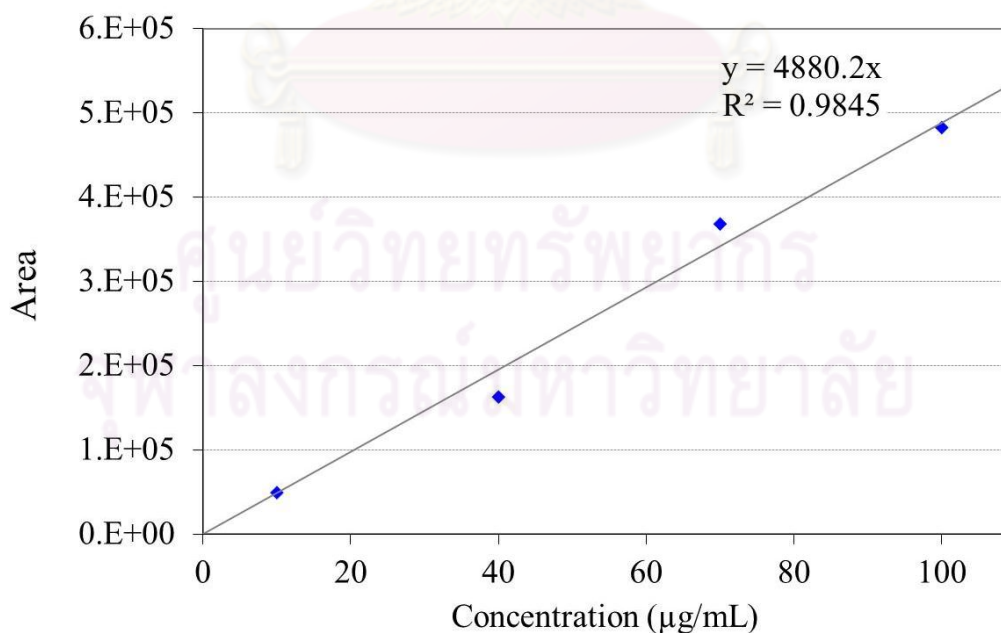


Figure A-12 Calibration curve of cellobiose standard after derivatization by method B.

Identification of the derivatized samples was carried out by two methods: comparing retention time with the standard, and MS identification by inject the same sample in GC-MS as shown in Figure A-13. In the MS identification, the order of eluted compounds is in the same sequence but not at the same retention time due to different column used by GC-FID and GC-MS. Noted that there could be more peaks present in GC-MS chromatogram due to some nitrogen compounds which do not show in FID.

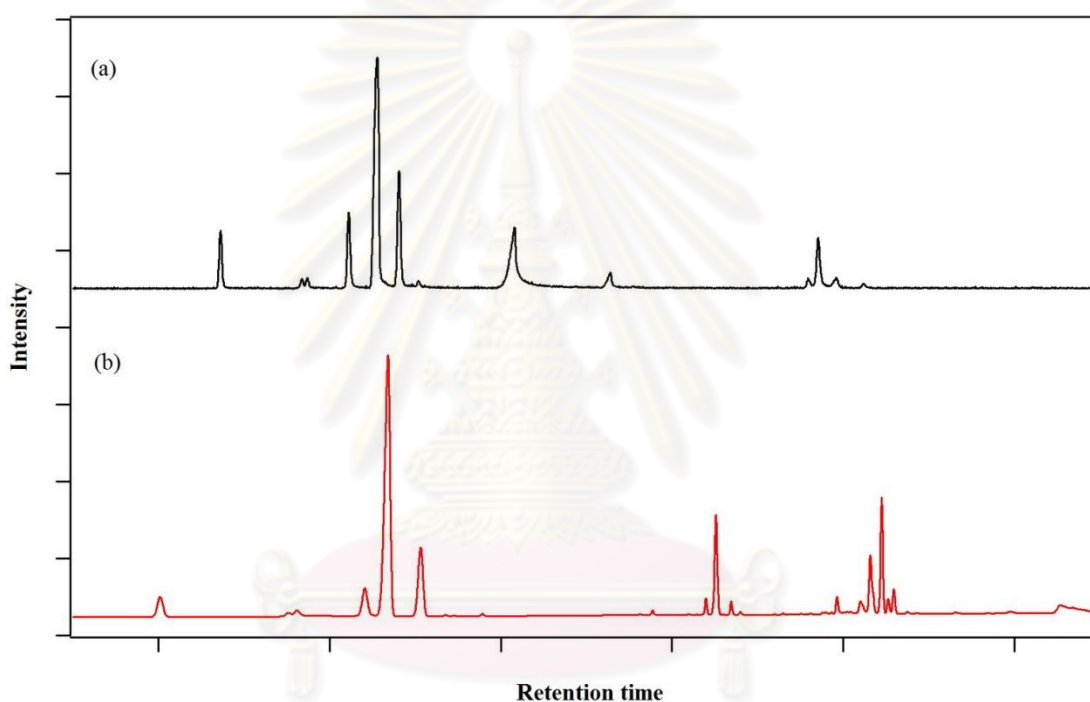
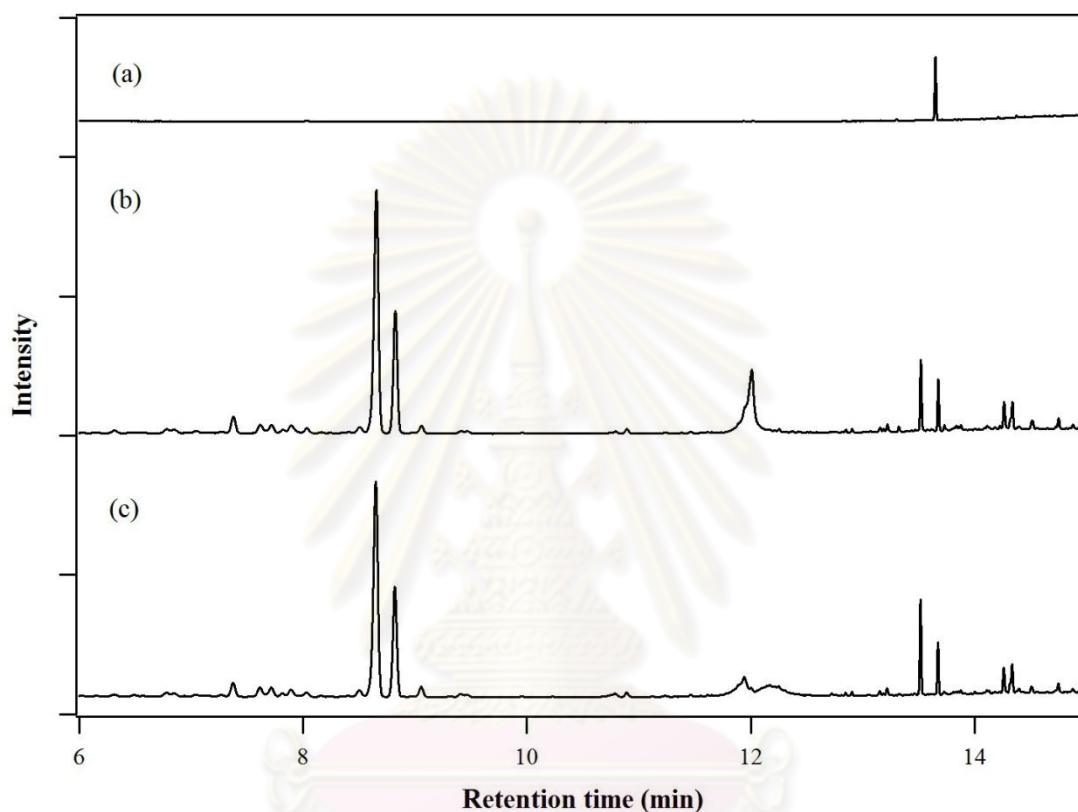


Figure A-13 Chromatogram of the same sample injected in (a) GC-MS (b) GC-FID

Another modification made to the derivatization procedure is neutralization step of the alkali samples. As shown in Figure A-14, the sample from base reaction does not derivatized unless the neutralization was done prior to the derivatization. From Figure A-14, both neutralization by acetic acid and oxalic acid



give the same result (peaks at 8.6 and 8.8 min) qualitatively and quantitatively.

Figure A-14 GC-FID chromatogram of samples from base reaction after derivatization (a) without neutralization (b) neutralized with acetic acid (c) neutralized with oxalic acid.

As mentioned in Chapter 2, the method employed for sugar analysis in this study is suitable for characterization of monomeric sugars, even though the cellobiose was also detected. Sugar oligomers are likely to exist in the liquid phase. It is reported that oligomers of glucose with degree of polymerization less than or equal to 6 are soluble in water [23]. In an autohydrolysis by water or typical diluted H_2SO_4 acid hydrolysis, the secondary hydrolysis to determine amount of oligomer can be done by adding acid or diluted with water to achieve final H_2SO_4 concentration of 4%, and then the mixture is heated at 121 °C for 1 h [27, 180, 227, 228]. This method is the resemble of the standard procedures publish by ASTM and NREL [79, 80]. However, in the oxalic acid hydrolysis, it is not possible to use secondary hydrolysis based on these standards. Therefore, the oligomers soluble in liquid product s were not analyzed. However, it is likely that there are oligomers in the liquid product since oligosaccharides were reported as intermediates for acid hydrolysis of biomass [27, 165, 176, 177].

Appendix B

Identification of Pyrolysis Products from Literature

Tables below are compilation of thermal degradation products from biomass for analysis of solid products by pyrolysis-gas chromatography technique presented in Chapter 4. Table B-1, B-2, and B-3 present compounds derived from polysaccharides, lignin, and lignin reacted with TMAH, respectively. Included in these tables are the name and other common names of the compounds, CAS number, origin of compounds, molecular weight, base peak, and m/z of mass spectrometry. Noted that the characteristic ion masses (m/z) were arranged in a sequence by their intensity in MS, where the base peak is the peak with the highest intensity. The m/z data was supplemented from outside literature in SciFinder, but m/z for some substances may not be available. This information is very useful for identification of the compounds and its origin in biomass. The order of elution is, however, depending on the column used, and not in the exact order as shown in the tables.

The polysaccharides term used in the Table B-1 represents for cellulose and hemicellulose degradation products, because both can produce the same compounds during pyrolysis and cannot be differentiated from each other. The lignin compounds were classified as H-, G-, and S-lignin, referring to Hydroxyphenyl, Guaiacyl, and Syringyl lignin, respectively, which are the type of lignin analogous to precursor units of lignin. There is also modified lignin, which cannot be identified the type of lignin because it has been modified during the reaction. The lignin-TMAH substances are the compounds derived from lignin that reacts with TMAH via methylation, which may occurred during reaction. Although TMAH can react with lignin in pyrolysis condition, it has been removed from solid residues by washing with water. When there is TMAH in the sample, the pyrogram will show intense peak of trimethylamine (TMA) peak. Also, the remaining TMAH in solid residues may

corrosive to the drying oven. Therefore, all the solid residues were thoroughly washed with water during collection from the reactor before drying.

Table B-1 Identified polysaccharides-derived compounds as pyrolysis products [147-152].

#	Compounds	CAS	Other names	Origin	MW	Base peak	m/z
P1	Carbon dioxide	124-38-9	-	Unknown	44	44	44/28
P2	Formaldehyde	50-00-0	-	Polysaccharides	30	29	29/30/28
P3	Methanol	67-56-1	-	Polysaccharides	32	31	31/32/29
P4	Formic acid	64-18-6	-	Polysaccharides	46	46	46/45/44
P5	Acetaldehyde	75-07-0	-	Polysaccharides	44	29	29/44/43
P6	Acetic acid	64-19-7	-	Polysaccharides	60	43	43/45/60
P7	Acetaldehyde, hydroxy-	141-46-8	Hydroxyacetaldehyde	Polysaccharides (Hexose polymer)	60	31	31/32/29
P8	1,2-Ethenediol	107-21-1	1,2-Dihydroxyethane	Polysaccharides	62	31	31/33/29
P9	1,2-Ethenediol	1571-60-4	1,2-Dihydroxyethene	Polysaccharides	60	31	31/42/60
P10	2-Propenal	107-02-8	-	Polysaccharides	56	56	56/55/37
P11	Propanal, 2-oxo-	78-98-8	Propanal-2-one	Polysaccharides	72	43	43/45/72
P12	2-Propanone, 1-hydroxy-	116-09-6	Hydroxypropanone	Polysaccharides (Hexose polymer)	74	43	43/31/74
P13	Propanal, 2-hydroxy-	598-35-6	-	Polysaccharides	74	45	45/43/46
P14	Propanal, 3-hydroxy-	2134-29-4	-	Polysaccharides	74	43	43/73/74
P15	Butanal	123-72-8	Butyraldehyde	Polysaccharides	72	44	44/43/72
P16	2-Butenal	4170-30-3	-	Polysaccharides	70	41	41/70/39
P17	2-Butanone	78-93-3	-	Polysaccharides	72	43	43/72/57
P18	2-Butanone, 1-hydroxy-	5077-67-8	-	Polysaccharides	88	57	57/31/56
P19	2-Propenoic acid, methyl ester	96-33-3	-	Polysaccharides	86	55	55/85/58
P20	Butanedial	638-37-9	-	Polysaccharides	86	58	58/43/57
P21	2,3-Butanedione	431-03-8	-	Polysaccharides	86	43	43/86/42
P22	3-Butenal, 2-oxo-	16979-06-9	2-keto-but-3-enal; 3-butenal-2-one	Polysaccharides (Hexose polymer)	84	84	84/55/56
P23	Butanal, 2-hydroxy-3-oxo-	473-80-3	2-hydroxy-3-ketobutanal; 2-hydroxy-3-oxobutanal	Polysaccharides (Hexose polymer)	102	43	43/42/102
P24	Butanedial, 2-hydroxy-	7724-28-9	-	Polysaccharides	102	44	44/43/74
P25	Acetic acid, 1,1'-anhydride	108-24-7	Acetic anhydride	Polysaccharides	102	43	43/42/45

Table B-1 Identified polysaccharides-derived compounds as pyrolysis products (continued).

#	Compounds	CAS	Other names	Origin	MW	Base peak	m/z
P26	Propanoic acid, 2-oxo-, methyl ester	600-22-6	2-Oxo-propanoic acid methyl ester	Polysaccharides	102	43	43/102/42
P27	2,4-Pentadienal	764-40-9	-	Polysaccharides	82	39	39/53/81
P28	2-Butenoic acid, methyl ester	18707-60-3	-	Polysaccharides	100	69	69/41/39
P29	2-propanone, 1-(acetyloxy)-	592-20-1	1-acetyloxypropane-2-one	Polysaccharides	116	43	43/42/86
P30	Butanal, 2-ethyl-	97-96-1	-	Polysaccharides	100	43	43/72/41
P31	2-Pentenoic acid, methyl ester	818-59-7	-	Polysaccharides	114	55	55/83/39/114
P32	3-Pentenoic acid, methyl ester	818-58-6	-	Polysaccharides	114	55	55/59/114
P33	5-Hexene-3-one, 4,5-dihydroxy-	121197-12-4	2,3-Dihydroxyhex-1-ene-4-one	Polysaccharides	130	43	43/57/43
P34	Furan	110-00-9	-	Polysaccharides	68	68	68/39/38
P35	3(2H)-Furanone	3511-31-7	-	Polysaccharides	84	84	84/54/55
P36	2(3H)-Furanone	20825-71-2	-	Polysaccharides	84	84	84/55/56
P37	2(5H)-Furanone	497-23-4	-	Polysaccharides Cellulose (Hexose polymer)	84	55	55/84/54
P38	2(3H)-Furanone, dihydro-	96-48-0	γ -Butyrolactone	Polysaccharides	86	42	42/41/86/56
P39	Furan, 2-methyl-	534-22-5	-	Polysaccharides	82	82	82/53/81
P40	Furan, 3-methyl-	930-27-8	-	Polysaccharides	82	82	82/53/81/39
P41	2-Furancarboxaldehyde	98-01-1	Furfural; Furaldehyde	Polysaccharides	96	96	96/95/39
P42	3-Furancarboxaldehyde	498-60-2	-	Polysaccharides	96	95	95/39/96
P43	2-Furanmethanol	98-00-0	Furfuryl alcohol	Cellulose	98	98	98/39/81/41
P44	3-Furanmethanol	4412-91-3	-	Polysaccharides	98	98	98/41/97/69
P45	2(3H)-Furanone, 5-methyl-	591-12-8	Tetrahydro-4-methyl-3-furanone	Polysaccharides Cellulose	98	55	55/43/98
P46	3(2H)-Furanone, dihydro-4-methyl-	89364-27-2	α -Angelicalactone; 2,3-dihydro-5-methylfuran-2-one	Polysaccharides	100	43	43/72/57
P47	2(5H)-Furanone, 3-methyl-	22122-36-7	3-Methyl-(5H)-furan-2-one	Polysaccharides	98	41	41/40/69/98
P48	2(5H)-Furanone, 4-hydroxy-3-methyl-	516-09-6	4-hydroxy-3-methyl-2(5H)-furanone	Polysaccharides	114	56	56/114/42
P49	2,4(3H, 5H)-Furandione, 3-methyl-	1192-51-4	-	Polysaccharides	114	56	56/114/42

Table B-1 Identified polysaccharides-derived compounds as pyrolysis products (continued).

#	Compounds	CAS	Other names	Origin	MW	Base peak	m/z
P50	2-Furancarboxaldehyde, 5-methyl-	620-02-0	5-methyl-2-furfural; 5-methyl-2-furaldehyde	Polysaccharides	110	110	110/109/53
P51	Ethanone, 1-(2-furanyl)-	1192-62-7	2-Acetylfuran	Polysaccharides	110	95	95/110/39
P52	2-Furancarboxaldehyde, 5-(hydroxymethyl)-	67-47-0	5-hydroxymethyl-2-furfural; 5-hydroxymethyl-2-furaldehyde	Polysaccharides Cellulose (Hexose polymer)	126	97	97/126/41
P53	2-Furancarboxylic acid, methyl ester	611-13-2	2-Furoic acid methyl ester	Polysaccharides	126	95	95/39/126
P54	2-Furancarboxaldehyde, tetrahydro-5-(hydroxymethyl)-3-oxo-	135192-83-5	-	Cellulose	144	-	57/69/70/82/85
P55	4-Cyclopenten-1,3-dione-	930-60-9	-	Polysaccharides	96	42	42/96/68/54
P56	2-Cyclopenten-1-one, 2-hydroxy-3-methyl-	80-71-7	-	Polysaccharides	112	112	112/55/69
P57	2-Cyclopenten-1-one, 3-hydroxy-2-methyl-	5870-63-3	-	Cellulose	112	-	55/71/84/112
P58	2H-Pyran-2-one, 5,6-dihydro-4-hydroxy-	55100-07-7	3-hydroxy-2-penteno-1,5-lactone; 4-hydroxy-5,6-dihydro-(2H)-pyran-2-one	Polysaccharides Cellulose (Pentose polymer)	114	114	114/58/57/85
P59	2H-Pyran-2,5(6H)-dione	112468-46-9	Pyran-2,5-dione	Polysaccharides (Pentose polymer)	112	-	112
P60	2H-Pyran-2-one, 3,6-dihydro-5-methyl-	60920-98-1	-	Polysaccharides	112	55	55/112/84
P61	4H-Pyran-4-one, 3-hydroxy-2-methyl-	118-71-8	-	Polysaccharides (Hexose polymer)	126	126	126/43/71
P62	4H-Pyran-4-one, 3,5-dihydroxy-2-methyl-	1073-96-7	-	Polysaccharides	142	142	142/43/85
P63	4H-Pyran-4-one, 2,3-dihydro-5-hydroxy-2-(hydroxymethyl)-	6380-97-8	-	Polysaccharides Cellulose	144	87	87/144/43
P64	alpha-D-Mannofuranose, 1,5:3,6-dianhydro-	4451-31-4	-	Polysaccharides	144	68	68/39/42

Table B-1 Identified polysaccharides-derived compounds as pyrolysis products (continued).

#	Compounds	CAS	Other names	Origin	MW	Base peak	m/z
P65	beta-D-Glucopyranose, 1,6-anhydro-	498-07-7	Levoglucofan	Polysaccharides Cellulose (Hexose)	162	60	60/57/73/43
P66	1,6-Anhydro, beta-D-galactopyranose	644-76-8	-	Polysaccharides	162	60	60/57/73/43
P67	1,6-Anhydro, beta-D-mannopyranose	14168-65-1	-	Polysaccharides	162	60	60/57/73/56
P68	1,6-Anhydro, beta-D-glucofuranose	7425-74-3	-	Polysaccharides	162	73	73/43/69/57/60
P69	1,6-Anhydro, alpha-D-galactofuranose	33818-21-2	-	Polysaccharides	162	73	73/43/69/61/45
P70	beta-D-Glucofuranose, 1,5:3,6-dianhydro-	4451-30-3	1,4:3,6-dianhydro-alpha-D-glucopyranose	Polysaccharides	144	69	69/57/41/70
P71	.beta.-L-Arabinofuranose, 1,5-anhydro-	51246-94-7	-	Polysaccharides	132	57	57/73/55/43
P72	.beta.-D-Xylofuranose, 1,5-anhydro-	51246-91-4	-	Polysaccharides	132	57	57/73/43/55
P73	Hexadecanoic acid	57-10-3	-	Lipid	256	43	43/73/60

Table B-2 Identified lignin-derived compounds as pyrolysis products [105, 147, 148, 150-152].

#	Compounds	CAS	Other names	Origin*	MW	Base peak	m/z
L1	Phenol	108-95-2	-	H-Lignin	94	94	94/39/66
L2	1,2-Benzenediol	120-80-9	Catechol; Pyrocatechol; 1,2-dihydroxybenzene	Modified Lignin	110	110	110/64/63
L3	Toluene	108-88-3	-	Lignin	92	91	91/92/65
L4	Benzene, metoxy-	100-66-3	Anisol	Lignin	108	108	108/78/65
L5	Benzaldehyde	100-52-7	-	Lignin	106	77	77/106/105/51
L6	Benzenemethanol	100-51-6	Benzylalcohol	Lignin	108	79	79/107/77
L7	Phenol, 2-methyl-	95-48-7	o-cresol	H-Lignin	108	108	108/107/79/77
L8	Phenol, 3-methyl-	108-39-4	m-cresol	H-Lignin	108	108	108/107/79/78
L9	Phenol, 4-methyl-	106-44-5	p-cresol	H-Lignin	108	107	107/108/77/79
L10	Phenol, 2-methoxy-	90-05-1	Guaiacol	G-Lignin	124	109	109/124/81
L11	Benzaldehyde, 4-hydroxy-	123-08-0	-	Lignin	122	121	121/122/93/65/39
L12	1,2-Benzenediol, 3-methyl-	488-17-5	Catachol, 3-methyl-	Lignin	124	124	124/78/123
L13	1,2-Benzenediol, 4-methyl-	452-86-8	Catachol, 4-methyl-	Modified Lignin	124	124	124/123/78
L14	1,2-Benzenediol, 3-methoxy-	934-00-9	Catachol, 3-methoxy-	Lignin	140	140	140/125/97/51

Table B-2 Identified lignin-derived compounds as pyrolysis products (continued).

#	Compounds	CAS	Other names	Origin*	MW	Base peak	m/z
L15	1,2-Benzenediol, 4-methoxy-	3934-97-2	Catachol, 4-methoxy-	Lignin	140	140	140/125/97/107/79
L16	1,4-Benzenediol, 2-methoxy-	824-46-4	-	G-Lignin	140	140	140/125/97
L17	Benzoic acid, 4-hydroxy-	99-96-7	4-carboxyphenol; p-hydroxybenzoic acid; p-salicylic acid	Lignin	138	121	121/138/93/65
L18	Benzene, 1,3/1,4-dimethyl-	108-38-3 106-42-3	-	Lignin	106	91	91/106/105
L19	Benzene, 1,2-dimethyl-	95-47-6	-	Lignin	106	91	91/106/105
L20	Benzene, ethyl-	100-41-4	-	Lignin	106	91	91/106/51
L21	Benzene, ethenyl-	100-42-5	Styrene	Lignin	104	104	104/103/78/51
L22	Ethanone, 1-phenyl-	98-86-2	Acetophenone	Lignin	120	105	105/77/120/51
L23	Benzene, 1-methoxy, 3-/4-methyl-	100-85-4 104-93-8	Anisol, 3-/4-methyl-	Lignin	122	122	121/107/77
L24	Phenol, 2,6-dimethyl-	576-26-1	-	Lignin	122	122	122/107/121/77
L25	Phenol, 2,4-/2,5-dimethyl-	105-67-9 95-87-4	-	Lignin	122	122	122/107/121/77
L26	Phenol, 2,3-dimethyl-	526-75-0	-	Lignin	122	122	122/107/121/77
L27	Phenol, 3,5-dimethyl-	108-68-9	-	Lignin	122	122	122/107/121/77
L28	Phenol, 2-ethyl-	90-00-6	-	Modified Lignin	122	107	107/122/77
L29	Phenol, 3-ethyl-	620-17-7	-	Lignin	122	107	107/122/77
L30	Phenol, 4-ethyl-	123-07-9	-	H-lignin	122	107	107/122/77
L31	Phenol, 4-ethenyl-	2628-17-3	4-vinylphenol	H-lignin	120	120	120/91/65
L32	Phenol, 2-methoxy-3-methyl-	18102-31-3	-	G-Lignin	138	123	123/138/77/95
L33	Phenol, 2-methoxy-4-methyl-	93-51-6	-	G-Lignin	138	138	138/123/95
L34	Phenol, 2,6-dimethoxy-	91-10-1	Syringol	S-Lignin	154	154	154/139/111
L35	Benzaldehyde, 4-hydroxy-3-methoxy-	121-33-5	Vanillin; Guaiacylaldehyde	G-Lignin	152	151	151/152/81/109
L36	Benzoic acid, 4-hydroxy-3-methoxy-	121-34-6	Vanillic acid	Lignin	168	168	168/153/97
L37	Phenol, 4-ethyl-2-methyl-	2219-73-0	-	Lignin	136	121	121/136/91
L38	Phenol, 2-propyl-	644-35-9	-	Lignin	136	107	107/136/77
L39	Phenol, 4-propyl-	645-56-7	-	Lignin	136	107	107/136/77
L40	Phenol, 4-allyl-	501-92-8	Phenol, 4-allyl-	Lignin	134	134	134/133/91
L41	Phenol, 4-(1Z)-propenyl-	85960-81-2	Phenol, 4-propenyl-(cis)	Lignin	134	134	134/133/91/135
L42	Phenol, 4-propenyl-(trans)	20649-39-2	Phenol, 4-propenyl-(trans)	Lignin	134	134	134/133/107/77
L43	Benzene, 1-methoxy, 2,4-/2,5-dimethyl-	6738-23-4 1706-11-2	Anisol, 2,4-/2,5-dimethyl-	Lignin	136	136	136/121/91/77

Table B-2 Identified lignin-derived compounds as pyrolysis products (continued).

#	Compounds	CAS	Other names	Origin*	MW	Base peak	m/z
L44	Phenol, 2-ethyl-4-methoxy-	13391-32-7	-	G-Lignin	152	152	152/137/109
L45	Phenol, 3-ethyl-2-methoxy-	97678-77-8	-	Lignin	152	152	152/137/109
L46	Phenol, 4-ethyl-2-methoxy-	2785-89-9	-	G-Lignin	152	137	137/152/122
L47	Phenol, 4-ethenyl-2-methoxy-	7786-61-0	4-vinylguaiacol	G-Lignin	150	150	150/135/107/7
L48	Phenol, 2,6-dimethoxy-4-methyl-	6638-05-7	-	S-Lignin	168	168	168/153/125
L49	Benzeneacetaldehyde, 4-hydroxy-3-methoxy-	5703-24-2	Homovanillin; Guaiacyl ethanal	G-Lignin	166	137	137/166/122
L50	Ethanone, 1-(4-hydroxy-3-methoxyphenyl)-	498-02-2	Acetoguaiacone; Guaiacyl ethanone	G-Lignin	166	151	151/166/123
L51	Benzoic acid, 4-hydroxy-3-methoxy-, methyl ester	3943-74-6	Vanillic acid, methyl ester	G-Lignin	182	151	151/182/123
L52	Benzaldehyde, 4-hydroxy-3,5-dimethoxy-	134-96-3	Syringaldehyde	S-Lignin	182	182	182/181/39
L53	Phenol, 2-methoxy-4-propyl-	2785-87-7	4-propylguaiacol	Lignin	166	137	137/166/138/122
L54	Phenol, 2-methoxy-4-(2-propen-1-yl)-	97-53-0	Eugenol	G-Lignin	164	164	164/149/77
L55	Phenol, 2-methoxy-4-(1-propen-1-yl)-	97-54-1	Isoeugenol	G-Lignin	164	164	164/149/131/77/103
L56	2,5-Cyclohexadien-1-one, 2-methoxy-4-(2-propen-1-ylidene)-	10570-85-1	-	Lignin	162	162	162/147/151/152
L57	Phenol, 2-methoxy-4-(1,2-propadien-1-yl)-	135192-85-7	-	Lignin	162	162	162/147/91/119
L58	2-Propanone, 1-(4-hydroxy-3-methoxyphenyl)-	2503-46-0	Guaiacylacetone; Guaiacylpropan-2-one	G-Lignin	180	137	137/180/43/122
L59	Phenol, 4-ethenyl-2,6-dimethoxy-	28343-22-8	4-Vinylsyringol; Syringylethane	S-Lignin	180	180	180/165/137
L60	2-Propenal, 3-(4-hydroxy-3-methoxyphenyl)	458-36-6	Coniferyl aldehyde	G-Lignin	178	178	178/135/77/147/107
L61	Phenol, 4-(3-hydroxy-1-propen-1-yl)-2-methoxy-	458-35-5	Coniferyl alcohol	G-Lignin	180	137	137/180/124/91
L62	Phenol, 3-ethyl-2,6-dimethoxy-	485385-57-7	Syringol, 3-ethyl-	S-Lignin	182	182	182/167/139
L63	Phenol, 4-ethyl-2,6-dimethoxy-	14059-92-8	Syringol, 4-ethyl-	S-Lignin	182	167	167/182/53
L64	1-Propanone, 1-(4-hydroxy-3-methoxyphenyl)-	1835-14-9	Propiovanillone, Propioguaiacone	G-Lignin	180	151	151/180/123

Table B-2 Identified lignin-derived compounds as pyrolysis products (continued).

#	Compounds	CAS	Other names	Origin*	MW	Base peak	m/z
L65	2-Propen-1-one, 1-(4-hydroxy-3-methoxyphenyl)-	2983-65-5	-	G-Lignin	178	151	151/178/137
L66	Benzenepropanol, 4-hydroxy-3-methoxy-	2305-13-7	Dihydroconiferyl alcohol	Lignin	182	137	137/182/138/122
L67	Benzeneacetaldehyde, 4-hydroxy-3,5-dimethoxy-	87345-52-6	Homosyringaldehyde; Syringylethanal	S-Lignin	196	167	167/196/53
L68	Ethanone, 1-(4-hydroxy-3,5-dimethoxyphenyl)-	2478-38-8	Acetosyringone; Syringylethanone	S-Lignin	196	181	181/196/43/153
L69	1,2-Propanedione, 1-(4-hydroxy-3-methoxyphenyl)-	2034-60-8	-	G-Lignin	194	151	151/123/152
L70	Phenol, 2,6-dimethoxy-4-(1-propen-1-yl)-	6635-22-9	Syringylpropene; 4-propenylsyringol	S-Lignin	194	194	194/91/179
L71	Phenol, 2,6-dimethoxy-4-(1Z)-1-propen-1-yl-	26624-13-5	cis-4-Propenylsyringol	S-Lignin	194	194	194/91/179/77
L72	Phenol, 2,6-dimethoxy-4-(1E)-1-propen-1-yl-	20675-95-0	trans-4-Propenylsyringol	S-Lignin	194	194	194/91/179/195
L73	Phenol, 2,6-dimethoxy-4-(2-propen-1-yl)-	6627-88-9	4-Allylsyringol	S-Lignin	194	194	194/167/91
L74	Phenol, 2,6-dimethoxy-4-propyl-	6766-82-1	4-propylsyringol	S-Lignin	196	167	167/196/168
L75	2,5-Cyclohexadien-1-one, 2,6-dimethoxy-4-(2-propen-1-ylidene)-	58623-87-3	-	Lignin	192	192	192/177/43/57/131
L76	Benzenepropanol, 4-hydroxy-3,5-dimethoxy-	20736-25-8	Dihydrosinapyl alcohol; Syringylpropanol	S-Lignin	212	167	167/168/212
L77	Phenol, 4-(3-hydroxy-1-propen-1-yl)-2,6-dimethoxy-	537-33-7	Sinapyl alcohol; Syringylpropanol	S-Lignin	210	-	-
L78	Phenol, 4-[(1Z)3-hydroxy-1-propen-1-yl]-2,6-dimethoxy-	104330-63-4	cis-Sinapyl alcohol	S-Lignin	210	149	149/192/106
L79	Phenol, 4-[(1E)3-hydroxy-1-propen-1-yl]-2,6-dimethoxy-	20675-96-1	trans-Sinapyl alcohol	S-Lignin	210	210	210/167/154
L80	2-Propenal, 3-(4-hydroxy-3,5-dimethoxyphenyl)-	87345-53-7	Sinapinaldehyde; Syringylpropenal	S-Lignin	208	208	208/165/180
L81	1-Propanone, 1-(4-hydroxy-3,5-dimethoxyphenyl)-	5650-43-1	Propiosyringone	S-Lignin	210	181	181/210/182

Table B-2 Identified lignin-derived compounds as pyrolysis products (continued).

#	Compounds	CAS	Other names	Origin*	MW	Base peak	m/z
L82	2-Propanone, 1-(4-hydroxy-3,5-dimethoxyphenyl)-	19037-58-2	Syringylacetone; Syringylpropanone	S-Lignin	210	167	167/43/210
L83	1,2-Propanedione, 1-(4-hydroxy-3,5-dimethoxyphenyl)-	6925-65-1	-	S-Lignin	224	181	181/43/182
L84	Benzene, 1-(1,1-dimethylethyl)-4-ethenyl	1746-23-2	p-tert-butyl-styrene	Lignin	160	145	145/160/117

* H-, G-, and S-lignin, referring to Hydroxyphenyl, Guaiacyl, and Syringyl lignin, respectively.

Table B-3 Identified lignin-TMAH derived compounds as pyrolysis products [105, 107-109, 112].

#	Compounds	CAS	Other names	Origin*	MW	Base peak	m/z
T1	Benzaldehyde, 4-methoxy-	123-11-5	-	H-Lignin	136	135	135/136/77
T2	Ethanone, 1-(4-methoxyphenyl)-	100-06-1	-	H-Lignin	150	135	135/150/77
T3	Benzene, 1-ethenyl-4-methoxy-	637-69-4	-	H-Lignin	134	134	134/119/91
T4	Benzene, 1,2-dimethoxy-4-methyl-	494-99-5	-	G-Lignin	152	152	152/137/109
T5	Benzene, 1,2,3-trimethoxy-	634-36-6	-	S-Lignin	168	168	168/153/110
T6	Benzaldehyde, 3,4-dimethoxy-	120-14-9	-	G-Lignin	166	166	166/165/95/77
T7	Benzoic acid, 4-methoxy-, methyl ester	121-98-2	-	H-Lignin	166	135	135/166/77
T8	Benzene, 4-ethenyl-1,2-dimethoxy-	6380-23-0	-	G-Lignin	164	164	164/149/121
T9	Ethanone, 1-(3,4-dimethoxyphenyl)-	1131-62-0	3,4-Dimethoxyacetophenone	G-Lignin	180	165	165/180/137
T10	Benzaldehyde, 3,4,5-trimethoxy-	86-81-7	-	S-Lignin	196	196	196/181/125
T11	Benzoic acid, 3,4-dimethoxy-, methyl ester	2150-38-1	Methyl 3,4-dimethoxybenzoate	G-Lignin	196	196	196/165/79
T12	Benzene, 1,2-dimethoxy-4-(1-propen-1-yl)-	93-16-3	-	G-Lignin	178	178	178/163/107/91
T13	Benzene, 1,2-dimethoxy-4-(1Z)-1-propen-1-yl-	6380-24-1	cis-Methyl isoeugenol cis-4-Propenyl veratrole	G-Lignin	178	-	-

Table B-3 Identified lignin-TMAH derived compounds as pyrolysis products (continued).

#	Compounds	CAS	Other names	Origin*	MW	Base peak	m/z
T14	Benzene, 1,2-dimethoxy-4-(1E)-1-propen-1-yl-	6379-72-2	trans-Methyl isoeugenol trans-4-Propenyl veratrole	G-Lignin	178	-	-
T15	2-Propenoic acid, 3-(4-methoxyphenyl)-, methyl ester	832-01-9	-	H-Lignin	192	161	161/192/133
T16	2-Propenoic acid, 3-(4-methoxyphenyl)-, methyl ester, (2Z)-	19310-29-3	cis(Z)-p-Methoxymethylcinna mate	H-Lignin	192	-	-
T17	2-Propenoic acid, 3-(4-methoxyphenyl)-, methyl ester, (2E)-	3901-07-3	trans(E)-p-Methoxymethylcinna mate	H-Lignin	192	161	161/192/133
T18	Benzene, 1,2-dimethoxy-4-[(1Z)-2-methoxyethenyl]-	163088-93-5	cis-1-methoxy-2-(3,4-dimethoxyphenyl) ethylene	G-Lignin	194	194	194/179/151
T19	Benzene, 1,2-dimethoxy-4-[(1E)-2-methoxyethenyl]-	136114-02-8	trans-1-methoxy-2-(3,4-dimethoxyphenyl) ethylene	G-Lignin	194	194	194/179/151
T20	2-Propanone, 1-(3,4-dimethoxyphenyl)-	776-99-8	-	G-Lignin	194	151	151/194/107
T21	Benzene, 1,2-dimethoxy-4-(2-methoxypropyl)-	175096-38-5	2-methoxy-1-(3,4-dimethoxyphenyl) propane	G-Lignin	210	-	151/152/210
T22	Ethanone, 1-(3,4,5-trimethoxyphenyl)-	1136-86-3	-	S-Lignin	210	195	195/210/43
T23	Benzeneacetic acid, 3,4-dimethoxy-, methyl ester	15964-79-1	-	G-Lignin	210	151	151/210/73
T24	Benzoic acid, 3,4,5-trimethoxy-, methyl ester	1916-07-0	-	S-Lignin	226	226	226/211/95
T25	Benzene, 1,2-dimethoxy-4-(1-methoxy-1-propen-1-yl)-	172896-22-9	-	G-Lignin	208	-	-
T26	Benzene, 1,2-dimethoxy-4-[(1Z)-1-methoxy-1-propen-1-yl]-	175096-33-0	cis-1-methoxy-1-(3,4-dimethoxyphenyl)-1-propene	G-Lignin	208	-	165/193/208
T27	Benzene, 1,2-dimethoxy-4-[(1E)-1-methoxy-1-propen-1-yl]-	175096-34-1	trans-1-methoxy-1-(3,4-dimethoxyphenyl)-1-propene	G-Lignin	208	-	165/193/208
T28	Benzene, 1,2-dimethoxy-4-(3-methoxy-1-propen-1-yl)-	58045-87-7	-	G-Lignin	208	177	177/208/146

Table B-3 Identified lignin-TMAH derived compounds as pyrolysis products (continued).

#	Compounds	CAS	Other names	Origin*	MW	Base peak	m/z
T29	Benzene, 1,2-dimethoxy-4-[(1Z)-3-methoxy-1-propen-1-yl]-	175096-32-9	cis-3-methoxy-1-(3,4-dimethoxyphenyl)-1-propene	G-Lignin	208	-	91/177/208
T30	Benzene, 1,2-dimethoxy-4-[(1E)-3-methoxy-1-propen-1-yl]-	84782-37-6	trans-3-methoxy-1-(3,4-dimethoxyphenyl)-1-propene	G-Lignin	208	-	91/177/208
T31	Benzene, 1,2,3-trimethoxy-5-[(1Z)-2-methoxyethenyl]-	71095-07-3	-	S-Lignin	224	209	209/224/181
T32	Benzene, 1,2,3-trimethoxy-5-[(1E)-2-methoxyethenyl]-	71095-06-2	-	S-Lignin	224	209	209/224/181
T33	2-Propenoic acid, 3-(3,4-dimethoxyphenyl)-, methyl ester	5396-64-5	-	G-Lignin	222	222	222/191/207
T34	2-Propenoic acid, 3-(3,4-dimethoxyphenyl)-, methyl ester, (2Z)-	30461-78-0	-	G-Lignin	222	-	-
T35	2-Propenoic acid, 3-(3,4-dimethoxyphenyl)-, methyl ester, (2E)-	30461-77-9	-	G-Lignin	222	-	-
T36	Benzenepropanoic acid, 3,4-dimethoxy-, methyl ester	27798-73-8	3-(3,4-dimethoxyphenyl) propanoic acid methyl ester	G-Lignin	224	151	151/224/164
T37	Benzene, 4-(1,3-dimethoxy-1-propen-1-yl)-1,2-dimethoxy-	477883-98-0	-	G-Lignin	238	-	-
T38	Benzene, 4-[(1Z)-1,3-dimethoxy-1-propen-1-yl]-1,2-dimethoxy-	175096-36-3	cis-1,3-dimethoxy-1-(3,4-dimethoxyphenyl)-1-propene	G-Lignin	238	-	-
T39	Benzene, 4-[(1E)-1,3-dimethoxy-1-propen-1-yl]-1,2-dimethoxy-	175096-37-4	trans-1,3-dimethoxy-1-(3,4-dimethoxyphenyl)-1-propene	G-Lignin	238	-	176/207/238
T40	Benzene, 1,2,3-trimethoxy-5-[(1Z)-1-methoxy-1-propen-1-yl]-	866217-09-6	-	S-Lignin	238	-	-
T41	2-Propenoic acid, 3-(3,4,5-trimethoxyphenyl)-, methyl ester	7560-49-8	-	S-Lignin	252	252	252/237/221
T42	2-Propenoic acid, 3-(3,4,5-trimethoxyphenyl)-, methyl ester, (Z)-	20329-97-9	-	S-Lignin	252	-	-

Table B-3 Identified lignin-TMAH derived compounds as pyrolysis products (continued).

#	Compounds	CAS	Other names	Origin*	MW	Base peak	m/z
T43	2-Propenoic acid, 3-(3,4,5-trimethoxyphenyl)-, methyl ester, (2E)-	20329-96-8	-	S-Lignin	252	-	-
T44	Benzenepropanoic acid, 3,4,5-trimethoxy-, methyl ester	53560-25-1	-	S-Lignin	254	-	-
T45	Benzene, 1,2,3-trimethoxy-5-(1-methoxy-1-buten-1-yl)-	350799-97-2	-	S-Lignin	252	-	-
T46	Benzene, 1,2-dimethoxy-4-(1,2,3-trimethoxypropyl)-	175096-35-2	1,2,3-trimethoxy-1-(3,4-dimethoxyphenyl) propane	G-Lignin	270	-	166/181/270
T47	Benzene, 5-[(1Z)-1,3-dimethoxy-1-propen-1-yl]-1,2,3-trimethoxy-	350482-89-2	-	S-Lignin	268	-	-
T48	Benzene, 1,2,3-trimethoxy-5-(1,2,3-trimethoxypropyl)-	279693-74-2	-	S-Lignin	300	-	-

* H-, G-, and S-lignin, referring to Hydroxyphenyl, Guaiacyl, and Syringyl lignin, respectively.

Appendix C

SEM Micrographs of Spruce and Solid Residues

As indicated in Chapter 5, additional SEM micrograph of 200 \times , 500 \times and 1000 \times magnification are shown in Appendix C. Each Figure shows SEM micrographs of spruce and the residues at different magnifications.

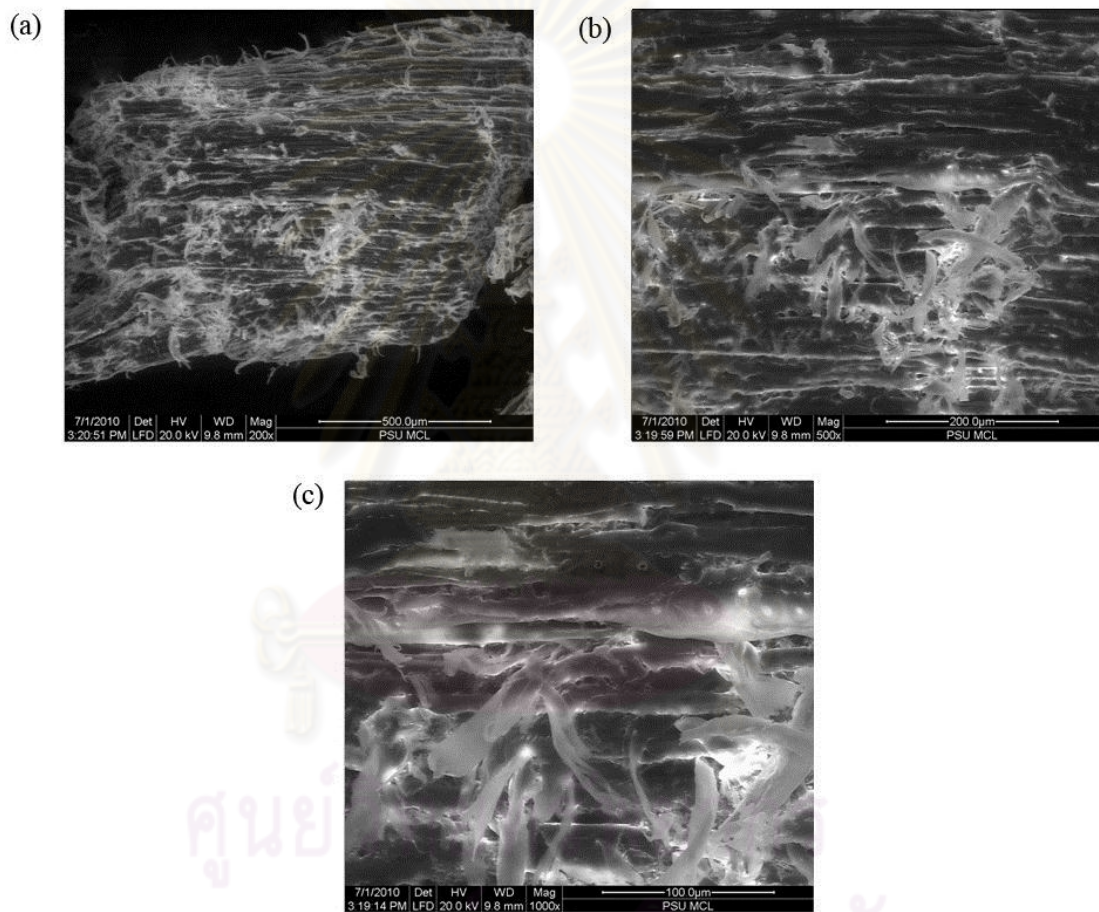


Figure C-1 SEM micrographs of spruce at various magnification. Designation: (a) 200 \times ; (b) 500 \times ; (c) 1000 \times .

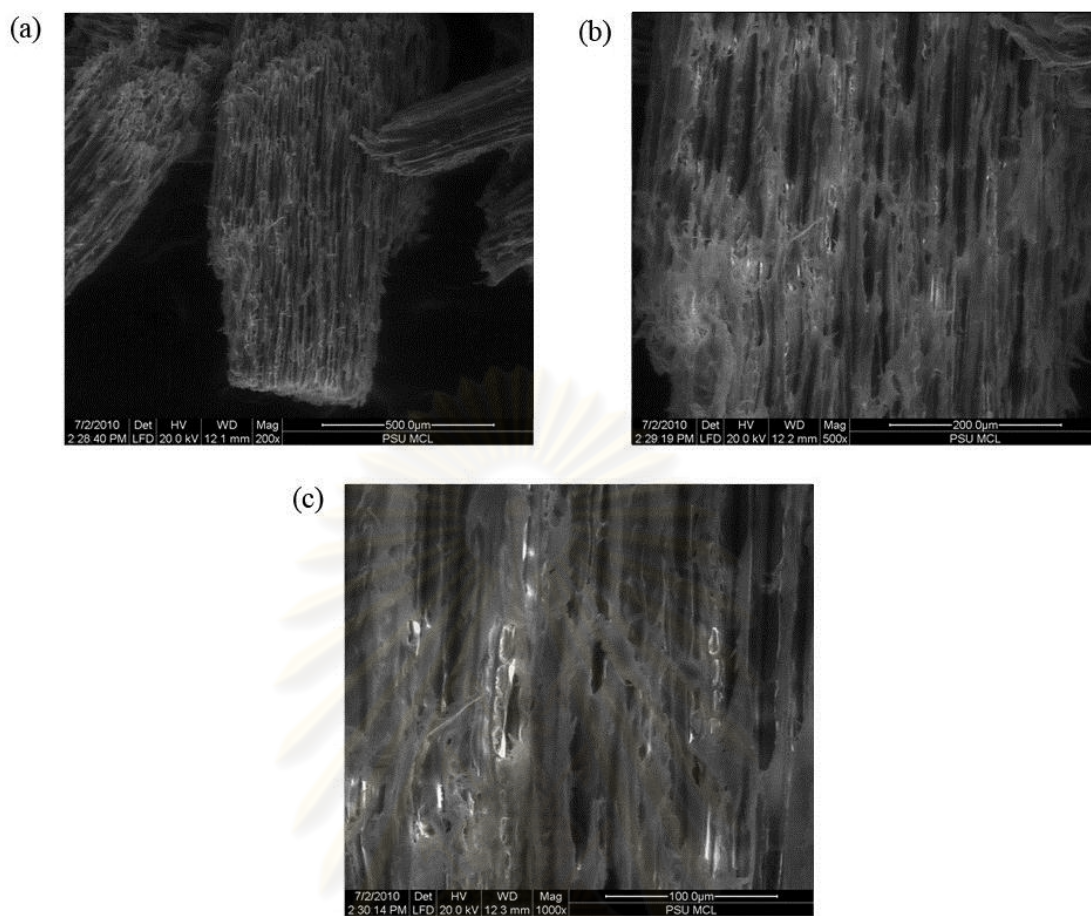


Figure C-2 SEM micrographs of water residues at various magnification.

Designation: (a) 200×; (b) 500×; (c) 1000×.

ศูนย์วิทยทรัพยากร
จุฬาลงกรณ์มหาวิทยาลัย

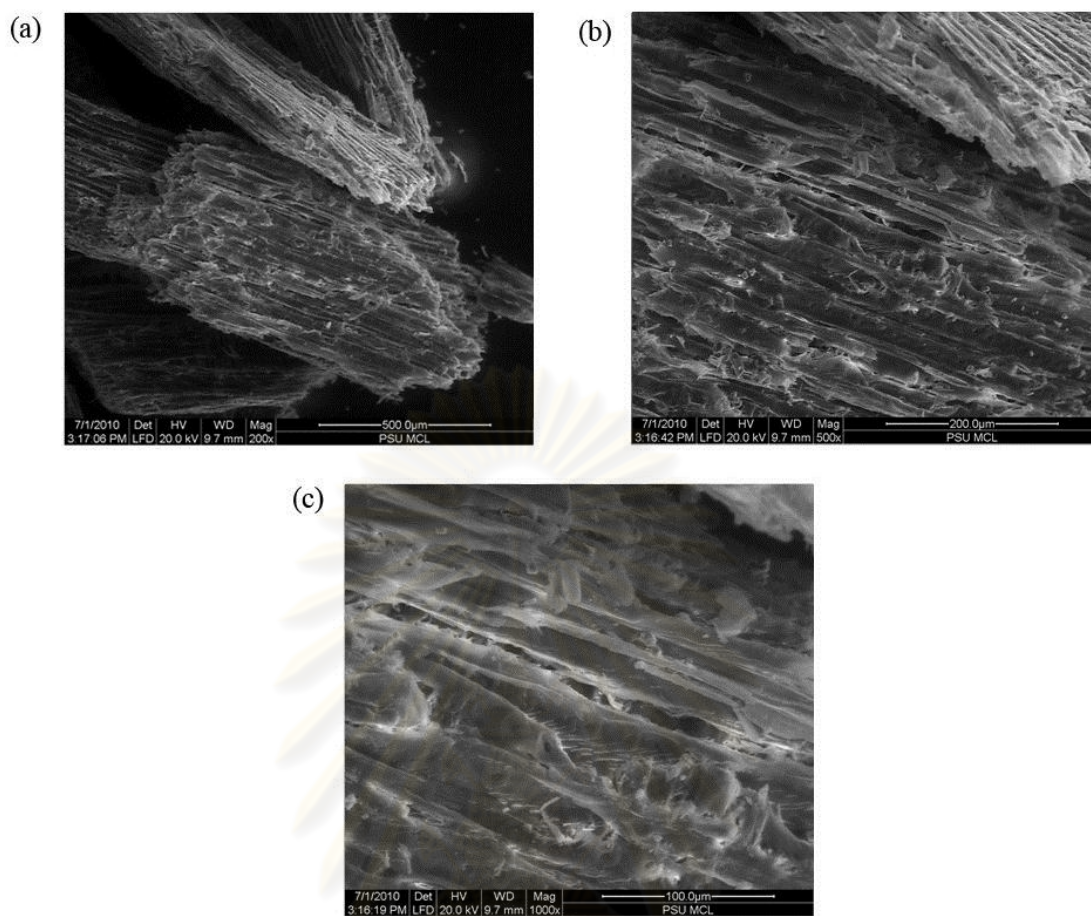


Figure C-3 SEM micrographs of acid residues at various magnification.

Designation: (a) 200 \times ; (b) 500 \times ; (c) 1000 \times .

ศูนย์วิทยทรัพยากร
จุฬาลงกรณ์มหาวิทยาลัย

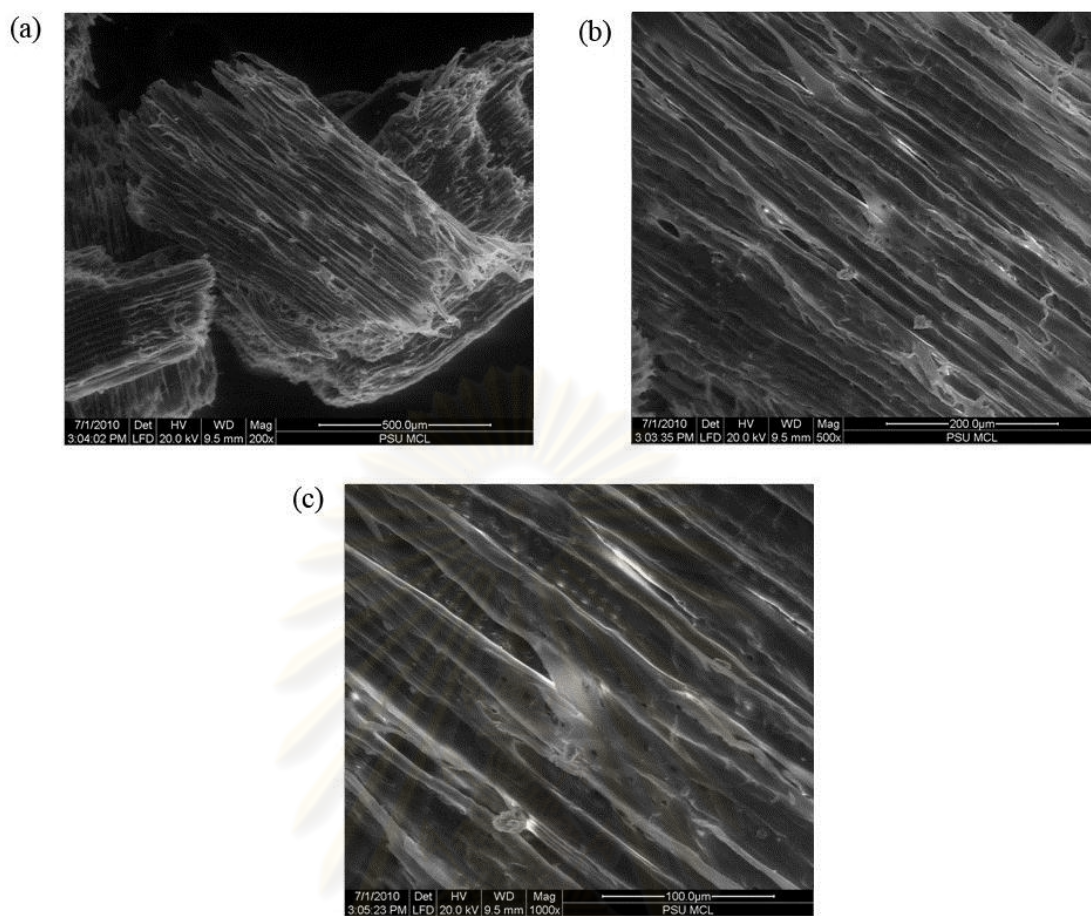


Figure C-4 SEM micrographs of base residues at various magnification.

Designation: (a) 200×; (b) 500×; (c) 1000×.

ศูนย์วิทยทรัพยากร
จุฬาลงกรณ์มหาวิทยาลัย

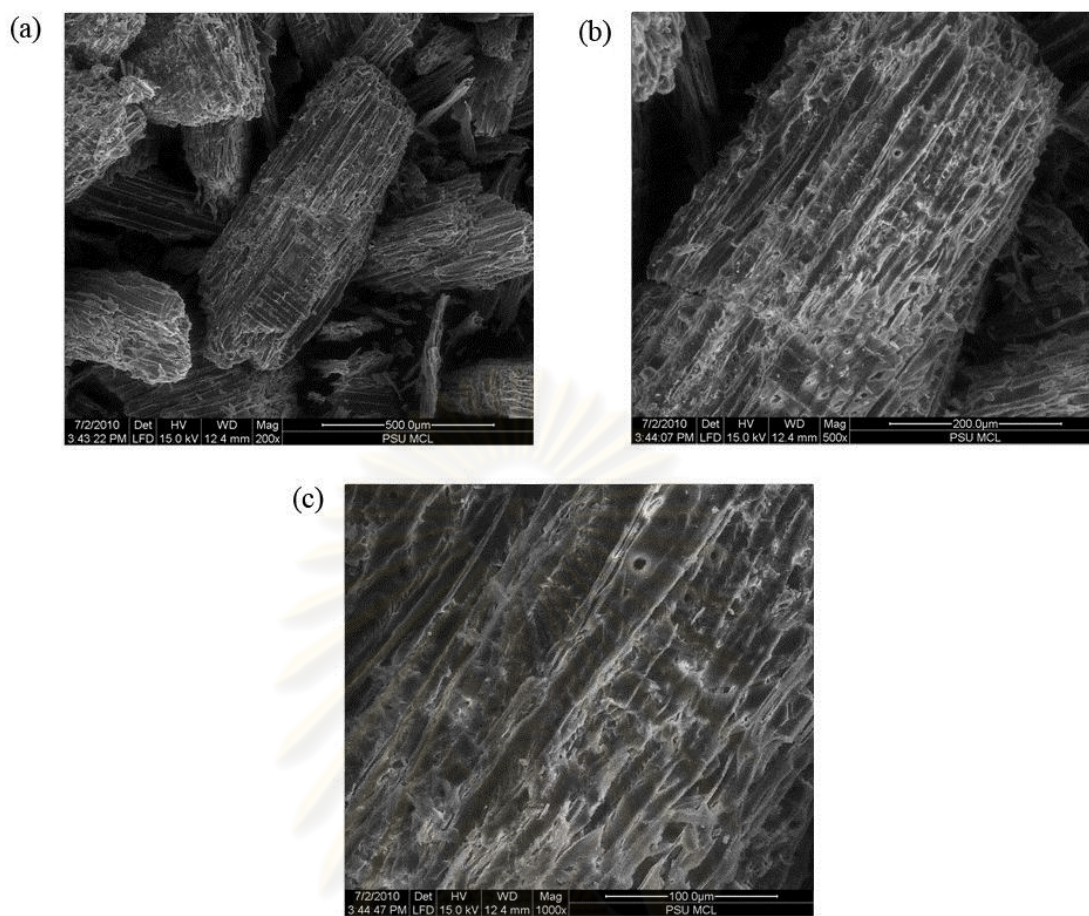


Figure C-5 SEM micrographs of A-A residues at various magnification.

Designation: (a) 200×; (b) 500×; (c) 1000×.

ศูนย์วิทยทรัพยากร
จุฬาลงกรณ์มหาวิทยาลัย

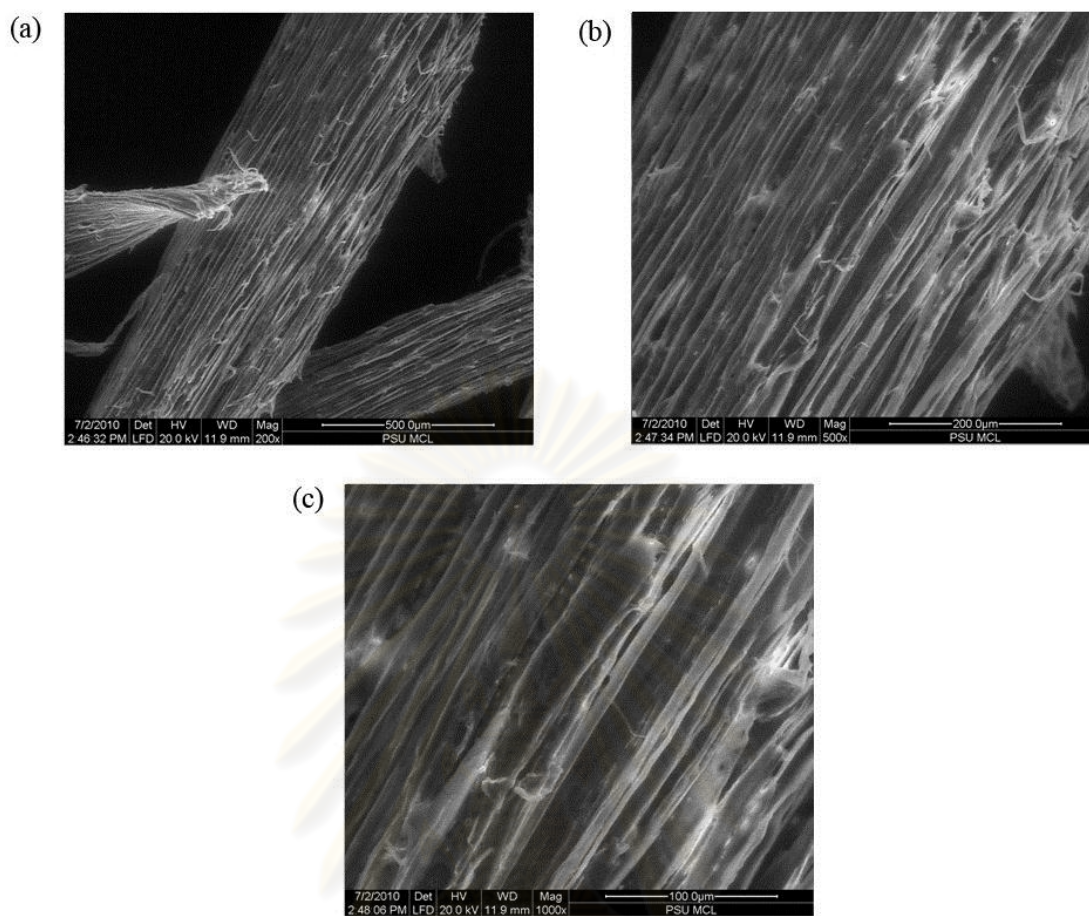


Figure C-6 SEM micrographs of B-B residues at various magnification.

Designation: (a) 200×; (b) 500×; (c) 1000×.

ศูนย์วิทยทรัพยากร
จุฬาลงกรณ์มหาวิทยาลัย

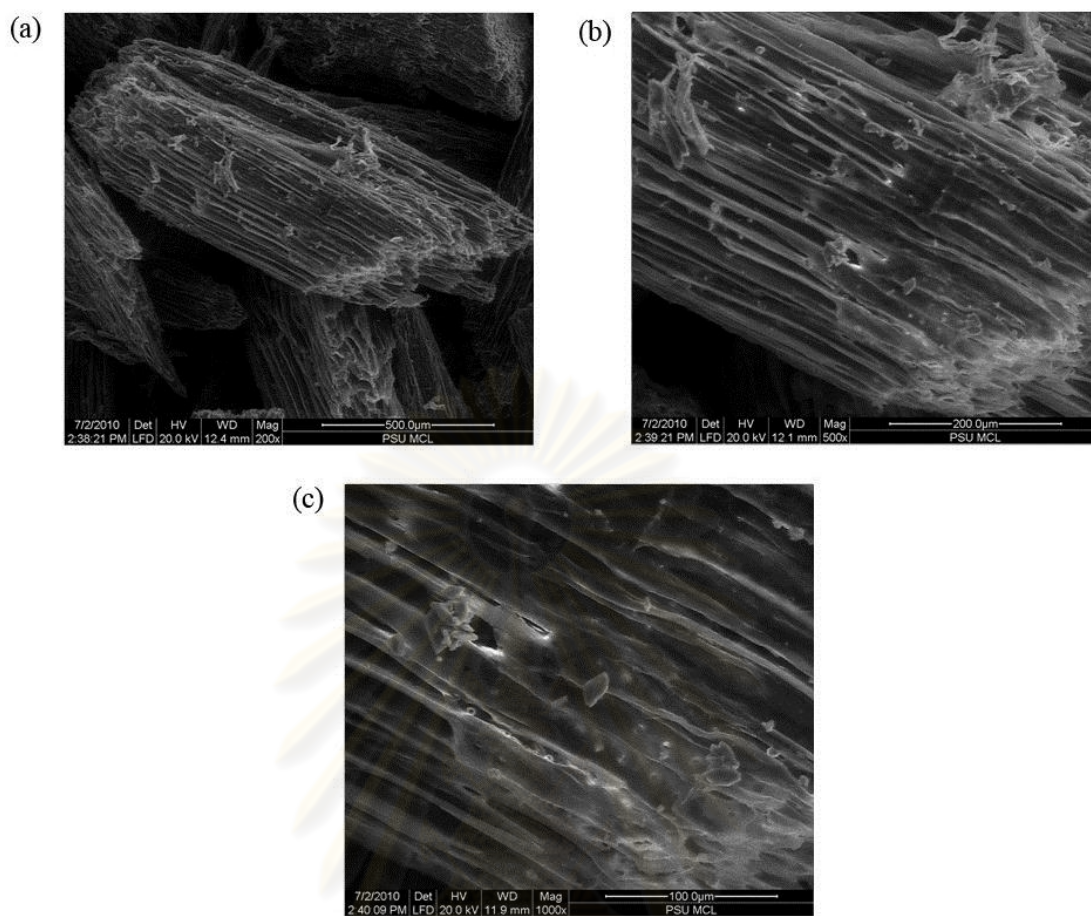


Figure C-7 SEM micrographs of B-A residues at various magnification.

Designation: (a) 200×; (b) 500×; (c) 1000×.

ศูนย์วิทยทรัพยากร
จุฬาลงกรณ์มหาวิทยาลัย

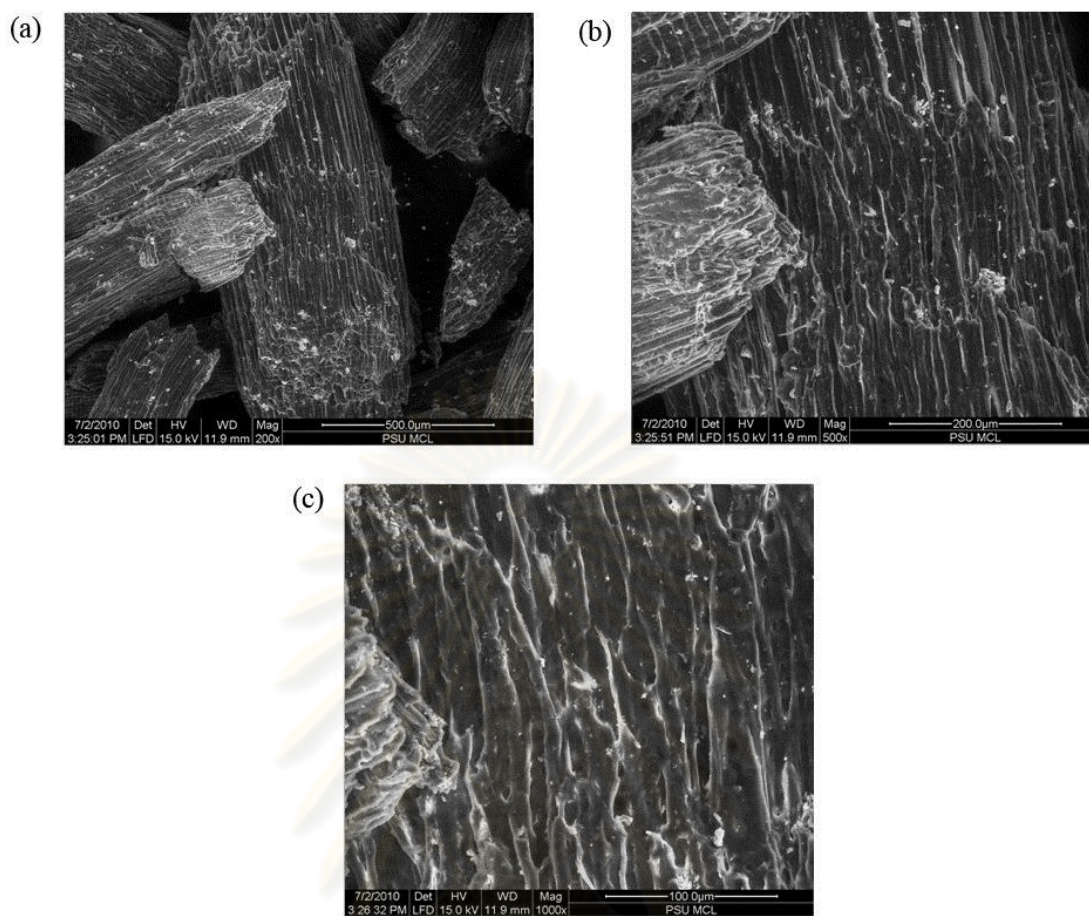


Figure C-8 SEM micrographs of A-B residues at various magnification.

Designation: (a) 200×; (b) 500×; (c) 1000×.

ศูนย์วิทยทรัพยากร
จุฬาลงกรณ์มหาวิทยาลัย

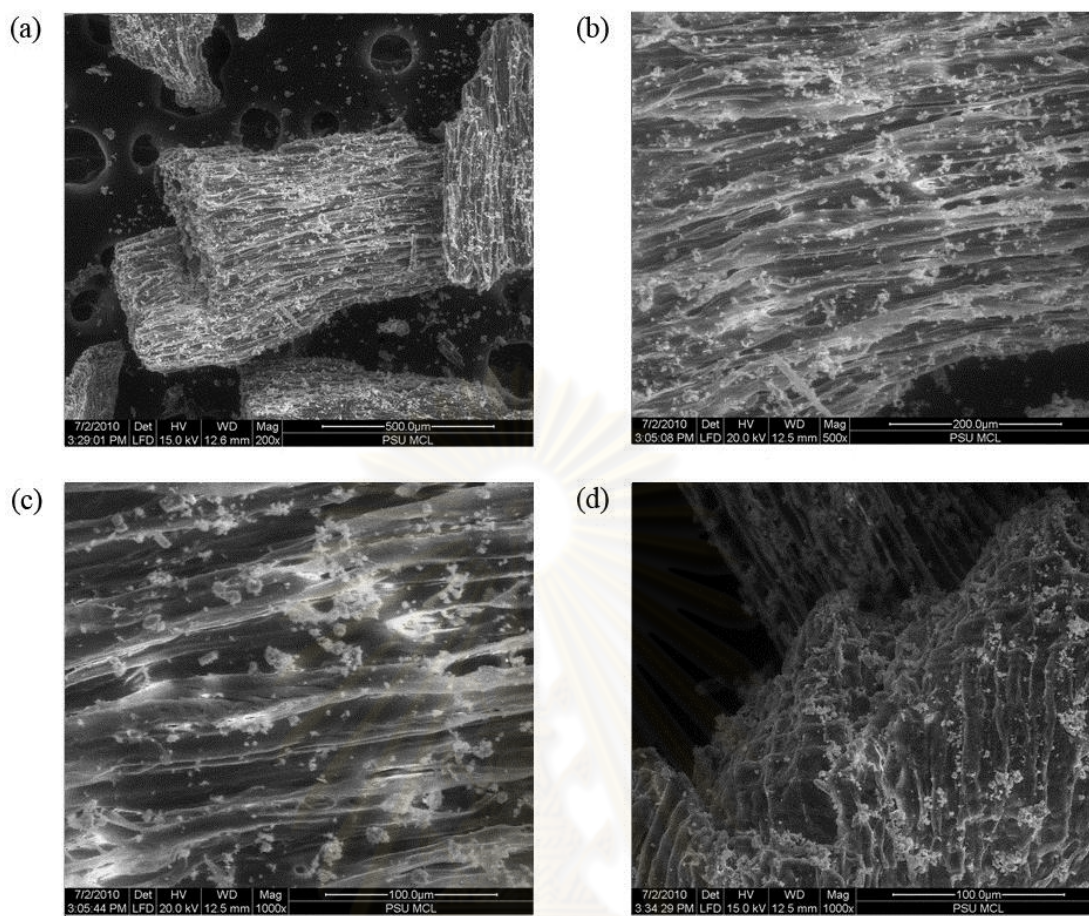


Figure C-9 SEM micrographs of A-B-A residues at various magnification.

Designation: (a) 200×; (b) 500×; (c) and (d) 1000×.

ศูนย์วิทยทรัพยากร
จุฬาลงกรณ์มหาวิทยาลัย

VITA

Miss Ungkana Wongsiriwan was born on December 31st, 1982 in Bangkok, Thailand. During her undergraduate years at Chulalongkorn University in 2004-2005, she was nominated to receive a scholarship for a student exchange program at the University of Washington and summer internship at the Dow Chemical Company, Freeport, Texas. In 2005, she received Bachelor Degree of Science (First class honors) in Chemical Engineering from the Department of Chemical Technology, Chulalongkorn University. Ungkana began her Ph.D. study at the Department of Chemical Technology, Chulalongkorn University and has received the Royal Golden Jubilee scholarship from the Thailand Research Fund since 2006. She was a teaching assistant at the Department of Chemical Technology for two undergraduate courses. As a part of her graduate study, she did collaborative research at the Energy Institute, College of Earth and Mineral Science, the Pennsylvania State University for almost 3 years during 2007-2010. Her paper “Lignocellulosic Biomass Conversion by Sequential Combination of Organic Acid and Base Treatments” was published in April, 2010 in “Energy and Fuels”. She participated in the 239th American Chemical Society conference on March 24, 2010 as a presenter in San Francisco, USA.

ศูนย์วิทยทรัพยากร
จุฬาลงกรณ์มหาวิทยาลัย